Emissions, physicochemical characteristics and exposure to coarse, fine and ultrafine particles from building activities

Department of Civil and Environmental Engineering
Faculty of Engineering and Physical Sciences
University of Surrey
Guildford, Surrey, UK

A thesis submitted for the fulfillment of
Doctor of Philosophy
by

Farhad Azarmi

Statement of Originality

The work presented in this dissertation was carried out by the author at the Department of Civil and Environmental Engineering, University of Surrey (UK), under the supervision of my principal supervisor, Dr. Prashant Kumar, and co-supervisor, Dr. Mike Mulheron. This thesis is my own work and contains nothing which is the outcome of my work performed in collaboration with others. Any published (or unpublished) ideas and/or techniques from the work of others are fully acknowledged in accordance with the standard referencing practices. In addition, no part of this thesis has already been, or is being concurrently submitted for any other degree, diploma or qualification.

This dissertation contains approximately 54,516 words, 48 figures and 24 tables.

Farhad Azarmi

University of Surrey

Friday, 11th of March, 2016

Acknowledgements

Firstly, I would like to express my sincere thanks and appreciation to my principal supervisor, Dr. Prashant Kumar for all his excellent supervision, constant support and kindness over the duration of my PhD. My discussions with Dr. Kumar and his insights always helped me to get back on the right direction. Dr. Kumar cared so much about my work and responded to all my queries and questions so promptly. His patient guidance and encouragement has given to me the confidence and assurance to carry on this research study. I also thank my co-supervisor, Dr. Mike Mulheron, for his valuable help and advice throughout the research duration.

I am very grateful to the Department of Civil and Environmental Engineering, University of Surrey for providing PhD funding support and cara for this work. I am thankful to Prof. Stephen Baker and Stuart Robinson for permitting the access of the demolition site. Thanks also to Prof. Vincent Emery, Dr. Norma Denny, Dr. Gary Fuller, Chris Burt, Alan Newland, Russell Bridges-Smith, Stephen Knight, Daniel Marsh, Shoaib Shafi and Nigel Mobb for all their helps during my PhD programme. Furthermore, I would like to thank Anju Goel, Omid Eshaghi, Hossein Jahangiri, Hesam Mehrabi, Zhenchun Yang, Abdullah Al-Dabbous, Dr. Siavash Adhami and Dr. Sanjay Mukherjee and all the faculty staff for their great supports and helps throughout my research study as a PhD student.

Last but not least, I would like to present my heartfelt thanks to my family for all their precious love, support and encouragement through my years of study.

Publications

The work described in this thesis appeared in the following published articles and presentations:

Journal Articles

Azarmi, F., Kumar, P., Mulheron, M., 2014. The exposure to coarse, fine and ultrafine particle emissions from concrete mixing, drilling and cutting activities. *Journal of Hazardous Materials* 279, 268-279.

Azarmi, F., Kumar, P., Mulheron, M., Colaux, J.L., Jeynes, C., Adhami, S., Watts, J.F., 2015. Physicochemical characteristics and occupational exposure to coarse, fine and ultrafine particles during building refurbishment activities. *Journal of Nanoparticle Research* 17, 343, doi: 10.1007/s11051-015-3141-z.

Azarmi, F., Kumar, P., Marsh, D., Fuller, G.W., 2015. Assessment of long-term impacts of PM_{10} and $PM_{2.5}$ particles from construction works on surrounding areas. *Environmental Science: Processes & Impacts* 18, 208-221.

Azarmi, F., Kumar, P., 2016. Ambient exposure to coarse and fine particle emissions from building demolition. *Atmospheric Environment* 137, 62-79.

Conference Articles and Presentations

Azarmi, F., Kumar, P., Mulheron, M., 2014. Coarse and fine particulate emissions from drilling activity. 4th Postgraduate research Conference, 3rd-4th February, Surrey University Conference, United Kingdom.

Azarmi, F., Kumar, P., Mulheron, M., 2015. Occupational exposure to coarse, fine and ultrafine particle emissions from building refurbishment activities. International Festival of Public Health, University of Manchester, United Kingdom, July 2015.

Azarmi, F., Kumar, P., 2015. Assessment of impact of coarse and fine particles from building demolition works on surrounding areas. 10th International Conference on Air Quality-Science and Application, 14th-18th March, Milan, Italy (accepted).

Book chapters

Kumar, P., Azarmi, F., Mulheron, M., 2012. Enlightening and noxious shades of nanotechnology application in concrete. In: Nanotechnology: Volume 9 Civil / Construction Engineering. (Studium Press LLC, USA; Govil, J.N. Eds.). ISBN: 1-62699-009-3). pp. 255-287.

News stories

DIY can be dangerous – but it's the invisible dust that may harm you the most, The Conversation, 20 August 2015

How the dust from DIY jobs can give you heart disease or cancer: Call for health and safety regulations to be updated to protect builders and amateur enthusiasts, Mail Online, 20 August 2015.

Warning to DIY enthusiasts and construction workers as dangerous dust emissions, Science Newsline, 19 August 2015.

DIY Techniques are found to be less productive, Nature World News, 27 August 2015.

Abstract

Building works include construction and demolition activities, which are common in cities across the world. Building-related activities contribute a considerable amount of the construction and demolition waste material worldwide. These activities have the potential to produce particulate matter (PM), including PM_{10} (≤10 μm), $PM_{2.5}$ (≤2.5 μm) and PM_{1} (≤1 μm), and airborne ultrafine particles (≤0.1 μm). Recent studies have indicated that the rate of building works undertaken each year is growing exponentially, to meet new urban design guidelines and respond to demand from the adoption of new building technologies, which highlights the importance of measuring the amounts of particle emissions from these sources. The principles of sustainable urban development are well established, but the extent of pollution due to construction and demolition activities is still unknown. Through laboratory and field studies, this thesis aims to comprehensively investigate the release of coarse (referred to as $PM_{2.5–10}$ fraction), fine ($PM_{2.5}$) and ultrafine particles from various building works, assess their physicochemical properties, and estimate the associated occupational exposure risk from them to on-site workers and individuals in the close vicinity.

Experiments for this thesis were carried out to measure PM and airborne ultrafine particles in the size range of (0.005–10 μm) using a fast response differential mobility spectrometer (DMS50), a tapered element oscillating micro balance (TEOM 1400), a GRIMM particle spectrometer (1.107 E) and OSIRIS (2315). Measurements were made in various locations: a controlled laboratory environment (i.e. concrete mixing, drilling, cutting), indoor field sites (i.e. building refurbishment) and at outdoor field sites (i.e. construction and

demolition). Moreover, dust samples were collected simultaneously for physiochemical analyses (e.g. SEM, EDS, XPS and IBA). Several important findings were then extrapolated during the analysis. These findings indicated that ultrafine particles dominated (74-97%) the total particle number concentrations (PNCs) while the coarse particles ($PM_{2.5-10}$) contributed to the majority of the total particle mass concentrations (PMCs), during the laboratory, indoor and outdoor field experiments. The highest proportion of PNCs and PMCs was found during the concrete cutting, drilling and wall chasing activities. In addition, the highest proportion of PMCs was observed in the excavator cabin during a building demolition at an outdoor field measurement site. Moreover, combining the results of SEM, EDS, XPS and IBA analysis suggested the dominance of elements such as Si, Al and S in the collected samples. The data were also used to assess the horizontal decay of the PMC through a modified box model to determine the emission factors and the occupational exposure to on-site workers and nearby individuals. The results confirmed that building-related works produce significant levels of coarse, fine and ultrafine particles, and that there is a need to limit particle emissions and reduce the occupational exposure of individuals by enforcing effective engineering controls. These findings could also be useful for the building industry to develop mitigation strategies to limit exposure to particulate matter during building works, particularly for ultrafine particles, which are currently non-existent.

Table of Contents

List of Figures

List of Tables

Glossary

List of Acronyms

AQS	Air Quality Strategy
AVG	Average
COSHH	Control of Substances Hazardous to Health
CS	Construction site
DF	Deposition fraction
DS	Demolition site
EBS	Elastic backscattering spectrometry
EDS	Energy dispersive x-ray spectroscopy
EF	Emission factor
EMEP	European Monitoring and Evaluation Programme
EEA	European Environment Agency
ENP	Engineered nanoparticles
EPA	Environmental Protection Agency
EU	European Union
FIB	Focused Ion Beam
GGBS	Ground Granulated Blastfurnace Slag
GPS	Global Positioning System

HEPA	High efficiency particulate air filter
HSE	Health and Safety Executive
IBA	Ion Beam Analysis
ICRP	International Commission on Radiological Protection
MMD	Mass median diameter
MLD	Minimum level of detection
MS	Monitoring station
NAEI	National Atmospheric Emission Inventory
NIST	National Institute of Standards and Technology
PFA	Pulverised Fuel Ash
PM	Particulate matter
PM_{10}	Particles with diameter $\leq$10 μm
$PM_{2.5}$	Particles with diameter $\leq$2.5 μm
PM_{1}	Particles with diameter $\leq$1 μm
PMC	Particle mass concentration
PMEF	Particle mass emission factor
PND	Particle number distribution
PNC	Particle number concentration
PIXE	Particle Induced X-ray Emission

PSL	Polystyrene Latex Sphere
PTFE	Polytetrafluoroethylene
PVC	Polyvinyl chloride
RDD	Respiratory deposited doses
SEM	Scanning electron microscope
STD	Standard deviation
UFP	Ultrafine particle
UK	United Kingdom
USA	United States of America
VT	Tidal volume
WD	Wind direction
WEL	Work Exposure Limit
WHO	World health organization
WS	Wind speed
XPS	X-ray Photoelectron Spectroscopy

Chapter 1. Introduction

This chapter provides an overview of the research in the context of emissions, physicochemical characteristics and exposure to coarse, fine and ultrafine particles from building activities. The chapter starts with the background and motivation for the study; this is followed by a summary of research objectives and approaches, and a conclusion briefly outlining the structure of the thesis.

1.1 Motivation

Exposure to particulate matter (PM), including PM_{10} (≤10 μm), $PM_{2.5}$ (≤2.5 μm) and PM_1 (≤1 μm), and ultrafine particles (≤0.1 μm), is of great concern to the air quality management community due to these particles' potentially adverse impacts on human health and the environment (Chow et al., 2006; Kumar et al., 2010a). There is substantial epidemiological and toxicological evidence to suggest that it is important to evaluate the influence of both particle number concentrations (PNCs) and particle mass concentrations (PMCs) on human health (Brunekreef and Forsberg, 2005; Heal et al., 2012). Particle size is important, as smaller particles can penetrate deeper into the respiratory system, increasing the potential to adversely affect human health (Hoet et al., 2004). Some studies have speculated that when considering exposure to ultrafine particles, PNC is a more important exposure metric than the particle mass-based metric (Hartog et al., 2005).

Typically, ultrafine particles are represented by PNCs, whilst the PM_{10}, $PM_{2.5}$ and PM_1 particles are represented based on PMCs (Kumar and Morawska, 2014).

Within urban environments there are a number of sources of ultrafine particles and PM. Vehicle emissions and road works are well-established sources of PNCs and PMCs (Amato et al., 2009; Kumar et al., 2013b; Pey et al., 2009). Previous studies have drawn attention to other sources of PM_{10}, $PM_{2.5}$, PM_1 and ultrafine particles, such as fossil fuel burning, mineral industries, mineral dust, and secondary aerosols (Querol et al., 2004; Yatkin and Bayram, 2008). There are many negative impacts on human health and the environment through exposure to PM and ultrafine particles , which may lead to higher rates of mortality around the world (Jacobson, 2005; Kumar et al., 2011a; Stjern et al., 2011).

Consequently, the continuous development of civil and urban infrastructures has led to the imposition of more stringent regulations on the use of construction materials, and on the way work is undertaken. Building-related activities have the potential to generate coarse (hereafter referred to $PM_{2.5–10}$ fraction), fine ($PM_{2.5}$) and ultrafine particles due to the increase in the world population and the growing need for construction and demolition works. However, the exact quantities of PM and ultrafine particles produced, and the occupational exposure level of operatives, are poorly understood. This is slowly changing as we become concerned with climate change and health issues, which highlighting a need to protect the environment, improve quality of life and sustain the liveable conditions in urban areas.

Whilst research studies have been undertaken to investigate the effects of PM and ultrafine particles on the environment and health, there is still very little and limited legal regulation, and a lack of guidelines for restricting public exposure to airborne particles – especially for ultrafine particles – within the urban environment and at construction and demolition sites. Setting up health and safety regulatory bodies as a basis for establishing such guidelines is very important, as there is a clear need to investigate the release of airborne particles. Therefore, the focus of this thesis remains mainly on building activities where very little is currently known.

1.2 Research objectives

The aim of this work is to understand how PM and ultrafine particles are emitted from various indoor and outdoor building sources and assess the physicochemical characteristics and exposure risks of PM_{10}, $PM_{2.5}$, PM_1 and ultrafine particles, in order to address concerns associated with the impacts of these particles from such sources. The specific objectives of this research work are to:

- Quantify the emission of particles released during building activities in the laboratory and field experiments.
- Understand the physical and chemical properties of particles, including assessing particles' shape, structure, size and composition.
- Assess the rate of mass and number emissions of particles during indoor and outdoor construction and demolition activities.
- Estimate the occupational exposure to on-site workers and people in the close vicinity of the building works.

1.3 Research approach

The above objectives are achieved by following the step by step research approach described in the following subsections.

1.3.1 Simulated laboratory investigations

Detailed investigations of the emission characteristics of ultrafine particles and PM were carried out in order to measure the quantities of coarse, fine and ultrafine particles produced from three simulated building activities (concrete mixing, drilling, cutting) at the Construction Materials Laboratory of Surrey University. These simulated activities included the mixing of fresh concrete, incorporating pulverised fuel ash (PFA) or Portland cement with ground granulated blastfurnace slag (GGBS), and the subsequent drilling and cutting of concrete cubes. A differential mobility spectrometer (DMS50) and GRIMM (model 1.107 E) instrument were used to measure number, mass and size distributions in the 5-10,000 nm range. The other objectives of this experiment were to compute the emission factors of PM_{10}, $PM_{2.5}$, PM_1 and ultrafine particles along with occupational exposure doses (i.e. respiratory deposition doses) of these particles. The results of these measurements are presented in Chapter 4.

1.3.2 Release of particles from indoor activities of building refurbishment

After achieving the above aim, 20 indoor building refurbishment activities, including various activities such as welding, wall chasing, sanding and cementing, were performed to measure particle mass (PMC) and number (PNC) concentrations. These measurements were taken in the Chemistry Laboratory at the University of Surrey using the DMS50 and GRIMM instruments for the measurements of particles in the 5-10,000 nm range. Particles

collected on the filters during background (pre-activity), activity and non-activity periods were analysed using a scanning electron microscope (SEM), through X-ray photoelectron spectroscopy (XPS), and through ion beam (IBA) analysis, to understand their nature and physicochemical properties, their potential effects on local air quality, and any health risks they posed. The emissions of these particles have also been investigated to help understand the effect of their associated occupational exposure on on-site workers undertaking building refurbishment. These results are presented in Chapter 5.

1.3.3 Assessment of PM_{10} and $PM_{2.5}$ particles from outdoor construction activities

The above-mentioned points in Sections 1.3.1 and 1.3.2 led to the performance of follow-up investigations for outdoor construction works. This part of the thesis assessed the impact of PM_{10} and $PM_{2.5}$ arising from construction works on the surrounding environment in London (UK). Measurements of PM_{10} and $PM_{2.5}$ were made at 17 different monitoring stations around three construction sites between 2002 and 2013. OSIRIS (2315) and tapered element oscillating micro balance (TEOM 1400) particle monitors were used to measure PM_{10} and $PM_{2.5}$ fractions in the 0.1-10 µm size range along with the ambient meteorological data (e.g. wind speed and direction). These secondary data were analysed using the openair package in R, including bivariate concentration polar plots and k-means clustering techniques. In addition, the polar concentration roses and the k-means cluster analysis were applied together to a pair of monitoring stations across the construction sites (i.e. one in downwind and the other in upwind) to estimate the contribution of construction sources to the measured concentrations. Moreover, the net concentrations from the

construction activities were then used to draw decay profiles of the PM emissions against distances. The results of these investigations are presented in Chapter 6.

1.3.4 Exposure to particles from outdoor building demolition activities

The final part of this thesis investigates the release of PM_{10}, $PM_{2.5}$ and PM_1 around a building demolition site in order to fill the existing research gaps in the literature. The measurements were carried out at (i) a fixed-site downwind of a demolished building; (ii) around the site during a demolition operation, through mobile monitoring; (iii) different distances away from the demolition site through sequential monitoring (10, 20, 40 and 80 m); and (iv) inside an excavator vehicle cabin and on-site temporary office for engineers and managers. A GRIMM particle spectrometer was used to measure the mass concentration and distribution of particles. A weather station (Kestrel 4500) was used to measure meteorological data (relative humidity and ambient temperature) every 10s at the measurement site. Furthermore, the position of the PM instrument was continuously recorded using a Global Positioning System during mobile measurements. The main objectives of this study were to investigate the quantities of produced particles, their physicochemical properties, and their potential effect on workers and the surrounding areas. The results were analysed using openair package in R and map source software (ArcGIS) to evaluate spatial variation of PMCs upwind and downwind of the demolition site. In addition, a modified box model was developed to determine the emission factors. The SEM and an energy-dispersive X-ray spectroscopy (EDS) were used to assess the morphology and chemical composition of particles such as their shape, structure and chemical composition. These results are presented in Chapter 7.

1.4 Thesis outline

This thesis consists of eight chapters, as presented in Figure 1.1. Chapter 1 discusses the importance and motivation behind this research, introduces the objectives, and sets out the approaches taken to achieve those objectives.

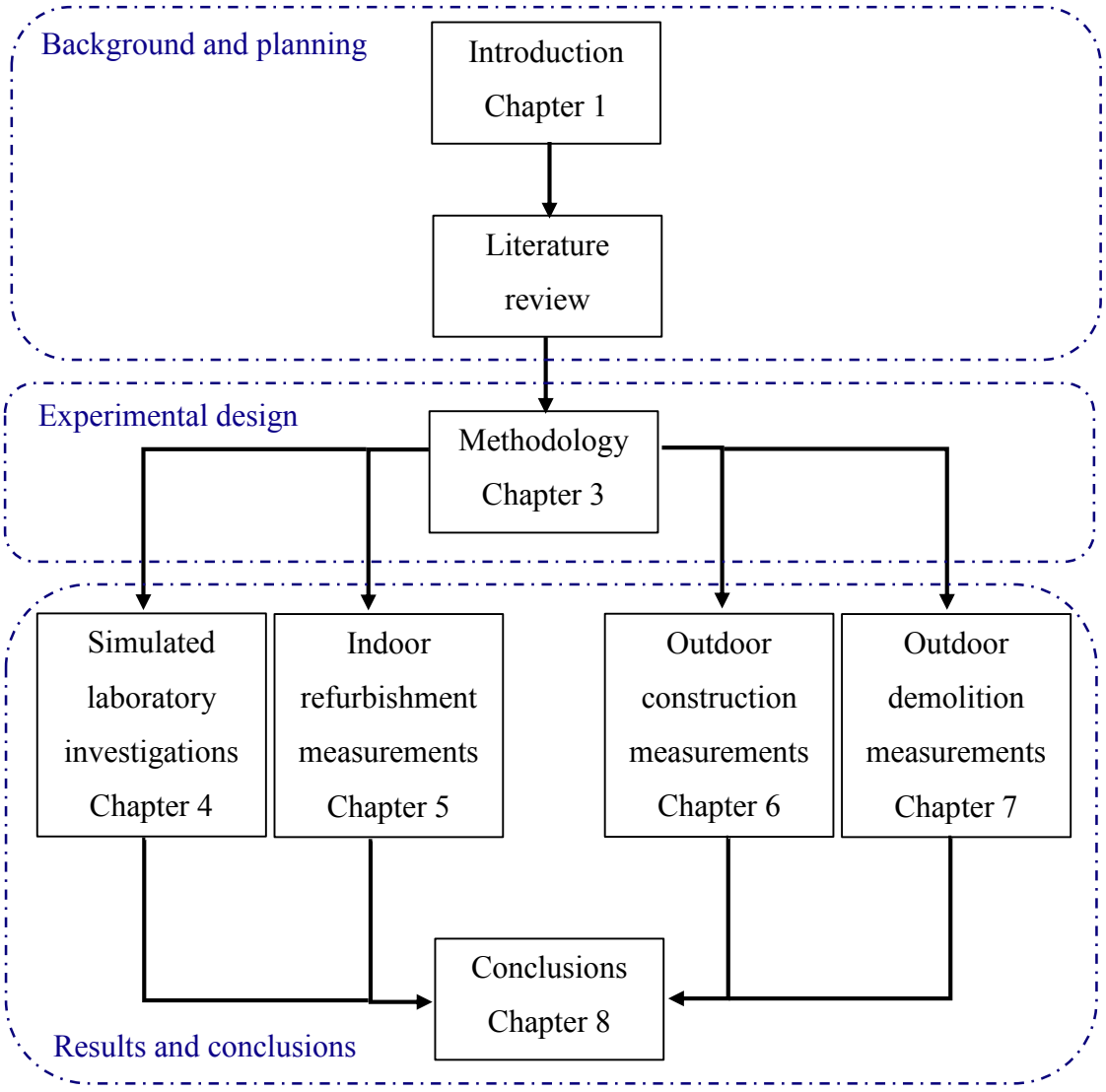

Figure 1.1: Report outline presenting the work breakdown structure for the main chapters.

Chapter 2 gives an introduction to the background concepts of this thesis and presents a review of the existing knowledge of airborne PM and ultrafine particles relating to the sources of the particles and their impacts on the environment and on human health.

Chapter 3 provides the methodologies and experimental set-up used in the experiments, as well as descriptions of the instruments used for measuring the particles and for performing physicochemical analysis, including SEM, EDS, XPS and IBA.

Chapter 4 presents the results gained from measurement of concrete mixing, drilling and cutting activities. This chapter also discuss the emission factors and occupational exposure doses.

Chapter 5 presents the results gained from the indoor building refurbishment activities. This chapter also discusses the emission characteristics of ultrafine particles and PM from these activities, and sets out a physiochemical analysis of the particles.

Chapter 6 presents the results gained form the assessment of the impact of PM_{10} and $PM_{2.5}$ arising from outdoor construction works on the surrounding environment in London.

Chapter 7 presents the results gained from the outdoor building demolition. This chapter also discusses quantities of produced particles, particle emission factors using a modified box model, the physicochemical features of particles, and their potential impact on workers and the surrounding areas.

Chapter 8 reviews the stated objectives of this research and presents a summary of the thesis, followed by an overall conclusion derived from the research. It offers suggestions for directions for future work.

Chapter 2. Background concepts and literature review

This chapter begins with the background, goes on to give an overview of PM and ultrafine particle emissions, and then provides a literature review related to the sources of these particles, including building and construction works. This chapter then presents a summary of the physicochemical characterisation and analysis of captured particles on the filters. Finally, the chapter presents a review of the existing knowledge of environmental and health impacts of PM and ultrafine particles.

2.1 General overview of PM and ultrafine particles

The air surrounding us contains a mixture of particles, commonly called particulate matter (PM), which is a complex mixture of organic and inorganic substances present in the atmosphere in either solid or liquid form (Heal et al., 2005). Ambient PM is a major source of air pollution and is known to have adverse impacts on human health (Kan et al., 2012). PM substances are divided into different sizes based on their aerodynamic diameter, including PM_{10} (≤10 μm), $PM_{2.5}$ (≤2.5 μm) and PM_1 (≤1μm). Aerodynamic diameter is defined as the diameter of a sphere with a standard density (i.e. 1000 kg m^{-3}; the density of a water droplet) that settles at the same terminal velocity as the particle of interest. Terminal velocity is the highest velocity reachable by an object as it falls through the air (DeCarlo et al., 2004). It occurs once particles experience a force, either due to gravity or due to

centrifugal motion, which will tend to move in a uniform manner in the direction exerted by that force. A diameter of a particle with irregular and non-spherical shape can be converted to an aerodynamic diameter using the Eq. (2.1) given by Hinds (1999):

$$da = dp\left(\frac{Pp}{Po.X}\right)^{1/2} \quad (2.1)$$

where d_a is the equivalent aerodynamic diameter, P_o is the standard particle density (1000 kg m^{-3}), X is dynamic shape factor, d_p is a particle diameter and P_p is the density of the particle. For example, the aerodynamic diameter for a quartz particle with a diameter of 18 µm and with a density of 2700 kg m^{-3} (Figure 2.1) can be calculated by using Eq. (2.1) as: $da = 18\left(\frac{2700}{1000\times1.36}\right)^{1/2}$ = 25.3 µm, where *X (=1.36)* is taken from Table 3.2 in Hinds (1999).

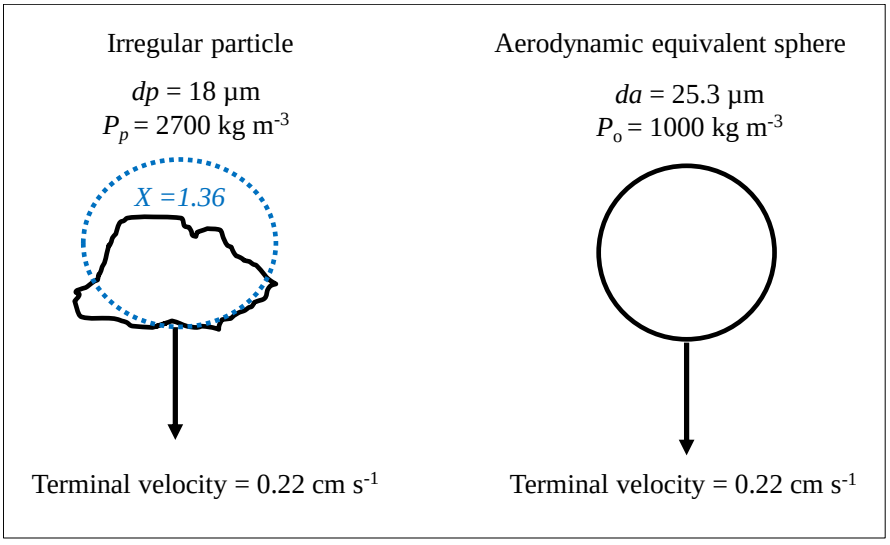

Figure 2.1: The aerodynamic equivalent diameter of an irregular and a spherical shaped particle (Hinds, 1999).

Particle mass concentration (PMC) is a common metric to measure the concentrations of PM_{10}, $PM_{2.5}$ and PM_1. On the other hand, particle number concentration (PNC) is a metric

to measure concentrations of ultrafine particles. These particles vary greatly in their ability to affect not only our health and quality of life, but also climate change and visibility (Hinds, 1999). The size of particles is important, as particles with different dimensions penetrate differently and smaller particles can move deeper into the respiratory system and as a result can potentially be the cause of serious negative health effects. In order to address the issues relating to these particles (PM and ultrafine particles), the subsequent sections discuss background information on particle size distribution (Section 2.2), particle mass and number concentrations (Section 2.3), sources of PM and ultrafine particles (Section 2.4), building activities and particle emissions (Section 2.5), physicochemical characteristics of particles (Section 2.6), health and environmental impacts of exposure to particles (Section 2.7) and regulations for PM and ultrafine particles (Section 2.8).

2.2 Particle size distribution, modes and fractions

Particle size is the most important parameter for characterising the behaviour of aerosols. The diameter of airborne particles (D_p) can vary from the nanometre size range (e.g. 1 nm) up to the micron scale (e.g. 10 μm) and beyond. Almost all properties of aerosols and also the nature of the laws governing their properties, depend on particle size (Hinds, 1999). There are three major factors influencing particle size: (i) the origin of the materials; (ii) the source of their emissions; and (iii) the processes of their formation (Morawska et al., 2008). Particle size range influences particle chemical and physical properties, health and environmental effects, and atmospheric lifetime (Buseck and Posfai, 1999). There are no standard terms used to represent particle size range specific to each particle mode, and so the terminology varies in the literature. Figure 2.2 shows the typical particle size

distribution in the urban environment, showing the nucleation (typically defined as particles <30 nm), accumulation (between 30-300) and coarse modes (over 300 nm) (ICRP, 1994; Kittelson 1998; Kumar et al., 2010). The nucleation mode particles are generally formed by gas-to-particle conversion due to the rapid cooling and dilution of emitted gaseous compounds in the atmosphere. Because of their high number concentration, especially near their source (e.g. roads), these small particles coagulate quickly with each other due to irregular wiggling and random Brownian motion in the air. Nucleation particles have relatively short lifetime in the atmosphere. Moreover, nucleation particles may cause the formation of cloud droplets and may subsequently be removed from the atmosphere by droplets of rain (Kumar et al., 2010; Hinds, 1999).

The accumulation mode consists primarily of combustion particles emitted directly into the atmosphere and also formed through the coagulation of the particles in the nucleation mode. For example, photochemical reactions of volatile organic and oxides of nitrogen formed the particles in the accumulation mode in the presence of strong sunlight. The particles in the accumulation mode can be removed from the atmosphere by washout or rainout, however, they coagulate very slowly to reach the coarse mode. The particles in accumulation mode account for most of the visibility effects of atmospheric aerosols and contains the wavelength of visual light.

The particles in coarse mode consist of large salt particles from sea spray, windblown dust and mechanically generated anthropogenic particles such as those from agriculture, construction and mining activities (Seinfeld and Pandis, 2006). Because of their large size, the coarse particles are affected by gravity and readily settle out or deposit on the available

surfaces, so their lifetime in the atmosphere could range from a few hours to days or weeks. Furthermore, meteorological variables such as wind speed can affect the lifetime of the suspended particles in the atmosphere. For instance, low wind speed reduces the concentration of windblown dust and soil particles while the high wind speed does the opposite (Hinds, 1999; Seinfeld and Pandis, 2006). It is worth noting that the definition of these particle size modes would change when referred to mass distribution. In any size range, the concentration of particles is related to the curve area in that range. As seen in Figure 2.3, the particle number distribution (PND) is often expressed in the form of the logarithmic function of the particle diameter dN/dlog*Dp* or the number of particles per cm^3 of air that have diameters in the size range from log (*Dp* + d*Dp*) (Kumar, 2009; Seinfeld and Pandis, 2006). The same plot can be generated for particle distribution on the basis of mass, surface area or volume (Kumar, 2009).

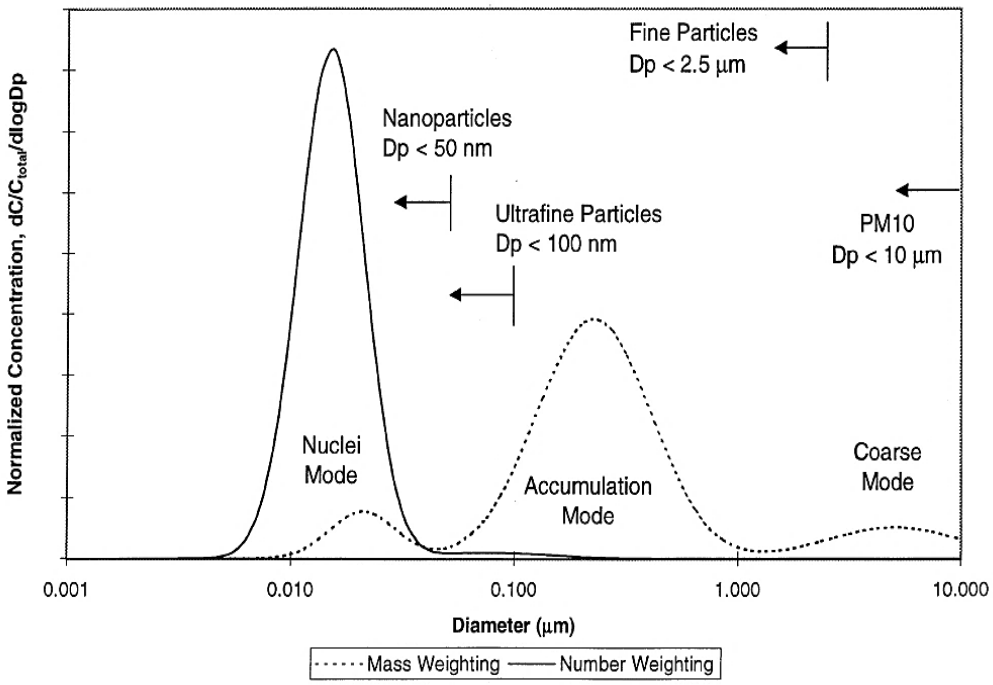

Figure 2.2: Typical particle size distribution by number and mass weightings showing different size modes (Kittelson, 1998).

2.3 Particle mass and number concentrations

Several epidemiological and toxicological evidences indicate that PMC is one of the most significant metrics and most commonly measured aerosol property to evaluate particle effects on human health and the environment (Brunekreef and Forsberg, 2005; Hinds, 1999). As described in Section 2.1, another common measure of concentration is number concentration, which determines the number of particles per unit volume of aerosols. PNCs in urban areas are dominated by particles in the nanometre range, though their mass is negligible in comparison with larger particles (Buseck and Adachi, 2008; Kumar et al., 2012b, 2013b).

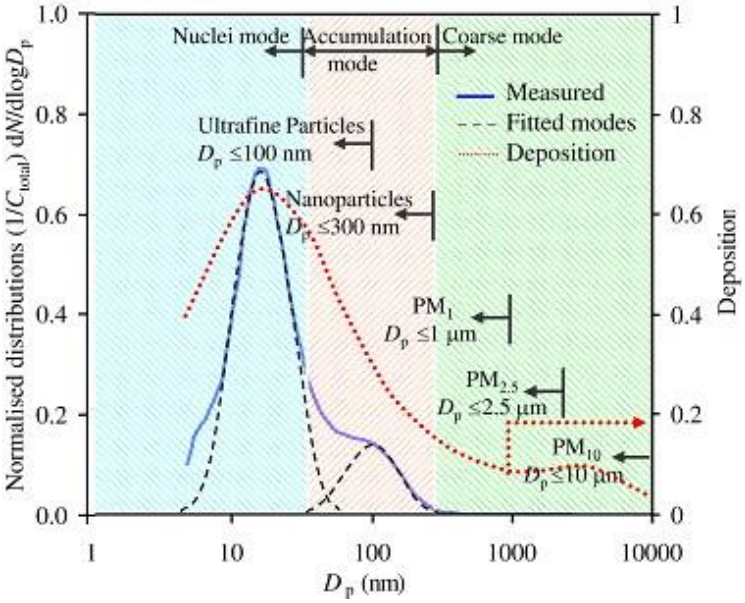

Figure 2.3: Typical example of ambient PNDs in a Cambridge street canyon (Kumar et al., 2010b). It is worth noting that nanoparticles are referred to a size range (<300 nm) which represent majority (>99%) of the total PNCs in the ambient urban environments.

Compared with coarse particles, ultrafine particles provide a larger surface area in total for absorbing harmful organic chemicals and penetrating deeper into the lungs (Donaldson et al., 2005; Oberdorster, 2000). A few studies have also speculated that the number of

particles may play a more important role than mass-based particle metrics, in causing adverse health effects and air pollution (Hartog et al., 2005; Knibbs, 2011).

2.4 Sources of PM and ultrafine particle emissions in the urban environment

PM types in the atmosphere originate from natural (e.g. rock debris, salt particles from sea spray, gas-to-particle conservation, soil and volcanic dust, photochemical sources) and anthropogenic sources (e.g. power plants, building works and construction, road dust and vehicular emissions, agriculture, wood burning) (Hinds, 1999).

PM_{10} particles in urban areas arise primarily from anthropogenic sources such as vehicular traffic and energy consumption (Hinds, 1999; Kittelson et al., 2004). For example, the main emission sources of PM_{10} in the typical urban EU environment are shown in Figure 2.4 (EEA, 2008). As noted in Section 2.1, PM_{10} concentrations are mainly affected by the emissions arising from local fugitive sources, such as vehicle exhaust due to fuel combustion, mostly because of ash particles formation through vaporisation and the subsequent condensation of inorganic matter present in the fuel during combustion (Cadle et al., 1999; Kean et al., 2000; Perez et al., 2010), non-vehicle exhaust sources (Chow et al., 2006; Hopke et al., 1980; Saliba et al., 2010), residential heating by wood and coal combustion (Junninen et al., 2009), road works and re-suspension of dust (Amato et al., 2009; Fuller et al., 2002; Fuller and Green, 2004; Tian et al., 2007; Woskie et al., 2002), emissions arising from industrial sources such as waste transfer stations and marble processing (Barratt and Fuller, 2014; Diapouli et al., 2013; Jaecker-Voirol and Pelt, 2000; Toledo et al., 2008) and activities related to air and sea transportation (Andrews et al., 2010; Corbett et al., 2007).

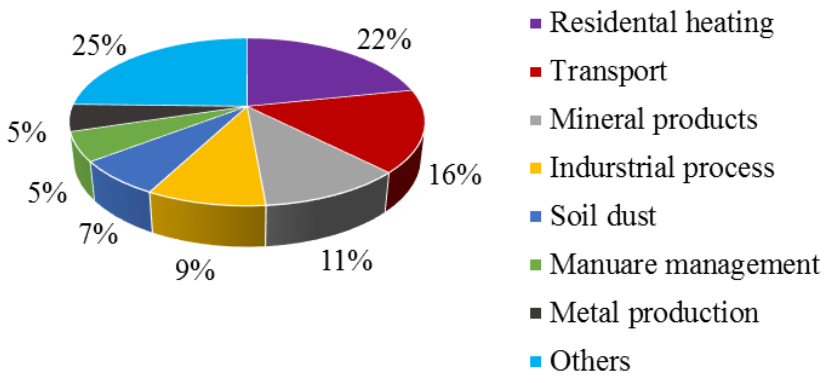

Figure 2.4: Emission sources of PM_{10} (Gg per year) in EU urban locations; adapted from EEA (2008). Others sources represented in this figure refer to agriculture, construction and secondary sources.

$PM_{2.5}$ particles in typical urban backgrounds mainly arise from vehicular sources due to incomplete combustion of fossil fuels and biomass because of the formation of fine ash particles during the process (Abu-Allaban et al., 2007; Dall'Osto et al., 2011; Pey et al., 2009), as well as the secondary gas-to-particle conversion processes that occur due to the condensation of vapours originating from lubricating oil (i.e. nitrates, sulphate and organic compounds) and unburned fuel in the atmosphere that take place after rapid cooling and dilution (Claeys et al., 2004; Heal et al., 2012). For instance, Figure 2.5 shows the important sources of $PM_{2.5}$ in EU urban locations which make significant contribution to $PM_{2.5}$ (EEA, 2008). In addition to secondary gas-to-particle formation and vehicular sources, $PM_{2.5}$ in the urban environment arises from non-vehicle exhaust sources (Cao et al., 2014), industrial sources (Rodriiguez et al., 2004), residential heating by wood and coal combustion (Ward and Smith, 2005), road works and re-suspension of dust (Ho et al., 2003) and measurements related to Saharan dust and ship emissions (Alastuey et al., 2005; Bates et al., 2008).

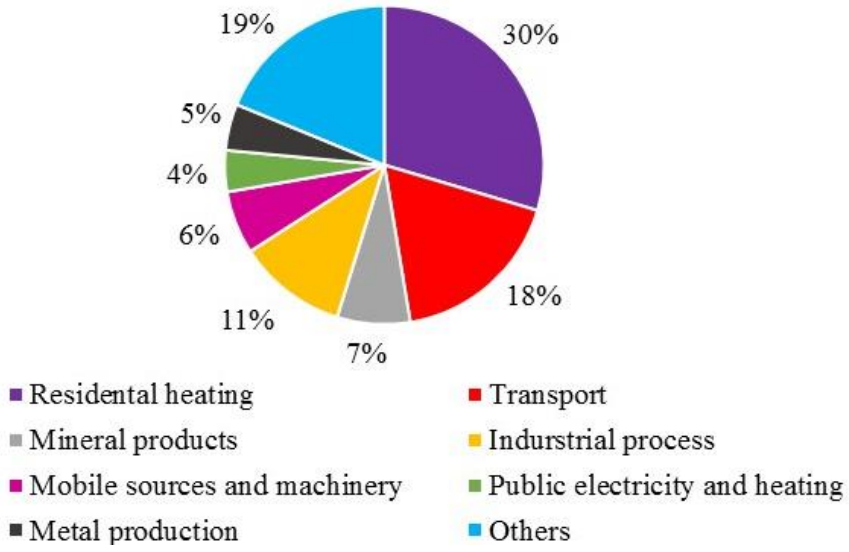

Figure 2.5: Emission source of ambient $PM_{2.5}$ (Gg per year) in EU urban locations; adapted from EEA (2008). Other sources in this figure refer to agriculture, construction and secondary sources.

Particles in the PM_1 size range are mainly produced from the process of gas-to-particle conversion, similar to the $PM_{2.5}$ production process. PM_1 concentration in the urban environmental is considerably affected by vehicular sources mainly through fuel combustion (Cheng et al., 2011) which is another important source of PM_1 emissions, non-vehicular emissions (Caggiano et al., 2010), soil dust (Labban et al., 2004), also industrial sources, such as the production of carbon black (Kuhlbusch et al., 2004) and coal combustion (Chen et al., 2011).

Ultrafine particles can also be generated in significant quantities in cities from vehicular sources (Charron and Harrison, 2003; Goel and Kumar, 2014; Kumar et al., 2010, 2011c). There are also other important sources of ultrafine particle emissions such as secondary particle formation, which may occur wherever the condensation of photochemically formed low volatility vapours leads to condensational growth, and sulphuric-acid induced

nucleation (Kumar et al., 2014), non-vehicular sources (Kumar et al., 2013b; Voliotis et al., 2014), ship emissions from ports (Saxe and Larsen, 2004), take-off and landing emissions from aircraft at airports (Hu et al., 2009), domestic biomass burning (Hosseini et al., 2010) and forest fires by wood burning (Reid et al., 2005).

2.5 Particle emissions from building activities

In many urban areas, fugitive dust from building construction, demolition, and road sources are important producer of PM and ultrafine particles. Particle emissions can occur during any stage of works, such as preparation of the land, land cleaning, earth moving and concreting. These emissions can differ significantly from day to day depending on the type of each activity, the level of activity, and the ambient meteorological conditions such as wind speed and direction (Cheng et al., 2010; Unal et al., 2011). Building-related sources of the PM_{10}, $PM_{2.5}$, PM_1 and ultrafine particles are discussed further in Sections 2.5.1 and 2.5.2. As mentioned in Section 2.4, there are a number of studies of PMCs of ambient PM_{10} and $PM_{2.5}$ in urban areas, but fewer studies have focused on the PM_1 fractions (Ragheb, 2011), with even less information relating to ultrafine particles released from building activities (Kumar et al., 2013b). This thesis investigates building-related works such as concrete mixing, drilling and cutting (Chapter 4), refurbishment (Chapter 5), construction (Chapter 6) and demolition (Chapter 7).

2.5.1 Importance of particle emissions from building activities

There may be greater understanding of PM_{10}, $PM_{2.5}$, PM_1 and ultrafine particles from construction and demolition sources in the future due to the development of sustainable urban infrastructures and growth in the world population, highlighting a need

for new construction, demolition, refurbishment or renovation of existing buildings (Kousa et al., 2002a; Balaras et al., 2007). Concerns associated with the by-products from construction and demolition sources, quantities of produced PM_{10}, $PM_{2.5}$, PM_1 and ultrafine particles, emission rates and occupational exposure to those particles, particularly ultrafine particles, are yet to be addressed. The contributions from these sources might be more localised and less studied compared with vehicular and industrial sources, but the combined contributions from building and construction sources could be comparatively large, particularly in close proximity to such sources (Kumar and Morawska, 2014). Furthermore, the physicochemical features of coarse, fine and ultrafine particles generated by building-related works may differ from those particles originating from other sources (e.g. vehicular, industrial sources), due to likely differences in the formation mechanisms, and this could have different health and environmental effects (Kumar et al., 2012a; Viana et al., 2008).

There are presently a limited number of legal thresholds and regulations governing PM_{10} and $PM_{2.5}$ (e.g. EU, USEPA, WHO), controlling the exposure of the public to airborne particle concentrations in the urban environment. The regulations and limits for PM_{10} and $PM_{2.5}$ particles that do exist are discussed further in Section 2.8. Furthermore, there are no guidelines or standards relating to the number concentrations of ultrafine particles, for numerous reasons, including the limited amount of published information, the lack of standardisation for sampling and measurement, and a lack of clear epidemiological evidence (Kumar et al., 2011c).

2.5.2 Building-related sources of PM and ultrafine particle emissions

This section focuses on PM_{10}, $PM_{2.5}$, PM_1 and ultrafine particle emissions from various building activities. A summary of relevant studies is provided in Table 2.1 and the subsequent text briefly discusses some of these key articles.

Table 2.1: Summary of past studies showing measured particle number and mass concentrations from various building activities.

PM Type	Activity type	Where	Source
PM_{10}	Sawing (cutting carbon nanofibre composite)	Indoor (National Institute for Occupational Safety and Health, USA)	Mazzuckelli et al. (2007)
PNC	Drilling of silica based nanocomposites	Indoor (Tarnamid T30, Azoty Tarnow, Poland)	Sachse et al. (2012)
PM_1	Building demolition	Outdoor (Demolition of an old four-story building on the premises of the university hospital of Essen, Germany)	Hansen et al. (2008)
PM_{10}	Construction activities	Outdoor (Construction and operational activities a port in Mumbai, India)	Joseph et al. (2009)
PM_{10} and $PM_{2.5}$	Earthmoving activities	Outdoor (Earth moving activities conducted at the two Kansas sites, Kansas city, USA)	Muleski et al. (2005)
PM_{10} and $PM_{2.5}$	Earthmoving activities	Outdoor (Road widening and related construction works in London, UK)	Font et al. (2014)
PM_{10}	Building implosion	Outdoor (22-story building in East Baltimore, USA)	Beck et al. (2003)
PM_{10}	Building demolition	Outdoor (Three public housing developments in Chicago, USA)	Dorevitch et al. (2006)
PM_{10}	Interaction between tyres and road pavement	Indoor (Road simulator, Swedish National Transport Research Institute, Linköping)	Gustafsson et al. (2008)
PM_{10}	Building and road works	Outdoor (At over 80 monitoring sites in and around London, UK)	Fuller and Green (2004)
$PM_{2.5}$ and PNC	Indoor sources (e.g. floor sweeping)	Indoor (Residential suburb in Brisbane, Australia)	He et al. (2004)
PM_{10}	Concrete grinding	Indoor (Laboratory simulation, Ohio, USA)	Akbar-Khanzadeh et al. (2007)

Concrete drilling, crushing and cutting are common activities both at construction sites and within domestic situations, and have the potential to generate significant airborne dust (Cook Jr and Harris, 1992; Kumar et al., 2012c). This is probably due to the higher rotational frequency, shear stresses and local energy density associated with drilling, crushing and cutting activities. Some studies have focused on PM_{10} (Akbar-Khanzadeh and Brillhart, 2002) and $PM_{2.5}$ (Flower and Sanjayan, 2007) and ultrafine particles (Kumar et al., 2012c) created during concrete grinding, manufacturing and crushing activities, respectively. For example, Kumar et al. (2012c) investigated the emission of ultrafine particles by simulating building activities, such as crushing concrete blocks in the laboratory environment and found notable quantities of ultrafine particles ($2.27\pm0.41 \times 10^4$ cm^{-3}) compared to the background level ($1.40\pm0.40 \times 10^4$ cm^{-3}). Despite the fact that such activities are undertaken on a daily basis around the world, surprisingly little is known about the associated exposure levels and physicochemical features of the particles produced (Broekhuizen et al., 2011). Further literature reviews on concrete mixing, drilling and cutting are provided in Chapter 4.

Building refurbishment or renovation typically includes bringing older buildings up to modern standards for improving lighting, heating and energy efficiency, as well as upgrading outdated buildings (Mickaityte et al., 2008; Sunikka and Boon, 2003). Activities related to building refurbishment have already grown in number in most European countries over the last 20 years (Kohler and Hassler, 2002), due to the increase in the rate of population growth within urban areas (Egbu, 1999). Refurbishment activities can have an associated carbon footprint of the order of 20% of the emissions that arose from the

original construction (Pacca and Horvath, 2002). However, the contribution of the building refurbishment activities to PM_{10}, $PM_{2.5}$, PM_1 and ultrafine particles and also the extent of the pollution caused due to refurbishment activities is still unknown. Further literature reviews on building refurbishment works are presented in Chapter 5.

Construction works involve the processes of building a structure or a facility in ways known to result in incremental increase of PM_{10} local concentrations, which may contain a wide variety of toxic and harmful substances and may adversely impact the health of nearby residents (Anderson, 2009; Davila et al., 2006; Heal et al., 2012; Loomis, 2000). These increments in PM_{10} concentration are typically thought to be due to construction activities including the resuspension of dust from any on-site vehicles at the construction sites. There are a few studies concerned with emissions of PM_{10} arising from outdoor construction works (Fuller and Green, 2004; Joseph et al., 2009; Font et al., 2014), but there is still very little work focusing on the fractions of $PM_{2.5}$ produced from construction activities (Muleski et al., 2005). For example, Fuller and Green (2004) studied the emission of PM_{10} particles generated by construction works in London, UK. It was found that the PM_{10} concentrations breached the 24-h mean EU limit (50 $\mu g\ m^{-3}$) for PM_{10} concentrations on numerous occasions at 25% of the monitoring stations. Further details of the literature on construction activities are provided in Chapter 6.

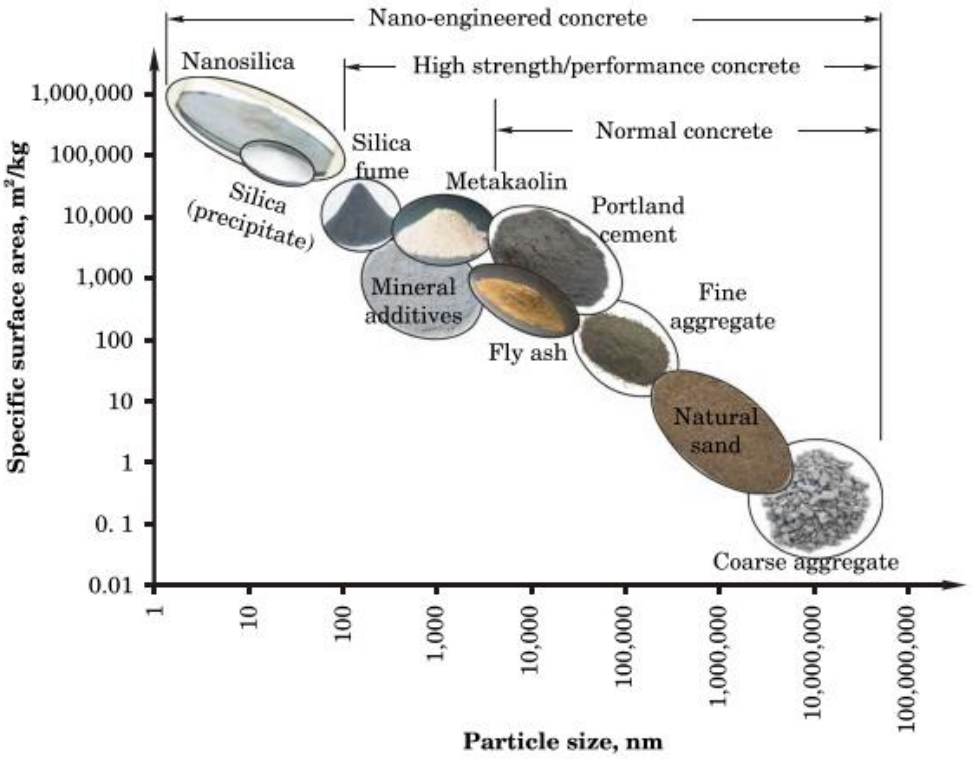

Figure 2.6: Particle size and specific surface area of concrete materials; taken from Kumar et al. (2012a).

As mentioned in Section 2.5, concrete is one of the most extensively used building materials in the construction industry, manufactured with Portland cement clinker and other binders (Kumar et al., 2012a). The increasing use of engineered nanoparticles (ENP) in construction materials, as well as in industrial and household applications, will very likely lead to the release of such materials into the environment (Nowack and Bucheli, 2007). For instance, combing nano-silica, carbon nanotubes, Fe_2O_3, SiO_2, Al_2O_3, TiO_2, etc. within concrete mixes improves workability, durability and compressive strength of concrete (Kumar et al., 2012b; Li, 2004; Rana et al., 2009; Shekari and Razzaghi, 2011), and leads to considerable changes in both surface morphology and surface energy, altering the basic features of nanomaterials (Figure 2.6). Some studies have measured the emissions of these

nano-sized particles through different generation methods (Tsai et al., 2012; Tsai et al., 2009) and a number of other studies have investigated exposure to them during handling and bagging processes at workplaces (Fujitani et al., 2008; Brouwer, 2010; Tsai et al., 2011).

Building demolition is the tearing-down of buildings and other structures, which involves taking a building apart while carefully preserving valuable elements for re-use. Each year, the number of buildings demolished is expected to growth by 4-time by 2016 in the UK from the levels of about 20,000 per year in 2008 (ECI, 2005; Roberts, 2008), in order to meet new building technology and urban design guidelines (Balaras et al., 2007; Kumar et al., 2015). Demolition and construction waste contribute about 33% of the total waste from all sectors, which about half of it is demolition waste (Balaras et al., 2007). Building demolition can be accomplished either mechanically or through implosion. Particles are then produced during the breaking up and demolition of building materials such as concrete slabs, iron beams, brick walls and also the shifting of the waste building material from the site that may lead to resuspension and further generation of particles. Demolition by both mechanical disruption (Dorevitch et al., 2006) and implosion (Beck et al., 2003) has the potential to produce significant amounts of PM_{10}, but still much less is known about $PM_{2.5}$ and PM_1, and also the impact of building demolition on the air quality of the surrounding areas (Beck et al., 2003). Further review of the literature on building works are presented in Chapter 7.

Recycling of construction waste is one of the effective ways to manage the related environmental problems, and also helps to save the limited space available of landfill

(Nakamura and Kondo, 2002). The enormous amount of construction and demolition waste produced reached a level where warnings about use were made. Among various types of materials, concrete waste accounts for about 50% of the total construction and demolition waste generated (Tam, 2008). After concrete structures are demolished or renovated, concrete recycling is an increasingly common method of utilising the rubble and remaining aggregates (Dosho, 2007; Rao et al., 2007). Aggregate recycling of concrete waste is a cost-effective method which can help the environment. However, there are a limited number of studies concerned with the exposure to particles generated by concrete recycling and the associated risks to the workers at recycling sites. For example, Kumar and Morawska (2014) investigated the exposure to ultrafine particles by simulating a concrete recycling activity and found significant exposure rate to be 24.83×10^{8} min^{-1} during measurements close to the source.

Earthworks cover the processes of soil-stripping, ground-levelling, excavation and landscaping. Common earthworks take place in roads, railway beds, causeways, dams, levees, canals, and berms (Smith et al., 2000). For example, Muleski et al. (2005) measured PM_{10} during the earth moving, track loading and track out works in Kansas, USA. Average PM_{10} emission factors were reported for earthmoving works (~0.41 kg veh^{-1} km^{-1}), track loading (~0.06 kg mg^{-1}) and track out works (~0.006 kg veh^{-1}), respectively. Track out is the transporting of dust and materials waste from the construction site onto the public road network, where it can be deposited and then re-suspended by vehicles using the network. This activity can take place when lorries leave the construction or demolition site with dusty materials which may then spill onto the road (Muleski et al., 2005). There are also a

number of studies concerned with PM_{10} and $PM_{2.5}$ emissions arising from road works (Fuller et al., 2002; Fuller and Green, 2004).

Welding is a common construction activity used to join metals (or other materials like PVC pipes) by causing fusion. During welding works, complex mixtures of aerosols and gasses are generated when a metal is heated above its boiling point and its vapours condense into solid particles. Despite improvements in control technologies, welding workers are yet exposed to welding fumes and gasses (Plog and Quinlan, 2002). For example, Buonanno et al. (2011) reported findings on the variation of PM_1 emissions produced during welding activities in automotive plants. High concentrations of PM_1 were observed at close distances to welding activities and the PM_1 emission rate was found to be 2.80×10^{15} min^{-1} close to the sources.

2.6 Physiochemical characteristics of particles

A general overview of applying different physicochemical analysis and techniques is presented in this section. Several studies have analysed the composition of particles derived from building sources and a number of attempts have been made to relate the observed elemental concentrations in collected particle samples to construction and demolition activities (Beck et al., 2003; Lioy et al., 2002; Mouzourides et al., 2015; Pattanaik et al., 2012). Understanding the chemical constituents, morphology (i.e. size, shape) and surface properties of particles released from building works is important for determining their toxicity and health effects (Lo et al., 2000; Senlin et al., 2008), which are currently poorly understood. A summary of relevant studies on physicochemical analysis is provided in Table 2.2.

Table 2.2: Summary of physicochemical analysis of particles collected during number of building-related activities.

Activity type	Technique used	Description	Source
Building destruction	SEM-EDS	It was found that the majority of particles were composed of building-related materials such as Ca, Si and S	McGee et al. (2003)
Building implosion	XRF	The elemental composition of particles collected in samples was dominated by Ca, Si, Al and Fe	Beck et al. (2003)
Building destruction	TEM/SEM-EDS	Elements such as Si (dominant), Ca, S, Zn, Al and Mg were found in collected samples	Lioy et al. (2002b)
Welding	TEM/SEM-EDS	Fe (dominant), Mn, S, K and Ca were found during analysis of welding fume particles	Jenkins and Eagar (2005)
Welding	TEM-PIXE	Elements such as Fe (dominant), Mn, Ni, and Cr were found during analysis of welding fume particles	Isaxon et al. (2009)
Drilling	TEM/SEM-EDS	The elemental composition was dominated by Zn, Si, Al and Fe via analysis of collected particles	Bello et al. (2010)
Grinding	SEM-EDS and ICP-MS	The presence of elements such as Fe, Cr, Mn, Si and Ni were found in samples collected during grinding activity	Iavicoli et al. (2013)

2.6.1 Scanning electron microscopy (SEM)

A SEM is a type of electron microscope that produces images of a sample by scanning it with a focused beam of electrons. Various signals are produced due to the interaction between the electrons and atoms that can be detected, and which contain information about an examined sample's surface composition and topography. A very fine probe of electrons with energies from a few hundred eV to tens of KeV is focused at the surface of the specimen and scanned across it in a raster or pattern of parallel lines. Signals

are amplified and used to vary the brightness of the trace on a cathode ray tube being scanned in synchrony with the probe. There is thus a direct positional correspondence between the electron beam scanning across the specimen and the fluorescent image on the cathode ray tube.

Mass measurements can now be carried out regularly on a wide range of molecular structures utilising elastically scattered electrons (Engel and Colliex, 1993). Recent progress in the acquisition and analysis of electron energy-loss spectroscopy data indicates that the scanning transmission electron microscope is an efficient tool for mapping the chemical composition of a biological sample. A few studies have utilised SEM for examining the solid-phase of metals and metalloids in house dust (Walker et al., 2011), determining the specific sources of lead in both household dust (Hunt et al., 1992) and the laser cleaning of building stones (Potgieter-Vermaak et al., 2005). Scanning electron microscopy together with focused ion beam milling (FIB-SEM) has been used to investigate the composition of atmospheric particles (Conny, 2013).

2.6.2 Energy-dispersive X-ray spectroscopy (EDS)

There are also techniques such as SEM for analysing morphology and the energy dispersive X-ray spectroscopy technique (EDS) to find elemental composition, which are used by numerous environmental studies (Kupiainen et al., 2003; Mouzourides et al., 2015; Paoletti et al., 2002). For example, Mouzourides et al. (2015) assessed the characteristics of bulk PM samples collected on polytetrafluoroethylene (PTFE) filters at an urban air pollution monitoring station in Nicosia (Cyprus) using SEM and EDS techniques. The results showed the presence of elements such as calcium (Ca), nitrogen (N) and lead (Pb)

in the samples. Likewise, Paoletti et al. (2002) studied the physicochemical characteristics and composition of particles in an urban area of Rome (Italy). They observed that elements such as carbon (C) and nitrogen (N) mainly originated from vehicular sources. McGee et al. (2003) also used SEM/EDS analysis to analyse the particles collected during the destruction of the World Trade Centre that caused the release of high levels of PM into the local environment in New York (USA). It was found that the majority of particles were composed of building related materials such as calcium (Ca), silicon (Si) and sulphur (S) (McGee et al., 2003). Currently, only a limited number of studies have reported physicochemical properties of particles released from building sources and therefore this is taken up for investigation in this thesis.

2.6.3 Ion Beam Analysis (IBA)

The conjunction of Particle Induced X-ray Emission (PIXE) and Elastic Backscattering Spectrometry (EBS) techniques represent powerful tools for measuring the elemental composition of fine atmospheric particles sampled on filters, as have been applied by Saitoh et al. (2003) during chemical characterisation of PM_{10} and $PM_{2.5}$ in diesel exhaust particles at the National Traffic Safety and Environment Laboratory in Tokyo (Japan). The major components of PM_{10} and $PM_{2.5}$ were found to be sodium (Na), silicon (Si), magnesium (Mg), chlorine (Cl), sulphur (S), iron (Fe), calcium (Ca) and zinc (Zn) as a result of the analysis. Similarly, Kothai et al. (2009) analysed the elemental composition of atmospheric PM at Vashi in Mumbai (India) and found the presence of components such as copper (Cu), chromium (Cr) and manganese (Mn) during the PIXE analysis, suggesting that they originated from anthropogenic sources. Despite these studies there remains a

considerable research gap with respect to the presence of elements such as arsenic (As), cadmium (Cd), chromium (Cr), lead (Pb), nickel (Ni), manganese (Mn) and zinc (Zn) within the particles arising from building activities.

2.6.4 X-ray Photoelectron Spectroscopy (XPS)

XPS is the most widely used surface analysis technique due to its relative simplicity of use and the ease of data interpretation. XPS has been demonstrated to be a powerful technique for examining the surface characteristics of various materials. XPS can perform elemental analysis for essentially the entire periodic table. The technique is surface-sensitive because the electrons whose energies are analysed arise from a depth of no greater than about 2-5 nm (He et al., 2007). Those electrons which are photo-excited, and which escape without loss of energy contribute to the characteristic peaks in the spectrum; those which suffer inelastic scattering and suffer energy loss contribute to the background of the spectrum. After a photoelectron has been emitted, the ionised atom must relax in some way. This can be achieved by the emission of an X-ray photon. The other option is the ejection of an electron as an Auger electron. Both types of relaxation are shown in Figure 2.7 (Watts, 1990). Several studies have been conducted using XPS to analyse the composition of particles derived from those sources which may contribute trace elements to urban aerosols and a number of attempts have been made to relate the observed elemental concentrations in collected aerosol samples to these sources (Adhami et al., 2012; Batonneau et al., 2004; Chen et al., 2000; Pattanaik et al., 2012; Roguala-Kozlowska et al., 2008). For example, Roguala-Kozlowska et al. (2008) studied the influence of vehicular traffic on the particle surface composition of PM_{10} and $PM_{2.5}$ in Zabrze (Poland) and found that the main components of the surface layer of these particles were carbon (C), nitrogen

(N) and oxygen (O). Batonneau et al. (2004) also analysed the particle composition of the generated PM_{10} within a 3-km zone of lead/zinc smelters in Noyelles-Godault (France) using XPS analysis. The results showed that lead (Pb) and zinc (Zn) were the main components of PM_{10}, and indicated that minor elements such as cadmium (Cd), mercury (Hg), and carbon (C) were more concentrated on the particle surface than in the bulk of PM_{10} generated by the smelting processes.

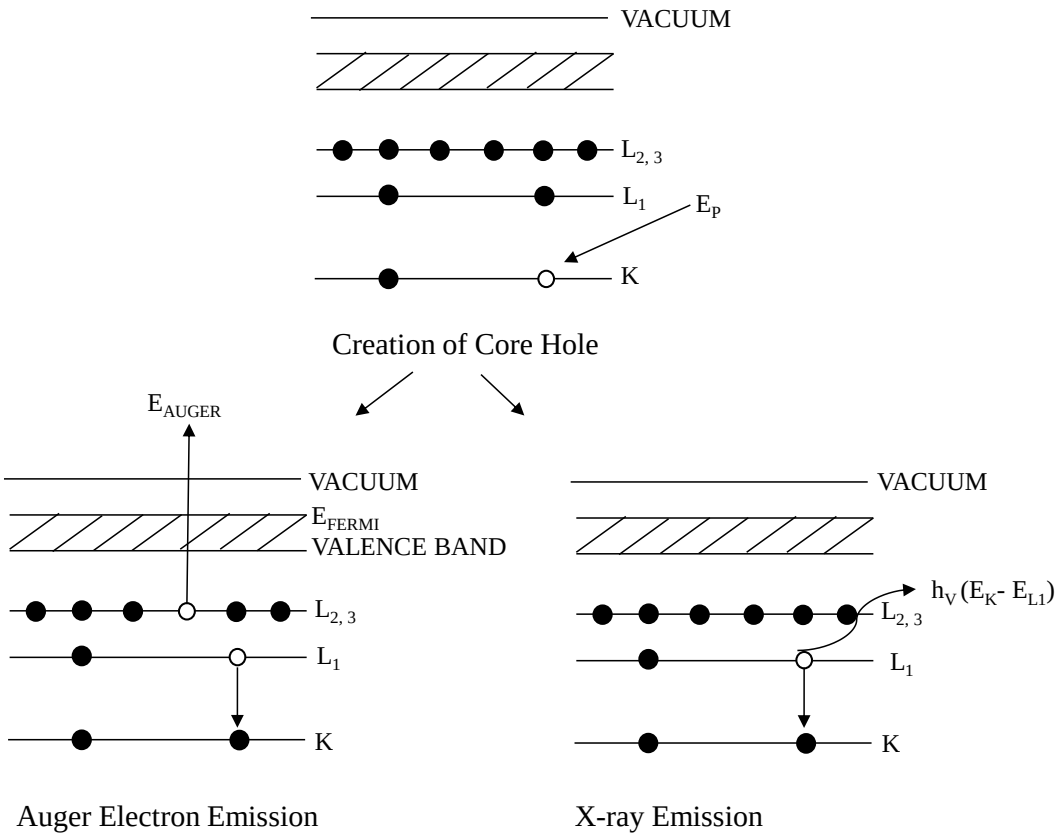

Figure 2.7: Relaxation of the ionized atom of Auger electron and X-ray electron emission (Watts, 1990).

2.7 Environmental and health impacts of exposure to atmospheric particles

The various activities associated with building works have the potential to produce considerable quantities of PM, including PM_{10}, $PM_{2.5}$, PM_1 and also ultrafine particles

(Kumar et al., 2012b, 2013b). These particles have serious environmental and health-related consequences because they may contain a variety of toxic organic and metallic compounds (Heal et al., 2012). Details about the impacts of exposure to PM_{10}, $PM_{2.5}$, PM_1 and also ultrafine particles on health, visibility and climate change are discussed in the following sections.

2.7.1 Health effects

PM_{10} in the urban environment is harmful since it can easily be introduced into the respiratory system (Davila et al., 2006), although $PM_{2.5}$ has been recognised as the 9th most powerful risk factor for disease globally (Lim et al., 2012). A number of epidemiological studies have shown that excess mortality comes from exposure to PM_{10} and $PM_{2.5}$ particles from sources such as road traffic and industry (Janssen et al., 2013; Kan et al., 2007; Namdeo and Bell, 2005). Furthermore, excessive inhalation of PM_{10} has been linked to a variety of respiratory diseases, such as lung cancer (Turner et al., 2011; Vineis et al., 2004) and asthma (Dorevitch et al., 2006; Eggleston et al., 1999). Also, a number of studies have linked excessive inhalation of $PM_{2.5}$ to renal (Spencer-Hwang et al., 2011; Weng et al., 2015) and cardiovascular diseases (Brook et al., 2010; Peng et al., 2008). There is also an increasing interest in the risks of PM_1 and ultrafine particles since these penetrate deeper into the lungs and are thought to be of greater concern for human health (Chaloulakou et al., 2003) as PM_{10} and $PM_{2.5}$ tend to penetrate into the gas exchange regions of the lung, but PM_1 and ultrafine particles can pass through the lungs to affect cells, tissues and organs of body. Number of studies have also confirmed the link between PM_1 exposure and morbidity (Pope and Dockery, 2006), and to several health issues such as cardiopulmonary (Zereini et al., 2012) and pulmonary diseases (Ostro et al., 2010). The smaller size of

ultrafine particles compared with PM_1 enables them to enter deeper into lungs, causing both acute and chronic adverse health effects such as asthma, and also cardiovascular and ischemic heart diseases (Goel and Kumar, 2014). However, the exact number of excess deaths and higher mortality rate due to exposure to ultrafine particles in the urban environment is yet unknown (Kumar et al., 2014).

Numerous studies have also reported the increased risk of death caused by PM_{10} and $PM_{2.5}$ due to ischemic heart disease among construction welders, plasterers and masons (Cavallari et al., 2007; Sjögren et al., 2002; Stern et al., 2001). PM_{10} and $PM_{2.5}$ have kinetic features, which mean they can be deposited in different internal parts of the body through the respiratory system and also can be translocated in the body through the circulatory system which supplies blood to the heart, liver and kidneys (Kampa and Castanas, 2008). Similar adverse health effects have even been observed among non-smoking workers at construction sites (Bergdahl et al., 2004; Verma et al., 2003), as well as depression problems among construction workers (Haynes and Savage, 2007). Some studies have shown that workers in construction and demolition industry dealing directly with cement and concrete materials are exposed to considerable PM_{10} and $PM_{2.5}$ emissions (Croteau et al., 2002; Flanagan et al., 2006) compared with those working in other industries such as the wood and metal industries (Fischer et al., 2005; Lim et al., 2010). Air pollution due to PM_{10}, $PM_{2.5}$, PM_1 and ultrafine particles from building activities can also adversely affect the health of people living close to the operation sites, particularly where measures to restrict and limit the amount of particles produced from the sites are insufficient (Kumar et al., 2012b). Hence, estimating the level of $PM_{2.5}$, PM_1 and ultrafine particles exposure

becomes even more important when such sites are situated within sensitive areas such as in the vicinity of hospitals and schools, or in densely built residential areas.

2.7.2 Visibility and climate change

There is sufficient evidence that building-related works such as earthmoving, building renovation and demolition considerably degrade the air quality of the surrounding environment (Beck et al., 2003; Font et al., 2014; Hansen et al., 2008; Joseph et al., 2009; Muleski et al., 2005). One of the most obvious indicators of air quality is visibility. Visibility is defined as the furthest distance in a given direction at daytime at which it is just possible to see and identify a prominent dark object against the skyline with the unaided eye (Tao et al., 2007). A number of studies have demonstrated that visibility is significantly influenced by the chemical composition, size and concentration of particles (Cheng and Tsai, 2000; Cheung et al., 2005). Nitrate and sulphate, which are generally formed at a considerably quicker rate in water droplets under high humidity conditions, are the main reasons for degraded the visibility (Mangelson et al., 1997; Tang and Munkelwitz, 1994). In rural regions of Europe, good visibility is usually considered to be 40-50 km, though anthropogenic works mainly account for reduction of visibility in urban areas (Horvath, 1995; Kim et al., 2001). Reduction in visibility is a result of processes such as light absorption by water vapor and scattering by aerosol particles such as PM_{10}, $PM_{2.5}$ and PM_1 (Majewski et al., 2014). Several studies have reviewed the impact of PM_{10} (Vajanapoom et al., 2001; Wan et al., 2012), $PM_{2.5}$ (Abby et al., 1994; Zhang et al., 2006) and PM_1 (Sabbagh-Kupelwieser et al., 2010; Shi et al., 2014) on decreasing visibility of the surrounding enviroment. For example, Wan et al. (2012) investigated the air quality impact of PM_{10} on atmospheric visibility in the Pearl River Delta (China) and found that visibility

was reduced to less than 8 km 22% of the time from 1998 to 2008, mainly due to PM_{10} emissions.

Climate change is a change in the statistical distribution of weather patterns and may refer to a change in average weather conditions, or a change in the time variation of weather based on longer-term average conditions. The effect of aerosols such as PM_{10} (D'amato et al., 2010), $PM_{2.5}$ (Tai et al., 2010), PM_1 (Vecchi et al., 2004), ultrafine particles (Feng et al., 2011) and greenhouse gasses (Meinshausen et al., 2009) is estimated through their global warming potential, which provides a measure of an aerosol's effect on global climate change relative to that of CO_2 for a given duration (Pearce et al., 1996). Generally, it is thought that aerosols change the radiative properties of the atmosphere and represent net negative radiative forcing, such as a cooling effect on climate and on the Earth's temperature. For example, PM_{10} particles may affect the earth's temperature by their effect on scattering the incoming solar radiation as they are bigger than the other particles in size with shorter lifetime in the air (Tiwari et al., 2009). $PM_{2.5}$ in the urban environment also mainly consists of black carbon, which is formed due to incomplete combustion of fossil fuels and biomass. $PM_{2.5}$ can stay in the atmosphere for several days or even weeks, which may cause a rise in the temperature of the Earth by absorbing sunlight and reducing albedo when deposited on snow (Lonati et al., 2007). PM_1 also affects the natural energy balance of the Earth, largely by reflecting and absorbing solar radiation, but also by influencing the reflective and absorbing features of clouds through condensation (Vecchi et al., 2004). However, the uncertainties relating to the direct effects of ultrafine particles on climate change remain significant and difficult to verify at the present time. However, in order to

control the rise in global temperature it is important to control the PM_{10}, $PM_{2.5}$, PM_1, ultrafine particles and greenhouse gas emissions, as greenhouse gasses have a much longer lifetime in the atmosphere (Coakley et al., 1983). Because of the above-mentioned health impacts and other problems such as acid rain, regulatory authorities must now more carefully control particulate emissions from building, vehicular and industrial sources, thereby leading to a rapid improvement in local air quality (Schopp et al., 1998).

2.8 Regulations, guidance and limits for PM and ultrafine particles

Environmental and health concerns associated with dust inhalation have led to a number of reduction and control initiatives of PM_{10}, $PM_{2.5}$, PM_1 and ultrafine particles in the construction and demolition industries. The UK Health and Safety Executive (HSE) has provided good practice guidelines to control and limit exposure to hazardous materials and substances at construction and demolition sites (HSE, 2006, 2011). Moreover, in the UK 'Best Practice Guidance' has been produced by London Councils at the local level, in partnership with the Greater London Authority which include a number of practical methods to control dust and emissions from construction and demolition works (Authority and Councils, 2006). In the US, the United States Environmental Protection Agency (USEPA) has provided guidelines on specific emission factors for different activities such as construction, demolition and mineral operations to control and limit PM emissions (EPA, 2011). These emission inventories are discussed further in Section 7.3.5. However, construction and demolition sites can be situated within very busy places, where meeting regulatory expectations and guidelines can often be challenging. Further details on the limit values of particles are provided in Table 2.3. Moreover, targets have been set by the

European Union Directive (1999) for year 2004 and 2010 to limit daily and annual mean values of PM_{10} at the European-wide level (Fuller and Green, 2004). For example, the limit by 2005 was to achieve a daily mean PM_{10} concentration of 50 µg m^{-3}, not to be exceeded on more than 35 occasions per year, and annual mean values of 40 µg m^{-3}. In addition, the target by 2010 was to achieve daily mean PM_{10} concentration of 50 µg m^{-3}, not to be exceeded on more than 7 occasions per year, and annual mean concentrations of 20 µg m^{-3}. However, the target values to be met by 2010 were not carried into Directive 2008/50/EC (Directive, 2008). Furthermore, a legal limit value for the three-year mean $PM_{2.5}$ concentration has been proposed by the EU, which cannot exceed of 25 µg m^{-3} by 2015 (Directive, 2008). In addition, World Health Organisation (WHO) guidelines (WHO, 2006) propose that the annual and daily mean concentrations of PM_{10} and $PM_{2.5}$, should not exceed (20 and 50 µg m^{-3}) and (10 and 25 µg m^{-3}), respectively. Table 2.3 presents the ambient PM standards enforced by the EU, USEPA, WHO, Japan and India. There are currently no national or international regulations or limits for controlling the release of PM_1 and ultrafine particles on buildings sites (Kumar et al., 2012c).

There are also number of studies available that quantify the level of exposure workers experience in workplace environments (e.g. coal- and gas-fired power plant workplaces) where PM_{10} (Stephenson et al., 2003), $PM_{2.5}$ (Kousa et al., 2002b), PM_1 (Hicks et al., 2012) and ultrafine particles (Methner et al., 2010) are produced. However, only limited guidelines, such as those produced by WHO and HSE, are available for controlling exposure to particles in workplaces. For example, the HSE recommended controlling exposure at source by carrying out all tasks, including packaging disposal, in a ducted fume

cupboard with a high efficiency particulate air filter (HEPA) and using another effective local exhaust ventilation, with a HEPA filter. In addition, HSE presented more recommendations by providing Control of Substances Hazardous to Health (COSHH) and Work Exposure Limits (WEL) guiltiness, which require employers to control workers' exposure to substances hazardous to health.

Table 2.3: Summary of ambient air quality limits and standards; (Directive, 2008; EPA, 2011; WHO, 2006; CPCB, 2010; Kumar, 2009). Please note that N.S. refers to not specified.

PM ($\mu g\ m^{-3}$)	Arithmetic Mean	EU	WHO	USEPA	Japan	India (Residential areas)
PM_{10}	Annual mean	40	20	Revoked[c]	N.S	60[g]
	24-hour mean	50[a]	50	150[d]	50	100[h]
$PM_{2.5}$	Annual mean	25[b]	10	15[e]	N.S	40[g]
	24-hour mean	N.S	25	35[f]	N.S	60[h]
PM_1	Annual mean	N.S	N.S	N.S	N.S	N.S
	24-hour mean	N.S	N.S	N.S	N.S	N.S

[a] The EU Directive 2008/50/EC stipulated that annual mean values of PM_{10} should not exceed a 24-hour mean of greater than 50 μgm^{-3} more than 35 days in a year.

[b] Three-year mean $PM_{2.5}$ concentration cannot exceed of 25 $\mu g\ m^{-3}$.

[c] The USEPA agency revoked the annual PM_{10} standard in 2006.

[d] Not to be exceeded more than once per year on average over 3 years.

[e] To attain this standard, the 3-year average of the weighted annual mean $PM_{2.5}$ concentrations must not exceed 15 $\mu g\ m^{-3}$.

[f] To attain this standard, the 3-year average of the 98th percentile of 24-h concentrations area must not exceed 35 $\mu g\ m^{-3}$.

[g] Annual Arithmetic mean of minimum 104 measurements in a year at a particular site taken twice a week 24 hourly at uniform intervals.

[h] 24 hourly 8 hourly or 1 hourly monitored values, as applicable shall be complied with 98% of the time in a year. 2% of the time, they may exceed the limits but not on two consecutive days of monitoring.

2.9 Chapter summary

This chapter has provided detailed information about the background to and primary concept of airborne PM and ultrafine particles. This chapter has reviewed the studies related to mass and number concentrations, particle distribution, sources of particle emissions, instrumentation, physicochemical analysis, exposure to the particles, health effects and current regulations. This review has suggested that adverse environmental and health effects can be expected with exposure to PM_{10}, $PM_{2.5}$, PM_1 and ultrafine particles at high mass and number concentrations. Several studies mentioned in this chapter highlighted the importance of PM and ultrafine particles emissions from building sources. The chapter has also covered the physicochemical characteristics of particles including their morphology and composition, using different form of analysis. The chapter concluded with a discussion of the potential impacts of PM and ultrafine particles on the surrounding environment and considered the associated regulations for controlling particle emissions. This chapter has highlighted the lack of studies about the release of airborne PM and ultrafine particles from major building activities such as construction, demolition and refurbishment, while acknowledging that numerous studies are available on dust emissions from different sources, such as vehicles and industrial sources. Further researches are needed to develop appropriate regulations for the control of PM_{10}, $PM_{2.5}$, PM_1 and ultrafine particles arising from building works in order to provide adequate protection for on-site workers and individuals living in nearby neighbourhoods. However, these investigations do not stop here, as further literature reviews are provided in the following chapters that relate to each individual objective.

Chapter 3. Materials and methods

This chapter presents a set of methods, instruments descriptions and the physicochemical analysis intended for achieving the research objectives.

3.1 Introduction

Experiments were conducted in the controlled laboratory, indoor and outdoor field sites, to study the emissions of PM_{10}, $PM_{2.5}$, PM_1 and ultrafine particles during building-related works such as concrete mixing, drilling, cutting, refurbishment, construction and demolition, as described in Section 1.3. The experimental studies in this section provide information on particle emission rates, together with methods used to calculate the respiratory deposition doses and physicochemical features including the morphology and chemical compositions of particles. Measuring particles in the required size range was performed using a DMS50 for measurements of PNCs and PNDs and using GRIMM (1.107 E), TEOM (1400) and OSIRIS (2315) instruments for measuring PMCs and PMDs (Table 3.1). A Kestrel 4500 weather station was also used to measure meteorological data (wind speed, direction, relative humidity and ambient temperature) at the measurement site. Furthermore, samples were collected on PTFE filters, and each of these samples was analysed using SEM, EDS, XPS and IBA analysis. The detailed descriptions of these instruments and their working principles are presented in the subsequent section, Section 3.2.

Table 3.1: Summary of the instruments used for measuring PM_{10}, $PM_{2.5}$, PM_1 and ultrafine particles during experiments.

Work type	Chapter number	Instrument used	Size range (µm)
Simulated laboratory investigations	Chapter 4	DMS50 GRIMM (1.107 E)	0.005–5 0.2–20
Indoor refurbishment measurements	Chapter 5	DMS50 GRIMM (1.107 E)	0.005–5 0.2–20
Outdoor construction measurements	Chapter 6	TEOM (1400) OSIRIS (2315)	0.1–10 0.4–20
Outdoor demolition measurements	Chapter 7	GRIMM (1.107 E)	0.2–20

3.2 Instrumentation

3.2.1 GRIMM (1.107 E)

A GRIMM particle spectrometer (model 1.107 E) was used to measure the mass distribution of particles per unit volume of air in 15 different channels covering the 0.2–20 µm in size range (Goyal and Kumar, 2013). The sensitivity of the instrument is 1 µg m^{-3}, and instrument reproducibility of size-resolved PMC is ±2% over the total measuring range. Optical signals pass through a multichannel size classifier to a pulse height analyser that classifies the signals based on size into appropriate channels. Ambient air was drawn into the unit every 6 second via an internal volume-controlled pump at a rate of 1.2 lit min^{-1} (Goyal and Kumar, 2013; Grimm and Eatough, 2009).

Two cross validation approaches were used to ensure the quality of the collected data. Firstly, the instrument was calibrated in a three-step process by the manufacturer prior to the on-site measurements, including verification of laser optics, gravimetric correlation verification and optical calibration against the known size-resolved distribution, density

and refractive index of known reference particles. This calibration used the National Institute of Standards and Technology (NIST) certified Polystyrene Latex Sphere (PSL) particles, which is a worldwide accepted standard method, giving a difference between standard instrument and my unit as ~5% (Table D1 in Appendix D). Secondly, on-site calibration was carried out by weighing (µg) the PTFE filters that collected particle mass during the on-site measurements and compared these mass with the data of PM mass produced by the instrument. The data of the PM mass (in µg) from the instrument was obtained by multiplying the total mass concentration (µg m^{-3}) with the sampling flow rate (2×10^{-5} m^3 s^{-1}) of the instrument and the total duration (s) of measured activity (Section D1). Results of this comparison are presented in Table D2, which shows an average difference of about 6% between the filter-based mass and the mass given by the instrument. Both these approaches provided a difference of ≤6% between the standard and the instruments unit, which was assumed to acceptable and no correction factor was applied to the data.

3.2.2 DMS50

The fast response differential mobility spectrometer (DMS50) was used to measure particles in the 5-560 nm size range. The DMS50 measures particles based on the electrical mobility equivalent diameter (D_p) and has a fast time response of up to 10 Hz for sampling ambient air with and a $T_{10\text{-}90}$% response time of 500 ms. The DMS50 samples air at a rate of 6.5 lit min^{-1} and further details of working principle of the DMS50 are described in the review by Kumar et al. (2010). The DMS50 provides real-time measurement of particle number spectrum from 5-560 nm sub-divided into 34 channels.

The DMS50 has been successfully used in the previous works involving measurements in indoor (Kumar and Morawska, 2014; Kumar et al., 2012c), outdoor (Al-Dabbous and Kumar, 2014), in-vehicles (Joodatnia et al., 2013a, b) and on-board vehicle (Carpentieri and Kumar, 2011) environments.

For quality assurance purposes, the DMS50 was calibrated by the manufacturer and the testing reported here was undertaken within the one year calibration period. The DMS50 was cleaned before each sampling day to remove dust particles accumulated on the electrometer rings. The DMS50 was set to average the samples every 10 sampling points (i.e. one second sampling rate) to improve the signal-to-noise ratio. Further detail of the DMS50 is presented in Table 3.2.

Table 3.2: Measuring capabilities of DMS50 (Kumar et al., 2010a) and GRIMM (Cheng, 2008).

DMS50			
Size range (nm)	Sampling rate (s)	Detectable diameter min/max	Measurable concentration range (cm^{-3})
5–2500	10	5 nm	$588–2.14 \times 10^{12}$
		2500 nm	$9–2.33 \times 10^{10}$
5–560	0.1	5 nm	$8233–4.97 \times 10^{12}$
		560 nm	$240–1.15 \times 10^{11}$
5–560	1	5 nm	$4209–4.97 \times 10^{12}$
		560 nm	$140–1.15 \times 10^{11}$
5–560	10	5 nm	$2628–4.97 \times 10^{12}$
		560 nm	$72–1.15 \times 10^{11}$
GRIMM			
Size range (nm)	Flow rate ($l\ s^{-1}$)		Measurable concentration range (cm^{-3})
0.2–20	0.02	-	$10^3–2 \times 10^9$

3.2.3 OSIRIS (2315)

Turnkey's Osiris instrument (model 2315) was used to measure the mass distribution of particles per unit volume of air in the 0.4 to 20 µm size range by light scattering technology in a mass concentration range of 0.1 to 6000 µg m^{-3} (Tasic et al., 2012). The Osiris is a portable device that is capable of sampling and measuring particle concentrations in real-time at high temporal resolution (1 s minimum). The air sample is continuously drawn into the instrument by a pump with a flow rate set by the microprocessor at a rate of 0.6 l min^{-1} through an inlet heated to 50 °C to minimise the effects of water droplets and particle bound water. Over 20,000 particles a second can be sized before coincidence effects occur. Several size selective inlets are also available for the instrument. These can be used to collect a size selected gravimetric sample on the instrument's filter and will measure in µg m^{-3}. Osiris also allows wind speed and direction, temperature and relative humidity to be recorded at the same time. Turnkey Instruments, OSIRIS monitors, have also been used for the assessment of indoor and outdoor PM levels as well as personal exposure in a number of past studies (Gulliver and Briggs, 2004a; Kim et al., 2008).

3.2.4 TEOM (1400)

The TEOM 1400 was used to measure mass of particles per unit volume of air in the size range of 0.1–10 µm. The instrument was capable of measuring particle mass concentration in the 0 to 1,000,000 µg m^{-3} range with a mass flow rate of 3 l min^{-1} (Cyrys et al., 2001). The sampling stream and filters were heated to 50 °C to maintain a stable temperature and eliminate interference from water on the filter. The mass measurement

relied on the measurement of the resonant frequency of an oscillating system that consists of the filter and glass element. A correction factor of 1.3 was recommended in the UK for comparison of PM_{10} measurements from TEOM with the EU Directive 1999/30/EC (Directive, 1999; Fuller and Green, 2004) prior to the development of a dynamic correction system (Defra, 2009; Green et al., 2009) and was applied in this study. Further details about the working principle and sensitivity of the TEOM 1400 can be found elsewhere (Ayers et al., 1999; Green et al., 2001; Meyer et al., 2000).

3.2.5 Kestrel 4500 weather station

A weather station (Kestrel 4500) was used for meteorological measurements (ambient temperature, relative humidity and barometric pressure), which was set up next to the measuring instruments. Meteorological information was logged on the Kestrel 4500 at 10 s resolution during all the experiments, though wind speed and direction were not considered during the simulated laboratory measurements since those measurements were undertaken in a controlled laboratory environment. Kestrel 4500 has also been used by past studies for their meteorological assessments (e.g. Burt and Eden, 2004; Al-Dabbous and Kumar, 2014).

3.2.6 GPS

A Global Positioning System (GPS) device (model: Garmin Oregon 350) was used to record sampling locations during the mobile measurements on a second basis (1 Hz). The data collected from the GPS in .gpx format was converted to Microsoft Excel through the map source software. Arcmap version 10.1 was used to plot spatial variations of PM_{10}, $PM_{2.5}$ and PM_1 during the different runs (Goel and Kumar, 2015).

3.3 Physicochemical analysis

3.3.1 SEM and EDS analysis

Samples collected during building refurbishment (Section 5.2.2) and demolition (Section 7.2.2) activities were analysed using a JEOL SEM (model: JSM-7100F) to provide information on the surface morphology of the particles collected on filters. The sample surface was scanned with a high-energy (~3.0 kV) beam of electrons in a raster pattern. The scanned area was between 6×6 and 200×200 μm^2 according to the magnification used. The electrons interact with the atoms that make up the sample producing signals, which contain information about the sample's surface topography, composition and other properties such as electrical conductivity (Watt, 1997; JEOL, 2015). In addition, each of the filter samples collected during building demolition activity (Section 7.2.2) were analysed using a JEOL SEM with a spatial resolution of 1.2 nm at 30 kV, equipped with energy dispersive X-ray spectrometer (EDS), to obtain information on the surface morphology and composition of the particles collected on filters (Chapter 7). The analyses were performed at The Microstructural Studies Unit of the University of Surrey (UK).

3.3.2 XPS analysis

X-ray Photoelectron Spectroscopy (XPS) analyses were also performed on a Thermo Scientific Theta Probe spectrometer (East Grinstead, UK) to analyse the surface chemistry of the particles collected in the filter samples collected during refurbishment activities (Section 5.2.2). XPS spectra were acquired by applying a Thermo digital twin anode source, which was operated using the Al Kα at 300W; quantitative surface chemical analyses were calculated from the high resolution, core level spectra following the removal of a non-linear background (Section B2). The manufacturer's software (Avantage version

4.74) was used to analyse the results. The software incorporates the appropriate sensitivity factors and corrects for the electron energy analyser transmission function and effective attenuation length. Further details of working principle of the XPS can be seen elsewhere (Watts and Wolstenholme, 2003).

3.3.3 IBA analysis

The non-destructive Ion Beam Analysis (IBA) was also applied on the samples collected during building refurbishment activities (Section 5.2.2) for investigating the chemical composition of PM sampled on the filters. Elemental analysis was carried out using 2.5 MeV proton beam, focused to about 6×6 μm² and scanned over an area of 1000×1000 or 2000×2000 μm² on the sample, with both particle backscattering (EBS) and particle-induced X-ray emission (PIXE) data collected and treated self-consistently (Jeynes et al., 2012) using the DataFurnace code, NDFv9.5e (Barradas and Jeynes, 2008). The EBS spectrum was essentially used for deriving the number of incident particles from the yield of the filter (i.e. C_2F_4). In principle, the particle spectrum also contains valuable information about the light elements (atomic number <12) for which the PIXE is essentially blind (due to the Be filter placed in front of the SiLi detector for stopping the intense flux of backscattering particles). In this case, the quantification was unfortunately not available due to the large signal of alpha particles emitted by the $^{19}F(p, \alpha_{0-4})^{16}O$ nuclear reactions. Besides, the strong gamma yield induced by the $^{19}F(p,p'\gamma)^{19}F$ nuclear reaction ($E\gamma$=110 and 197 keV) drastically increased the background of the PIXE spectrum, making the minimum detection limits significantly higher than usual. Despite these limitations, interesting information about the elements with an atomic number >12 became available

from the PIXE analysis.

3.4 Emission factors

3.4.1 Simulated laboratory investigations

The emission factors (EFs) calculated for the various operations (i.e. mixing, drilling and cutting) investigated were estimated in terms of particle number and mass emissions per unit time (s^{-1}), mass (kg^{-1}) and a combination of both (s^{-1} kg^{-1}). This approach was used for calculating EFs in Chapter 4. The net EFs were determined by subtracting the background mass or number concentrations during the "pre-activity (background)" period from the total measured during the "activity" period. Using this approach, both the particle number- and mass-based EFs were estimated for all the four activities (mixing with GGBS and PFA, drilling and cutting) across the three of the phases described. EFs on a number basis are estimated in terms of particle number released by an activity per second (# s^{-1}), per kilogram (# kg^{-1}) and per second per kilogram (# s^{-1} kg^{-1}). For PM_{10}, $PM_{2.5}$ and PM_1, the EFs were calculated particle mass per second (µg sec^{-1}), per kilogram (µg kg^{-1}) and per second per kilogram (µg s^{-1} kg^{-1}).

For mixing activities, EF of mixing with GGBS and PFA were determined separately. Mixing activities included both dry and wet mixing periods and the average of both periods is estimated for each mixing activity. The dry mixing is the period when the water was not added to the cement, aggregate and sand mixtures. The wet mixing is the period when water for hydrating the cement and admixtures for producing concrete was used. To state the EF in terms of number or mass of particles emitted per second (# s^{-1} or µg s^{-1}), the number or

mass concentrations of particles per centimetre cube of sample air (# cm^{-3} or µg cm^{-3}) were multiplied by the sample flow rate of DMS50 (108.33 cm^3 s^{-1}) and GRIMM (20 cm^3 s^{-1}).

The EF based on particles released per second from each kg of material mixed (i.e. # s^{-1} kg^{-1} or µg s^{-1} kg^{-1}) was calculated by dividing the above-noted time based EF (# s^{-1} or µg s^{-1}) by the total 21 kg mass of the fresh concrete mix; this mass was 0.12 and 0.08 kg for cutting and drilling, respectively. Furthermore, multiplication of the above-noted EF (i.e. # s^{-1} kg^{-1} or µg s^{-1} kg^{-1}) by the typical total time taken by mixing activity (taken here as a typical time of ~420 s) produced mass-based particle number or mass EFs in # kg^{-1} or µg kg^{-1}. Typical times for drilling and cutting activities depends on the hole depths and rotational speeds of machines, and these were assumed as 60 s for the both the activities (Oberg, 2004).

3.4.2 Building demolition

The approach presented in this section was applied to calculate particle EFs for the outdoor building demolition works in Chapter 7. The PMEFs are defined as the mass of emitted particles per unit area of demolition per second (µg m^{-2} s^{-1}). These were estimated for PM_{10}, $PM_{2.5}$ and PM_1 fractions separately using the data collected during the fixed-site measurements in the downwind of the demolished building (Section 7.2). Generalising the methods used in this section, to other real field operations is helpful as they provide a basis to estimate the realistic values of total particle mass emissions from a demolition activity. A box model was initially developed, and then modified to take into account the horizontal decay of PM fractions, using the mass balance concept for the assessment of demolition-related PMEFs (Figure 3.1). Similar modelling approach to estimate the PMEFs has been

used by previous studies (Font et al., 2014; Jamriska and Morawska, 2001; Kumar et al., 2011a).

It has been assumed that the box has a width, length and the maximum height where the pollutants mix as L, W and H_m, respectively. Formulation of the box model assumes that the demolition site acts as a control volume (box), and that the air in the box is well mixed with uniform (U_x in m s^{-1}) and exchange (U_z in m s^{-1}) wind velocities in the x– and z–directions, respectively. The model also assumes that there is no change in PMCs through transformation processes in the box (Kumar et al., 2011a). The removal of PM due to deposition and gravitational settling are assumed to be negligible.

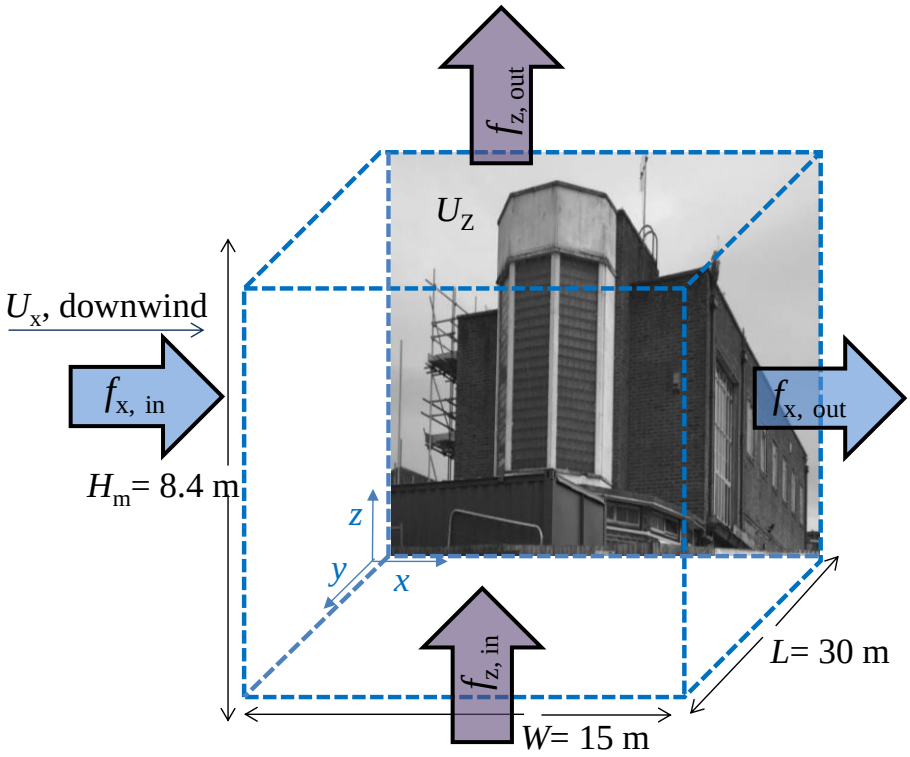

Figure 3.1: Schematic diagram of the box model, showing various dimensions and parameters; f_x and f_z refer to the particulate mass flow rate entering and leaving the box in the x and z directions, respectively. U_x and U_z refer to wind velocities in the x and z directions; L and W refer to length and width of the box, respectively, and H_m refers to maximum mixing height.

On a dimensional basis, it is assumed that the mass flow rate (μg s^{-1}) due to the emissions from the demolition site is equal to the product of PMEFs (μg m^{-2} s^{-1}) and the surface area (m^2) (Font et al., 2014).

$$\text{Mass flow rate} = \text{PMEF} \times \text{L} \times \text{W} \quad (3.1)$$

Further, consideration of the conservation of mass for PM gives their mass flow rate in the box as: Net mass flow rate due to demolition activity = mass flow entering and leaving the box through horizontal advection (f_x) + mass flow through vertical exchange (f_z). Eq. (3.1) can then be written as:

$$\text{PMEF} \times \text{L} \times \text{W} = [(\text{PM}_{\text{activity}} \times U_x \times H_m \times L) - (\text{PM}_{\text{background}} \times U_x \times H_m \times L)] + [(\text{PM}_{\text{activity}} \times U_z \times W \times L) - (\text{PM}_{\text{background}} \times U_z \times W \times L)] \quad (3.2)$$

Vertical exchange wind velocity is assumed to be negligible, and thus the calculation for mass flow entering and leaving the box through vertical advection was overlooked from the calculations of the particle emissions rates. With this assumption, Eq. (3.2) becomes:

$$\text{PMEF}_i \times \text{L} \times \text{W} = [(\text{PM}_{i,\text{activity}} \times U_x \times H_m \times L) - (\text{PM}_{i,\text{background}} \times U_x \times H_m \times L)] \quad \textit{or}$$

$$\text{PMEF}_i \times \text{W} = \Delta\text{PM}_i [U_x \times H_m] \quad (3.3)$$

where ΔPM_i (μg m^{-3}) is the subtraction of the PMC during the "background" period from the total PMCs measured during the "activity" period (i.e. ΔPM_i = PM (activity, downwind) – PM (background); subscript *i* of PM and PMEF refers to size fractions of PM (i.e. PM_{10}, $PM_{2.5}$ and PM_1).

Since the measurements were taken at ~10 m away from the site, there will be a *dilution* between the source (i.e. demolition site) and the monitoring station. Hence the emission factors using these measured concentrations at a distance away from the source will underestimate the PMEFs. Therefore, the horizontal decay profiles (Eq. 3.4) were developed through the sequential measurements in Section 7.3.4 to account for the dilution between the emission source and sampling location, and back-calculate PM_{10}, $PM_{2.5}$ and PM_1 concentrations closest (~0.1 m away from demolition site) to the emission source before putting them in Eq. (3.3).

$$\Delta PM_i = -a \ln(x) + c \tag{3.4}$$

where x (m) is a distance from the demolition site. The values of the empirical coefficient a (μg m^{-3}) are 13.57, 8.51 and 1.77 for PM_{10}, $PM_{2.5}$ and PM_1, respectively (Section 7.3.4). Likewise, c (–) is a constant with values as 92.57, 40.60 and 11.59 for PM_{10}, $PM_{2.5}$ and PM_1, respectively. Substitution of Eq. (3.4) into Eq. (3.3) gives:

$$PMEF_i \times W = [-a \ln(x) + c]\,[U_x \times H_m] \tag{3.5}$$

Furthermore, the value of H_m is taken as 8.4 m, which is the height of the building; the similar assumption was taken from Jamriska and Morawska (2001). Since the value of average synoptic wind speed (U_{15}) were available from at a height of 15 m above the ground level and that the PMC measurements were taken at a height of about 1.8 m (Section 7.3.1), the log-law was applied to predict the wind speed (U_x) at a height (z) of 1.8 m using the Eq. (3.6):

$$U_x = \frac{u^*}{k} \ln\left(\frac{z-d}{z_0}\right) \tag{3.6}$$

where u^* (= 0.26 m s^{-1}) is surface friction velocity, k (= 0.40) is a constant, z_0 (= 0.5 m) is surface roughness length, and d (= 1 m) is the zero displacement height (Britter and Hanna, 2003). Substitution of Eq. (3.6) into Eq. (3.5) gives the final equation to estimate the PMEFs as:

$$\mathrm{PMEF}_i = \frac{[-a \ln(x) + c] \times H_m \times \left(\frac{u^*}{k} \ln\left(\frac{z-d}{z0}\right)\right)}{W} \tag{3.7}$$

3.5 Estimation of exposure doses for health risk analysis

The analysis of the potential health risk of occupants associated with inhalation exposure of PMs and ultrafine particles was carried out based on estimated respiratory deposition dose rates. Construction workers are frequently exposed to inhale particles, particularly ultrafine particles, at building refurbishment sites.

The total dose received by an individual is related to the breathing rate, the period of exposure and the difference between the number of particles inhaled and exhaled during each breath (Hofmann, 2011). Including algebraic and semi empirical deposition models, the inhalation and deposition of particles through the respiratory tract can be estimated in a number of ways. The deposition fraction model of the International Commission on Radiological Protection (ICRP, 1994) is a commonly accepted approach, which is applied here and also adopted by Azarmi et al. (2014) and Goel and Kumar (2015).

3.5.1 Exposure doses of ultrafine particles

Tidal volume and breathing rate depend on age, gender and the level of activity (Int Panis et al., 2010; Joodatnia et al., 2013a). Multiplication of the tidal volume and the breathing frequency determines the so-called one minute ventilation (VE).

There are two approaches for calculating the dose rate. The first method utilised size-dependant DFs that were taken by the ICRP respiratory deposition model (Hofmann, 2011; ICRP, 1994) and the other uses average size resolved PNCs for each activity. The second method utilised a single DF and the average PNC for each activity. The latter approach is usually applied in situations where information on size-resolved concentration distributions is not available. The measurements provided the detailed size distributions of particles and therefore both the fixed– and variable–DF approaches were used to estimate the dose rate in this study using Eqs. (3.8) and (3.9), respectively;

$$\text{Deposited Dose (with constant DF)} = (\text{VT} \times f) \times \text{DF} \sum_{i=1}^{32} \text{PNC}\,(i) \qquad (3.8)$$

$$\text{Deposited Dose (with variable DF)} = (\text{VT} \times f) \sum_{i=1}^{32} \text{PNC}(i) \times \text{DF}(i) \qquad (3.9)$$

Where PNC_i and DF_i are the number concentration and deposited fraction of particles in each size range (i), respectively. VT is tidal volume that is considered equal to 800 cm^{-3} per breath for male; f is the typical breathing frequency for male in working light exercise, which is taken as 0.34 breath per second (Hinds, 1999) and a constant DF value is taken as 0.65 (Chalupa et al., 2004; Int Panis et al., 2010).

3.5.2 Exposure doses of PM_{10}, $PM_{2.5}$ and PM_1

The mass–based respiratory deposited doses (RDD), based on deposition fraction (DF) values, for various PM fractions are estimated using the Eq. (3.10):

$$\text{Deposited Dose} = (VT \times f) \times DF_i \times PM_i \tag{3.10}$$

where DF values are estimated (see Figure 3.2) based on the mass median diameter (d_p) of PMCs in various size ranges using the Eqs. (3.11-3.12) given by Hinds (1999):

$$DF = IF\ (\ 0.058 + \frac{0.911}{1+\exp(4.77+1.485\ln dp)} + \frac{0.943}{1+\exp\ (0.508-2.58\ln dp)}) \tag{3.11}$$

where *IF* is the inhalable fraction that is computed as:

$$IF = 1 - 0.5(1 - \frac{1}{1+0.00076\ dp^{2.8}}) \tag{3.12}$$

VT is tidal volume that is considered equal to 1920 (1360) and 1250 (990) cm^3 per breath during heavy and light exercises for men, respectively; the values in parenthesis are for females (Hinds, 1999). *f* is the typical breathing frequency, which is taken as 0.45 (0.55) and 0.34 (0.35) breath per second during heavy and light exercises for male, respectively; the values in parenthesis are for females (Hinds, 1999). The resulting product of VT, *f* and DF to PM_{10}, $PM_{2.5}$ and PM_1 values provide mass-based RDDs.

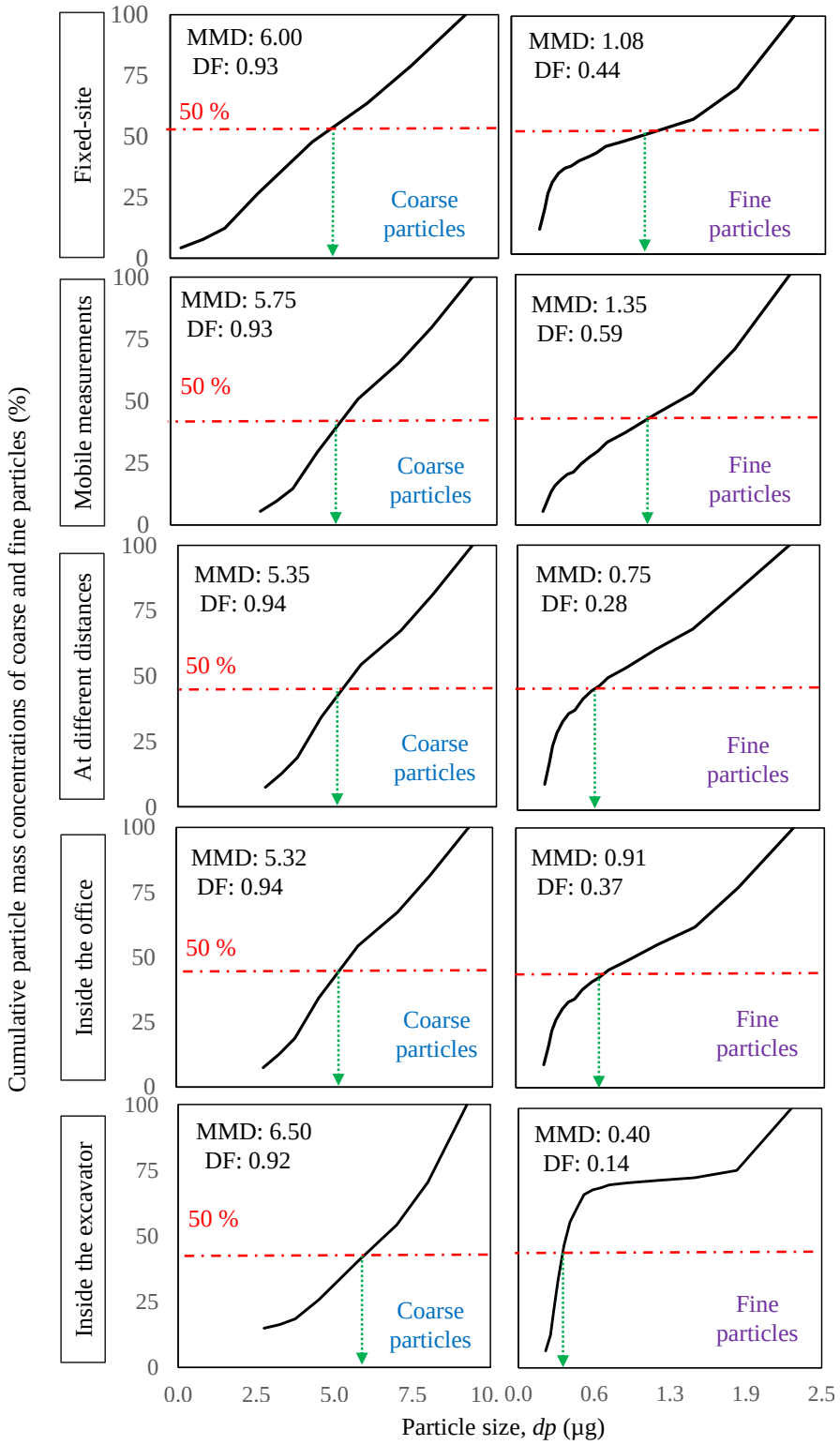

Figure 3.2: Finding mass median diameter (MMD) of coarse and fine particles using cumulative particle mass concentrations measured during each activity. DF refers to deposition fraction which has been estimated using MMD in Eq. (3.11).

3.6 Chapter summary

This chapter summarises the set of instruments and materials used for measuring the particle number and mass concentrations, and also presents the methods used to estimate particle emission factors and occupational exposures. Furthermore, this chapter covers the physicochemical characterisation of particles using SEM, EDS, XPS and IBA analysis. This chapter ends by providing descriptions of the instruments used for measuring the particles, including DMS50, GRIMM (1.107 E), OSIRIS (2315) and TEOM (1400), during the laboratory, indoor and outdoor field experiments as well as the devices which were used for measuring meteorological parameters and for recording sampling locations. Further information about the results of the experiments in the controlled laboratory environment (i.e. concrete mixing, drilling, cutting), indoor field sites (i.e. building refurbishment) and outdoor field sites (i.e. construction and demolition) are presented in Chapters 4, 5, 6 and 7, respectively.

Chapter 4. Simulated laboratory investigations

This chapter presents the results of release of ultrafine particles and PM from indoor simulated building activities (i.e. concrete mixing, drilling and cutting). The chapter also provides assessments of particles emission factors followed by estimations of exposure doses.

4.1 Introduction

There have been a number of studies of PMCs of ambient PM_{10} in urban areas, but less work has focused on the $PM_{2.5}$ and PM_1 fractions arising from building activities (Ragheb, 2011) with even less information relating to particles below 100 nm (Kumar et al., 2013). Whilst research has been undertaken into the effects of ultrafine particles on the environment and health (Kumar et al., 2011a), there is currently no legal regulation, or guidelines, for controlling the public exposure to airborne PNCs within the urban environment, including construction sites (Kumar and Morawska, 2014).

Construction activities such as the mixing, drilling and cutting of concrete have the potential to generate coarse, fine and ultrafine particles. The manufacture of fresh concrete typically involves the mixing of coarse and fine aggregates with cement, water and admixtures in a rotating drum mixer generating considerable airborne dust (Kumar and Morawska, 2014). Concrete drilling (employing hardened drill bits) is a common activity

both at construction sites and within domestic situations and is known to generate coarse and fine particles (Cook Jr and Harris, 1992). Similarly, the cutting of concrete is common during refurbishment, maintenance and demolition activities and can also produce coarse and fine particles. Despite the fact that such activities are undertaken on a daily basis around the globe, surprisingly little is known about the associated emissions and exposure levels of the particles produced (Akbar-Khanzadeh and Brillhart, 2002; Broekhuizen et al., 2011; Kumar et al., 2012b).

Many studies have experimentally measured particle number and size distributions during manufacturing, handling and usage of engineered nanomaterials (Kumar et al., 2014a, 2010a). For example, PNCs in the 0.06–6.36 $\times 10^4$ cm^{-3} range were measured during a simulated sanding process. Some studies have also measured emissions of nano-sized particles during different generation methods (Tsai et al., 2012; Tsai et al., 2009), or their exposure during handling and bagging processes at workplaces (Fujitani et al., 2008; Tsai et al., 2011). However, most of these studies are related to engineered nanomaterials and there are hardly many investigations that deal with the construction and demolition processes.

There are a few studies concerned with PM emissions arising from the drilling and cutting of materials such as carbon nanofibre as well as composite and silica based nanocomposites (Sachse et al., 2012), the demolition of structures (Dorevitch et al., 2006), concrete recycling (2014) and other building and road works (Fuller et al., 2002; Fuller and Green, 2004). A summary of relevant studies is presented in Table 2.1. The importance of particle emissions from construction sources is likely to increase as the development of urban

infrastructure across the globe is expected to reflect world population growth (Kumar et al., 2012b). In addition, there remain significant uncertainties concerning exposure risk because the particles characteristics from construction sources may be different from other, more established sources such as vehicle exhaust (Charron and Harrison, 2003; Kumar et al., 2010, 2011b) and non-vehicle exhaust sources (Kumar et al., 2013; Voliotis et al., 2014). Further information about the other sources of PM_{10}, $PM_{2.5}$, PM_1 and ultrafine particles in the urban environment is described in Section 2.4 (Chapter 2). None of the studies to date have presented coarse, fine and ultrafine particles emissions and associated exposure to on-site workers from either of the mixing, drilling or cutting activities (see Table 2.1), which is the focus of this study.

Taking advantage of research gaps, this work investigates the release of particles in the 5-10,000 nm range from three (simulated) construction activities (concrete mixing, drilling and cutting) carried out under controlled conditions in indoor laboratory environment. The objectives were to analyse the size distributions and proportions of both particle number and mass concentrations in the studied size range, compute emission factors (EFs) and exposure to on-site workers.

4.2 Methodology

4.2.1 Experimental setup

Experiments were conducted to measure the release of PM_{10}, $PM_{2.5}$, PM_1 and ultrafine particles arising from the manufacture of fresh concrete (mixing), and subsequent processing of hardened concrete by drilling and cutting. The aim of the experiments was to simulate the activities that occur on typical construction sites and consider the

implications for workers who are exposed to such procedures. In addition, using approaches described in Sections 3.4 and 3.5 in Chapter 3, both the particle number- and mass-based EFs and occupational exposure doses were estimated for all the four activities (mixing with GGBS and PFA, drilling and cutting) across the three of the phases described.

A total of four different experiments were performed: (i) concrete mixing with a blended cement incorporating Portland cement with 35% by weight Ground Granulated Blastfurnace Slag (GGBS), (ii) concrete mixing with a blended cement incorporating Portland cement with 35% Pulverised Fuel Ash (PFA), (iii) the drilling of hardened concrete, and (iv) the cutting of hardened concrete. During each experiment the measurement of particle emissions was divided into three distinct time periods: (i) the pre-activity baseline (i.e. background levels in the ambient indoor environment), (ii) the simulated activity (carried out over a fixed time to enable the EFs and exposure doses to be estimated), and (iii) the post-activity background level.

The levels of particle emissions arising during each experiment were measured using a DMS50 and GRIMM instruments (see Section 3.2 in Chapter 3) for measurements of number and size distributions in the 5-10,000 nm range such that both the particle number and mass concentrations (PM_{10}, $PM_{2.5}$, PM_1) could be obtained. KESTREL 4500 was also used for measuring the meteorological data (relative humidity, barometric pressure and ambient temperature), which was set up next to the DMS50 and GRIMM instruments. Meteorological information was logged on the Kestrel 4500 during all the experiments although wind direction and speed were not recorded since all of the measurements reported here were undertaken in a controlled laboratory environment.

Table 4.1: Summary of sampling data during concrete mixing, drilling and cutting activities.

Date	Time	Sampling time (seconds)	Name of activities
03/07/2013	14:40:46 15:27:03	2,777	Mixing with GGBS
04/11/2013	13:28:28 14:39:23	4,255	Mixing with PFA
04/11/2013	14:47:38 15:20:01	1,953	Drilling
04/11/2013	15:21:00 15:41:48	1,248	Cutting

Concrete mixing was carried out using a rotating drum mixer, manufactured by ELE International (model: EL34-3540/01, Bedfordshire, United Kingdom), with a 100 litre capacity operating at 60 rpm. Two different concrete mixes were manufactured using the mix specification shown in Tables A1-A2 (Appendix A) incorporating Portland cement blended with either GGBS or PFA. Measurements of particle levels were obtained during the pre-activity and both during the mixing process itself (which took place over a period of ~180–300 seconds) and subsequently during the measurement of the slump test of the resulting fresh concrete mix (see Table 4.1). Slump test is used at construction sites to measure the workability of freshly made wet concrete. This test was carried out following the method described in BS EN 12350-2. Concrete was filled in a steel slum test cone in three equal layers to measure the "slump (settlement)" of freshly made concrete after lifting up the test cone. The test does not involve any mechanical stresses and the probable source of coarse particles appears to be resuspension of dust from the floor and nano-sized particles from the chemical reactions undergoing in the fresh mix of concrete.

The fresh concrete was subsequently cast into steel moulds (150×150×500 mm) to provide specimens of hardened concrete with known composition for subsequent post-processing drilling and cutting. During this experiment the sampling tube was positioned 1 m away from the source and the DMS50 was allowed to equilibrate, prior to establishing the pre-activity (background) readings (Figure 4.1). Care was taken to clean the internal tubes of the equipment prior to each experiment and parts of dust deposits from previous experiment.

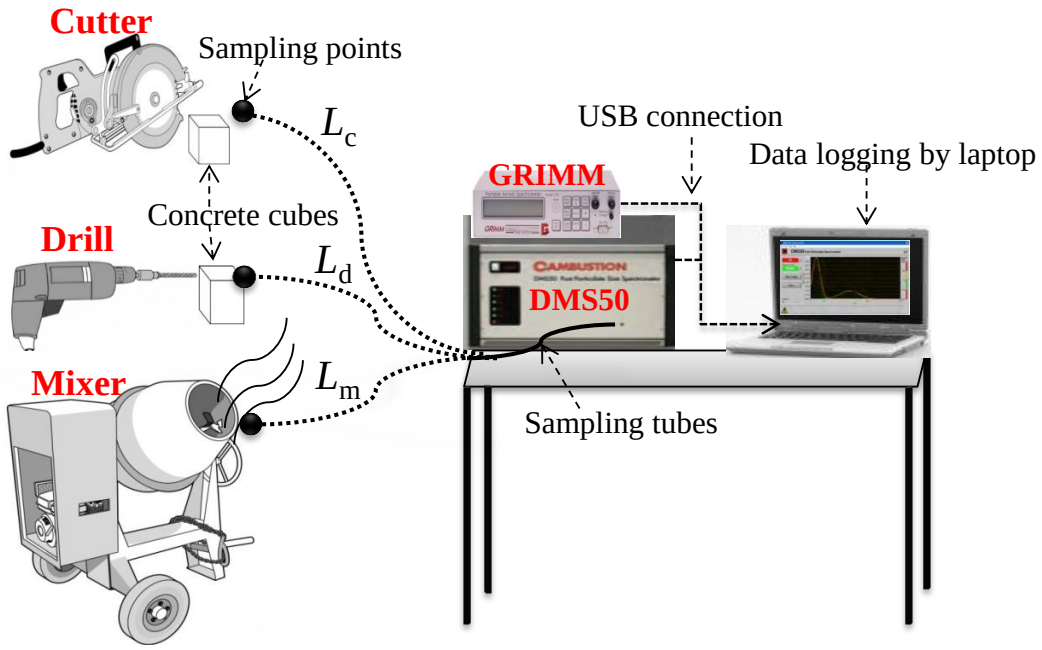

Figure 4.1: Schematic of the experiment showing instrumentation used and distances; L_c, L_d and L_m represents the length between the DMS50 and the sampling points from cutter, drilling and mixer, respectively. Length of all these sampling tubes is 1 m.

Dry drilling of concrete was carried out using a Kango 501 Rotary Drill with 10 mm masonry drill-bit. A hardened concrete prism (with a characteristic compressive strength equivalent to a grade $C_{30/40}$ concrete) was subject to the creation of a number of 25 cm deep holes, each produced in succession. During the drilling process a water spray was employed

to mimic good construction practice and the sampling tube was positioned at 1 m from the source in each case (Figure 4.1). Dry cutting was carried out on a hardened concrete prism (150×150×500 mm) using a Norton BBL527 model, diamond wheel with a blade shaft speed of 2400 rpm and a 55.88 cm diameter blade of 1.5 mm thickness. Again the sampling point was 1 m away from source (Figure 4.1).

4.3 Results and discussion

4.3.1 Particle size distributions

The spectrums of particle number distribution (PND) obtained during the simulated building activities are presented in Figure 4.2a-b (mixing of concrete) and Figure 4.2c-d (drilling and cutting). It can be seen that during each "activity" period there is a significant change in the PND over background levels. As expected the post-activity levels are lower than those obtained during the activity but were somewhat above the original background reflecting the time taken by particles to disperse after the activity (Section 4.3.2). For mixing activities undertaken with GGBS and PFA the peak PND values obtained were 2.31×10^4 and 3.80×10^4 cm^{-3} being ~3.0 and 12-times higher than peak background PNDs, respectively. In terms of nucleation mode particles (those below 30 nm; (Kumar et al., 2008)) and new particle release, peak PNDs produced during mixing with PFA were ~1.64-times higher than those obtained with GGBS. This is thought to reflect the particle size, density and adhesion of the two materials as the mixing process was the same. As seen in Figure 4.2a-b there is an increase in PNDs in the ultrafine size range during the mixing process. Figure 4.2c-d show the PND spectrums obtained during the drilling and cutting of samples of hardened concrete. The peak PND values obtained were 37.10×10^4 and

118.80×10^4 cm^{-3}, respectively, being ~3.5 and 8-times higher than the background peak PNDs. A significant increase in nucleation mode particles was observed with cutting producing a greater release of new particles (over background) than drilling, reflecting the larger surface area of concrete subject to abrasion. These observations confirm that significantly more ultrafine particles are released during cutting and drilling activities in comparison to mixing activities. These results are dissimilar to the findings of Kumar et al. (2012c), both in terms of peak diameters and the shape of PNDs obtained during their investigations for estimating the release of particles below 100 nm arising from the crushing of hardened concrete cubes, the fracture of concrete slabs and the recycling of concrete debris. For example, their work found peak PNDs at ~20.73×10^4 and 20.86×10^4 cm^{-3} during demolition and dry recycling of concrete, respectively, which is ~2- and ~6-times larger to that obtained for the drilling and cutting activities reported here.

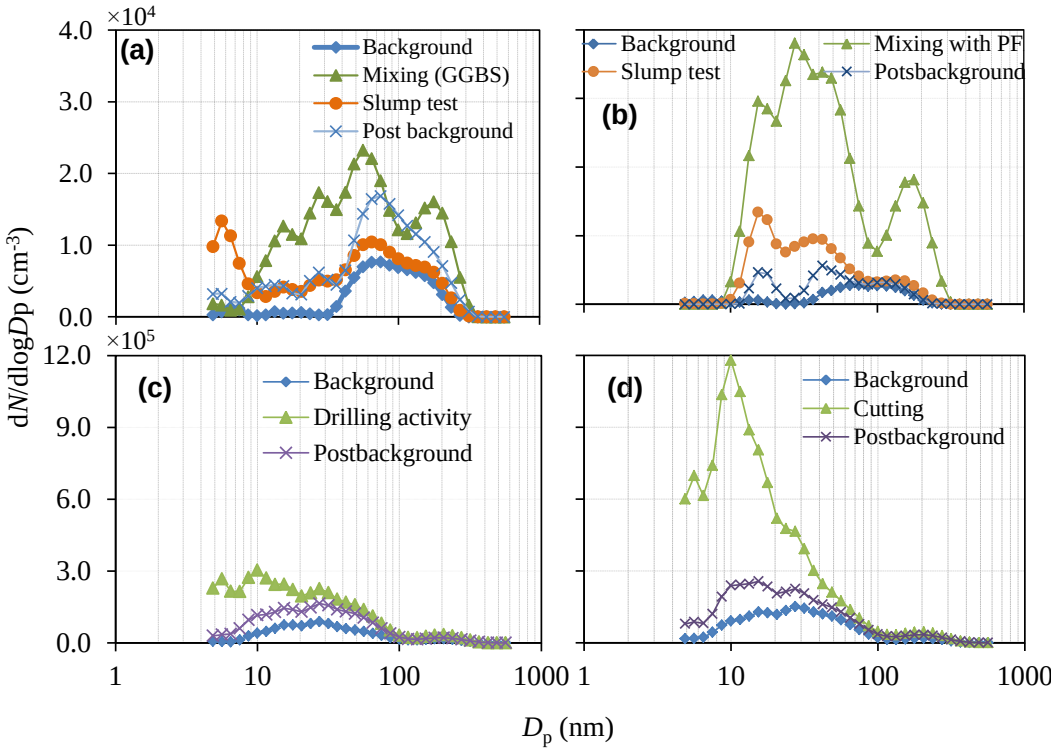

Figure 4.2: PNDs for the (a) mixing with GGBS and (b) mixing PFA, (c) drilling, and (d) cutting.

4.3.2 Particle number concentrations

Figure 4.3 and Figure 4.4 show the total PNCs and distribution of particles in various size ranges obtained during mixing (with GGBS and PFA), drilling and cutting, respectively. Average PNCs during the activity periods in size ranges 5-30, 30-100, 100-300 and 300-560 nm were 21.27±2.02 $\times 10^3$, 30.97±16.51 $\times 10^3$, 279.11±61.92 $\times 10^3$ and 732.27±442.51 $\times 10^3$ cm^{-3} for mixing with GGBS, PFA, drilling and cutting, respectively. Average PNC values during mixing with GGBS and PFA were ~4 and 15-times above the background levels, Table 4.2.

Table 4.2: Average concentration, Geometrical mean diameter and fractions for particles number during mixing, drilling and cutting activities.

Experiments	Time period	Average ± STD (# cm^{-3}) $\times 10^3$	Geometrical mean diameter	Ultrafine particles fraction (%)
Mixing with GGBS	Background	5.26±1.24	58.96±2.56	68
	Mixing with GGBS	21.72±2.02	53.01±2.50	74
	Slump test	11.12±6.10	35.95±3.23	78
	Post background	11.88 ±2.25	67.49±2.36	65
Mixing with PFA	Background	1.98±1.42	63.15±2.39	66
	Mixing with fly ah	30.97±16.61	41.93±2.28	82
	Slump test	8.61±6.09	34.97±2.15	88
	Post background	4.08±1.67	4.08±1.67	80
Drilling	Background	69.85±7.15	30.90±2.34	90
	Drilling	279.11±61.92	19.55±2.50	95
	Post background	146.64±24.35	26.41±2.33	94
Cutting	Background	127.32±16.65	27.68±2.28	93
	Cutting	732.27±442.51	15.10±2.17	97
	Post background	233.64±133.57	23.23±2.40	93

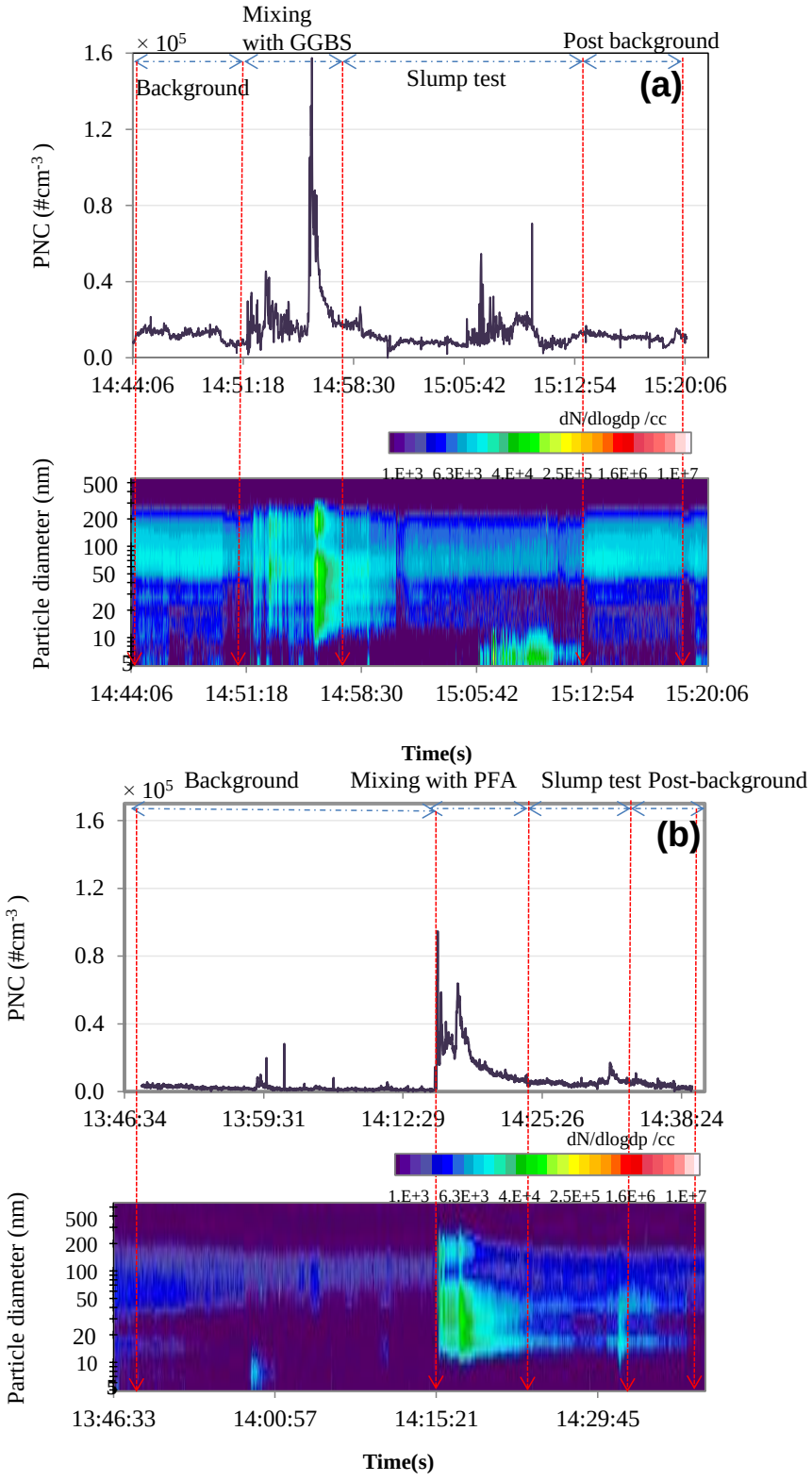

Figure 4.3: Temporal evolution of PNC and their contour plots during (a) mixing with GGBS, and (b) mixing with PFA.

The average PNCs during the drilling activity changed relatively little. For example, these were ~1.38-times higher for the second hole than during the first hole (Figure 4.4a). Average values over the period of drilling periods were ~ 4–times higher than background level (69.85±7.15 $\times 10^3$ cm^{-3}), as seen in Table 4.2. For all the activities, the ultrafine size range (below 100 nm) contributed most of the total PNCs. For example, their proportion to total PNCs during the mixing with GGBS, mixing with PFA, drilling and cutting activities was 74, 82, 95 and 97%, respectively (see Figure A1 in Appendix A). The peak value for the "dry" drilling activity was 5.14×10^5 cm^{-3} and decreased by ~40% to 3.08×10^5 cm^{-3} when water spraying was employed as a suppression method since particles are less able to become airborne (Rosenfeld et al., 2001).

The average PNC measured during concrete cutting was 732.27±442.51 $\times 10^3$ cm^{-3}, which is ~14–times greater than the background value, Table 4.2. Taken together Figure 4.3 and Figure 4.4 demonstrate that for both the drilling and cutting activities there is an increase in PNC with time and the magnitude of PNC are much higher than occurred during the mixing of fresh concrete. This is thought to reflect the higher rotational frequency, shear stresses and local energy density associated with drilling and cutting activities. Again these results are in agreement with those of Kumar et al. (2012c) who reported an increase of between 2– and 17–times in the total PNC over the background PNCs for various concrete demolition related activities. After adjusting for background concentrations, the net release of PNCs during cube crushing and 'dry' recycling of concrete events were measured as ~0.77 and 22.70 ($\times 10^4$) cm^{-3}, respectively. The corresponding results reported by Kumar et al. (2012c) were about (2.76, 0.09), (4.02, 0.13), (36.23, 1.22) and (95.06, 3.22) times

smaller than values for mixing with GGBS, with PFA, drilling and cutting activities, respectively.

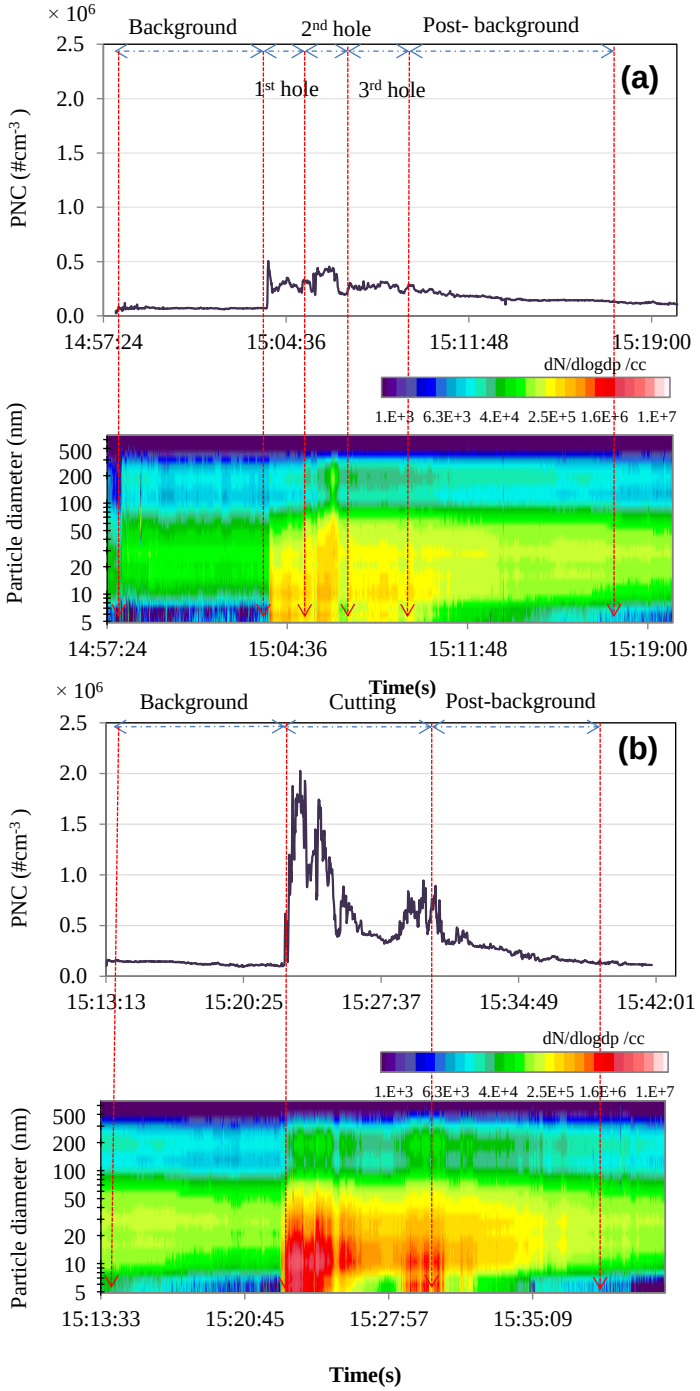

Figure 4.4: Temporal evolution of PNC and their contour plots during (a) drilling, and (b) cutting activities.

The values of PNC obtained during these processes are not directly comparable but can be put in perspective of the average roadside and urban background PNCs. The corresponding values of PNCs in European environments were reported as $3.15\pm1.60 \times10^4$ cm^{-3} and $1.63\pm0.82 \times10^4$ cm^{-3}, respectively (Kumar and Morawska, 2013; Kumar et al., 2014), indicating that studied activities may produce particles at levels (above background) that are comparable to, or greater than, those which arise from vehicle exhausts. Given that construction and demolition activities occur within urban areas this raises important questions about the need to understand the associated exposure levels to urban dwellers, building operatives and the need to establish suitable standards and controls.

4.3.3 Particle mass concentrations

Figure 4.5 shows the PMC arising from the mixing of concrete with GGBS and PFA. The average PM_{10}, $PM_{2.5}$ and PM_1 determined during mixing were 1.89×10^3, 0.78×10^3, 0.56×10^3 µg m^{-3} and 1.98×10^3, 0.94×10^3, 0.63×10^3 µg m^{-3}, respectively (see Figure A2 in Appendix A). PMC values showed a rapid increase immediately after the start of mixing. The peak values of PM_{10}, $PM_{2.5}$ and PM_1 reached $4.10\times10^{3,}$ 3.65×10^3 and 2.42×10^3 µg m^{-3} for the concrete containing GGBS. The corresponding values obtained for the mix containing PFA were 3.66×10^3, 2.35×10^3 and 1.04×10^3 µg m^{-3}, which are many times higher than those for the mixing with the GGBS reflecting the same trend as seen for the PNCs (see Section 4.3.2). The results of the drilling and cutting activities show a considerable increase in PMC over background levels. Moreover, the average PM_{10}, $PM_{2.5}$ and PM_1 were calculated as 2.82×10^3, 1.19×10^3, 0.80×10^3 µg m^{-3} for drilling and 3.77×10^3, 1.34×10^3, 0.86×10^3 µg m^{-3} for cutting, Table 4.3.

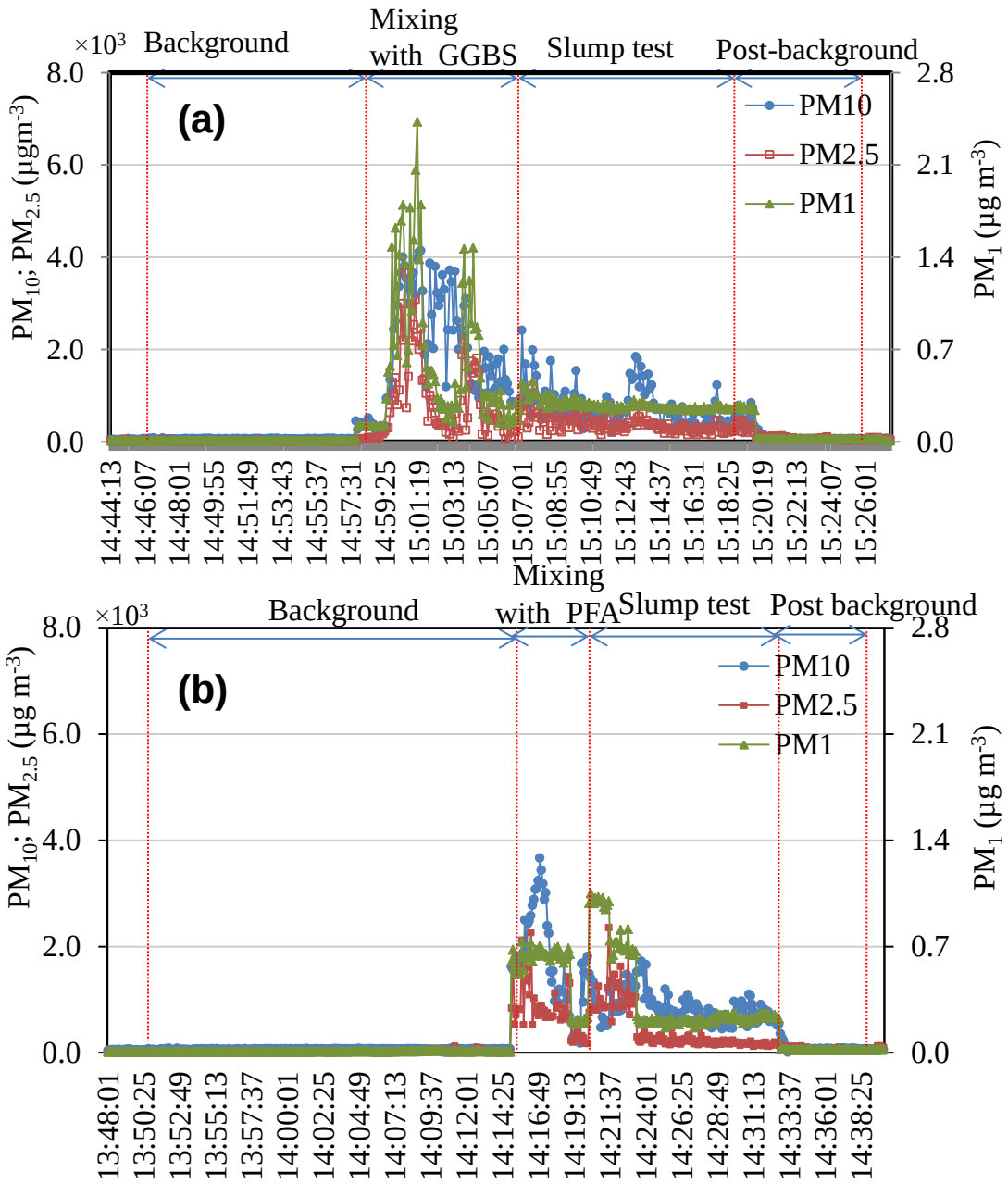

Figure 4.5: Mass concentration against time for (a) mixing with GGBS, (b) mixing with PFA, (c) drilling, and (d) cutting activities.

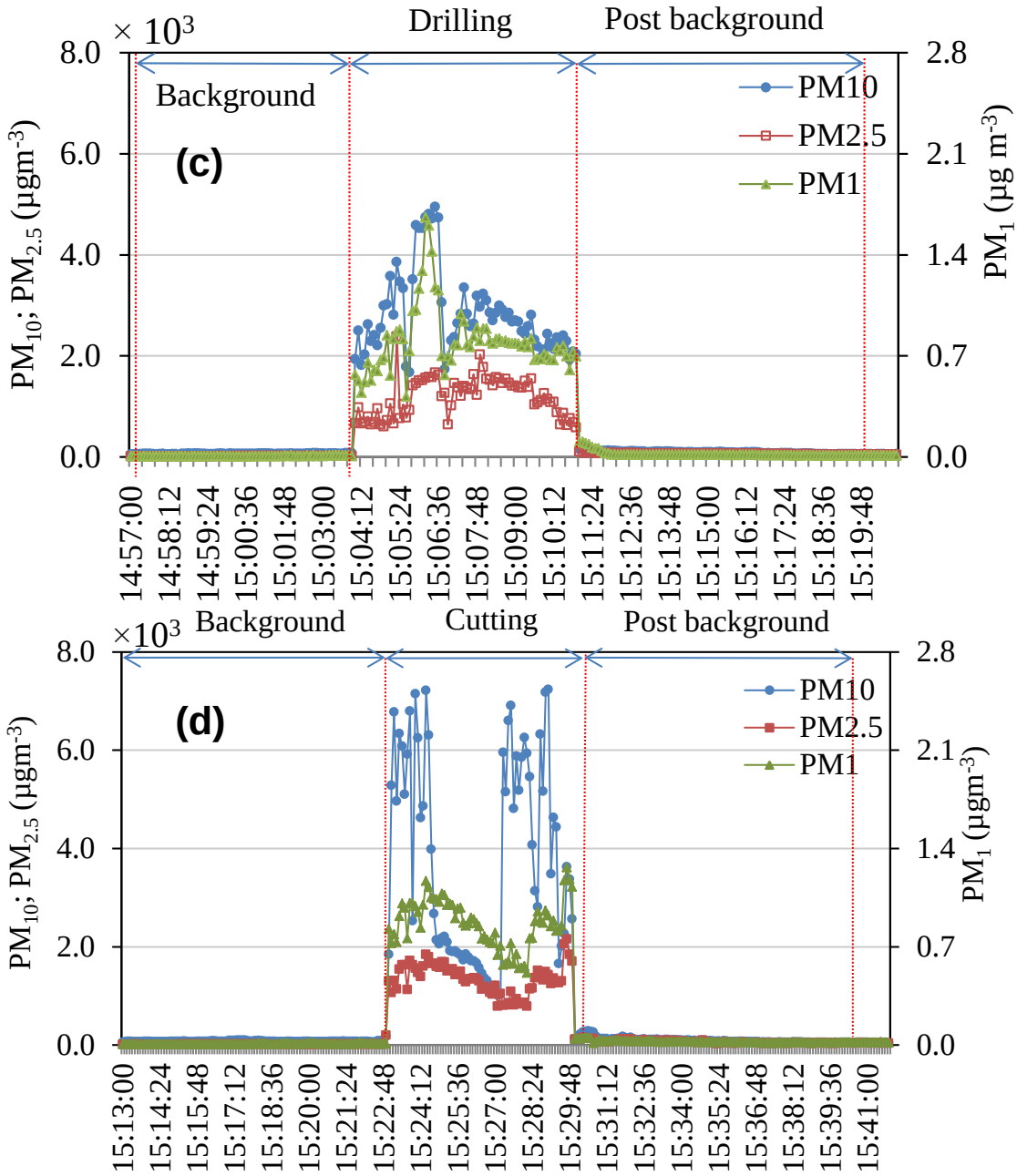

Figure 4.5: Mass concentration against time for (a) mixing with GGBS, (b) mixing with PFA, (c) drilling, and (d) cutting activities.

The peak PMC values of PM_{10}, $PM_{2.5}$ and PM_1 during drilling were 4.94×10^3, 2.38×10^3 and 1.65×10^3 µg m^{-3}, which are higher than the values of 7.21×10^3, 2.05×10^3 and 1.26×10^3 µg m^{-3} for the cutting activity. This substantiates the fact that the cutting activity not only produces more particles, by number (Section 4.3.2) but also greater particle mass emissions compared with the drilling activity.

Overall, the results in Figure 4.5 show an increase in the average PMC over background levels during the various activities reflecting the release of new particles. PM_{10}, $PM_{2.5}$ and PM_1 are 32, 58 and 86 times the background during the mixing of concrete with GGBS and 32, 50, 89 times when mixing concrete with PFA. In the same way PM_{10}, $PM_{2.5}$ and PM_1 for the drilling activity were 45, 80 and 115 times the background during the drilling activity, and 50, 80 and 122 times higher during the cutting activity. Depending on the source the values of PMCs varied, however, in all cases the PMC values increased with increasing PNCs (see Section A1 in Appendix A).

It is interesting to compare these results with the work of Hansen et al. (2008) who carried out environmental sampling of PM during demolition of a hospital building. They found a 2.9-times increase in concentration for particles higher than 0.5 µm and 3.3-times for particles about 1 µm. This increase was less marked than that of demolition by implosion (Dorevitch et al., 2006) which has been shown to be associated with short-term concentrations of PM, 10-times higher than pre-implosion levels.

Table 4.3: The concentrations of PM_{10}, $PM_{2.5}$ and PM_1 during the activity period. STD and percentage fraction (PF) represent standard deviation and particles fraction of mixing with GGBS, PFA, drilling and cutting, respectively.

Activities		PM_{10} Avg ± STD (μg m^{-3})	$PM_{2.5}$ Avg ± STD (μg m^{-3})	PM_1 Avg ± STD (μg m^{-3})
Mixing with GGBS	Background	58.45±9.19	13.37±5.46	6.52±0.65
	Mixing with GGBS	1891.28±1212.20	780.65±769.99	562.23±541.26
	Slump test	736.12±416.50	366.44 ±165.26	278.27±40.13
	Post background	73.70 ±60.84	59.96 ±25.43	17.76±3.80
Mixing with PFA	Background	61.60±8.41	18.71 ±14.88	7.14±1.99
	Mixing with PFA	1986.12±824.44	945.30±405.7	636.61±48.21
	Slump test	846.44±335.68	409.71±402.17	353.67±269.35
	Post background	79.63±48.70	62.63±28.71	18.52±2.16
Drilling	Background	63.40±7.47	14.98±3.17	6.95±2.42
	Drilling	2827.27±820.99	1193.41±391.18	801.49± 228.81
	Post background	86.74±25.56	61.25±13.72	18.87±18.72
Cutting	Background	74.50±13.547	16.76±18.77	7.12±2.55
	Cutting	3777.18±2065.46	1345.85±310.474	867.75±172.37
	Post background	89.03±50.42	61.12±28.65	21.95±7.87

4.3.4 Emission factors

EFs for any activity are calculated in accordance with method described in Section 3.4.1. It was made to identify the number and mass of particles being released from the source and to indicate how many particles can be inhaled by an occupant during the

activities. Figure 4.6 and Figure 4.7 show the EF based on the concentrations measured at occupational exposure range, within 1 meter. It was shown that the EF not only depends on PNCs and PMC but also depends on volume of the drilled or cut area and on the size and sharpness of the cutting tool.

The EFs during the mixing with GGBS, PFA, drilling and cutting activities were 8.25±4.09 $\times 10^4$, 14.95±7.83 $\times 10^4$, 18890.12±4944.36 $\times 10^4$ and 80905.12±56954.83 $\times 10^4$ s^{-1} kg^{-1}, respectively. Relatively higher EF during mixing with PFA compared with GGBS could possibly be due to the differences in hydration and reaction rates of GGBS and PFA with the Portland cement (Li and Zhao, 2003). The higher EF for cutting compared with drilling is possibly due to the high surface area and rotational frequencies, shear stresses and local energy density associated with cutting. It is worth noting that the EFs are expected to be slightly underestimated, given the fact that the sampling was carried out ~1 m away from the source due to a possible dilution between the source and the sampling point. The corresponding values of mass-based EFs for PM_{10}, $PM_{2.5}$ and PM_1 are presented in Table A3 (Appendix A).

Generalising the lab results to real site experiments is helpful as they provide a basis to estimate the realistic values of total particle number (or mass) emissions from an individual activity. For instance, the commercial mixers in construction sites produce on average about 30-40 $m^3 h^{-1}$ (or 20-27 kg s^{-1}) of concrete, depending on the type of concrete being poured (Dhir et al., 2002). Assuming an average value of ~35 $m^3 h^{-1}$ (or 23 kg s^{-1}), and the EFs (in # kg^{-1}; see Table A4 in Appendix A) for average production of mixers on construction sites gives per unit particle number emission of ~7.98×10^8 s^{-1} and 14.44×10^8

s^{-1} during mixing with GGBS and PFA, respectively. Similar estimates can be made for the cutting and drilling activities in order to assess the extent of total particle number emissions from these activities.

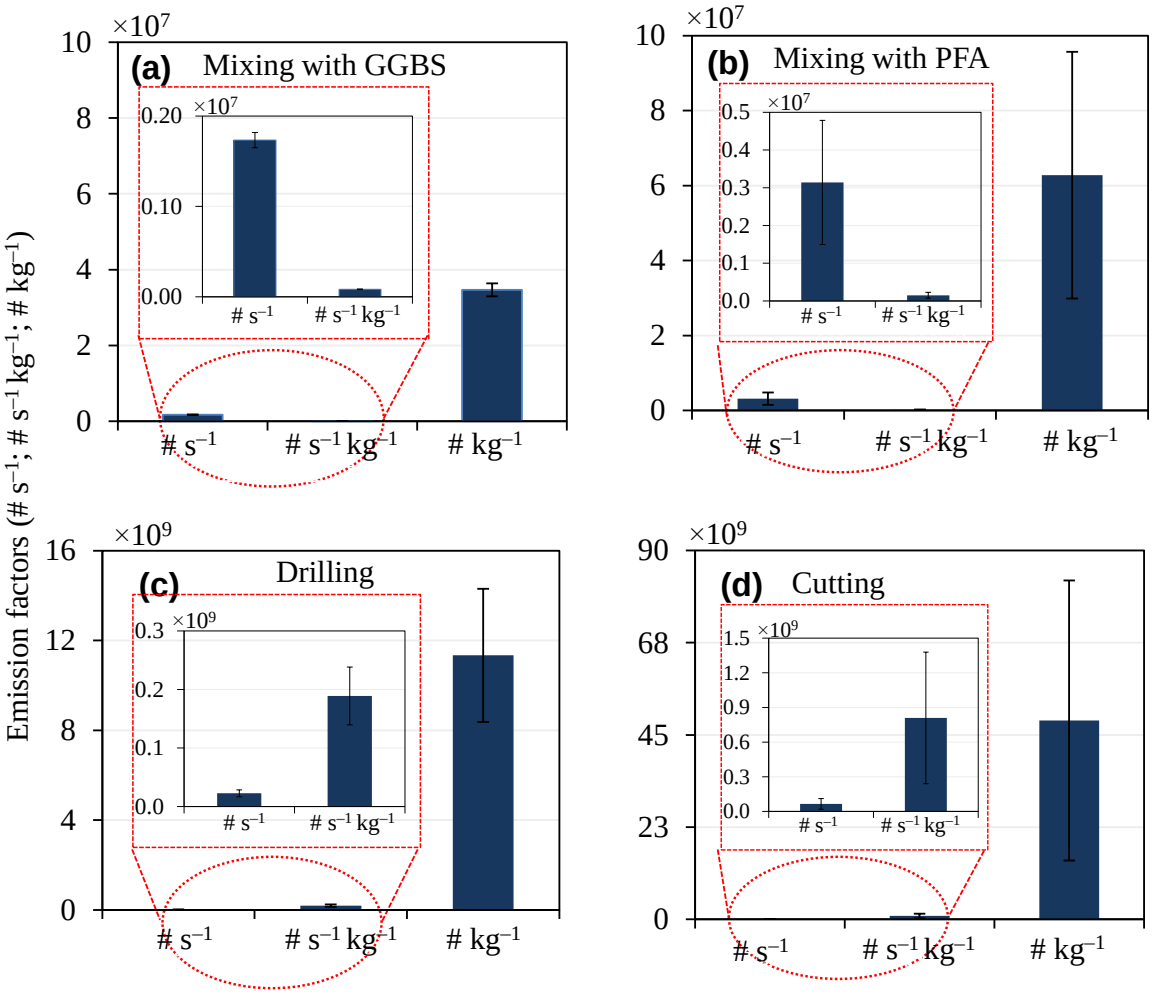

Figure 4.6: Particle number concentration based EFs for all the four activities. Please note that these are net EFs estimated using the net sum of PNCs (i.e. total during the activity period minus the background PNCs during pre-activity period).

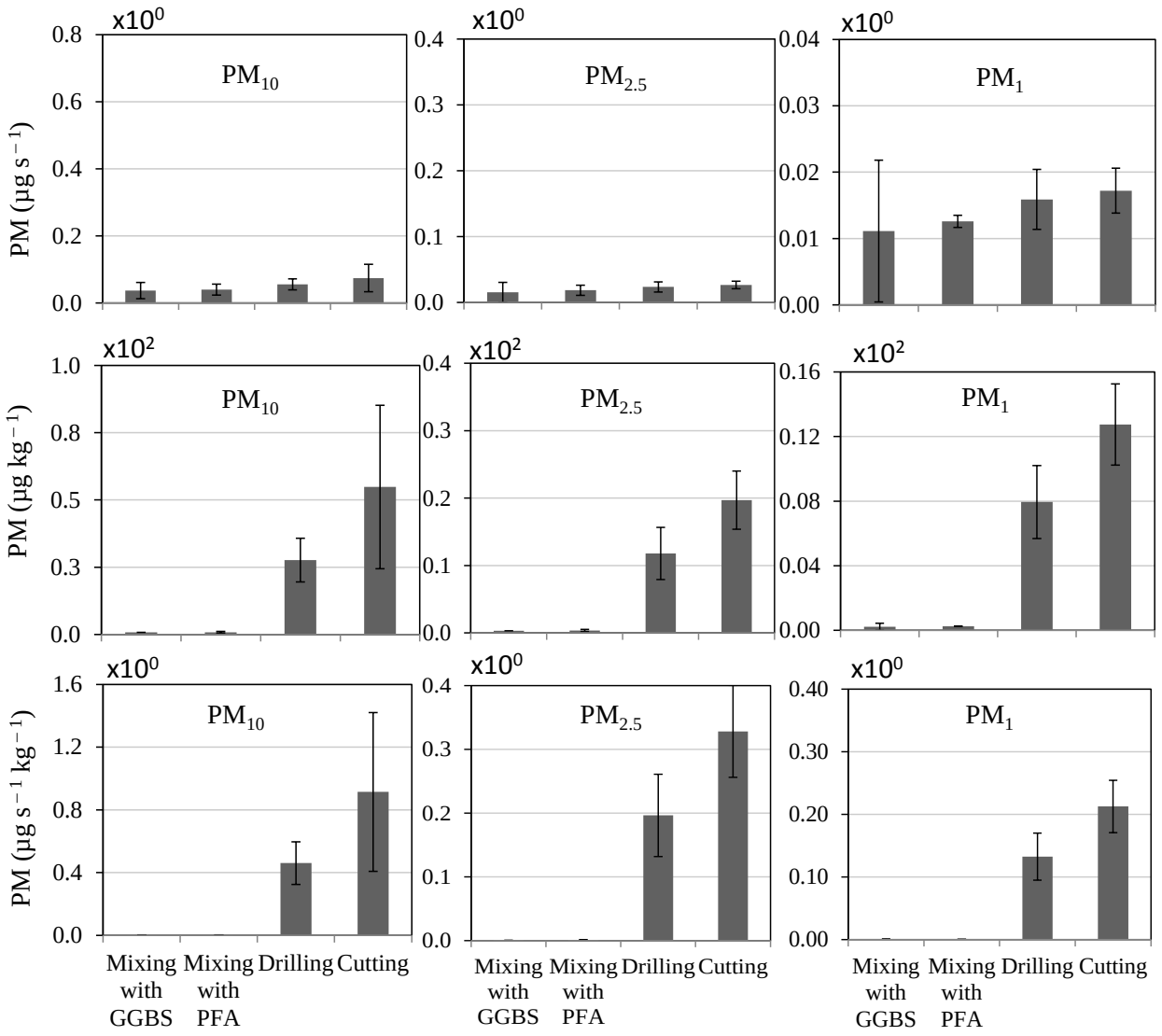

Figure 4.7: Particle mass concentration based EFs for all the four activities. Please note that these are net EFs estimated using the net sum of PMCs (i.e. total during the activity period minus the background PMCs during pre-activity period).

4.3.5 Exposure assessment

Measuring the occupational exposure to ultrafine particles and PM at construction sites is subject to several factors, which influence the level of particles exposure. The first is the size range of the measured particles and their concentration. The average dose rates

over the activities for particle numbers were estimated using (i) constant DF, and (ii) size-dependant DFs and (as described in Section 3.5). The approach (ii) provided the total deposited doses as 2.35±0.31 $\times 10^8$ min^{-1}, 3.40±2.17 $\times 10^8$ min^{-1}, 32.97±9.41 $\times 10^8$ min^{-1} and 88.25±58.82 $\times 10^8$ min^{-1} for mixing with GGBS, with PFA, drilling and cutting, respectively (see Table A5 in Appendix A). Figure 4.8 shows the overall differences between the two approaches. In general, exposure studies using constant DF values can provide a satisfactory approximation of the dose inhaled by commuters. However, an underestimation of dose can be seen for cases in which the vast majority of inhaled particles are in the nucleation mode (i.e. those below 30 nm in diameter).

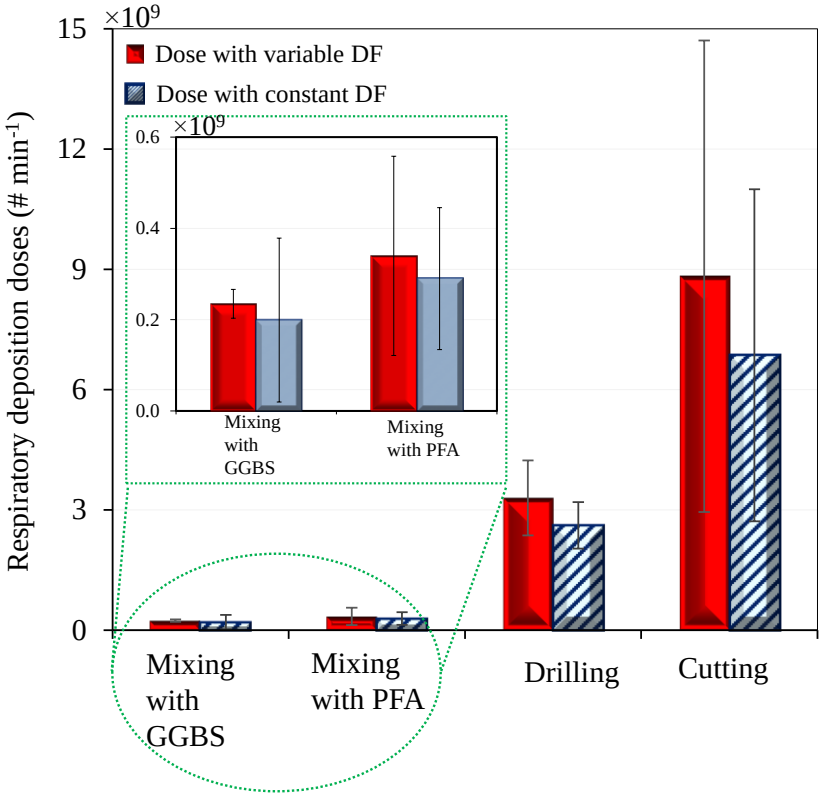

Figure 4.8: Respiratory tract deposition dose rate (# min^{-1}) calculated using (i) size-dependent DFs and average size-resolved PNCs, and (ii) a constant DF and the average PNC for each activity.

There is currently no data available for direct comparison of results of this study with other exposure studies. Therefore the closest possible exposure studies have been picked for this purpose. For example, Kumar and Morawska (2014) reported results on exposure to airborne particles during simulated concrete recycling activity. The deposited fraction of total PNCs were found to be 24.83×10^{8} min^{-1} during exposure close to the source. The deposited fraction for mixing with GGBS, with PFA, drilling and cutting was found to be ~0.09, 0.13, 1.32, and 3.55 times higher, respectively, compared with those obtained by Kumar and Morawska (2014) for concrete recycling. Urban exposure study of Joodatnia et al. (2013a) estimated the average dose rates over the 30 car journeys in Guildford (UK) using used size-dependant DFs as $5.50\pm5.09\times10^{8}$ min^{-1}. These come out ~0.43, 0.62, 5.99 and 16.05 times smaller than those for mixing with GGBS, with PFA, drilling and cutting, respectively. Similarly, Int Panis et al. (2010) calculated the dose rate for cycling and car journeys in Brussels (Belgium) by applying a constant DF (0.63) as 9.02×10^{8} min^{-1} and 1.49×10^{8} min^{-1}, respectively. These are about (0.26, 1.58), (0.38, 2.28), (3.66, 22.12) and (9.78, 59.22) times smaller than those for mixing with GGBS, with PFA, drilling and cutting, respectively.

4.4 Chapter summary and conclusions

A DMS50 and GRIMM were used to measure particle number and size distributions in the 5–10,000 nm size range of particles released by mixing, drilling and cutting activities. The objectives were to understand the number and mass emission characteristics of particles in various size ranges during these simulated building activities, along with

estimating the emission factors and exposure of site workers to ultrafine particles and PM from these activities.

- The cutting was found to produce the highest release of new particles in terms of both PNCs and PNDs, followed by the drilling and mixing activities. Overall, the results confirm that the simulated building activities studied here have the potential to release ultrafine particles at levels above that encountered in the normal background. The use of water sprays as a controlling measure worked well to suppress associated dust release.
- Ultrafine particles were found to dominate the total PNCs with 74, 83, 95 and 97% during the mixing (with GGBS and PFA), drilling and cutting activities respectively, with the highest proportion of ultrafine particles arising from the cutting of concrete. Particles number distributions were dominated by the 5-100 size range during the both drilling and cutting activities.
- The net average PNC after subtracting the background from the PNCs during the mixing with GGBS, PFA, drilling and cutting activities were found to be 1.60, 2.89, 20.92 and 60.49×10^4 cm^{-3}, respectively, showing up 38-times higher values of average PNCs for cutting activity compared with those for mixing with the GGBS.
- The results demonstrate the highest proportion of the total PMCs for coarse particles with 52% during mixing with PFA, and 58, 59 and 64% for the drilling, mixing with GGBS and cutting activities, respectively.
- The average mass concentration of $PM_{2.5}$ and PM_1 during mixing with GGBS, PFA, drilling and cutting were measured as (780.65, 562.23), (945.30, 636.61), (1193.41,

801.49) and (1345.85, 867.75) µg m^{-3}, which shows many times higher values for cutting, and drilling than mixing activities.

- Particle number based emission rates were estimated as 173.41±8.43 $\times 10^4$, 314.01±164.55 $\times 10^4$, 2266.81±593.32 $\times 10^4$ and 6553.34±4613.34 $\times 10^4$ s^{-1} for mixing with GGBS, PFA, drilling and cutting, respectively, which are much lower than the emission rate obtained from floor sweeping activity as 2×10^9 s^{-1} (He et al., 2004).

This study has presented hitherto missing information concerning the potential for concrete mixing, drilling and cutting activities to produce ultrafine particles in significant quantities. This has implications both for the owners of buildings and structures and regulatory bodies, who appear to be unaware of the potential for building works to give rise to ultrafine particles at levels significantly above typical background exposures. Further work now needs to be carried out to compare the results of these laboratory based studies with data from real indoor and outdoor field sites and establish the exposure levels that can occur for those carrying out such activities, and those that live or work adjacent to such sites. For this purpose, the measurements of particles during indoor field activities (i.e. building refurbishment activities) were carried out and the results are presented in Chapter 5.

Chapter 5. Indoor building refurbishment activities

This chapter presents the results of measurements of PM and ultrafine particles measurements, taken during the indoor building refurbishment activities (e.g. welding, wall chasing, sanding and crushing) at an operational refurbishment site. The chapter also provides information on morphology and composition of the particles through SEM, XPS and IBA analysis followed by occupation exposure assessments.

5.1 Introduction

The principles of sustainable urban development are well established, but the extent of pollution due to refurbishment activities is still unknown. The aim of building refurbishment is typically to adapt the existing space to meet the needs and expectations of occupants and bring older buildings up to modern standards for heating, lighting and energy efficiency, as well as to give outdated buildings an upgrading and redesign that goes beyond the cosmetic. The drive for sustainable refurbishment includes both the provision of improved lighting, insulation, ventilation and facilities to ensure the comfort and needs of users as well as related measures to reduce energy consumption in buildings (Mickaityte et al., 2008; Omer, 2008; Sunikka and Boon, 2003).

Within many existing urban environments, refurbishment has become a major, and increasingly important, activity and it is predicted to become the dominant construction activity in the years ahead (Sartori et al., 2008). Due to the increase in rate of population within urban areas (Egbu, 1999; Kumar et al., 2013a), activities related to refurbishment of the building stock as a percentage of all building work have already grown in most European countries over the last 20 years (Kohler and Hassler, 2002). Refurbishment activities are expected to grow further as more than 60% of the world's population are likely to be living in urban areas by 2035 (GroBmann et al., 2013). Such long-term changes in building demand within Europe will constrain the building professions to shift their focus from new construction to the maintenance and refurbishment of existing buildings (Kohler and Hassler, 2002).

In recognition of changes in the age of structure and population rate within urban environments, significant sectors of the construction industry have concentrated on developing innovative refurbishment techniques. However, the various demolition and construction activities associated with building refurbishment are known to produce copious PM, including coarse, fine and ultrafine particles (Kumar et al., 2012b, 2013b). PM has serious environmental and health-related consequences because it contains a wide variety of toxic organic and metallic compounds (Heal et al., 2012). Urban dust, particularly PM_{10}, is harmful since it can be easily introduced in the respiratory system (Davila et al., 2006), although there is increasing interest in $PM_{2.5}$ and ultrafine particles since these penetrate deeper into the lungs and are thought to be of greater concern for human health (Chaloulakou et al., 2003). Building activities produce both airborne dust

(Batonneau et al., 2004) and the emissions of ultrafine particles (Azarmi et al., 2014; Kumar and Morawska, 2014) which are causally involved in greater inflammatory responses than the coarse particles per given mass (HEI, 2013; Kumar et al., 2014). Refurbishment activities are important part of building construction since these can have an associated carbon footprint of the order of 20% of the emissions that arise from the original construction (Pacca and Horvath, 2002). Therefore, the development of efficient monitoring strategies to study the concentration and distribution of urban particles can help in mitigating the effects of urban pollution on public health. As a consequence, it is essential to determine the exposure levels of operatives involved in building refurbishment as well as understanding the distribution and propagation of particulate materials into the surrounding environment.

As described in Section 2.4 (Chapter 2) it has now been established that various size of particles arising from vehicle exhaust and non-vehicle exhaust sources enhance their concentrations in certain areas (Dall'Osto et al., 2011; Hopke et al., 1980; Kumar and Morawska, 2014; Kumar et al., 2010, 2011b, 2013b). A few studies have also reported the particle number and mass emissions arising from the demolition of buildings and transport structures (Dorevitch et al., 2006; Hansen et al., 2008), concrete recycling (Kumar and Morawska, 2014) and road works (Fuller et al., 2002; Fuller and Green, 2004). Several studies have also analysed the composition of particles derived from such sources and a number of attempts have been made to relate the observed elemental concentrations in collected particle samples to such activities (Adachi and Tainosho, 2004; Adhami et al., 2012; Adhami et al., 2014; Batonneau et al., 2004; Chen et al., 2000; Mouzourides et al.,

2015; Pattanaik et al., 2012). Further information about the SEM, XPS and IBA analysis of the particles is presented in Section 2.6 (Chapter 2).

Over the past 35 years, there has been ~20% increase in refurbishment work in relation to the total volume of UK construction output (Egbu, 1999). This study investigates the release of particle number distribution (PNDs) and concentrations (PNCs) in sub-micrometre range, along with PMCs in PM_{10}, $PM_{2.5}$ and PM_1 size range, arising from a number of refurbishment activities and associated occupational exposure for construction workers. The characteristics of these particles have also been investigated to help understand their physicochemical nature and the potential impact of associated exposure on operatives undertaking building refurbishment.

5.2 Materials and methods

5.2.1 Site description and sampling setup

Experiments were carried out at an indoor refurbishment site (Chemistry Laboratory) at the University of Surrey that was 31 m long and 15.5 m wide to measure the PM_{10}, $PM_{2.5}$, PM_1 and ultrafine particles released from refurbishment activities (Figure 5.1). The data were collected for a total of 55 working hours between 08:00 and 18:00 h (local time) over a period of 8 days; of which, one day was without any activity that enabled us to evaluate the levels of local background (Figure 5.2).

The refurbishment site had 1 m wide and 0.32 m deep windows that were slightly open most of the sampling duration (Figure 5.2). However, the ambient wind speed during the sampling period was relatively low (<1.5 m s^{-1}), giving almost steady dilution conditions at the site during the study period. There were also three door openings towards a main

corridor (Figure 5.2) but these doors were covered with a thick plastic sheet acting as a temporary protection shield for trapping the particles released on the site. Further details of the description of site can be seen in Section B1, Appendix B.

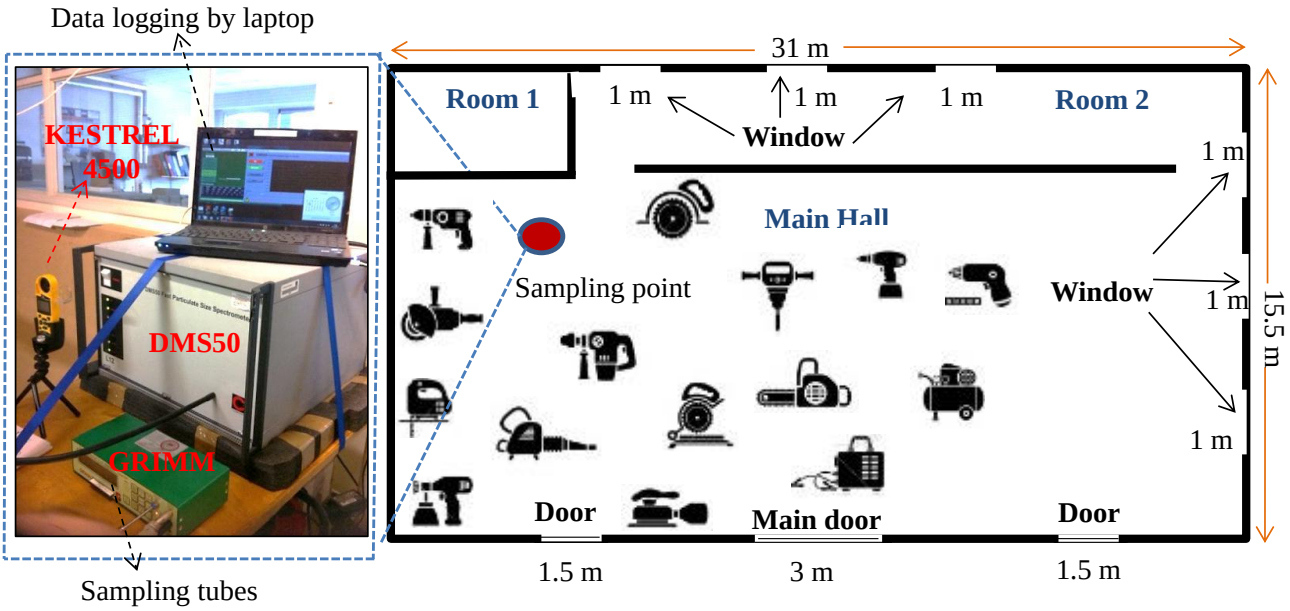

Figure 5.1: Schematic diagram of the experimental set-up, showing instrumentation used and sampling locations.

An exhaustive list of a number of refurbishment activities performed during the sampling period is presented in Table B1 in Appendix B. Over 20 different refurbishment activities were counted, including some of the most frequent ones such as general demolition and cutting of concrete, welding, wall chasing, painting, cutting abrasive blasting, hammering, impact driving, sawing and cementing (Table B1 and Figure B1). Emitted particles were measured in the 5-10,000 nm size range using a GRIMM particle spectrometer (model 1.107 E) and a DMS50, as described in Section 3.2 (Chapter 3). The time stamp of both the instruments was set same to local GMT time. The instrument was placed at the closest safe place (~2 m from the closest activity) at the site (Figure 5.2). Five different samples were also collected on Polytetrafluoroethylene (PTFE) filters by the GRIMM instrument

for the purpose of their physicochemical analysis. These filters collected all the particles above the pore size (0.12 µm) of filters.

Figure 5.2: Number of typical activities involved in refurbishment works including (a) drilling of wood, (b) drilling of concrete slab, (c) cutting, (d) hammering, (e) sanding and (f) ceiling drilling activities.

5.2.2 Collection of PM mass on PTFE filters for SEM, IBA and XPS analysis

Five samples, namely samples 1-5, were collected on PTFE filters that had a diameter of 47 mm and a nominal thickness of ~1000 µg cm^{-2}. Mass of particles was collected on filters 1, 2 and 5 during the refurbishment activities. In order to evaluate the background levels of particles, sample 3 was collected on the same site but on a separate day when the refurbishment activities were completed. Sample 4 was a "blank filter" which was not exposed to any experimental activity. This sample was analysed to set the baseline levels of various elemental species present within the filters. Details on the sampling duration and mass collected on the sampled filters are provided in Table 5.1. Furthermore, SEM, IBA and XPS analysis were conducted on the samples collected on the filters which details of these analysis are described in Section 3.3 in Chapter 3.

Table 5.1: Summary of samples collected on PTFE filters during the refurbishment activity.

Name	Date of sampling	Net time for sampling (min^{-1})	Net mass of particles collected on the filter (µg cm^{-2})
Sample 1	2 and 3 July 2013	804	21.8
Sample 2	4 and 5 July 2013	647	24.4
Sample 3	6 July 2013	459	4.6
Sample 4	Blank	0	0
Sample 5	9, 10 and 11 July 2013	1333	0.6

5.3 Results and discussion

In order to understand the characteristics of particles during different refurbishment and non-refurbishment periods, the measured data of particles in the 5-10,000 nm size

range is divided into three time periods. These included: (i) the "background period" at the site that was measured at one of the weekend days when no refurbishment work was taking place at the site to establish local background concentrations, (ii) the "activity period" when different refurbishment activities were taking place at the site during the working hours, and (iii) the "non-activity period" which represent times during the activity period on working days when workers did not perform any activity for at least an hour or more due to lunch breaks or some other reasons. The non-activity period was important to understand the levels of particle concentrations with respect to background and activity periods.

5.3.1 Number and size distribution of particles

Figure 5.3 presents an overall picture of the average PNDs measured during the background, activity and non-activity periods. The PND spectrum during the activity period was found to be multi-modal and higher than those obtained during the non-activity period (Figure 5.3).

Background periods showed notably lower magnitude of PNDs compared with the activity and non-activity periods that exhibited two clear peaks at about 27 and 80 nm. These two peaks were non-existent during background measurements, clearly showing a significant release of particles from the refurbishment activities in the ultrafine particles size range. These observations are in line with the earlier laboratory studies (Azarmi et al., 2014), showing release of ultrafine particles during the construction activities.

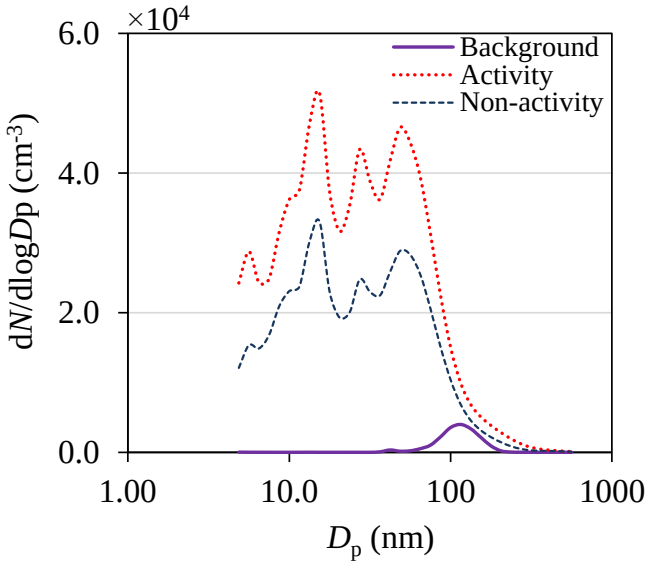

Figure 5.3: Average PNDs during the background, activity and non-activity periods.

A number of individual refurbishment activities were identified during the activity period. Their name and associated time periods are presented in Table B1. Figure 5.4 presents the average PND spectrums measured during these activities and corresponding peak diameters observed are presented in Table B2. These individual activities show remarkably different PND spectrums, with multiple modes and varying peak diameters. One of the interesting observations seen from Table B2 in Appendix B is that activities such as sawing and sanding that involve wood present lower peak diameters compared with those activities such as grinding and cutting involving concrete. These differences can be attributed to the differences in the mechanical process that create these particles, which are also expected to have different material composition. However, one of the common features of the PND from all the activities observed is that the majority of particles are in ultrafine particles range. This range was dominated by a significant proportion of sub–30 nm size particles that contributed up to 90% of total PNCs (Figure 5.4). Earlier work of Kumar et al. (Kumar and Morawska, 2014) on concrete recycling also found multimodal PNDs, showing peak

diameters at ~15, 27 and 56 nm with significant quantities of the particles below 30 nm in diameter.

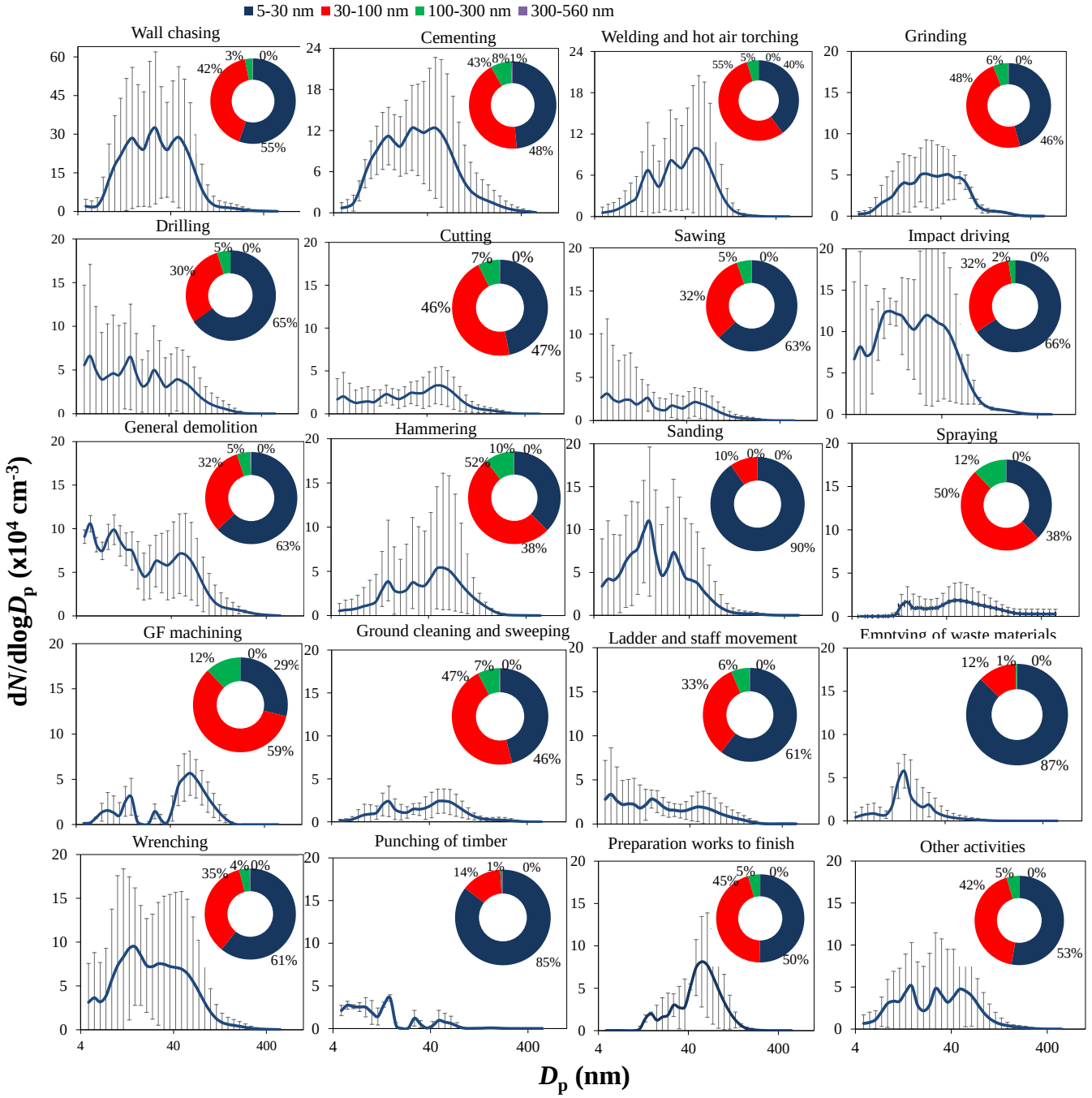

Figure 5.4: Average PNDs and proportion of PNCs in various size ranges for the individual activities. Other activities refer to painting, oiling, carrying metal bars to the site and moving demolished debris.

Wall chasing activity was observed to produce a greatest concentration in terms of release of new particles, reflecting the effect of abrasion between the wall surface and the chasing drill material. An overall increase over the background levels (Figure 5.4) during these activities clearly indicates the emissions of new particles. However, these results did not allow us to draw conclusions on their formation pathways, i.e. whether these emissions are arising from electric motors of different tools used such as those analysed by He et al. (2004) or through other novel mechanism, suggesting a need of dedicated studies in future. In addition, transformation processes such as coagulation, condensation, nucleation and deposition act simultaneously on the number and size distributions of particles. These processes lead to both increase (e.g. nucleation) and decrease (e.g. coagulation and deposition) in PNCs (Kumar et al., 2011a). Coagulation is an aggregation of particles and this aggregation is a function of both the residence time of particles in an experimental setting and their ambient number concentrations (Hinds, 1999). A typical average concentration was measured in the range of ~10^4 cm^{-3} (Section 5.3.2) with the highest PNCs being of the order of ~10^6 cm^{-3} during wall chasing (see Table B3 in Appendix B). The time taken for the 10^4 and 10^6 cm^{-3} in doubling the size of particles through monodisperse coagulation is about 16 days and 4h, respectively (Hinds, 1999). This time is much greater than both the sampling rate (10 Hz) and the air exchange rates at the site (a few 10's of minutes), meaning that the effect of aggregation on measured PNCs can be overlooked.

5.3.2 Particle number concentrations

Average PNCs on a daily basis including background, activity and non-activity periods are summarised in Table 5.2 and their proportions in various size ranges are shown in Figure 5.5. The overall average PNCs (49.14±32.80 $\times 10^3$) during the activity periods were significantly above the background level (1.17±0.80 $\times 10^3$) and showed noteworthy variation from day to day with maximum values being about twice the average. However, the fraction of average PNCs in the 5–30 nm, 30–100 nm and 100–300 nm ranges during the activity and non-activity periods remained nearly unchanged Figure 5.5. There was a much larger change to PNCs in the 5–30 nm size range that, for example, increased from ~0.2% during background to 56 and 55% during activity and non–activity periods, respectively. Such a change was modest (within 6%) between background and activity/non-activity periods for the particles in the 30–100 nm range.

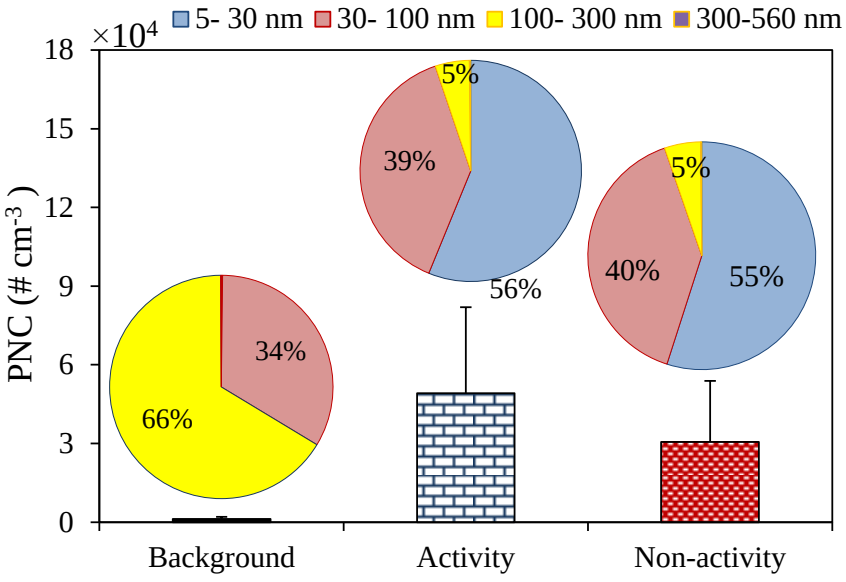

Figure 5.5: Average PNCs during the background, activity and non-activity periods.

Figure 5.6 shows the average PNCs measured over each sampling day and their fractions in various size ranges for individual activities (irrespective of their use on materials type such as concrete, bricks or metal) are presented in Table B3. Average PNCs during all the various activities significantly exceeded measured background levels. The results also demonstrate that drilling of concrete produces much higher PNCs in comparison with drilling of metal or other materials like polyvinyl chloride. For all these activities, the ultrafine size range (5–100 nm) accounted for the majority of the total PNCs (Figure 5.6 and Figure B1 in Appendix B). For example, their proportion to total PNCs during the wall chasing, general demolition, cementing, welding, cutting, wrenching with using gas grips and impact driving on woody boards was between 91 and 97% (Figure 5.4). A major fraction of these ultrafine particles is below 30 nm (Figure 5.5), which are generally formed through gas-to-particle conversion (Kumar and Morawska, 2014; Kumar et al., 2010), but information of such precursor gases were unavailable. It may be the case that the attrition between the surfaces of equipment and building materials during high rotational frequency have produced precursor gases, however, further investigations are clearly needed to reach to a clear consensus. The average values of PNCs during the general demolition activity at refurbishment site were ~2–times lower than those reported by Kumar et al. (2012c) during simulation of slab demolition in the laboratory. Furthermore, results of average PNCs during the drilling activity ($5.22\pm4.44 \times 10^4$ cm^{-3}) was ~5-times lower compared with laboratory studies of Azarmi et al. (2014). This is expected because the emissions in laboratory work were measured close to the source. However, the activities in this work occurred a few meters away from the sampling point to give emission relatively larger time to dilute before measurements.

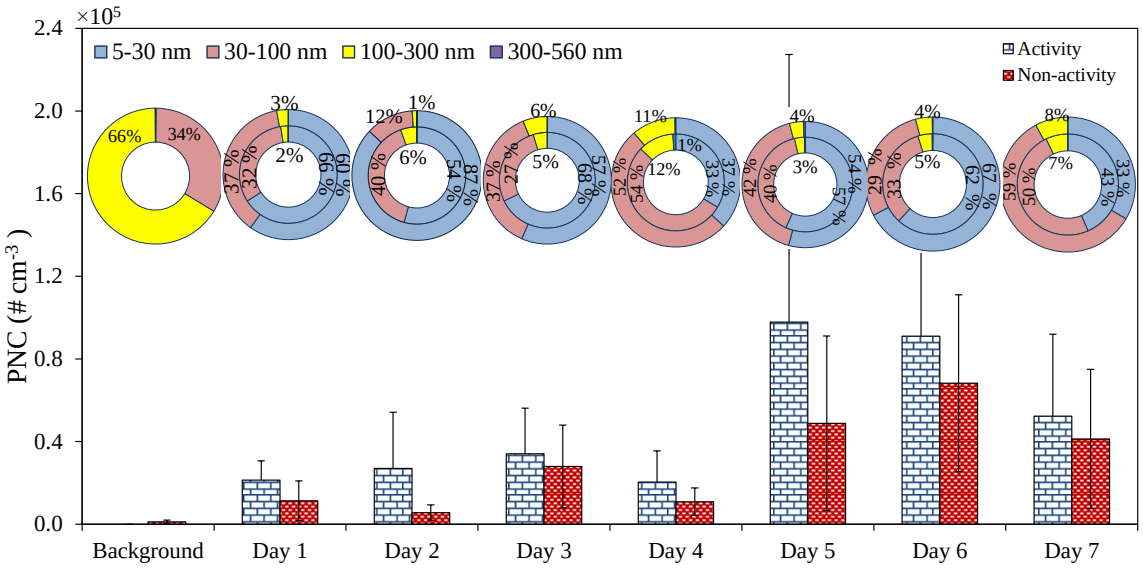

Figure 5.6: The Average PNCs on a daily basis during the background, activity and non-activity periods. The inner and outer circles represent fractions of PNCs in various size ranges during the activity and non-activity periods, respectively.

Table 5.2: Average values of PNCs during the background, activity and non-activity periods on different days.

Activity days	Background	PNC during activity periods ± Standard deviation (# cm^{-3})	PNC during non-activity periods ± Standard deviation (# cm^{-3})
	$1.17\pm0.80 \times10^3$	---	---
1	---	$21.37\pm9.34 \times10^3$	$11.33\pm9.63 \times10^3$
2	---	$26.99\pm27.18 \times10^3$	$5.60\pm3.70 \times10^3$
3	---	$34.09\pm22.07 \times10^3$	$27.90\pm20.06 \times10^3$
4	---	$20.357\pm15.11 \times10^3$	$10.89\pm6.66 \times10^3$
5	---	$97.84\pm129.50 \times10^3$	$48.76\pm42.31 \times10^3$
6	---	$91.04\pm51.07 \times10^3$	$68.24\pm42.74 \times10^3$
7	---	$52.31\pm39.68 \times10^3$	$41.27\pm33.65 \times10^3$
Overall average	$1.17\pm0.80 \times10^3$	$49.14\pm32.80 \times10^3$	$30.57\pm23.28 \times10^3$

5.3.3 Particle mass concentrations

Figure 5.7 shows the overall average of PM_{10}, $PM_{2.5}$ and PM_1 during the background, activity and non-activity periods. These PM fractions were found to be significantly above the background levels (Table 5.3). For instance, PM_{10}, $PM_{2.5}$ and PM_1 were up to 2- and 43-times larger during the activity periods than those during subsequent periods of non-activity and background, respectively (Figure 5.8). Results of this study are not directly comparable to other studies, but similar trend in increased concentrations were observed by the other field studies. For example, Hansen et al. (2008) found a 2.9- and 3.3-times increase in concentration for particles larger than 0.5 and 0.1 μm in size, respectively, during the demolition of a hospital building. The average PM_{10} concentrations measured during refurbishment activities found to exceed by about 20-times the 24-h mean European limit values of 50 μg m^{-3} (Directive, 1999).

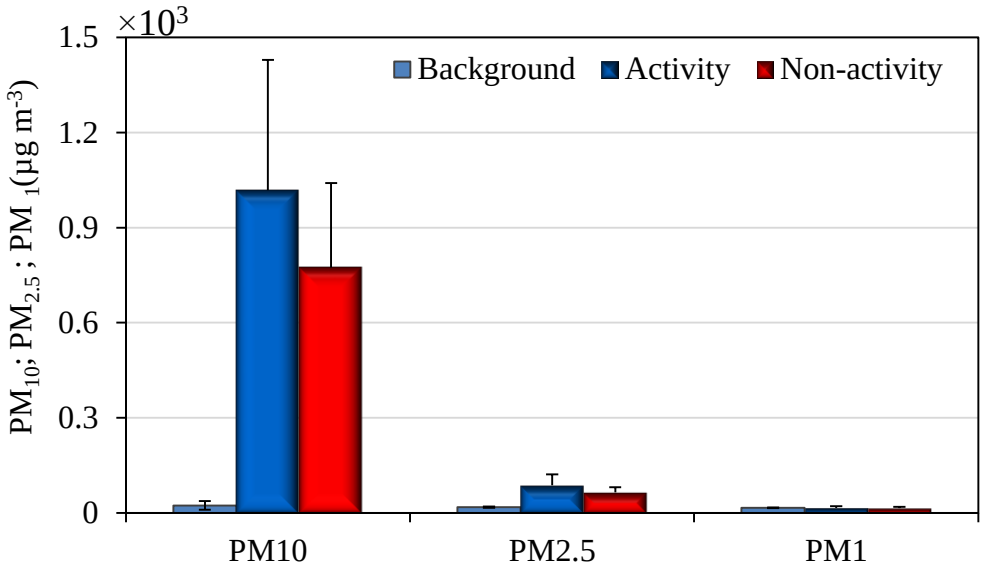

Figure 5.7: The concentrations of PM_{10}, $PM_{2.5}$ and PM_1 during the background, activity and non-activity periods.

Table 5.3: The concentrations of PM_{10}, $PM_{2.5}$ and PM_1 during the background, activity and non-activity periods on different days.

Sampling days	PM_{10} Average± Standard deviation ($\times 10^2$ µg m^{-3})		$PM_{2.5}$ Average± Standard deviation ($\times 10^2$ µg m^{-3})		PM_1 Average± Standard deviation ($\times 10^2$ µg m^{-3})	
Background	-	0.19±0.04	-	0.16±0.01	-	0.14±0.00
	Activity	Non-activity	Activity	Non-activity	Activity	Non-activity
1	6.11±6.08	5.32±3.21	0.49±0.27	0.45±0.14	0.14±0.03	0.14±0.01
2	10.32±7.37	10.16±5.48	0.69±0.46	0.69±0.33	0.11±0.05	0.11±0.03
3	12.87±12.93	8.34±7.78	0.96±0.94	0.66±0.53	0.13±0.09	0.10±0.04
4	15.93±12.28	7.83±8.94	1.43±0.83	0.63±0.59	0.20±0.92	0.19±0.08
5	7.51±5.32	7.04±3.99	0.69±0.41	0.65±0.37	0.12±0.05	0.11±0.05
6	5.05±3.53	3.81±1.93	0.62±0.35	0.50±0.20	0.17±0.82	0.15±0.05
7	13.45±7.64	11.60±3.65	1.18±0.75	0.95±0.26	0.24±0.86	0.19±0.03
Overall average	10.18±4.10	7.73±2.67	0.87±0.33	0.64±0.16	0.16±0.04	0.14±0.03

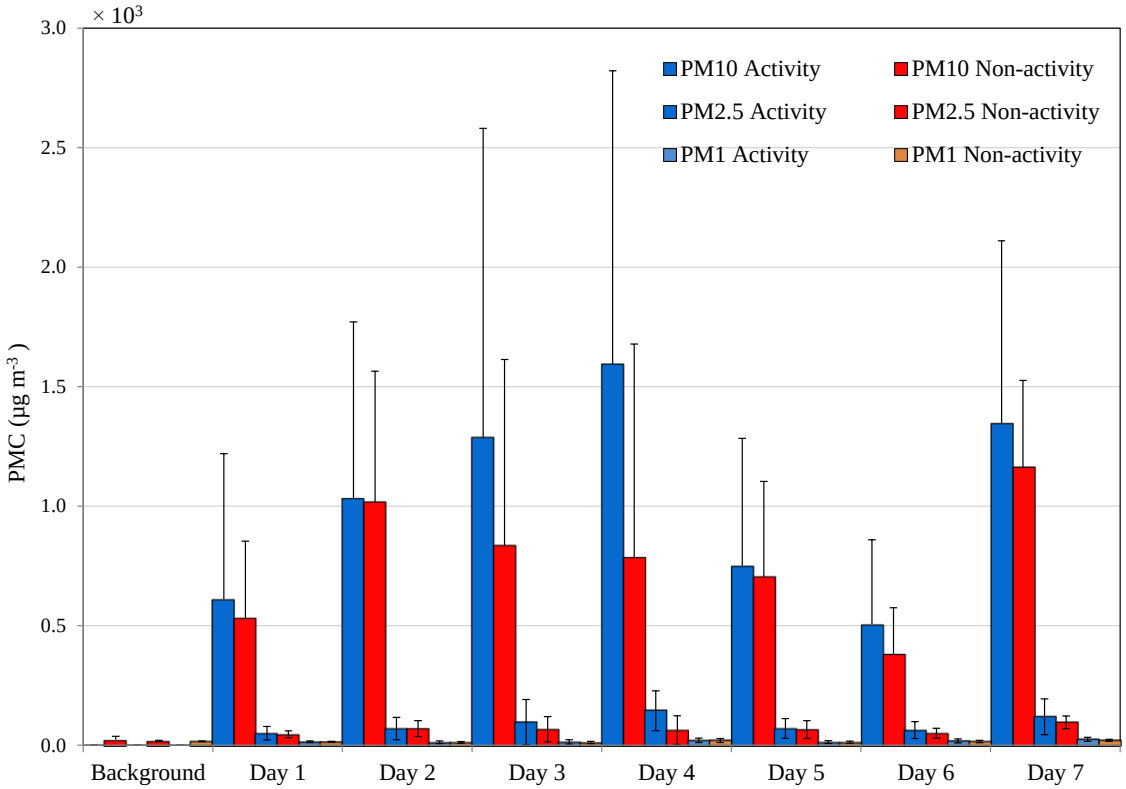

Figure 5.8: The average concentrations of PM_{10}, $PM_{2.5}$ and PM_1 during the background, activity and non-activity period for each day of activity.

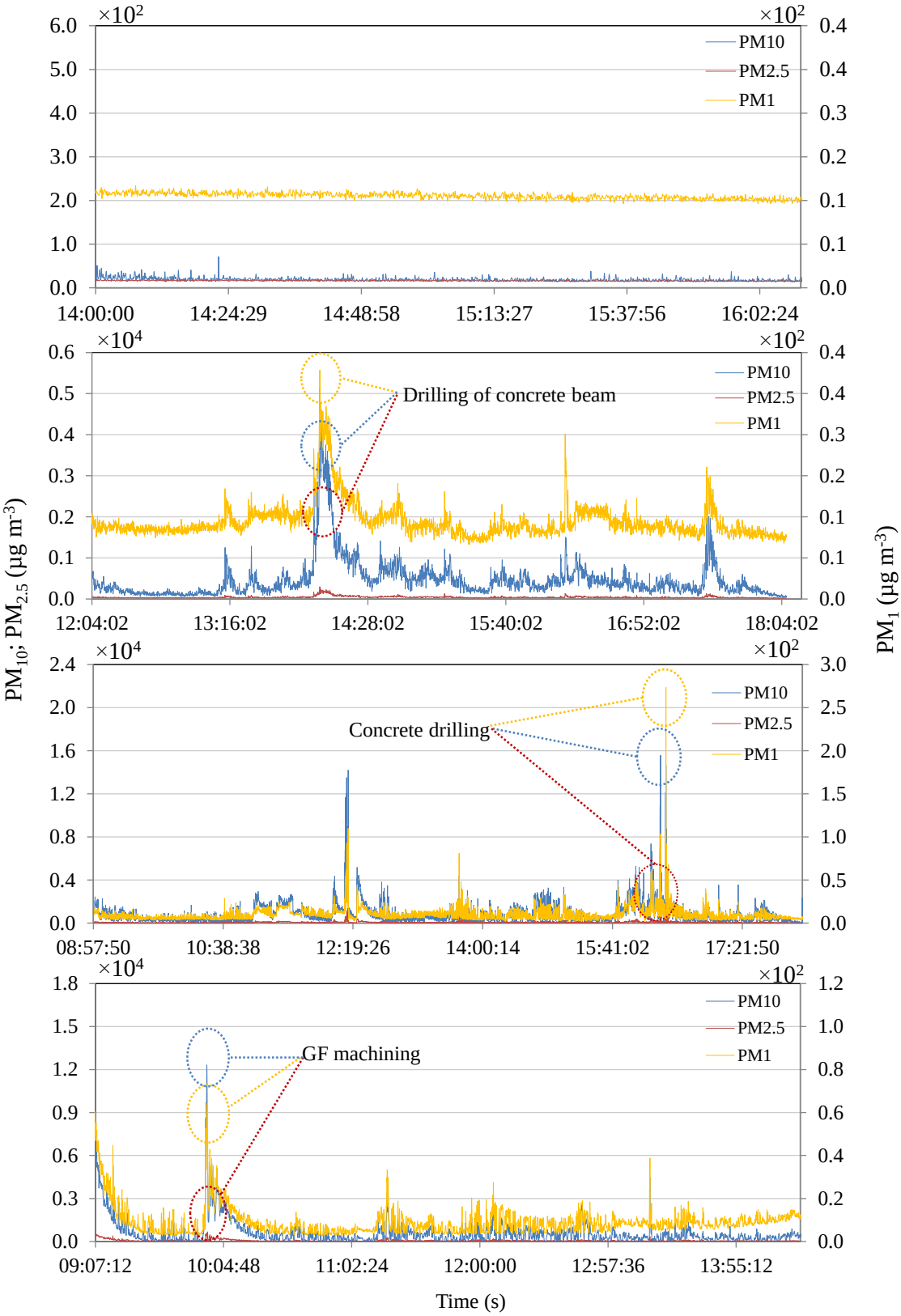

figure continues on next page

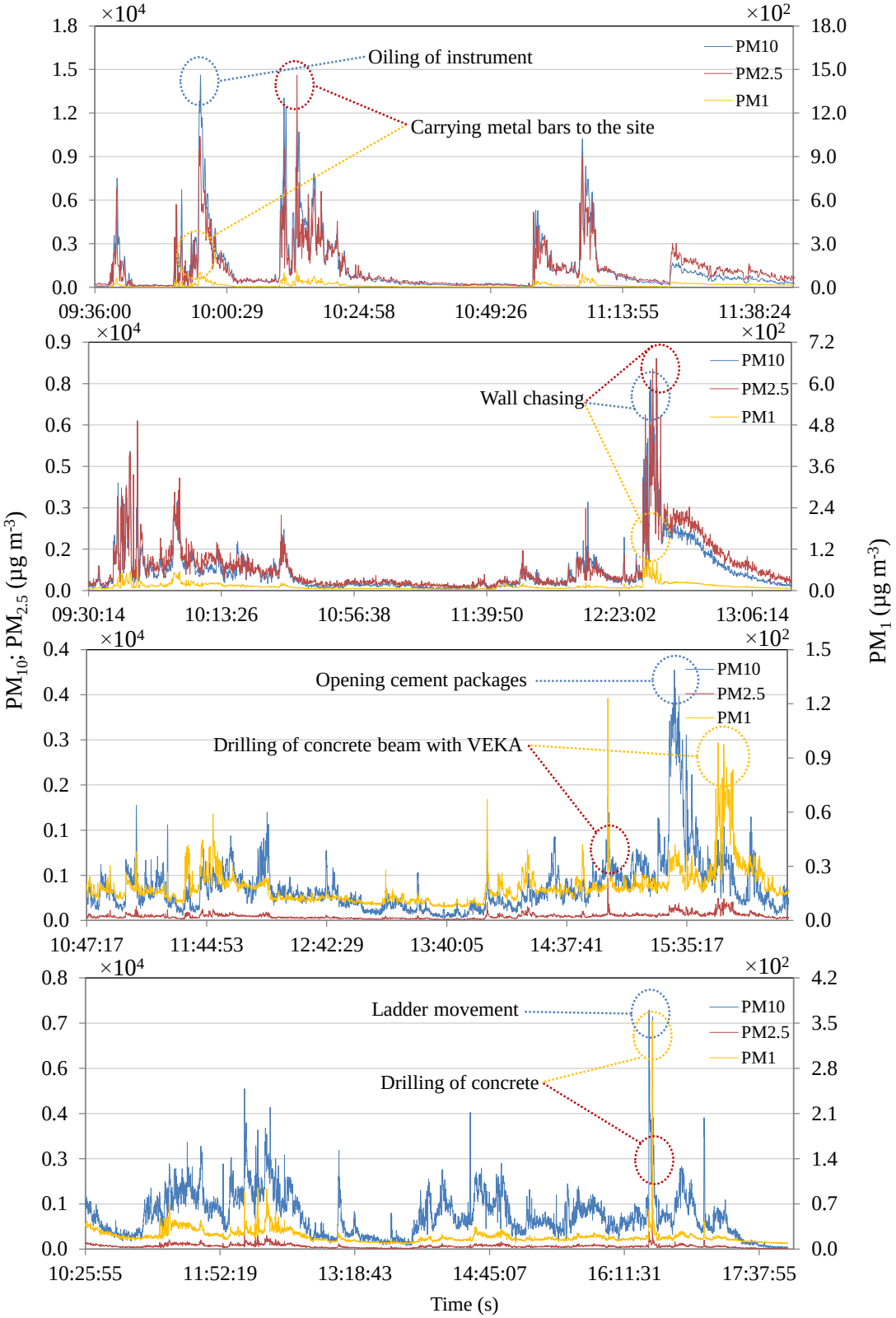

Figure 5.9: The concentrations of PM_{10}, $PM_{2.5}$ and PM_1 during the background and activity period (details of each activity time period is listed in Table B1).

The previous field studies have also found increase in PMCs levels during the activity periods over the background levels. For example, Dorevitch et al. (2006) measured PM_{10} during the demolition of a reinforced concrete building and found 6h averaged concentrations up to about 10-times higher compared with pre-demolition levels which are background concentrations in this case. Likewise, Beck et al. (2003) found ambient levels of PM_{10} to increase by between 8 and 3000-times during implosion of a building compared with pre-demolition levels, depending on the distance of measurement point from the source.

Figure 5.9 confirms that PMC values exhibit a sharp increase immediately after the start of any activity and reach a peak value within a few seconds. The highest peak values for PM_{10}, $PM_{2.5}$ and PM_1 obtained for the drilling activity were 155.60, 19.10 and 3.54 ($\times 10^2$) $\mu g\ m^{-3}$, respectively, which is about 819, 119 and 25-times higher than the background levels. Interestingly, the wall chasing activity produced a higher PNC, but lower PMCs, than those measured during drilling operation, suggesting that the particle sizes produced by the wall chasing were (on average) smaller than those produced by drilling (see Table B3 in Appendix B). Possible reasons for this could be a much greater mechanical attrition between the surfaces of wall and drilling bit materials, generating coarse size particles in higher quantities during drilling.

5.4 Morphology assessment and chemical characterization

SEM, IBA and XPS experiments were conducted on the samples collected on the filters for understanding the morphology and chemical composition of particles such as their shape, structure and chemical composition.

5.4.1 XPS and SEM analysis

Table 5.4 shows the elemental composition of all the five samples described in Table 5.1. The blank filter sample and background contained the main characteristics of Teflon type materials. The shape of the spectrum (see Figure B2 in Appendix B) indicated a thin layer of about 5 mm on the background and blank filters. A very strong peak for fluorine (F) was observed, followed by carbon (C) and oxygen (O) in the background (sample 3) and blank (sample 4) filters. The samples 1, 2 and 5, which were taken during activity periods, also contained calcium (Ca), silicon (Si), copper (Cu), aluminium (Al) and sulphur (S).

The chemical state of Si can be associated to either organosilane or silicon dioxide (SiO_2), depending on the binding energy of the peak (see Figure B2). This is because Si is capable of reacting with an organic compound and it is found to be present in an oxide form. Some of the Al and S compounds and organic hydrocarbons were also found on the surfaces of the filters collected during activity periods (i.e. samples 1, 2 and 5), which were thought of arising from activities such as drilling of aluminium or steel stuff, spraying (galvanizing), cementing and cutting of concrete.

Table 5.4: The elemental composition of the all the filters (quantitative XPS analyses).

Sample 1		Sample 2		Sample 3 (background)		Sample 4 (blank)		Sample 5	
Name	Fraction (%)	Name	Fraction (%)	Name	Fraction (%)	Name	Fraction (%)	Name	Fraction (%)
C	37.4	C	34.9	C	31.2	C	30.3	C	34.3
O	11.1	O	8.2	O	1.2	O	1.0	O	21.5
F	50.5	F	55.3	F	67.6	F	68.7	F	37.5
Ca	0.9	Ca	0.6					Ca	1.5
		Si	0.5					Si	2.2
		Cu	0.2					Cu	0.3
		S	0.4					S	1.2
								Al	2.0

Further analysis showed that the sample 5 contained relatively heavier particles of elements such as Cu. In addition, the intensity of the peaks of other elements such as C, Si and Al was found to be increasing, mainly due to the longer exposure time and thereby leading to larger amount of absorbed particles on the filter. Considering (i) the increment in the intensity of O peak, (ii) its ratio with other peaks such as Si, Al and Ca, and (iii) comparison of the shape of the C1s peak and all the fitted peaks contributing toward it, suggested that these elements appear to be associated with grinding, drilling and welding activities where aluminium oxide, calcium oxide, calcium carbonate, copper oxide compounds are expected to be produced.

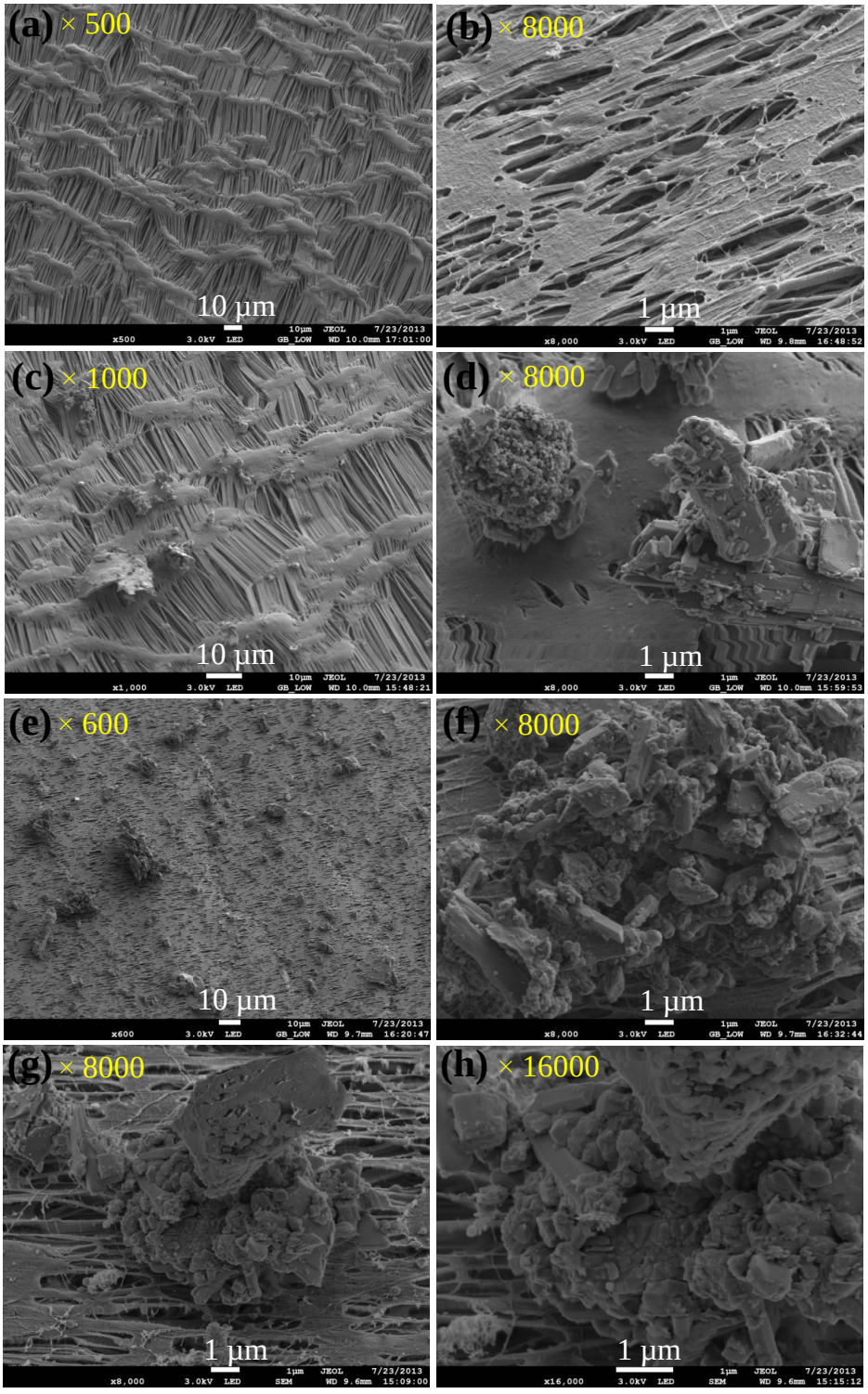

Figure 5.10: SEM images of (a) blank filter at ×500, (b) background measurements at ×8000, (c) sample 1 at ×1000, (d) sample 1 at ×8000, (e) sample 2 at ×600, (f) sample 2 at ×8000, (g) sample 5 at ×8000, and (h) sample 5 at ×16000.

SEM images of the particles collected on filters were taken for understanding the morphology of particles (Figure 5.10). A heterogeneous structure of the sampled particles was found where the irregular shaped aggregated and spongy particles can be seen. A few irregular shaped black holes can also be seen, which represent the porosity of the filters. Differences between particles deposited on the background (sample 3) and blank (sample 4) filters and those collected during the activity periods (samples 1, 2 and 5) represents the presence of new elements (Ca, Si, Cu, S and Al) arising from the refurbishment activities, and some of these elements could be in oxide form as evident by the presence of O (Table 5.4).

5.4.2 IBA analysis

Weight of elemental contents in parts per million (ppm) together with analysis uncertainties and the minimum level of detection (MLD) are shown in Table B4. The filters analysed in this work were much thicker (~3500 µg cm^{-2}) than expected (~1000 µg cm^{-2}) leading to degradation of the accuracy generally achievable for this kind of analysis (Cohen et al., 1996). The Fe-containing nanoparticles tend to form large aggregates of tens of microns size. The possible reason for the high presence of Ca, Si and K is thought to be due to activities related with concrete material (e.g. drilling, cutting and general demolition), which is typically made of cement, water, admixtures and aggregates (Kumar and Morawska, 2014). Furthermore, cement is made of constituents such as silicon oxide (SiO_2), calcium oxide (CaO), aluminium oxide (Al_2O_3), ferric oxide (Fe_2O_3) and sulphate ($\bar{S}$) that acts to bind the components of concrete together. This forms a nonporous, highly cohesive, complex structure containing 10–50 nm diameter capillary pores in well hydrated form (Raki et al., 2010). This suggests that the breaking of concrete containing small pores

may produce particles in various size ranges, as seen in Figure 5.4 (Kumar and Morawska, 2014). The comparison between the results of this section with those presented in Section 5.4.1 shows that Fe and Zn were detected by the IBA but not by the XPS analyses. This difference is possibly due to the different detection levels of sample depth between the IBA and XPS analyses.

5.5 Exposure assessment

The size range of the measured particles and their concentration are key factors for the assessment of occupational exposure to ultrafine and PM. The average respiratory disposition doses of PNCs were estimated using the approach described in Section 3.5.1 for both constant and size-dependant DFs (see Section B3).

The constant and size-dependent DFs provided the total deposited doses as 5.70±5.42 $\times 10^8$ min^{-1}, 2.86±2.17 $\times 10^8$ min^{-1} as well as 7.03±6.65 $\times 10^8$ min^{-1} and 3.57±2.72 $\times 10^8$ min^{-1} for refurbishment activities during the activity and non-activity periods, respectively (see Table B5). These figures show much higher doses for the size-dependent DFs compared to those obtained using the constant DFs (Figure 5.11), mainly due to dominance of particles below 100 nm which is a fraction that also have the largest deposition (ICRP, 1995). This highlights the importance of the availability of size distributions for an accurate exposure assessment.

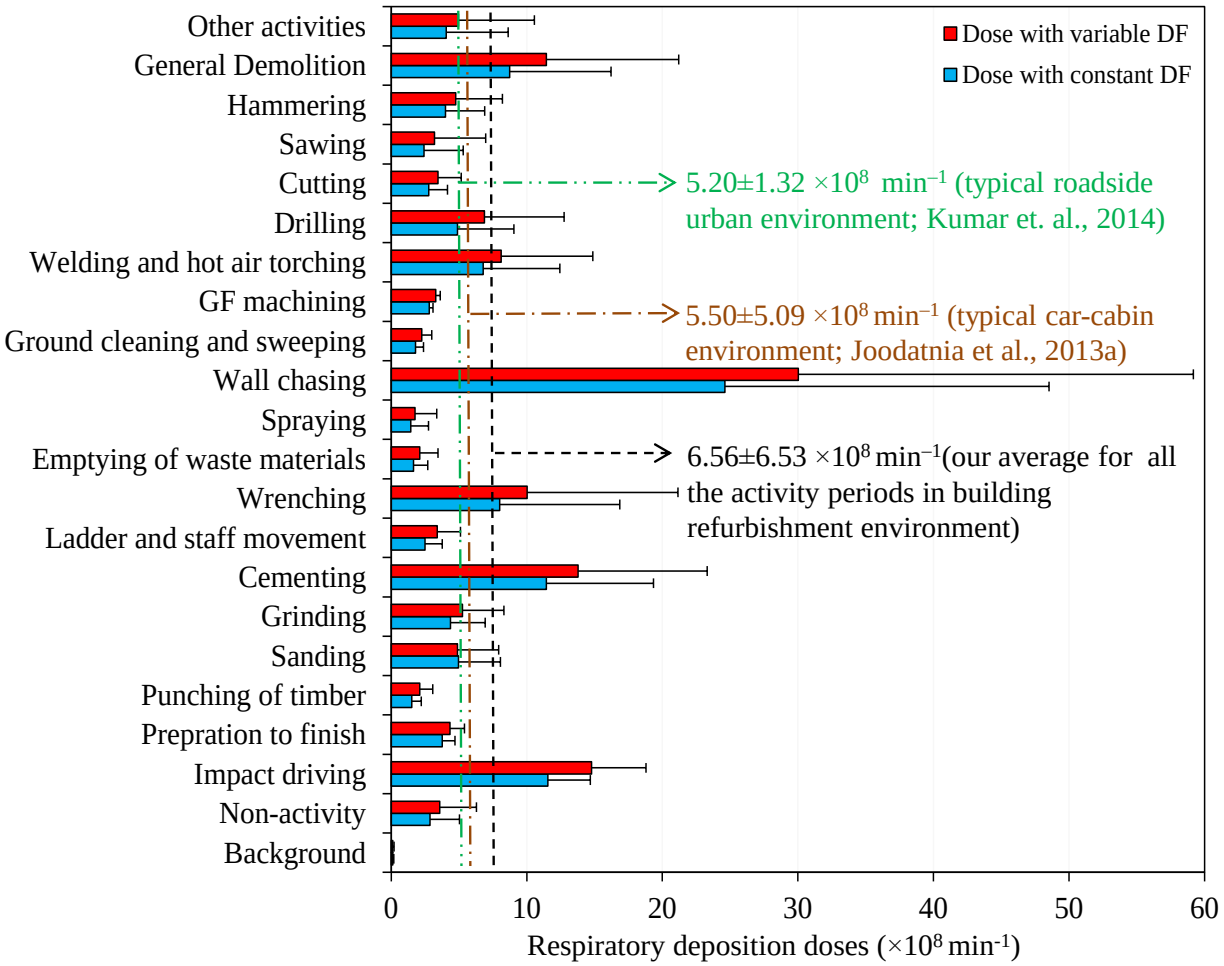

Figure 5.11: Respiratory tract deposition dose rate (# min^{-1}) calculated using (i) a constant DF and the average PNC during each activity and (ii) size-dependent DFs and average size-resolved PNCs.

Lack of exposure assessment studies during refurbishment works make it challenging to directly compare results of this study with published literature. It was tried to pick the closest possible exposure studies for putting the results in a broad perspective. For instance, Kumar et al. (2014) summarised results of 45 sampling locations in 30 different European cities to estimate the respiratory deposition doses of PNCs in urban roadside environments. The corresponding values of such doses were found to be 5.20±1.32 ×10^8 min^{-1} in roadside European environments. Likewise, Joodatnia et al. (2013a) estimated the average

respiratory doses as 5.50±5.09 $\times 10^8$ min^{-1} over 30 car journeys in Guildford, UK. Respiratory deposited doses for refurbishment activities are nearly one and a half times higher than those shown by both studies. These observations clearly indicate that the occupational exposure to workers on refurbishment site is much higher than those experienced in roadside environments. Needless to mention that emission sources (e.g. tailpipe of vehicles) are closest to the roadsides and therefore already high PNCs are expected at such locations (Fujitani et al., 2012; Kumar et al., 2008). For the first time the above findings clearly highlight that workers at the refurbishment sites spend long hours and they are exposed to much higher PNCs than those experienced in outdoor ambient or micro-transport environments, indicating a clear need for limiting occupational exposure at such sites.

5.6 Chapter summary and conclusions

A DMS50 and GRIMM were used to measure number and size distributions of particles in the 5–10,000 nm size range released by numerous activities. While the DMS50 data was used to analyse the PNCs, the data measured from the GRIMM allowed us to assess PMCs in PM_{10}, $PM_{2.5}$ and PM_1 fractions. Mass of bulk particles were also collected on the PTFE filters during background as well as activity periods for understand their physicochemical properties. The objectives were to understand the number and mass emission characteristics of particles in various size ranges during these building activities and assess their physical and chemical properties. The following conclusions are drawn:

- The refurbishment activities were found to release ultrafine particles at levels well-above the local background PNCs. The ultrafine particles were found to dominate (91-

97%) the total PNCs. Average PNCs during the periods of refurbishment activities were found up to 84-times higher than the average PNCs during the background period. The largest PNCs were observed during the wall chasing activity, followed by the drilling and general demolition activities (Table B3).

- Results showed that highest mass concentrations of PM_{10}, $PM_{2.5}$ and PM_1 (i.e. 20.01, 1.52, 0.18 $\times 10^2$ µg m^{-3}) were obtained during general demolition. The peak value of PMC was observed up to about 815-times higher over the background value during the drilling in comparison with the other activities. The mechanical attrition between the surfaces of instrument and materials during the activities and re-suspension of existing particles appears to be a likely source to produce larger-sized particles.
- Combining the results of XPS, SEM and IBA gives the capability of characterising both the micro- and nano-sized particles. The increase of the surface composition of new peaks and decrease of the F and C-F peaks shows higher level of deposition of the particles on the filter and that the Fe-containing particles tend to form aggregates of few 10 µm. These analyses showed the presence of the elements such Ca, Si, Cu, K, S, Zn and Al on the collected samples. These elements were presumably released from the building equipment and materials (e.g. concrete, bricks and metals) involved in the refurbishment activities.
- Occupations exposure to workers on the building refurbishment sites were found to contribute much higher exposure compared with typical roadside urban environments. Peak respiratory deposition doses during activity periods were over two orders of

magnitude higher than those during the background periods, showing a broad diversity in the emission strengths of various refurbishment activities.

The study presented hitherto missing information that the refurbishment activities produce ultrafine particles in dominant proportions. These high levels of ultrafine particle suggest that there is a need to design appropriate risk mitigation strategies to limit exposures of on-site workers. Further information about the particle emissions from an outdoor field site (i.e. construction site) can be found in Chapter 6.

Chapter 6. Outdoor construction activities

This chapter presents the results of measurements of PM_{10} and $PM_{2.5}$ concentrations arising from outdoor construction activities along with meteorological data on the surrounding environment in London. The chapter also provides information on analysis using bivariate concentration polar plots, followed by k-mean analysis.

6.1 Introduction

Construction developments in both the developing and developed world are common. However, the impact of PM emitted in coarse and fine particle size range from such activities on the surrounding areas is yet poorly understood. Construction and demolition of structures is known to result in higher local concentrations of PM_{10}, which contains a wide variety of toxic organic substances and may adversely affect the respiratory health of nearby residents (Anderson, 2009; Brunekreef and Holgate, 2002; Davila et al., 2006; Heal et al., 2012; Loomis, 2000). There is also an increasing interest in $PM_{2.5}$ since it penetrates deeper into the lungs and is of even greater concern for human health (Chaloulakou et al., 2003; Pekkanen et al., 1997; Pope, 2000). For this reason, exposure to $PM_{2.5}$ is globally the 9th most powerful risk factor for diseases burden (Lim et al., 2013; Oberdörster, 2000). Further information about the health and environmental impacts of the particle emissions is presented in Section 2.7 (Chapter 2). Until recently, only limited research has focused on exposure to the PM_{10} and even less research on exposure to the

$PM_{2.5}$ fractions arising from outdoor construction activities and understanding their potential impact on local air quality (Table 2.1). As described in Section 2.4 in Chapter 2, besides the construction activities, PM_{10} concentrations are also affected by the emissions arising from local fugitive sources such as road works (Amato et al., 2009; Fuller et al., 2002; Fuller and Green, 2004; Ho et al., 2003; Tian et al., 2007), vehicle exhaust (Abu-Allaban et al., 2007; Cadle et al., 1999; Kean et al., 2000; Kumar et al., 2010; Kumar et al., 2011a) and non-vehicle exhaust sources (Chow et al., 2006; Dall'Osto et al., 2011; Hopke et al., 1980; Kumar and Morawska, 2014; Kumar et al., 2013; Saliba et al., 2010). At the same time, many activities associated with the air and sea transportation produce particles across the range of PM_{10} and $PM_{2.5}$ (Andrews et al., 2010; Bates et al., 2008; Corbett et al., 2007). A few studies have investigated the PM_{10} emissions arising from industrial sources such as waste transfer stations (Barratt and Fuller, 2014). There are also a few studies concerned with PM_{10} emissions arising from the outdoor construction activities (Beck et al., 2003; Dorevitch et al., 2006; Hansen et al., 2008; Joseph et al., 2009). However, there is still very little work focusing on the $PM_{2.5}$ fractions arising from construction activities (Muleski et al., 2005).

The importance of particle exposure from construction sources is expected to increase with the ever growing world population (Egbu, 1999; Kousa et al., 2002a). In addition to concerns associated with the short-term exposure to airborne PM at the time of construction activities, there is also a potential for long-term exposure to PM that settles across the

nearby community and then is available for inhalation or ingestion after resuspension (Abu-Allaban et al., 2006; Beck et al., 2003; Lioy et al., 2002).

European Union Directive (1999) set the targets to limit daily and annual mean values of PM_{10} at the EU level for year 2004 and 2010 (Fuller and Green, 2004). The legal limit by 2005 was to achieve daily mean PM_{10} concentration of 50 μg m^{-3}, not exceeded on more than 35 occasions per year and annual mean values of 40 μg m^{-3}. Also the target by 2010 was to achieve daily mean PM_{10} concentration of 50 μg m^{-3}, not exceeded on more than 7 occasions per year and annual mean concentrations of 20 μg m^{-3}. These target values to be met by 2010 were not carried forward in the Directive 2008/50/EC (Directive, 2008). For example, Fuller and Green (2004) noted that the PM_{10} emissions generated by building and road works in and around London breached EU limits of daily mean PM_{10} concentrations (50 μg m^{-3}) on several occasions. In this work, a series of PM_{10} and $PM_{2.5}$ measurements at 17 monitoring stations around construction sites were carried out during 2002–2013 to assess their impact on the air quality in surrounding areas.

6.2 Materials and methods

6.2.1 Description of the sites and sampling set ups

Measurements were carried out around three outdoor construction sites, which are referred hereafter as CS_1, CS_2 and CS_3, respectively. CS_1, CS_2 and CS_3 covered an area of about 260×10^4, 54×10^4 and 3×10^4 m^2, respectively (Figure 6.1). There were 17 monitoring stations (i.e. MS_1–MS_{17}) around these three outdoor construction sites (CS_1, CS_2 and CS_3), which represented a diverse range of construction activities. The locations of the

monitoring stations around these sites are shown in Figure 6.1, but the specific details about the location have been kept anonymous for the protection of confidential information.

Continuous air quality monitoring was carried out at 17 different monitoring stations around three construction sites to measure the concentration of PM_{10} and $PM_{2.5}$. The measurements of PM concentrations analysed in this paper were during the periods of construction, and there were no similar measurements made before and/or after construction works. Measurements were undertaken continuously and divided into working hours (referred to as working period) in weekdays between 08:00 and 18:00 h (local time) and non-working hours (referred to as non-working period), which covered the weekdays between 18:00 and 08:00 h and the weekends.

Data were collected over a period of about 4000 days for about 12 years between 2002 and 2013 at these 17 different monitoring sites around CS_1-CS_3 (Table 6.1). A diverse range of construction works during the different phases of the construction were anticipated at the studied sites. However, I did not have access to information of the different phases of the construction processes at each site, except the overall duration of the works.

Data were analysed with reference to the EU Limit Values for annual and daily PM_{10} concentrations. In addition, bivariate plots were drawn to qualitatively assess the effects of wind speed and direction on the measured concentrations in upwind and downwind directions from construction sites. The k-means clustering technique was then applied to assess contribution of probable local construction sources, which were identified through bivariate polar plots of paired monitoring stations (i.e. one in upwind and the other in

downwind). The k-means clustering technique helped to identify the range of increments in particle mass concentrations due to the construction operations, including the resuspension and emissions from any on-site vehicles (Carslaw and Ropkins, 2012). Also frequency and variation in PM_{10} and $PM_{2.5}$ concentration in prevailing wind direction were evaluated with changes in distance from sources by pairing the sites in downwind of the CS_1-CS_3 in order to assess the decay profile of the PM emissions, which is important to understand the impact of the construction works on the air quality in surrounding areas.

PM concentrations at CS_1 were collected using TEOM 1400 and those at CS_2 and CS_3 were measured by Osiris instrument (model 2315) as described in Sections 3.2.3 and 3.2.4 in Chapter 3. Practical constraints such as space and cost, were important factors in the instrument selection.

The meteorological data were produced taking a mean from a number of different monitoring locations across the monitoring stations and construction areas where the meteorological equipment is considered to be working well and the data shows a good correlation. The measurements were made using cup anemometers and wind vanes (as opposed to sonic anemometers) mainly made by Campbell Scientific. This equipment was located at a height of about 10 m.

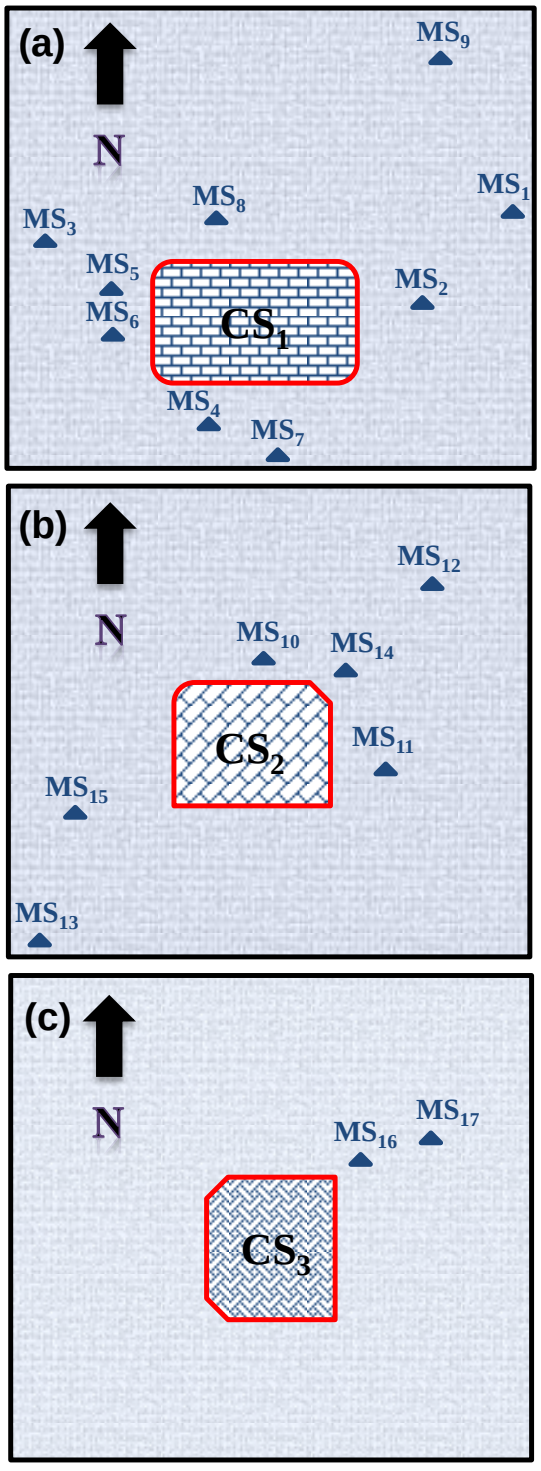

Figure 6.1: Schematic map of the experimental set-up, showing monitoring stations (MS) and construction sites: (a) one (CS_1), (b) two (CS_2) and (c) three (CS_3). Please note that the figure is not to scale and distances are presented in Table 6.1.

Table 6.1: Description of monitoring stations around the construction sites. Monitoring stations S1-S9, S10-S15, and S16-S17 below are around the CS_1, CS_2 and CS_3, respectively.

Site Code	Duration	Species Monitored	Instrument used	Location (distance of MS from CS)
MS_1	January 2002- January 2007	PM_{10}	TEOM 1400	CS_1 (3000 m)
MS_2	January 2002- January 2007	PM_{10}	TEOM 1400	CS_1 (500 m)
MS_3	January 2002- January 2007	PM_{10}	TEOM 1400	CS_1 (500 m)
MS_4	January 2002- January 2007	PM_{10}, $PM_{2.5}$	TEOM 1400	CS_1 (100 m)
MS_5	January 2002- January 2007	PM_{10}, $PM_{2.5}$	TEOM 1400	CS_1 (200 m)
MS_6	January 2002- January 2007	PM_{10}, $PM_{2.5}$	TEOM 1400	CS_1 (200 m)
MS_7	January 2002- January 2007	PM_{10}, $PM_{2.5}$	TEOM 1400	CS_1 (500 m)
MS_8	January 2002- January 2007	PM_{10}, $PM_{2.5}$	TEOM 1400	CS_1 (500 m)
MS_9	January 2002- January 2007	PM_{10}, $PM_{2.5}$	TEOM 1400	CS_1 (4000 m)
MS_{10}	January 2009- December 2013	PM_{10}	OSIRIS 2315	CS_2 (100 m)
MS_{11}	December 2009- May 2013	PM_{10}	OSIRIS 2315	CS_2 (200 m)
MS_{12}	November 2008- December 2013	PM_{10}	OSIRIS 2315	CS_2 (1000 m)
MS_{13}	January 2009- December 2013	PM_{10}	OSIRIS 2315	CS_2 (3000 m)
MS_{14}	May 2013- December 2013	PM_{10}	OSIRIS 2315	CS_2 (100 m)
MS_{15}	January 2009- October 2014	PM_{10}	OSIRIS 2315	CS_2 (400 m)
MS_{16}	June 2011- August 2012	PM_{10}	OSIRIS 2315	CS_3 (100 m)
MS_{17}	June 2011- August 2012	PM_{10}	OSIRIS 2315	CS_3 (50 m)

6.3 Results and discussion

6.3.1 Bivariate concentration polar plots

Bivariate polar plots were used to recognise different sources of PM and their characteristics at the construction sites (Mouzourides et al., 2015; Westmoreland et al., 2007). Figure 6.2 shows the polar plots that were constructed by partitioning wind speed and direction data and their corresponding hourly mean PM concentration data into wind speed and direction bins (Carslaw and Ropkins, 2012). These plots are presented as smoothed surfaces showing variations in concentrations, depending on the local wind direction and wind speed at a receptor (Carslaw and Beevers, 2013). The results presented in Figure 6.2 show evidence of increased PM_{10} and $PM_{2.5}$ concentrations levels when the wind direction is from the construction sites to the monitoring stations.

Closer inspection of polar plots at all 17 monitoring stations around each of the three sites indicates the following. Firstly, whenever there are monitoring stations in the downwind side of the construction sites, high concentrations of PM_{10} (Figure 6.2) and $PM_{2.5}$ (Figure 6.3) are seen, indicating a potential contribution from the construction activities (Figure 6.2). Secondly, pockets of high PM concentrations can also be seen in some cases (for example, see MS_2 for PM_{10} and MS_9 for $PM_{2.5}$ in Figure 6.2a and Figure 6.3, respectively) despite the monitoring stations being in the upwind of east and south-west wind directions. This is expected due to long-range transport of PM_{10} during easterly winds from European countries (Liu and Harrison, 2011; Smethurst et al., 2012) and the effect of generated sea salt on $PM_{2.5}$ from the south-westerly winds (Jones et al., 2010; Liu and Harrison, 2011).

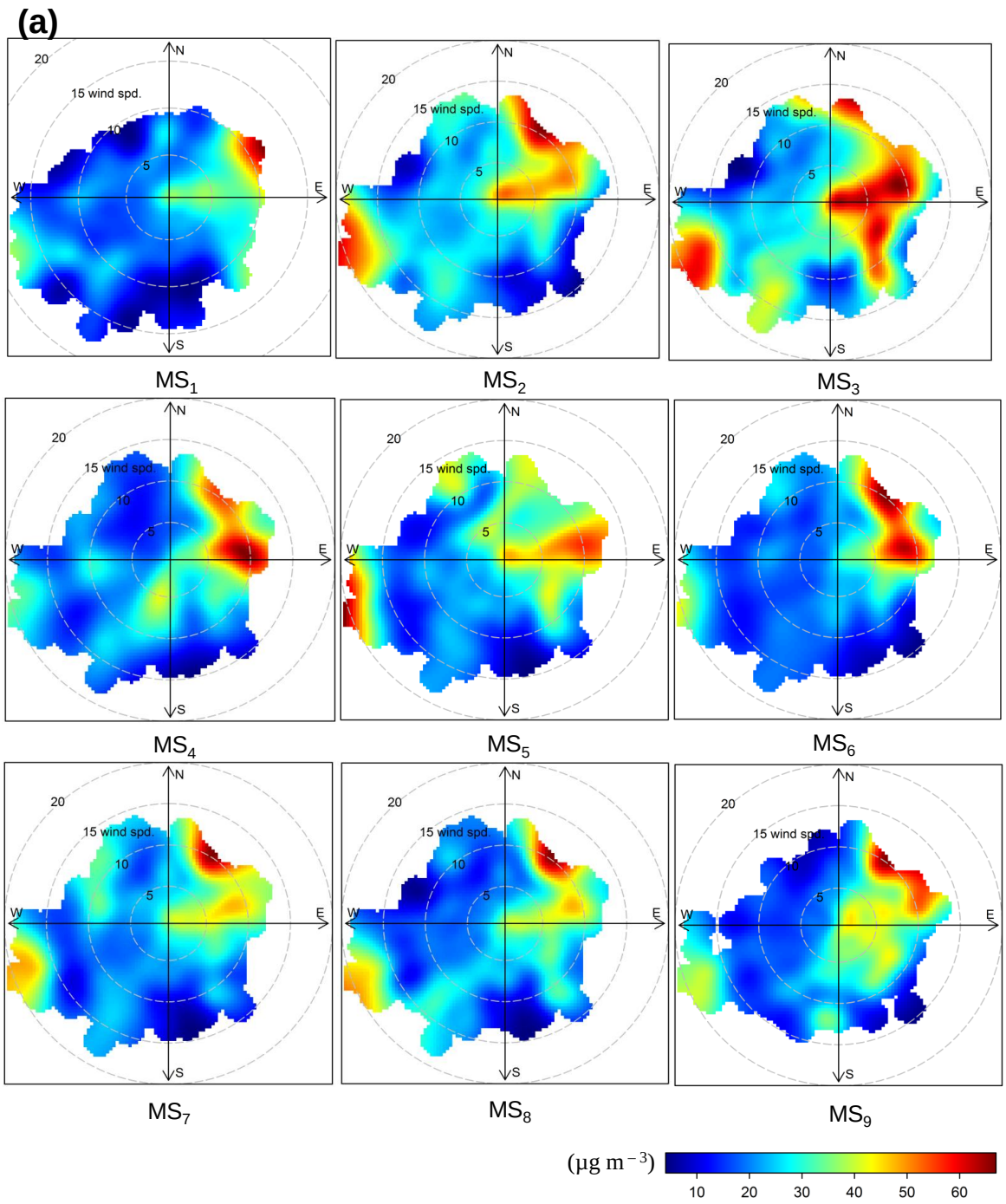

Figure 6.2: Polar plots for PM_{10} at the (a) CS_1, (b) CS_2 and (c) CS_3; hourly average values during 24-h measurements were used for all pollutants. These plots present as smoothed surfaces how concentrations vary depending on the local wind speed and wind direction.

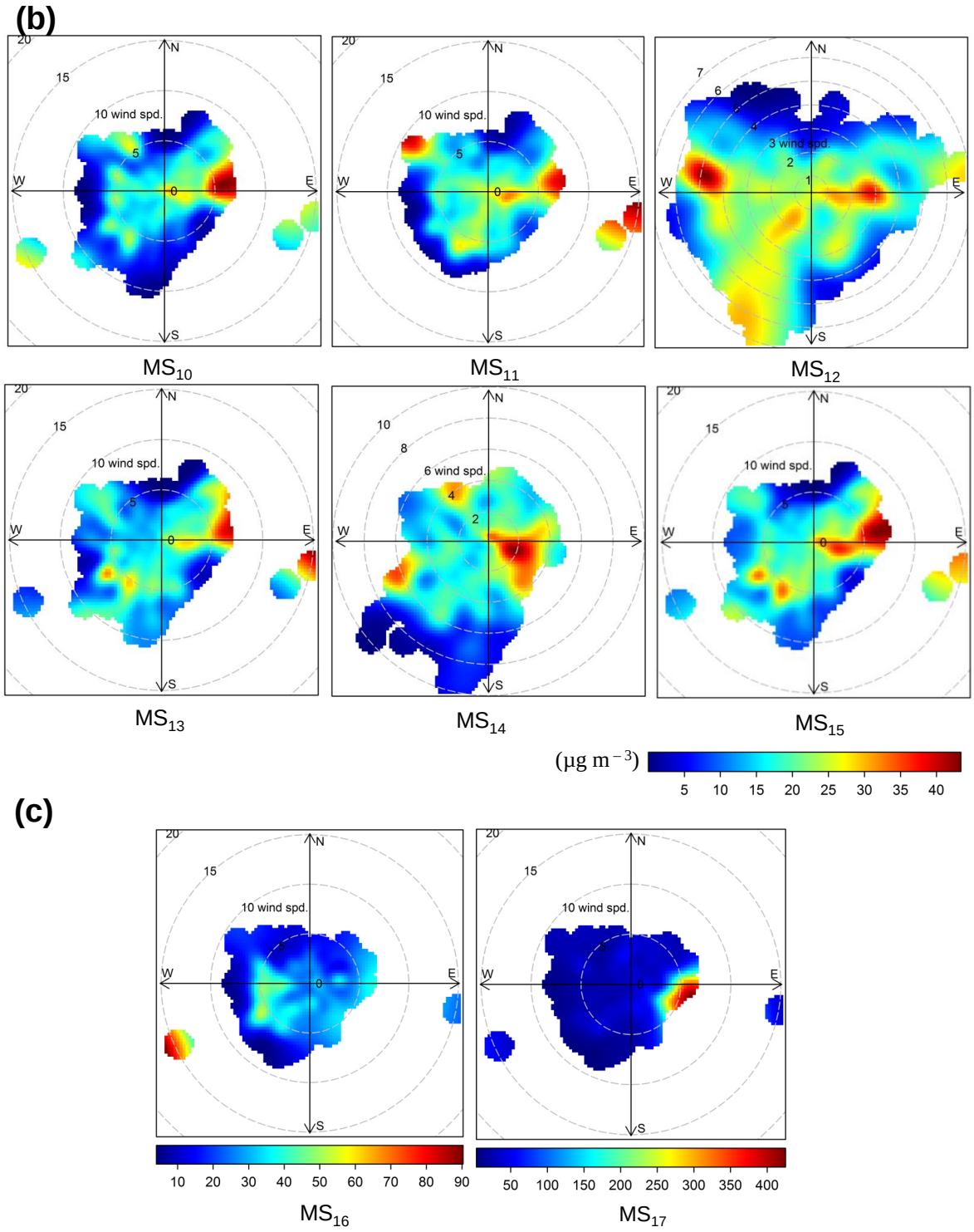

Figure 6.2: Polar plots for PM_{10} at the (a) CS_1, (b) CS_2 and (c) CS_3; hourly average values during 24-h measurements were used for all pollutants. These plots present as smoothed surfaces how concentrations vary depending on the local wind speed and wind direction.

This observation also suggest that the concentrations measured in downwind of construction sites include some contribution of emissions from these sources and are not solely the emissions from construction activities. However, this analysis is inadequate to conclusively report that the measured downwind emissions are from construction. Therefore, paired-site analysis (Section 6.3.2) and k-means cluster analysis (Section 6.3.3) were performed to better understand the contributions of construction emissions during varying wind directions.

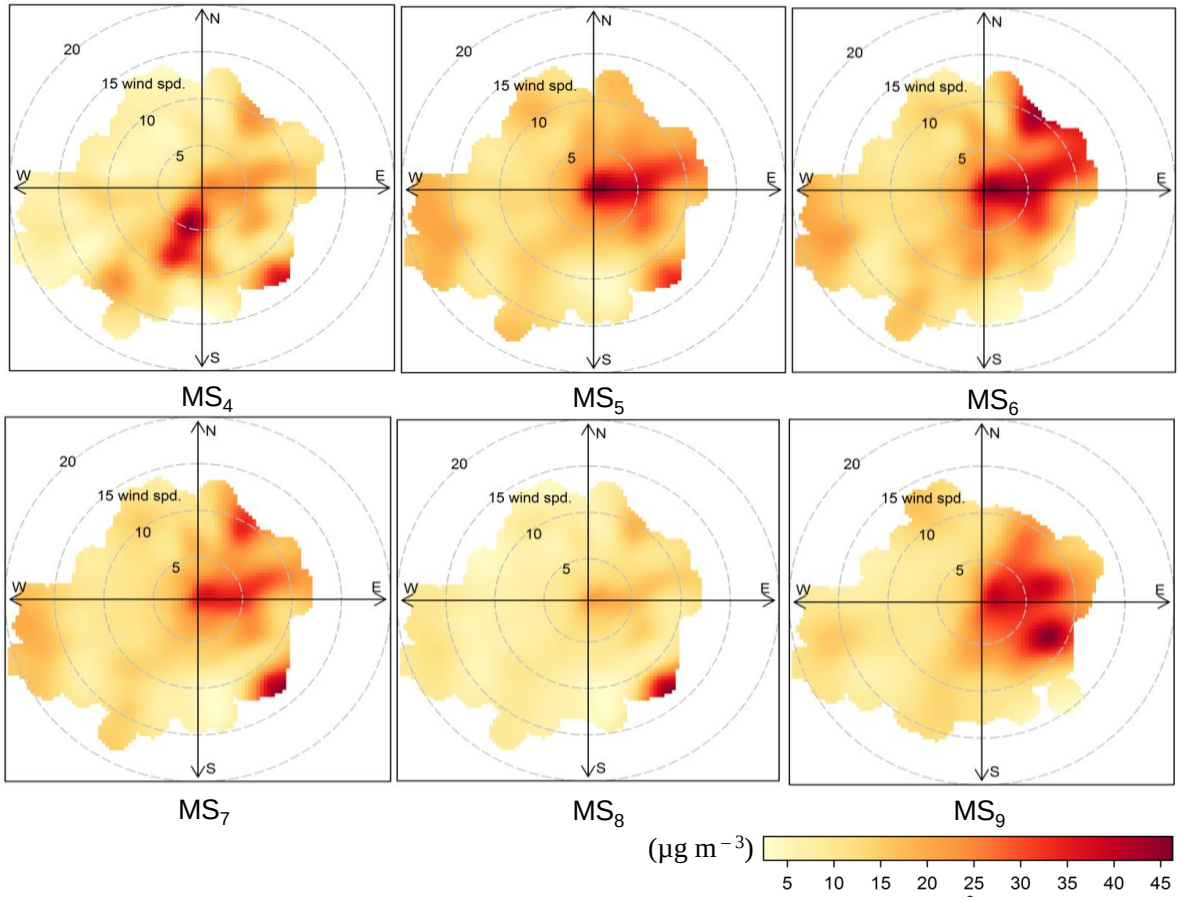

Figure 6.3: Polar plots for $PM_{2.5}$ (hourly average values during 24-h measurements were used for all pollutants) at the CS_1. These plots present as smoothed surfaces how concentrations vary depending on the local wind speed and wind direction.

6.3.2 Assessment of paired sites for examining differences in PM concentrations

The monitoring stations opposite to each other were paired in the upwind and downwind of the construction sites to assess the relative change in the concentrations that may have been contributed by the construction emissions (Figure 6.4). Two pairs of paired monitoring stations were found each for PM_{10} and $PM_{2.5}$ around CS_1 (Figure 6.4a) and another two pairs for PM_{10} around CS_2 (Figure 6.4b), giving a total of 6 paired monitoring stations. This pairing allowed us to measure changes in concentrations (i.e. ΔPM_{10} and $\Delta PM_{2.5}$) as air mass crosses the construction sites and the results are presented in Figure 6.4. For example, the hourly mean differences in PM_{10} and $PM_{2.5}$ at CS_1 measured in two pairs of opposite monitoring stations (MS_1, MS_4 and MS_7, MS_8), which were estimated as MS_4 minus MS_1 and MS_7 minus MS_8. Likewise, hourly mean differences at CS_2 were calculated using MS_{14} and MS_{15} as opposite monitoring stations, which was MS_{15} minus MS_{14}. Subtraction of results in upwind polar plots from those in downwind polar plots clearly shows increment in concentrations of PM_{10} and $PM_{2.5}$ at all the sites, with all the values being positive and high concentration zone reflecting emissions from construction sites. Cross-comparison of results between different PM types suggest that the differences are larger for coarse particles compared with fine particles, suggesting a relatively greater extent of PM_{10} emissions than those of $PM_{2.5}$ from construction works. Similar observations were reported by previous studies (Font et al., 2014) where they found greater increments in PM_{10} compared with $PM_{2.5}$ from the road widening works in London.

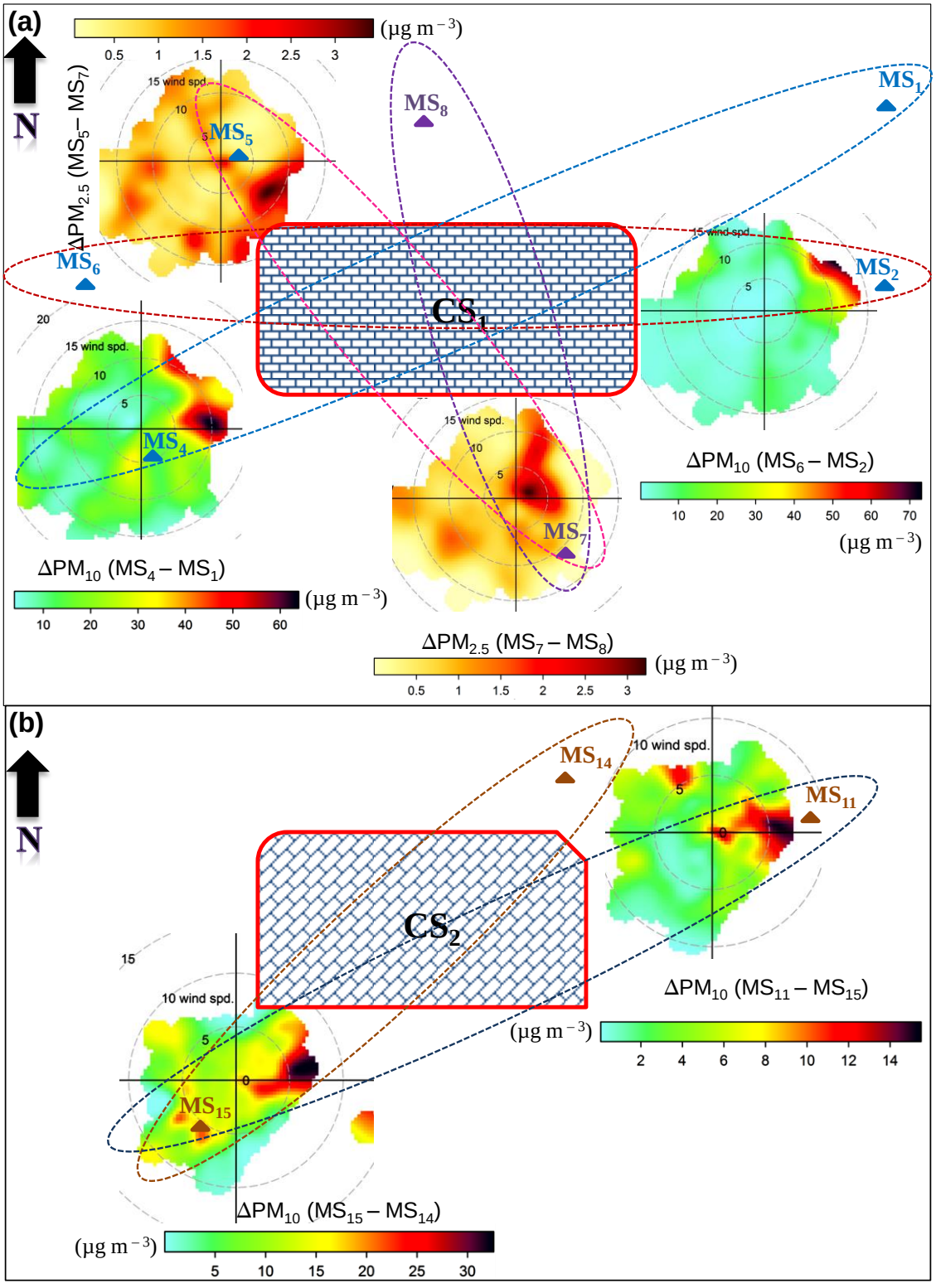

Figure 6.4: The polar plots for the paired monitoring stations across each construction site, for ΔPM_{10} and $\Delta PM_{2.5}$ (a) at the CS_1 and (b) for ΔPM_{10} at the CS_2, respectively.

6.3.3 k-means clusters analysis

In order to identify and independently assess the contribution of local sources, k-means cluster analysis was applied on the 6 paired monitoring stations that were identified and discussed in Section 6.3.2. Eight different clusters were chosen that were found to be optimal for separating the local source contribution from external sources, based on the recommendations from previous studies (Carslaw and Beevers, 2013; Elangasinghe et al., 2014; Everitt et al., 2011; Wood, 2006).

Figure 6.5 and Figure 6.6 show the contribution of each cluster in polar plots of ΔPM_{10} and $\Delta PM_{2.5}$. Also are shown the temporal variation of ΔPM_{10} and $\Delta PM_{2.5}$ contributed by each cluster on an hourly, weekly and monthly basis. Based on the ΔPM_{10} and $\Delta PM_{2.5}$ concentrations showing the high concentration peaks in polar plots (Figure 6.4), clusters 5–7 can be identified to represent the concentrations of ΔPM_{10} (Figure 6.5) and $\Delta PM_{2.5}$ (Figure 6.6) due to construction sources. If look at these clusters in the temporal variation plots, peaks can be seen during the weekdays which are missing during the weekends. This is also demonstrated by the increments in PM_{10} and $PM_{2.5}$ concentrations during 08:00 and 18:00 h, which we referred to as "working hours". While looking at the temporal plots on a monthly basis, the identified clusters (i.e. 5-7) showed relatively lower concentrations during the cold months (i.e. December, January and February) compared with the rest of the months.

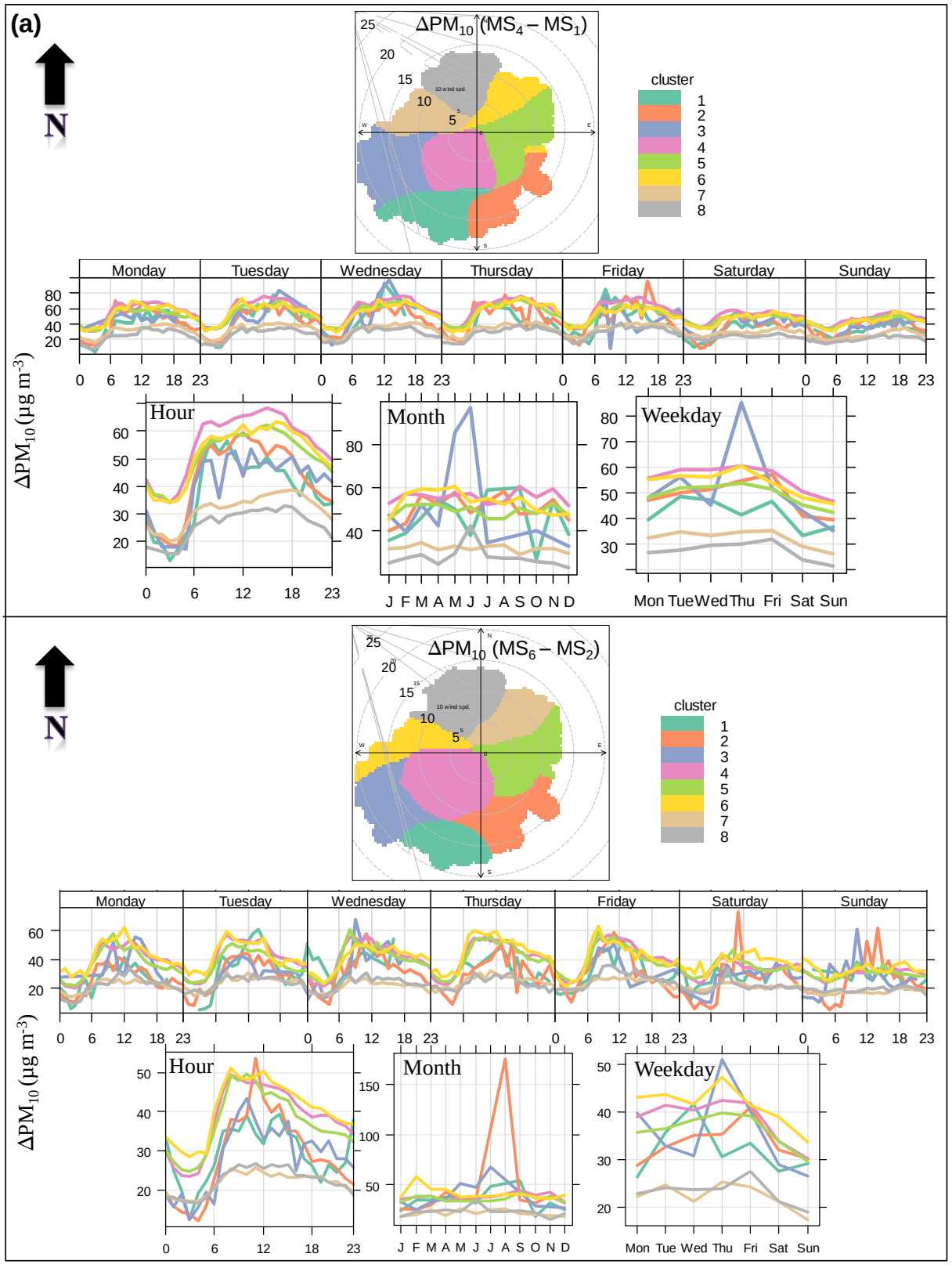

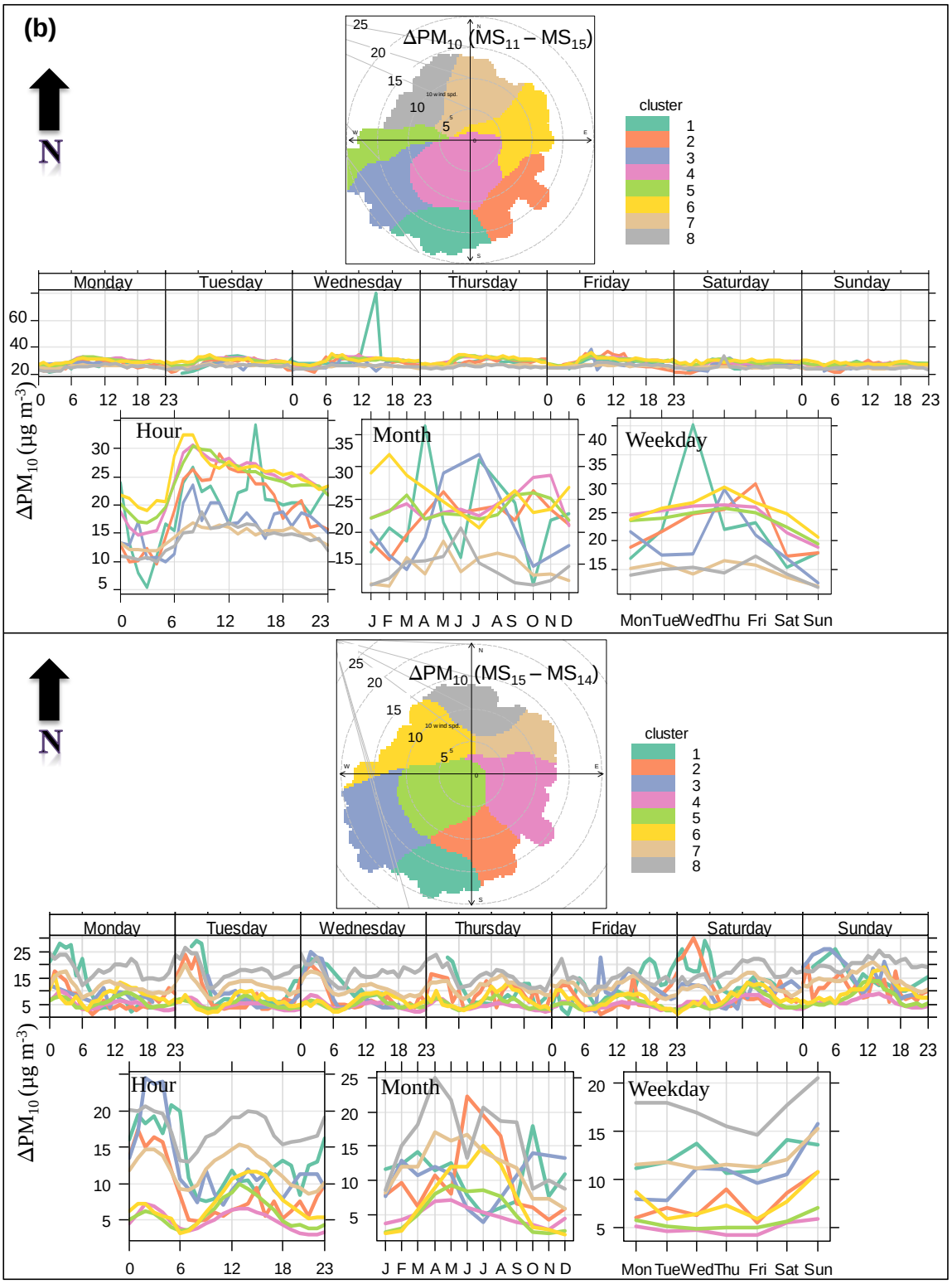

Figure 6.5: Clusters identified at CS_1 and CS_2 sites for PM_{10} concentrations for 8 clusters. The shading shows the 95% confidence intervals in the mean. The data have been normalised in each case by dividing by the mean.

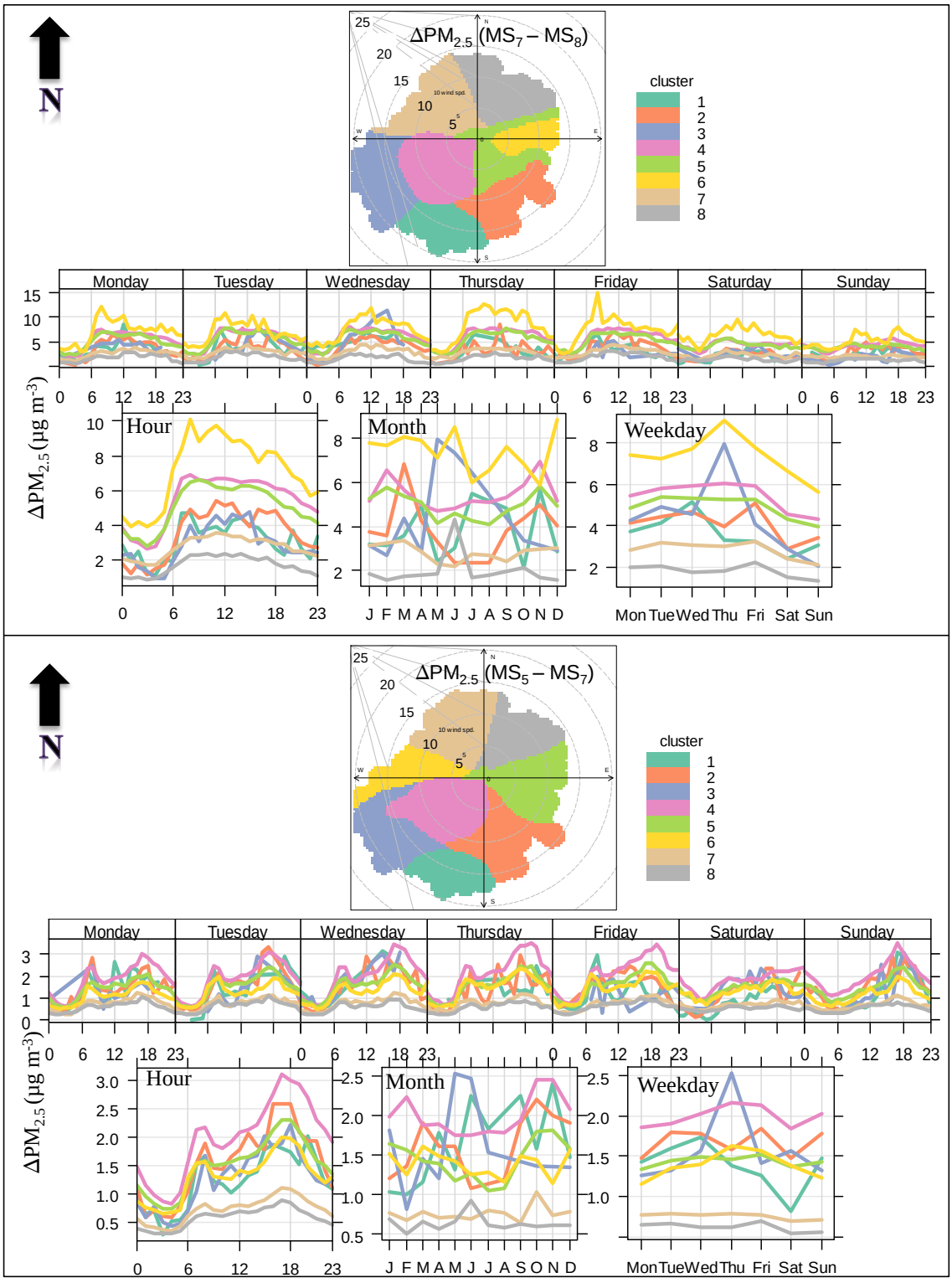

Figure 6.6: Clusters identified at CS_1 for $PM_{2.5}$ concentrations for 8 clusters. The shading shows the 95% confidence intervals in the mean. The data have been normalised in each case by dividing by the mean.

There could be two possible reasons for these lower concentrations: (i) lesser construction activity compared to normal, and (ii) weather conditions suppressing the emissions and transport of particles due to relatively wetter conditions than the other months, and also affecting the normal construction due to adverse weather conditions. For example, mean precipitation and relative humidity is expected to be higher during winter months (e.g. 256 mm and 85% to 213 mm and 70% during summer, respectively) and low temperature (e.g. mean ~4^0C to 15^0C during summers) (Jenkins et al., 2009). Past studies have found wet conditions such as water spraying an effective method to supress coarse particle emissions by up to 13-times during construction works (Kumar et al., 2012c). Detailed receptor modelling studies could help further in drawing firm conclusions.

6.3.4 Particle mass concentrations during working and non-working hours

Figure 6.7 shows the annual mean PM_{10} and $PM_{2.5}$ concentrations at all the three construction sites.

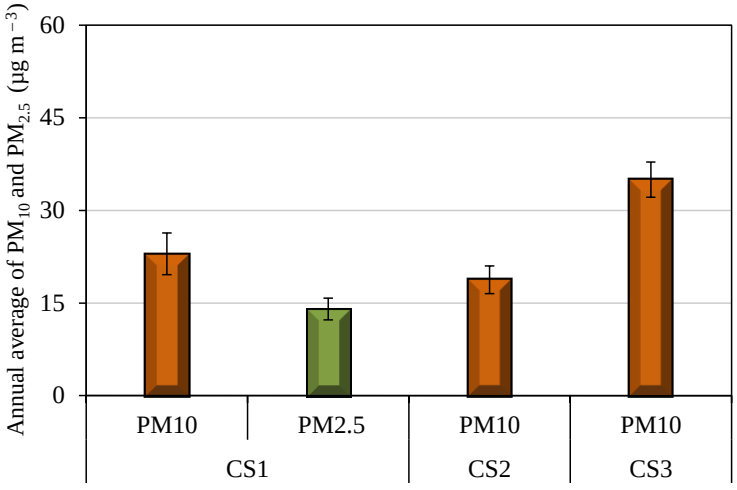

Figure 6.7: The annual average concentrations of PM_{10} (17 monitoring stations) during 2002-2013 period at the (a) CS_1, (b) CS_2, and (c) CS_3.

The annual average in PM_{10} concentrations were found to be 22.96±3.37 μg m^{-3}, 18.77±2.24 μg m^{-3} and 34.98±2.85 μg m^{-3} at CS_1 (Table 6.2), CS_2 (Table 6.4) and CS_3 (Table 6.5), respectively, while the annual average $PM_{2.5}$ concentrations were 14.01±1.76 μg m^{-3} at CS_1 (Table 6.3). These averages include both the working and non-working hours and the averages for these separate durations are presented in Figures C1a and C2 and described in Appendix C, Sections C1-C2. Depending on the source and distance from the monitoring stations, the values of PM_{10} and $PM_{2.5}$ varied and the concentrations in all cases increased as the working period started (see Figures C1-C4).

In general, concentrations during the working hours were higher than those during the non-working hours (see Tables C1-C4), presumably due to construction activities and the other emission sources such as road vehicles in operation during working hours. Overall, PM_{10} values were about ~24, 18 and 120% larger during the working periods compared with those during non-working periods at the CS_1, CS_2 and CS_3, respectively. Also at the CS_1, there was an increase of about 11% in $PM_{2.5}$ values during the working period compared with non-working periods (see Figure C2).

Table 6.2: The annual average concentrations of PM_{10} including the working and non-working periods at the CS_1; ± refers to standard deviation and "–" to the unavailability of data.

	Monitoring stations								
Year	MS_1	MS_2	MS_3	MS_4	MS_5	MS_6	M S_7	MS_8	MS_9
2002	_	21.94±12.28	19.14±11.20	29.59±22.38	27.56±20.95	23.61±15.62	19.37±10.58	19.42±10.21	24.36±14.42
2003	_	24.57±15.75	21.25±12.98	36.73±32.14	26.80±18.65	31.31±27.93	22.16±14.03	23.87±15.54	22.15±13.71
2004	19.18±11.59	21.25±11.99	17.32±9.52	28.94±23.59	21.81±13.14	25.15±25.55	18.72±11.33	20.56±11.83	25.91±17.08
2005	19.60±10.66	23.93±12.13	17.41±10.95	26.71±21.57	23.23±14.18	23.95±19.40	19.15±10.44	19.66±10.23	_
2006	20.45±11.21	24.51±23.57	18.82±9.86	24.88±18.03	24.51±20.86	22.96±15.56	20.67±10.83	21.22±11.77	_
Overall average	19.96±11.15	23.24±15.14	18.79±10.90	29.37±23.54	24.78±17.56	25.39±20.81	20.02±11.44	20.95±11.92	24.14±9.04

Table 6.3: The annual average concentrations of $PM_{2.5}$ including the working and non-working periods at the CS1; ± refers to standard deviation and "–" to the unavailability of data.

	Monitoring stations								
Year	MS_1	MS_2	MS_3	MS_4	MS_5	MS_6	MS_7	MS_8	MS_9
2002	_	_	_	17.3±17.9	13.0±8.0	12.5±8.0	12.0±8.1	11.8±7.2	12.6±7.9
2003	_	_	_	15.5±13.6	14.5±10.3	14.0±9.9	14.2±10.4	15.5±10.7	17.4±10.1
2004	_	_	_	17.0±18.4	12.6±7.4	11.5±7.9	11.5±7.4	12.1±7.5	19.4±13.3
2005	_	_	_	15.4±16.3	12.9±8.2	11.9±8.2	11.9±7.5	12.0±7.4	_
2006	_	_	_	14.6±12.9	13.0±8.0	12.1±8.0	12.1±7.8	12.9±7.4	_
Overall average	_	_	_	16.0±15.8	13.2±8.4	12.9±8.4	12.4±8.2	12.9±8.0	16.5±6.2

Table 6.4: The annual average concentrations of PM_{10} including the working and non-working periods; ± refers to standard deviation and "–" to the unavailability of data.

	Monitoring stations					
Year	MS_{10}	MS_{11}	MS_{12}	MS_{13}	MS_{14}	MS_{15}
2009	24.86±15.54	18.28±11.09	19.34±11.60	14.75±7.90	_	15.55±9.22
2010	23.68±16.89	17.27±11.23	_	15.74±13.93	_	14.81±10.31
2011	25.10±18.34	18.78±12.69	_	20.40±11.88	_	20.05±13.24
2012	22.20±16.17	18.68±13.71	_	16.42±9.77	_	18.07±15.49
2013	19.71±12.86	15.64±9.40	_	20.03±11.20	17.43±12.76	19.16±13.60
Overall average	23.11±16.17	17.73±12.35	19.34±11.60	17.47±11.28	17.43±12.79	17.53±13.11

Table 6.5: The average concentrations of PM_{10} including the working and non-working periods at the CS_3; ± refers to standard deviation.

	Monitoring stations	
Year	MS_{16}	MS_{17}
2011	37.36±33.08	35.39±31.24
2012	28.56±24.36	38.61±24.66
Overall average	32.96±19.31	34.98±18.16

Comparison of 24 hour average concentrations of PM_{10} with the EU Directive 2008/50/EC (Directive, 2008), as described in Table 6.6, suggests a number of exceedences each year (Table 6.7 and Figure C5). However, these exceedences are not expected to be due to construction works alone, given that the winds were blowing from various directions (Figure 6.1 and Figure 6.2) and the nearby sources could have also made contribution to these exceedences. Therefore, the data was filtered based on the wind directions at each monitoring station (Figure 6.8). The monitoring stations downwind of construction sites

were then considered for the comparison with the 24 hour mean EU limit value of 50 µg m^{-3} to observe the influence of construction works on the exceedences. The values in parenthesis in Table 6.7 shows these exceedences possibly due to the construction activities which were, except on two occasions in 2003 (Table 6.7), less than the allowable 35 exceedences per year (Table 6.6). Unlike previous occasions when Fuller and Green (2004) reported exceedences of daily mean PM_{10} concentrations over the EU limit value of 50 µg m^{-3} on several occasions during the monitoring of emissions from road and building works in London, exceedences in this study are within the regulatory limits and could also be attributed to the construction works, given that the paired polar roses and k-means clusters analysis in Sections 6.3.1-6.3.3 suggested a clear contribution of construction works on downwind monitoring stations.

Table 6.6: Summary of EU air quality limit values against AQS objectives (Directive, 1999; Directive, 2008; Fuller and Green, 2004).

		EU limit value	
Pollutant	Period of averaging	Limit values	Dates to achieve
PM_{10}	24 hour mean	50 µg m^{-3} not to be exceeded more than 35 times a year	January 2005
	Calendar year	40 µg m^{-3}	January 2005
	24 hour mean	50 µg m^{-3} not to be exceeded more* than 7 times a year (target limit value)	January 2010
	Calendar year	20 µg m^{-3}(target limit value)*	January 2010
		UK government AQS objective	
	24 hour mean	50 µg m^{-3} not to be exceeded more than 10-14 times a year	January 2010
	Calendar year	23-25 µg m^{-3}	January 2010

*The EU Directive 1999/30/EC stipulated that annual mean values of PM_{10} should be less than 20 µgm^{-3} and should not exceed a mean of greater than 50 µgm^{-3} more than 7 days in a year as per 2010 target limit values. These target values to be met by 2010 were not carried forward in the Directive 2008/50/EC (Directive, 2008).

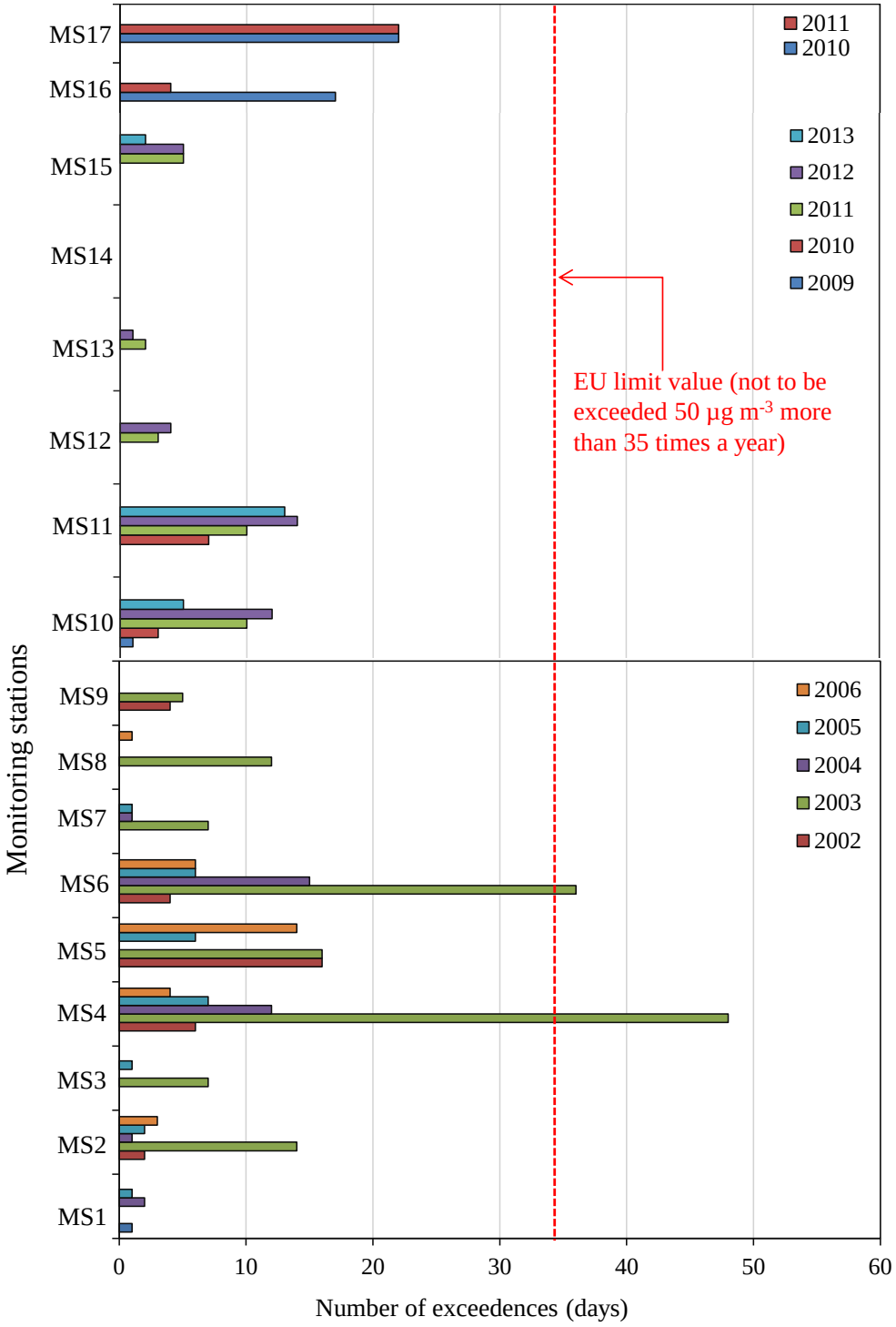

Figure 6.8: Numbers of exceedences over the EU limit value at the individual monitoring stations.

Table 6.7: Number of exceeded days from the EU standard limit and UK government objective (AQS). Please note that the excedances presented in the parenthesis against each exceedance number represent the exceedances belonging to the 24 hours.

	Monitoring Years											
Monitoring stations	2002	2003	2004	2005	2006	2007	2008	2009	2010	2011	2012	2013
MS_1	0(0)	0(0)	2(2)	1(1)	0(0)	_	_	_	_	_	_	_
MS_2	3(2)	17(14)	3(1)	2(2)	5(3)	_	_	_	_	_	_	_
MS_3	1(0)	9 (7)	0(0)	1(1)	0(0)	_	_	_	_	_	_	_
MS_4	9(6)	60(48)	19(12)	11(7)	5(4)	_	_	_	_	_	_	_
MS_5	18(16)	22(16)	1(0)	6(6)	15(14)	_	_	_	_	_	_	_
MS_6	7(4)	42(36)	16(15)	9(6)	6(6)	_	_	_	_	_	_	_
MS_7	1(0)	11(7)	1(1)	1(1)	1(0)	_	_	_	_	_	_	_
MS_8	0(0)	14(12)	2(0)	1(0)	1(1)	_	_	_	_	_	_	_
MS_9	4(4)	6(5)	3(0)	0(0)	0(0)							
MS_{10}	_	_	_	_	_	_	_	3(1)	17(3)	28(10)	12(12)	6(5)
MS_{11}	_	_	_	_	_	_	_	0(0)	11(7)	31(10)	16(14)	13(13)
MS_{12}	_	_	_	_	_	_	_	0(0)	0(0)	3(3)	5(4)	0(0)
MS_{13}	_	_	_	_	_	_	_	0(0)	0(0)	3(2)	1(1)	0(0)
MS_{14}	_	_	_	_	_	_	_	0(0)	0(0)	0(0)	0(0)	0(0)
MS_{15}	_	_	_	_	_	_	_	0(0)	0(0)	7(5)	6(5)	2(2)
MS_{16}	_	_	_	_	_	_	_	_	_	20(17)	4(4)	_
MS_{17}	_	_	_	_	_	_	_	_	_	25(22)	33(22)	_

6.3.5 Decay profiles of PM_{10} and $PM_{2.5}$

The purpose of this section is to evaluate the variation in concentrations of PM_{10} and $PM_{2.5}$ at different distances from the construction sites. This analysis assisted in understanding how far the PM concentrations can go to affect the surrounding areas as well as help in planning for emission mitigation measures, particularly for construction sites close to sensitive areas such as hospitals or schools.

Figure 6.9 shows the decay profiles of PM_{10} and $PM_{2.5}$ concentrations with the changing distance from the CS_1 and CS_2. Both the logarithmic (Figure 6.9a) and exponential (Figure 6.9b) best fit functions were applied to ΔPM_{10} and $\Delta PM_{2.5}$. The logarithmic decay function (Figure 6.9a) was chosen as a best fit to the data based on better R^2 values than those given by an exponential decay profile as 0.79, 0.90 and 0.89 for PM_{10} (CS_1), PM_{10} (CS_2) and $PM_{2.5}$ (CS_1), respectively (Figure 6.9b). The differences between hourly averages of PM_{10} and $PM_{2.5}$ concentrations (ΔPM_{10} and $\Delta PM_{2.5}$) during the working and non-working time periods provided the net concentrations from the construction activities, which were then used to draw decay profiles (Figure 6.9). Further, the calculated concentrations for PM_{10} and $PM_{2.5}$ were filtered on the basis of prevailing wind direction. The decay profile of PM_{10} concentrations at CS_1 was drawn using the data measured at MS_4, MS_5, MS_7 and MS_3 which were 100, 200, 500 and 1000 m away from the CS_1, respectively. Also the data measured at MS_4, MS_6 and MS_7 were used to draw the decay profile of $PM_{2.5}$ at CS_1 which were 100, 200 and 500 m away from the CS_1. Furthermore the decay profiles of PM_{10} concentrations were measured at 100, 200 and 400 m away from the CS_2 at MS_{10}, MS_{11} and MS_{15}, respectively.

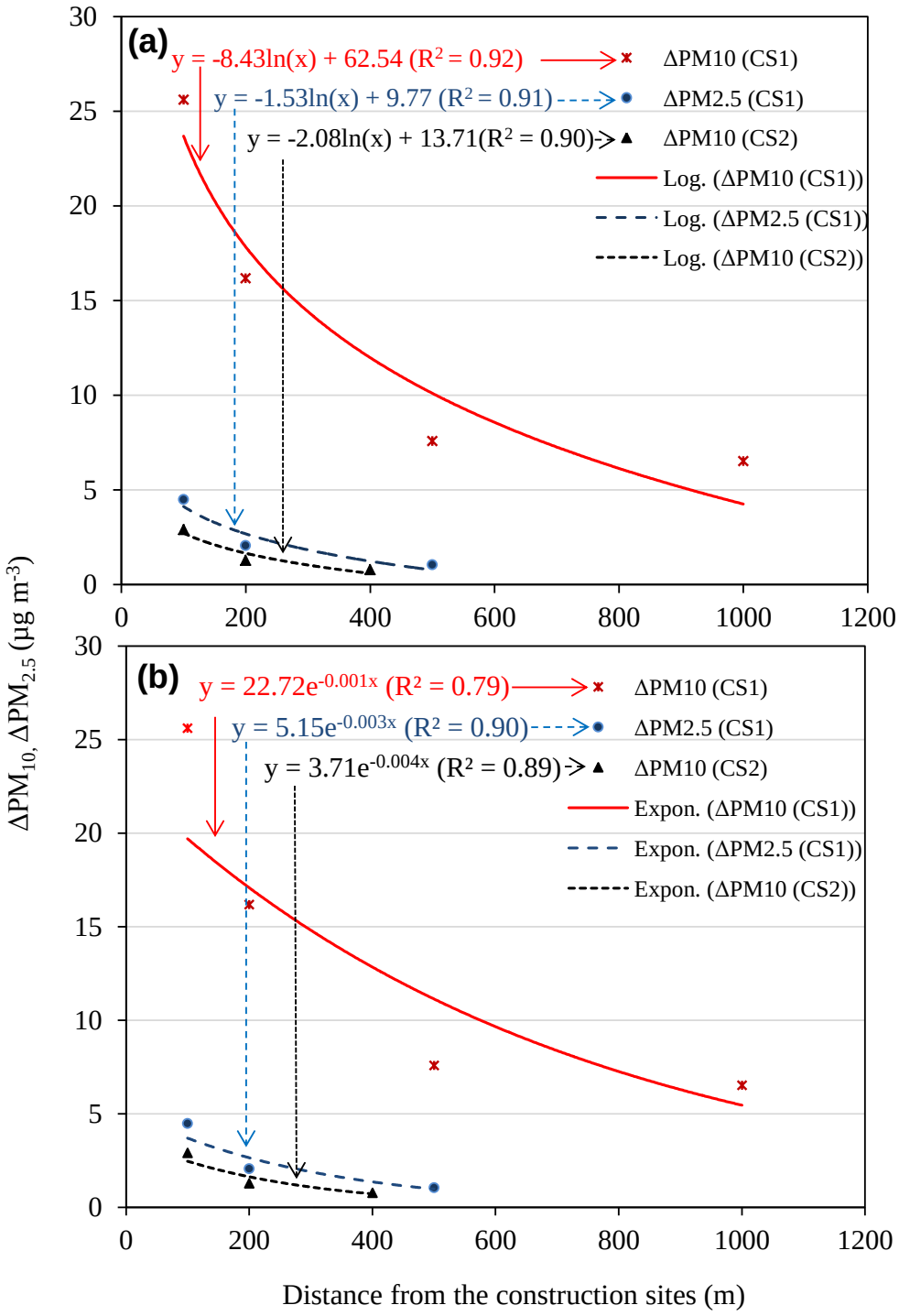

Figure 6.9: ΔPM_{10} and $\Delta PM_{2.5}$ concentration decay at CS_1 and CS_2 versus distance in the direction of wind blowing from construction sites, showing (a) logarithmic, and (b) exponential best fit functions.

Because of atmospheric dilution, the mass concentration dramatically dropped with increased distance from the construction site to approximately half of its value at a distance between 100 and 200 m. The best fitting logarithmic decay equations for PM_{10} were drawn, which gave R^2 values as 0.92 and 0.91 for the CS_1 and CS_2, respectively (Figure 6.9a). A much higher rate of change in PM concentrations can be seen close to the construction site compared with those at farther distances. For instance, the rate of change in PM_{10} (CS_1) concentration with per meter distance is 0.06 μg m^{-3} in between 100 and 200 m, which decreases to 0.030 and 0.013 μg m^{-3} per meter distance in the 200-400 m, and 400-1000 m range, respectively (Figure 6.9a). These observations suggest to measure the PM within a few 100 meter distance from the construction sites to capture the rapid decay in PMCs. The total mean $PM_{2.5}$ levels around the CS_1 were also correlated well with the distances. A logarithmic decay profile with R^2 value of 0.90 represented the measured data very well.

Although studies measured decay of PM concentrations around the construction sites are rare, it was tried to compare the data of this study with the most relevant studies. For example, Hitchins et al. (2000) determined the PM_{10} concentration at increasing distances from a road at two sites in Australia. They found that $PM_{2.5}$ and ultrafine particles decayed by up to half of their maximum initial concentrations within a distance of 100–150 m from the road. Likewise, Buonanno et al. (2009) found PM_{10} concentration values to decrease exponentially away from the freeway in Italy during weekly traffic conditions.

6.4 Chapter summary and conclusions

OSIRIS (model 2315) and TEOM 1400 were used to measure mass concentration of particles in the 0.1–10 μm size range around the three construction sites at 17 monitoring

stations over a period of 12 years between January 2002 and December 2013. The objectives were to understand the emission characteristics of coarse and fine particles from the construction activities, identifying contribution to the ambient levels of PM concentrations in the vicinity of these sites, and their spatial decay away from the construction sites.

The following conclusions are drawn from this work:

- The source characteristics of PM_{10} and $PM_{2.5}$ were investigated using bivariate concentration polar plots and k-means clustering techniques. The high concentrations of PM_{10} and $PM_{2.5}$ were observed at the paired monitoring stations during the construction works when the winds were blowing from construction sites toward the monitoring stations. K-means clustering technique provided a useful development to the bivariate polar plots to assess the contribution of construction and other local sources.
- Three clusters (5, 6 and 7) from a total of selected 8 clusters showed strong evidences of a downward increase in PM_{10} and $PM_{2.5}$ levels during the weekdays. These clusters were identified to represent construction activities.
- PM_{10} were found about ~24, 18 and 120%, and $PM_{2.5}$ about 11%, larger during the working periods compared with those during non-working periods at the CS_1, CS_2 and CS_3, respectively. These increments were attributed to the construction works as indicated by the bivariate concentration polar plots and k-means clustering analysis. In addition, downwind concentrations of PM_{10} were found to be relatively more influenced by construction works at the CS_1 than $PM_{2.5}$ concentrations.

- The 24-hour mean EU limit of value of 50 μgm^{-3} set by EU Directives for PM_{10} not to be exceeded more than 35 times a calendar year was breached on two occasions due to construction operations on downwind monitoring stations during measurements between 2002 and 2013.
- Both the total PM_{10} and $PM_{2.5}$ values during the working periods in downwind direction found to be well correlated with the distances with R^2 values over 0.90 in a logarithmic form. These concentrations reduced to half of their initial concentrations within a few 100 meters. This indicates that placing a monitoring station around a site within this peripheral distance could help capturing the rapid decay of particles escaping from the construction sites.

The result presented in this study highlight the contributions of PM_{10} and $PM_{2.5}$ from construction works. The increase in concentrations of PM_{10} and $PM_{2.5}$ at the downwind monitoring stations suggest that there is a need to design more detailed and appropriate risk mitigation strategies to limit exposures to onsite workers and people who live in the surrounding environment. Further research is required to monitor and understand the emission levels of particles arising from other filed building works within urban areas in order to establish suitable exposure limits for both on-site workers and passer-by urban people. For this purpose, the measurements of particles during outdoor field activities (i.e. building demolition works) were carried to assess particles emissions and also physicochemical features which allows to differentiate between the properties of particles from indoor and outdoor sources. The results are presented in Chapter 7.

Chapter 7. Outdoor building demolition activities

This chapter presents the results of release of PM_{10}, $PM_{2.5}$ and PM_{1} from outdoor building demolition activities. The chapter also provides assessments of physicochemical properties of those particle and potential impact on workers and individuals in the surrounding.

7.1 Introduction

Construction and demolition waste contribute up to about 33% of the total waste from all the streams; about half of which is demolition waste (Balaras et al., 2007). Construction and demolition of structures generate in excess of 450 million tonnes of waste each year in Europe, with about 53 million tonnes per year in the UK alone (Lawson et al., 2001; Rao et al., 2007). However, the number of buildings demolished each year is expected to increase by 4-fold by 2016 in the UK from the levels of about 20,000 per year in 2008 (ECI, 2005; Roberts, 2008). This increased rate of building demolition could be linked to growing population of the urban areas and the need for improvements to meet new urban design guidelines and adopt building technologies (Balaras et al., 2007; Kumar et al., 2015). For example, the global urban population is expected to increase by about 60% in 2035 from the 2013 levels (GroBmann et al., 2013; Kumar et al., 2013a).

Building demolition can be accomplished through either implosion or mechanical means

(e.g. excavator and wrecking ball). Demolition by both mechanical disruption (Dorevitch et al., 2006) and implosion (Beck et al., 2003) produce significant amount of PM, but the impact of implosion demolition on surrounding areas air quality is generally short-lived and severe (Beck et al., 2003). Recent studies have shown that workers in construction industry dealing directly with concrete and cement products are exposed to notable PM emissions (Azarmi et al., 2014; Croteau et al., 2002; Flanagan et al., 2006; Kumar et al., 2012b) compared with those working in metal and wood industries (Fischer et al., 2005; Lim et al., 2010). There are sufficient evidences that activities such as demolition, earthmoving and building renovation are important sources of PM and degrade the surrounding air quality (Azarmi et al., 2015a; Beck et al., 2003; Font et al., 2014; Hansen et al., 2008; Joseph et al., 2009; Muleski et al., 2005). In addition, PM pollution from demolition activity can adversely impact the health of people living close to demolition sites, especially when the measures to restrict particles released from sites are inadequate (Kumar et al., 2012a). Therefore, assessment of PM exposure becomes even more important when such sites are situated within the densely built residential areas or sensitive areas such as schools and hospitals.

Understanding the chemical constituents, morphology (i.e. size, shape) and surface properties of particles released from building demolition are important for determining their toxicity and health effects (Lo et al., 2000; Senlin et al., 2008). Currently, limited studies have reported physicochemical properties of particles released from the building demolition and therefore this is taken up for investigation in this study. However, further details about the physicochemical analysis of the particles from demolition and

construction sources is presented in Section 2.6 in Chapter 2. Health concerns related to dust inhalation have led to a number of dust control and reduction initiatives in demolition industry. The US EPA have provided specific emission factors for different operations such as demolition, construction and mineral operations to control PM emissions (EPA, 2011). In addition, the UK Health and Safety Executive (HSE) developed a good practice guideline to limit exposure to hazardous substances at the demolition sites (HSE, 2006, 2011). Furthermore, at local level, "Best Practice Guidance" is produced by London Councils in partnership with the Greater London Authority in the UK, which contains a number of practical methods to control dust and emissions from demolition activities (Authority and Councils, 2006). However, demolition sites can be situated within extremely busy places where meeting regulatory expectations, or strictly following associated guidelines, are often challenging.

In order to fill the existing research gaps in the literature, this study investigates the release of PM_{10}, $PM_{2.5}$ and PM_1 and associated exposure around a real-world building demolition site. The aims were to: (i) quantify the emission and exposure rates of particles and their dispersion in the downwind of demolished building, (ii) assess the horizontal decay of the PM emissions, (iii) understand the physical and chemical properties, (iv) computation of particle mass emission factors (PMEFs), and (v) determining the occupational exposure to on-site workers and people in the close vicinity of the demolition site.

7.2 Materials and methods

7.2.1 Sampling set up and site description

PMCs were measured at the fixed-sites in the downwind of demolition site, around the demolished building through the mobile monitoring as well as at different distances (10, 20, 40 and 80 m) from the demolition site through sequential measurements (Figure 7.1). Monitoring was also carried out inside the cabin of an excavator vehicle and in on-site canteen offices for engineers. Figure 7.2 shows the sampling locations around the demolition site, which was situated ~10 m away from a busy road that was closed during the demolition activity (i.e. sampling period). The demolished building was 30×15×8 m (length × breadth × height) and was located in Haywards Heath in West Sussex, United Kingdom (Figure 7.2). Construction material of building floors, stairs and supporting columns was reinforced concrete while the walls were made of brick. The data were collected for a total of 54 working hours between 08:00 and 18:00 h (local time) over a period of 7 days; of which, one day was without any activity that enabled us to evaluate the local background levels.

Table 7.1 presents the detailed summary of sampling durations. The background measurements were made at 15 m from the demolition site. Fixed site measurements were made at a distance of ~10 m in the downwind of the demolition site (Figure 7.3) while mobile measurements were made in loops of ~100 m (route A) and ~ 600 m (route B) around the demolition site (Figure 7.2). Mobile routes were intentionally changed to capture the exposure of on-site workers around the demolition site (route A) and the people in nearby vicinity of the site (route B). A total of 24 runs were made at routes A and B

during the demolition works; the runs were spread equally between morning and afternoon hours (Table 7.1). A GRIMM particle spectrometer (model 1.107 E) was used to measure the mass distribution of particles per unit volume of air in 15 different channels as described in Section 3.2.1 in Chapter 3.

Figure 7.1: Sample of demolition works at the demolition site.

Table 7.1: Description of sampling duration and monitoring sites.

Day number	Date	Start-end time (sampling duration in minutes)	Measurement type	Measurement location with respect to demolition site (x)
1	28 June 2015	10:00:00–14:00:00 (~240)	Background	At 15 m downwind of demolition site
2, 3	1, 3 July 2015	08:56:01–17:00:07 (~500) 08:33:01–16:56:37 (~500)	Fixed-site	At 10 m downwind of the demolition site
4, 5	6, 8 July 2015	08:46:01–17:01:13 (~500) 08:35:01–16:59:25 (~500)	Mobile measurements	Around the demolition site in ~100 m (route A) and ~600 m (route B) loop
6, 7	9, 10 July 2015	14:12:01–16:46:43 (~150) 08:39:01–16:44:01 (~500)	Sequential measurements	At 10, 20, 40 and 80 m downwind of demolition site
7	10 July 2015	11:03:00–14:40:00 (~220)	Excavator cabin	At 5 m downwind inside the vehicle cabin
2, 3, 4, 6, 7	1, 3, 6, 9, 10 July 2015	15:10:00–15:49:00 (~40) 13:25:00–14:00:00 (~35) 14:30:00–15:00:00 (~30) 14:10:00–14:40:00 (~30) 15:00:00–15:10:00 (~10)	Engineer's on-site office	At 16 m downwind inside the office

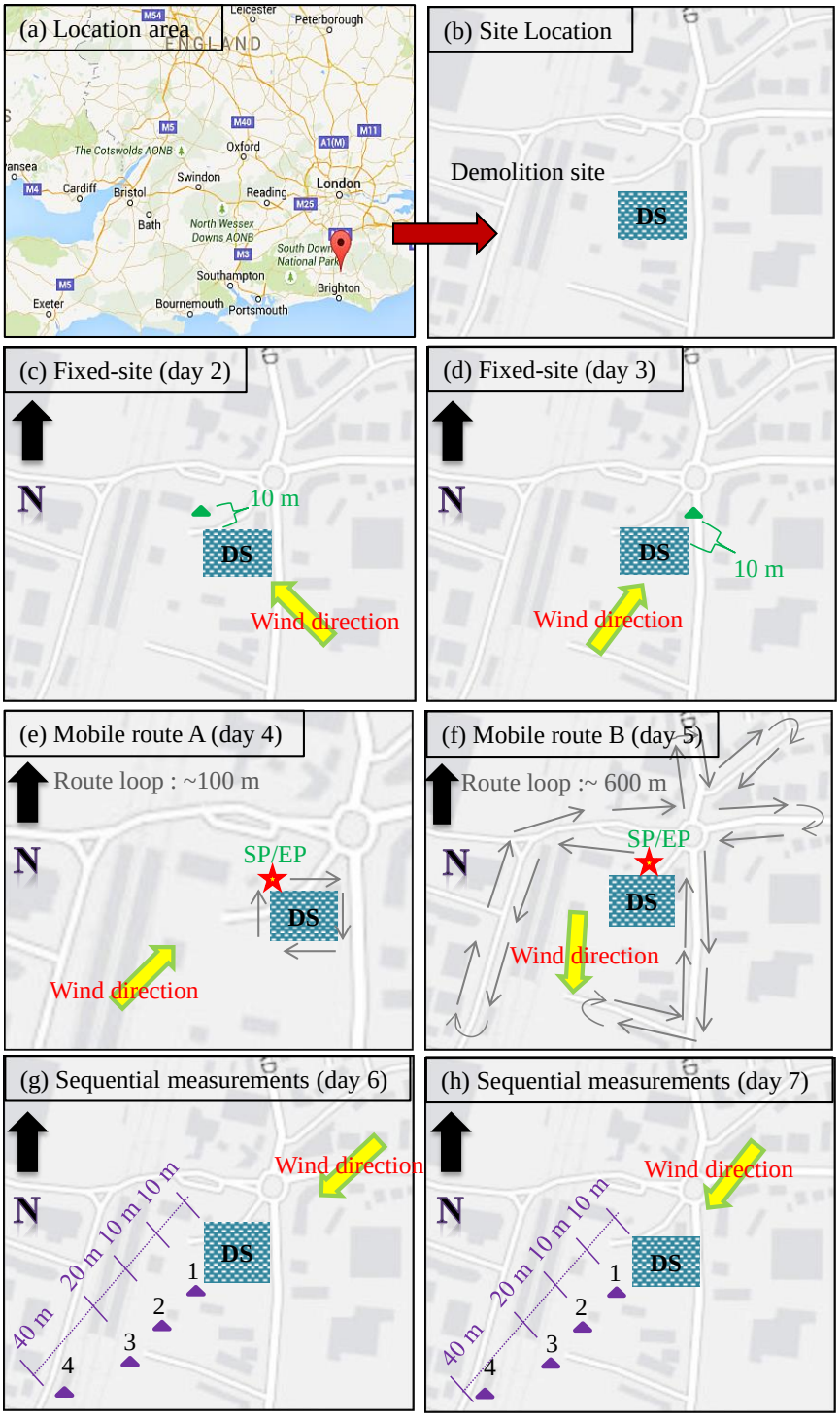

Figure 7.2: Schematic map of the experimental set-up, showing (a, b) monitoring stations around the demolition site (DS) during (c) fixed site measurements at day 2, and (d) day 3. Route of mobile measurements around the DS during (e) day 4, and (f) day 5. SP and EP refer to the start and end points, respectively, while the arrows represent the path of mobile measurements.

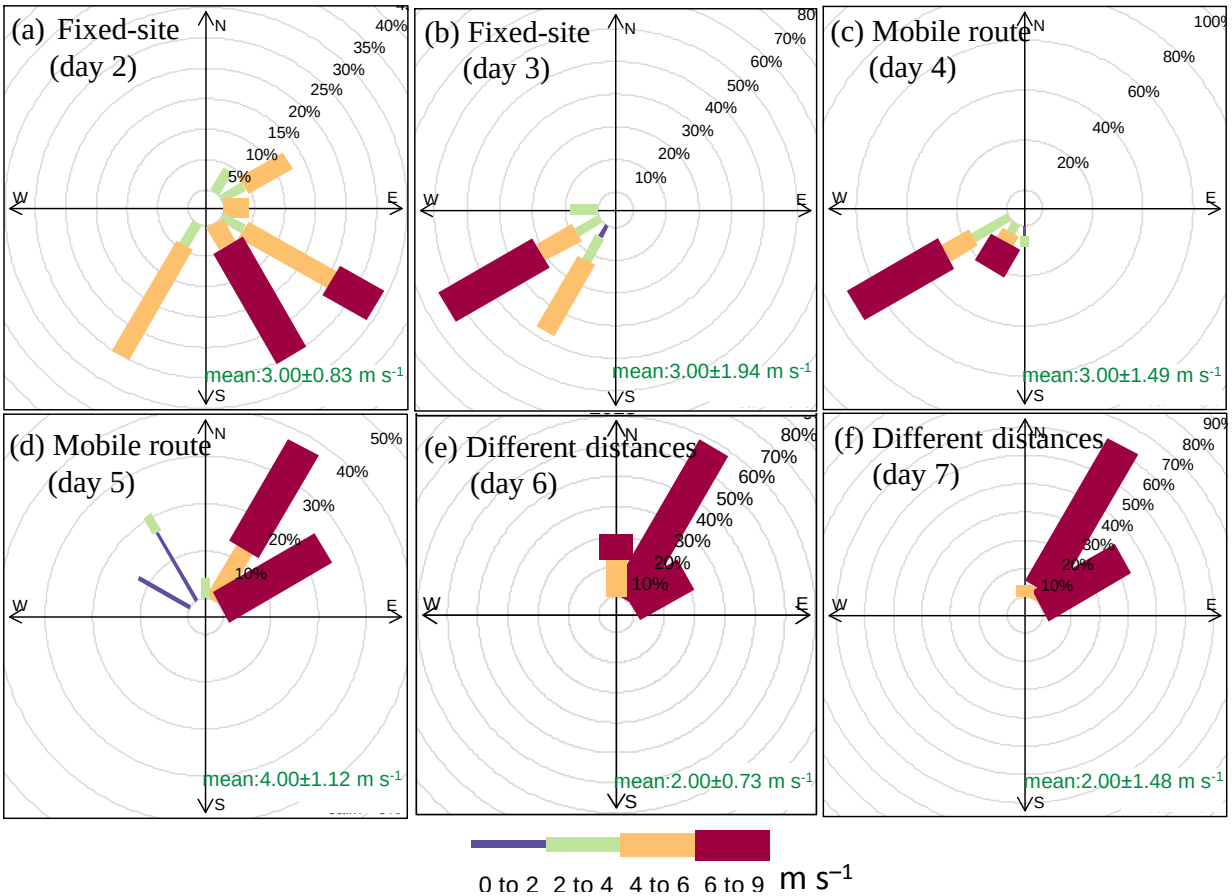

Figure 7.3: Wind roses diagrams depict the hourly frequency distribution of the wind speed and direction during the fixed site measurement on day 2 (a) and day 3 (b), as well as during the mobile measurements on day 4 (c) and day 5 (d), for sequential distances at day 6 (e) and day 7 (f).

7.2.2 Collection of PM mass on PTFE filters for SEM and EDS analysis

Five different samples (1-5) were collected on PTFE filters that had a diameter of 47 mm and a nominal thickness of ~1000 µg cm^{-2} (Table 7.2). Filter sample 1 was treated as a "blank" while mass on sample 2 was collected during the background period (pre-demolition). Mass on filter samples 3, 4 and 5 were collected during fixed-site (days 2 and 3), mobile (days 4 and 5) and sequential measurements (days 6 and 7), respectively. Further details on the sampling duration and mass collected on the sampled filters are provided in Table 7.2. Each of these five filter samples were analysed using a JEOL SEM (model: JSM-

7100F), equipped with EDS (see Section 3.3 in Chapter 3), to obtain information on the surface morphology and composition of the particles collected on filters. The sample surface was scanned with a high-energy (~3.0 kV) beam of electrons in a raster pattern. The scanned area was between 6×6 and 200×200 μm^2 in accordance with the magnification applied (JEOL, 2015).

Table 7.2: Summary of samples collected on PTFE filters during the demolition activity.

Name	Date of sampling	Time for sampling (min^{-1})	Mass of particles collected on the filter per unit area ($\mu g\ cm^{-2}$)[a]
Sample 1	Blank (reference)	-	-
Sample 2	28 June 2015	240	0.3
Sample 3	1 and 3 July 2015	1000	19.5
Sample 4	6 and 8 July 2015	1000	14.7
Sample 5	9 and 10 July 2015	650	16.1

[a]The mass of collected particles on the filter per unit area ($\mu g\ cm^{-2}$) has been calculated by dividing the collected mass over the area of a filter (~ 69.3 cm^2).

7.3 Results and discussion

7.3.1 PMCs downwind of the demolition site

Figure 7.4a and Figure 7.4b show the average PMCs and their fractions in various size ranges, respectively, from the building demolition activity during the fixed–site measurements (see Figure D1 in Appendix D). Polar concentration rose were also plotted to identify the locations of the source during different wind directions (Figure 7.4c-e). These polar plots clearly showed increments in PM_{10} (Figure 7.4c), $PM_{2.5}$ (Figure 7.4d) and PM_1 (Figure 7.4e) when the prevailing wind was from demolition to monitoring sites. In

fact, the overall average of PM_{10}, $PM_{2.5}$ and PM_1 concentrations were found to be 133.1±17.2 μg m^{-3}, 15.0±6.3 μg m^{-3} and 7.9±5.2 μg m^{-3}, with a fraction of about 89, 5 and 6% in $PM_{2.5-10}$, $PM_{1-2.5}$ and PM_1 size ranges, respectively (Section D2 in Appendix D). Fraction of coarse particles (i.e. $PM_{2.5-10}$) was found to be about 39% higher over the background level, compared with fine particles (i.e. $PM_{2.5}$) that reduced by about similar percentage, against the background level during the demolition periods. This observation clearly suggests a much higher increase of coarse particle emissions from building demolition (Figure 7.4).

As far as the regulatory metrics are concerned, the average concentrations of PM_{10}, $PM_{2.5}$ and PM_1 were found to be up to 11-times higher during the demolition periods than the background levels of PM_{10} (12.0±6.3 μg m^{-3}), $PM_{2.5}$ (6.07±2.6 μg m^{-3}) and PM_1 (2.0±1.1 μg m^{-3}; Figure 7.3a). Published studies on this topic are limited for direct comparison but results of this study were analogous to that observed by previous studies. For example, Dorevitch et al. (2006) measured PM_{10} during the demolition of a brick-walled reinforced concrete building and average concentrations were reported to be up to 10-times higher compared with background levels. Later, Hansen et al. (2008) measured PM_1 particles from the demolition of a brick-walled concrete building and found about 3-fold increase in concentration during the demolition over the background values. The differences in *peak* concentrations with respect to the background levels changed drastically. For example, the *peak* values of PM_{10}, $PM_{2.5}$ and PM_1 during the demolition period increased to about 7358, 348 and 42 μg m^{-3}, which were 615-, 60- and 30-times higher than the background levels, respectively. Closer inspection of the log-sheets indicated these peak increments to be

coinciding with the periods of intense breaking of the ceiling and side walls at the upper floors of the demolished building (Figure 7.4).

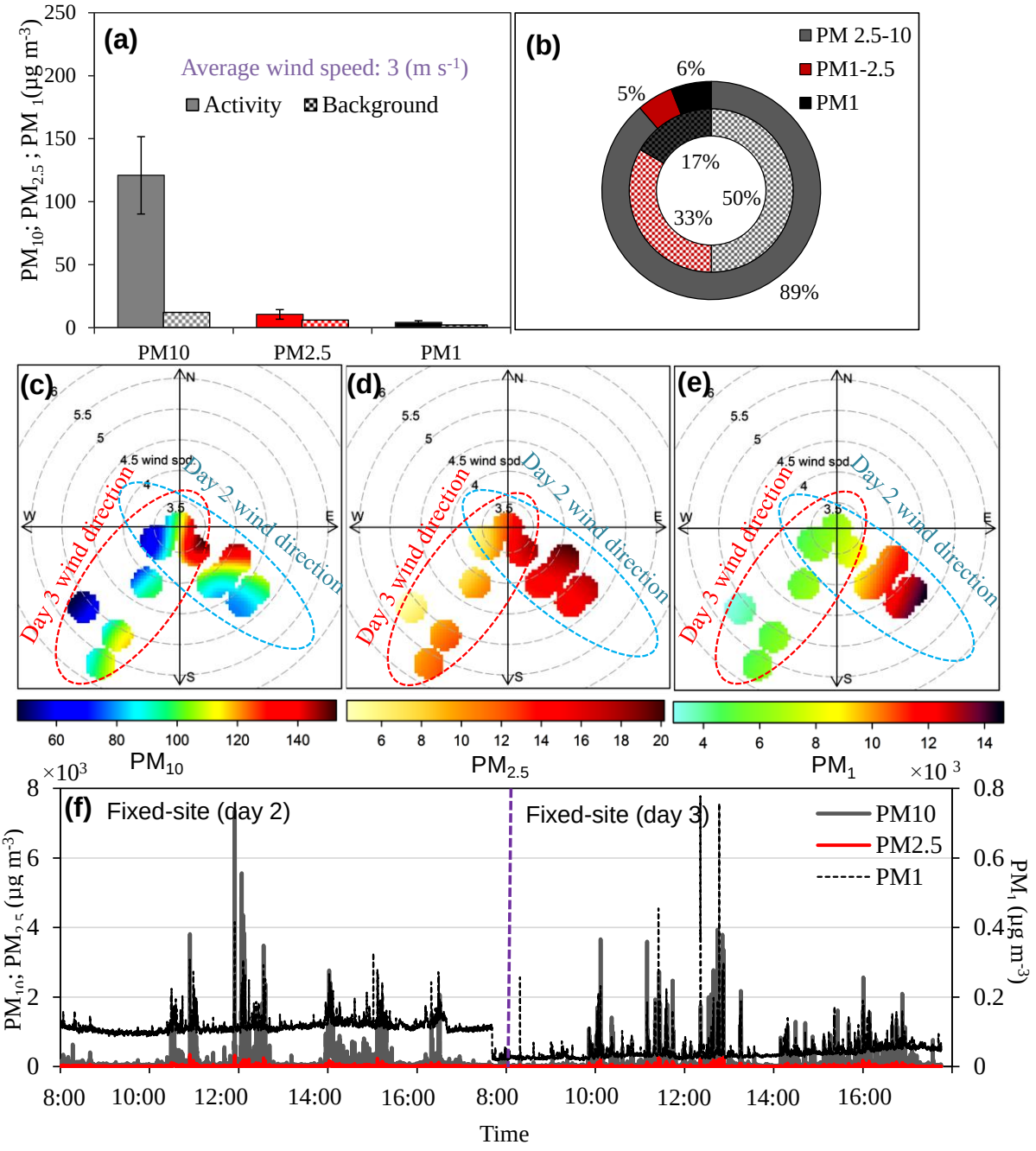

Figure 7.4: (a) The average concentrations of PM_{10}, $PM_{2.5}$ and PM_1 with average of prevailing wind direction, during all days of fixed site measurements. The inner and outer circles represent fractions of PMCs in various size range.

Histograms of PM_{10}, $PM_{2.5}$ and PM_1 concentration were made using the SPSS statistical software for comparing measured concentrations against the air quality standards (SI Figure D2). The EU Directive 2008/50/EC (Directive, 2008) and WHO guidelines (WHO, 2006) suggest the daily mean concentrations of PM_{10} and $PM_{2.5}$, not to exceed of 50 μg m^{-3} (on more than 35 occasions per year) and 25 μg m^{-3}, respectively. The results showed that a cumulative percentage of concentrations for about 42% exceeded the EU daily limit value for PM_{10} and about 11% of the time the daily mean WHO limits of $PM_{2.5}$.

The above observations clearly suggest increased concentrations above the background and exceedances over the regulatory limits, especially for daily mean PM_{10}, for over 2/3rd of total demolition period. On the other hand, the exceedances of $PM_{2.5}$ were minimal, indicating that more efficient preventive measures (e.g. wind barriers, building sealing by impermeable plastic foil or water spraying (Kumar et al., 2012b) is needed to contain the PM_{10} emissions within the site boundaries in order to decrease the exposure to public in the downwind of such sites.

7.3.2 Spatial variations of PM during mobile measurements

In order to understand the exposure to people around the demolition site, the spatial variation of PM_{10}, $PM_{2.5}$ and PM_1 concentrations were assessed on the routes A and B that have a closed "mobile monitoring" loop of about 100 and 600 m, respectively, around the demolition site. The average PM_{10}, $PM_{2.5}$ and PM_1 for the route A were measured as 162.7±48.4, 15.5±0.8 and 4.7±1.2 μg m^{-3} (Figure 7.5a), respectively, with about 4- and two-times lower PM_{10} (37.2±9.1 μg m^{-3}) and $PM_{2.5}$ (7.5±3.6 μg m^{-3}) and slight decrease in PM_1 (3.5±1.0 μg m^{-3}) at the route B (Figure 7.5b). Fractions of coarse (and fine) particles

were found about 90% (10%) and 79% (21%) at route A and route B, respectively (see Figure D3). The higher PMC and fraction of coarse particles at the route A was expected, given that this route was around the periphery of the site compared with route B which was further apart from the demolition site (Table 7.3).

The increase in PMC during the mobile measurements cannot be directly attributed to the demolition activity since the collected data also included the periods when the mobile sampling location was in the upwind of the routes A and B. Therefore, to separate the upwind (primarily baseline, or background, PM concentrations arriving at the site) and downwind concentrations (primarily baseline plus the contribution from the building demolition), firstly the spatially averaged PM concentrations (Figure 7.6) were plotted and then divided the upwind and downwind data set to identify contribution from the demolition activity.

For both routes, the PMCs were much higher in downwind than those in upwind of the site and these differences were highest for the PM_{10}, followed by $PM_{2.5}$ and PM_1. For example, the average PM_{10} $PM_{2.5}$ and PM_1 in downwind (217.4, 21.0 and 6.6 μg m^{-3}) were about 7.7, 2.3 and 2.1 times higher than those in upwind (28.3, 9.3 and 3.1 μg m^{-3}) areas of the demolition site on the route A; with corresponding values on the route B being 63.6, 12.3 and 4.7 μg m^{-3} (in downwind) and 21.0, 3.1 and 2.0 μg m^{-3} (in upwind).

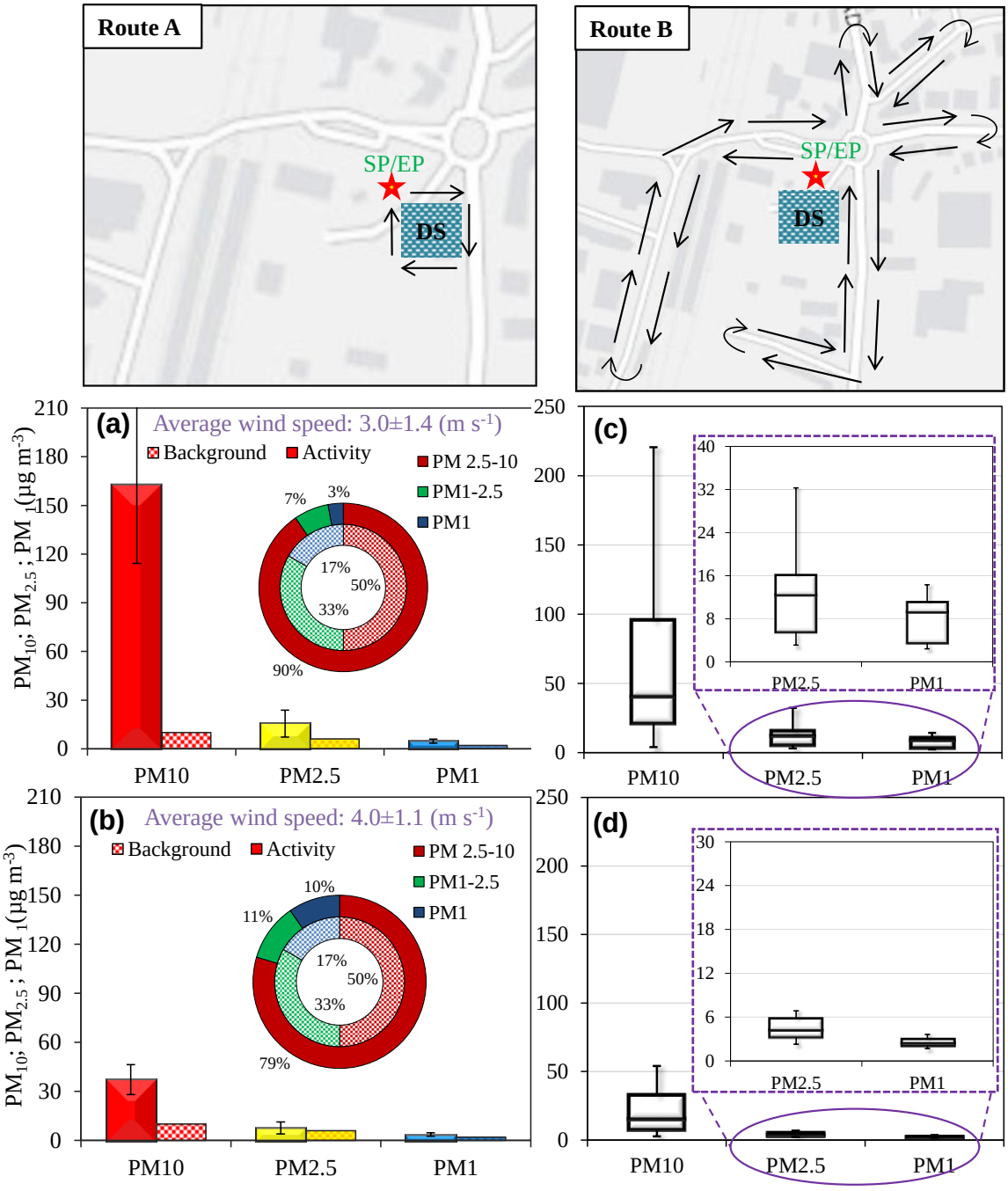

Figure 7.5: The average concentrations of PM_{10}, $PM_{2.5}$ and PM_1, at (a) route A and (b) route B, during all days of mobile measurements. The inner and outer circles represent fractions of PMCs in various size ranges during the background and activity periods. Please note that SP and EP refer to the start and end points, respectively.

Peak concentrations are usually reflection of the intense emission activities, which reached to 3510.9 (PM_{10}), 244.5 ($PM_{2.5}$) and 31.2 μg m^{-3} (PM_1) which were 16.2, 11.6 and 4.7-times over the average PMCs on the downwind of the route A. The manual log of activities showed these peak PMCs corresponding to intense breaking of reinforced concrete beams and shifting the waste material from the site that may have led to generation and resuspension of particles from the site. It was clear from the results that the close vicinity (route A) of the demolition site in downwind wind direction was significantly more influenced by PM emissions and that the most influenced size range was PM_{10}.

It will be interesting to put measurements of this study in the context of relevant mobile measurement studies. For example, Gulliver and Briggs (2004) reported results on variation of PM_{10} concentration during walking on the suburban routes in Northampton, UK. Their average PM_{10} concentrations (38.1±25.1 μg m^{-3}) were ~6 and 2-times lower than those found in downwind of routes A and B of this study, respectively. Furthermore, Kaur et al. (2005) found the average concentration of $PM_{2.5}$ to be 27.5 μg m^{-3} during the measurement of pedestrian exposure during walk along a major road in London (UK) which was slightly higher (~1.3) than averaged downwind $PM_{2.5}$ of this work (21.0 μg m^{-3}). The measured downwind $PM_{2.5}$ on the route A were about 3-times higher than those found inside the car (6.60 μg m^{-3}) by Weichenthal et al. (2014) in Toronto (Canada).

This is clear from the above contextualisation that while PM_{10} concentrations can be much higher in the downwind of demolition sites compared to those the most polluted roadside environments in urban areas; the $PM_{2.5}$ emissions from demolition are generally less pronounced and comparable to urban walking and in-vehicle studies.

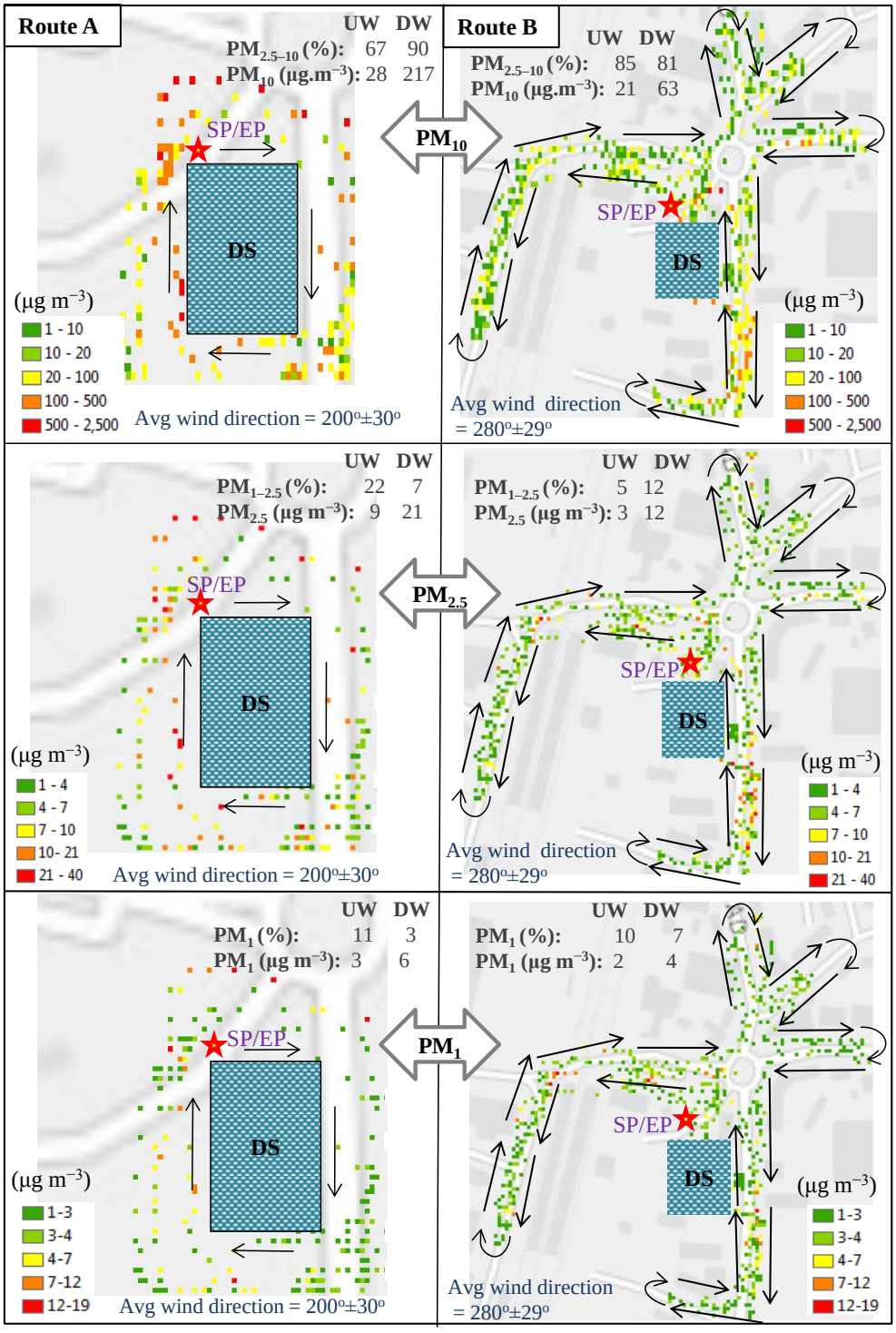

Figure 7.6: The spatially averaged concentrations of PM_{10}, $PM_{2.5}$ and PM_1 during mobile measurements at (a) route A and (b) route B. The words Avg, DW and UW in the figure represent average, downwind and upwind, respectively. A number of parallel points at each route were due to the sensitivity of GPS device, which varied within ±3.5 m at the same route.

Table 7.3: PM_{10}, $PM_{2.5}$ and PM_1 concentrations (μg m^{-3}) during mobile measurements at routes A and B.

Route A				Route B			
	PM_{10}	$PM_{2.5}$	PM_1		PM_{10}	$PM_{2.5}$	PM_1
Run 1A	48.8±20.7	12.2±2.1	4.3±0.6	Run 1B	35.0±5.1	12.2±0.5	4.7±0.4
Run 2A	29.6±2.7	9.8±0.1	3.9±0.2	Run 2B	28.4±7.8	9.1±1.3	3.9±0.7
Run 3A	133.9±83.5	19.4±5.3	8.3±1.3	Run 3B	61.7±56.8	12.2±5.2	4.9±1.2
Run 4A	202.4±198.0	19.9±12.1	5.8±1.3	Run 4B	32.9±9.6	9.3±1.6	4.5±1.1
Run 5A	331.7±204.1	27.0±9.3	6.7±1.0	Run 5B	75.8±81.3	10.5±6.3	3.5±1.7
Run 6A	24.4±6.6	8.3±1.6	4.2±1.3	Run 6B	28.2±20.4	7.4±1.1	4.0±0.9
Run 7A	53.3±37.1	7.0±4.5	2.2±0.4	Run 7B	23.5±11.6	4.6±0.7	2.7±0.8
Run 8A	440.1±358.5	30.9±24.3	5.2±2.2	Run 8B	29.9±37.6	5.0±1.2	3.1±0.4
Run 9A	171.4±96.8	13.5±4.5	4.1±0.6	Run 9B	25.3±15.6	5.5±0.4	3.2±0.6
Run 10A	155.5±91.7	12.9±1.9	4.4±0.9	Run 10B	58.2±54.5	6.4±3.2	2.7±0.6
Run 11A	150.8±56.8	11.4±1.7	3.5±0.3	Run 11B	29.5±22.9	5.1±1.2	3.0±0.4
Run 12A	210.8±114.4	13.8±4.7	3.4±0.8	Run 12B	17.9±8.7	3.3±0.4	2.2±0.2
Overall average	162.7±48.4	15.5±0.8	4.7±1.2	Total	37.2±9.1	7.5±3.6	3.5±1.0

7.3.3 Concentrations inside the excavator cabin and temporary on-site office

Excavator vehicle and on-site temporary offices are integral part of demolition sites where drivers and on-site workers remain present. In order to understand how the concentration levels change during the demolition periods in these settings, the measurements made showed the *average* (and *peak*) concentrations of PM_{10}, $PM_{2.5}$ and PM_1 inside the excavator cabin as 455±349 (54124), 109±54 (12401) and 75±14 (699) μg

m^{-3}, respectively (Figure 7.7a), which were about 38 (4500), 18 (2060) and 37 (350) times higher than those during the background periods, respectively. These relatively higher average concentrations and the notably high peak values inside the excavator cabin, compared with fixed-site (Section 7.3.1) and mobile measurements (Section 7.3.2), were expected due to a very close proximity (~5 m) of the excavator cabin from the demolition site.

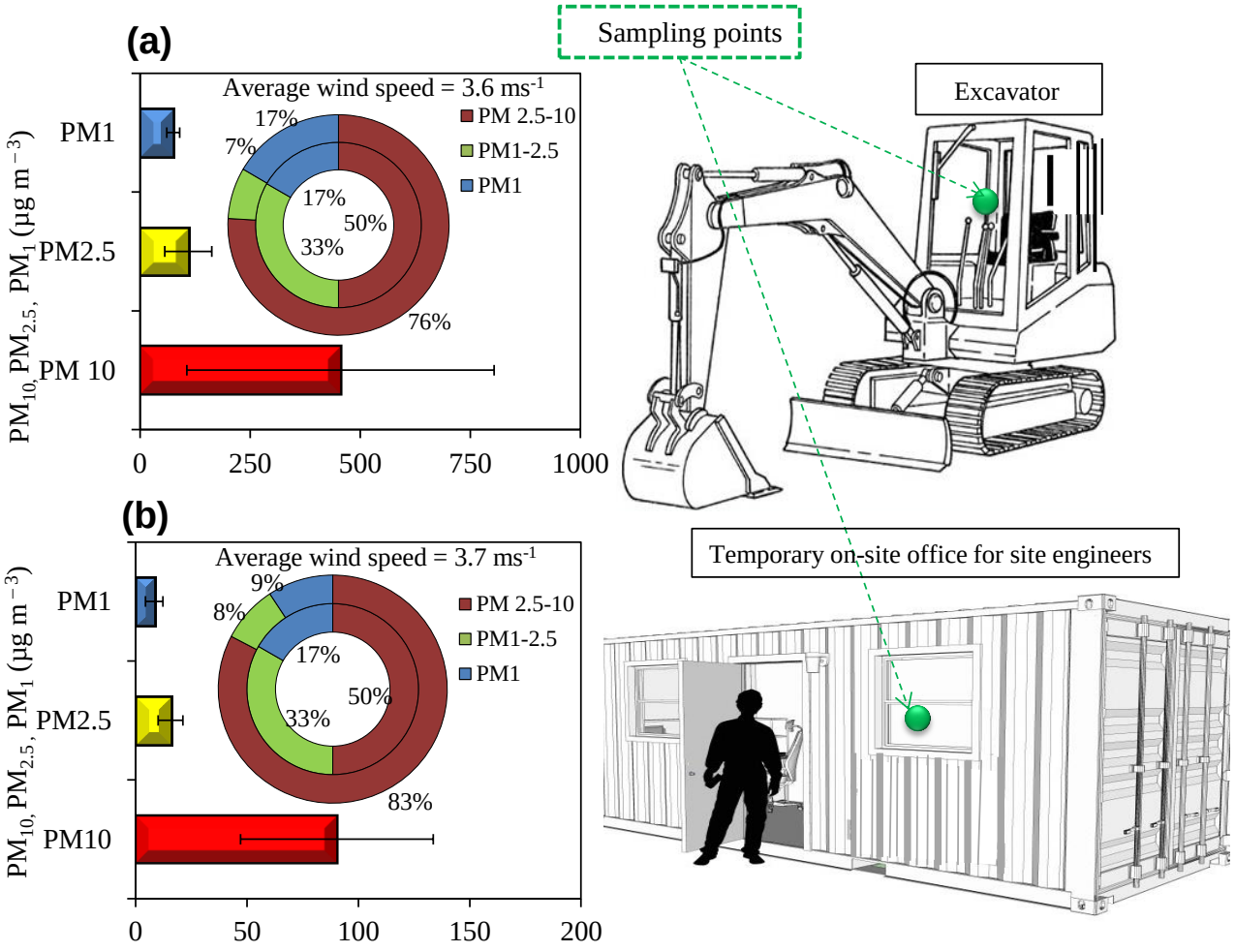

Figure 7.7: The concentrations of PM_{10}, $PM_{2.5}$ and PM_1, at (a) the excavator cabin and (b) temporary on-site office for site engineers and managers during the background and working periods, respectively.

As for the concentrations in on-site temporary office, the *average* (and *peak*) concentrations of PM_{10}, $PM_{2.5}$ and PM_1 were measured as 90±4 (2566), 16±6 (341) and 8±4 (26) μg m^{-3} during the days of measurements, respectively (Figure 7.7b). The corresponding *average* (and *peak*) PM_{10}, $PM_{2.5}$ and PM_1 increased to 8 (214), 9 (57) and 7 (13) times higher over the background levels during the building demolition periods. These peak values for on-site office were recorded during the time of intense demolition of the building's ceiling and falling of demolished materials such as brick and concrete pieces from heights to the ground level at the site. Furthermore, a greater fraction of coarse particles (i.e. 83%), compared to that (~76%) in excavator cabin, was found in on-site temporary offices (Figure 7.7). This higher fraction could be expected due to much higher ventilation, and hence penetration of particles, to the site office through windows and doors openings as opposed to the much air tighter excavator cabin.

The above results clearly reflect that drivers of excavator vehicle and the other on-site workers, engineers or supervisors are exposed to relatively high level of PM concentrations at the demolition sites. The levels of concentrations, as expected, reduce with the distance from the source (i.e. demolition site in this case) and release of emissions from demolition activity is much larger in PM_{10} size fraction compared with $PM_{2.5}$ (Figure 7.7).

7.3.4 PM decay profiles

The PM data collected at different downwind distances (i.e. at 10, 20, 40 and 80 m) was plotted for evaluating the horizontal decay in concentrations of PM_{10}, $PM_{2.5}$ and PM_1 in the downwind of demolition site (Figure 7.8). In order to find the best fit function, both the logarithmic (Figure 7.8) and exponential (see Figure D4) best fit functions were applied to net ΔPM_{10}, $\Delta PM_{2.5}$ and ΔPM_1 concentrations, which were determined by subtracting the background PMCs from the measured concentrations during the demolition period. The ΔPM concentrations at downwind distances showed a negatively correlated logarithmic form (Figure 7.8), with R^2 values as 0.94 (ΔPM_{10}), 0.93 ($\Delta PM_{2.5}$) and 0.84 (ΔPM_1). For the discussion purposes, the logarithmic decay function (Figure 7.8) was chosen as a best fit to the data due to better R^2 values than those given by an exponential decay profile as 0.85, 0.89 and 0.68 for ΔPM_{10}, $\Delta PM_{2.5}$ and ΔPM_1), respectively (see Figure D4).

The decay profiles suggest a higher rate of change in PM concentrations close to the demolition site compared with those at farther distances. For example, the rate of change in ΔPM_{10}, $\Delta PM_{2.5}$ and ΔPM_1 concentration with per meter distance are (1.60, 0.51, 0.27) $\mu g\ m^{-3}$ between 10 and 20 m, which decreases to (0.27, 0.45, 0.04) and (0.19, 0.06, 0.01) $\mu g\ m^{-3}$ per meter distance in the 20-40 m, and 40-80 m range, respectively (Figure 7.8). Furthermore, the average PM_{10}, $PM_{2.5}$ and PM_1 concentrations reached to half of their initial concentrations within 80, 50 and 50 m from the demolition site, respectively (Figure 7.8).

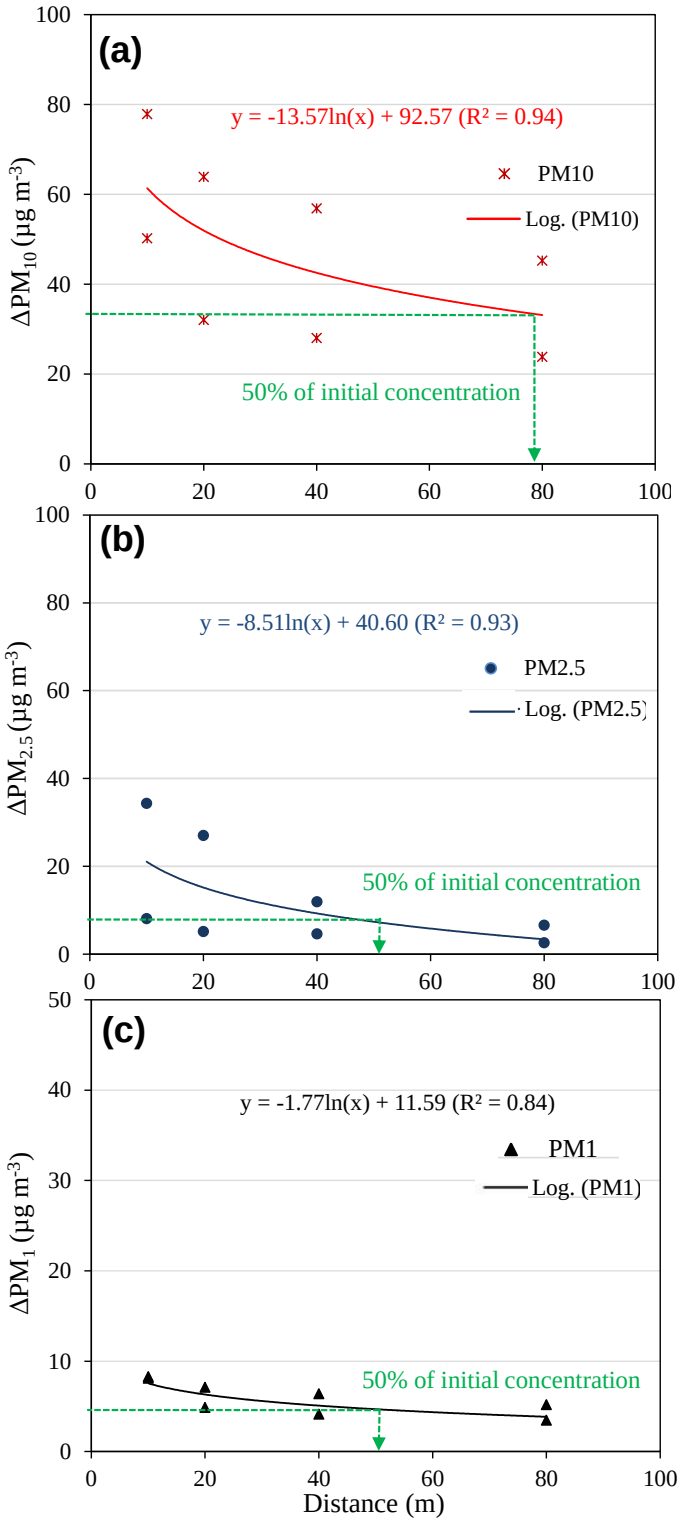

Figure 7.8: (a) Horizontal decay profiles of ΔPM_{10}, (b) $\Delta PM_{2.5}$ and (c) ΔPM_1 at the demolition site during the sequential measurements; *x* and *y* expresses distance from the demolition site and ΔPM values, respectively.

Similar decay profiles from demolition works are not available for comparison but other studies for construction or roadside (Buonanno et al., 2009; Hagler et al., 2009; Hitchins et al., 2000) have either logarithmic or exponential decay profiles. For example, Azarmi et al. (2015b) and Buonanno et al. (2009) found the decay profiles of PM_{10} and $PM_{2.5}$ for the construction works in London (UK) and at the highway in Cassino (Italy) as logarithmic and exponential, respectively.

In order to understand how far the initial concentrations from demolition site reaches to meet the standard limits, the daily limits of the EU Directive 2008/50/EC (Directive, 2008) for PM_{10} and WHO guidelines for $PM_{2.5}$ (WHO, 2006) were compared with decaying concentrations of this study (Section D3 in Appendix D). PM_{10} and $PM_{2.5}$ took 50 and 15 m in the downwind of demolition site to meet the EU and WHO daily mean standard values, respectively (see Figure D5). This distance could be taken as a public exclusion zone in the downwind direction of such demolition sites during demolition days.

7.3.5 The PMEFs for building demolition

Using the modified box model described in Section 3.4.2 and the PM data monitored downwind of the building demolition at the fixed-site (Section 7.3.1), the average PMEFs for PM_{10}, $PM_{2.5}$ and PM_1 were estimated as 35±1, 17±4 and 4±0.5 µg m^{-2} s^{-1}, respectively (see Table D2). While there are numerous field studies available for emission factors from road traffic (Kumar et al., 2011b), limited studies are available for road works (Font et al., 2014) and almost none for building demolition activity. For example, Font et al. (2014) estimated emission factors for PM_{10} from road works in London as 0.0022 kg m^{-2} $month^{-1}$ which was about 6-fold smaller than those observed

(0.013±0.004 kg m^{-2} $month^{-1}$) in this study (Section D4). This difference clearly suggest much larger emissions of PM_{10} during building demolition, which is expected given its dry and intense nature compared with less intense construction activities in relatively open areas such around roads. Results of this study were about 19-fold higher than those reported in the UK National Atmospheric Emissions Inventory (NAEI) for the PM_{10} as 0.0007 kg m^{-2} $month^{-1}$ (NAEI, 2013) and about 2-fold greater than European emission inventory median value (0.0068 kg m^{-2} $month^{-1}$) (EMEP-EEA., 2013) for the demolition and construction activities (see Figure D6). The PMEF of $PM_{2.5}$ and PM_1 from demolition, construction or road works are currently unavailable and hence estimates of this wok provide hitherto missing information for future experimental and modelling studies.

7.3.6 Morphology and chemical characterisation

SEM and EDS analyses were performed on the bulk mass of particles collected on the filters (Table 7.4) for assessing their shape, size, composition and structure (Section D5). Figure 7.9 shows the SEM images of the samples, indicating a heterogeneous structure with crystal and aggregated shaped particles during the demolition works; the irregular shaped holes show the porosity of PTFE filters. EDS analysis suggested the dominance of silicon, Si (10.5-17.8%) and aluminium, Al (4.2-5.1%; Table 7.4).

The crystal shaped particles are thought to be Si released from concrete debris (Srivastava et al., 2009) while the aggregated shaped particles shows the presence of metals such as Al (Falkovich et al., 2001). The EDS analysis also showed the presence of other elemental species (Table 7.4), with a strong peak for carbon (C) and fluorine (F) in the blank "reference" filter, with an additional peak of nitrogen (N) in the background sample (see

Figure D7). C and F are thought to be the material of PTFE filters while presence of N in the background filter is possibly from the regional background in a nitrate form due to secondary gas-to-particle aerosol formation (Schaap et al., 2004; Viana et al., 2008). The differences between particles deposited on the reference (sample 1) and background (sample 2) filters and those collected during the demolition activity periods (samples 3, 4 and 5) signify the presence of *new* elements (Figure 7.9). Apart from the dominating fraction of Si and Al, the additional elements during the demolition periods were found to be sulphur (S), chlorine (Cl), magnesium (Mg), sodium (Na) and Zinc (Zn), as shown in Table 7.4. The potential sources of these elements in urban environments are summarised in Table D3.

Some of the deposited elements could be in oxide form because of presence of O during the demolition activities. The increment in the intensity and ratio of O peak compared with other peaks like Si, Al and S suggested that these elements appear to be strongly related with building demolition sources where aluminium oxide, sulphur oxide and silicon dioxide compounds are expected to be formed. The main source of Si is likely to be building related activities, particularly those involving concrete material such as breaking concrete slabs, which is typically made of cement, admixtures, water and aggregates (Kumar and Morawska, 2014). Si can be found in asbestos-containing hazardous building materials and it is also one of the key constituents of cement in the form of celite (tetracalcium aluminoferrite), belite (dicalcium silicate) and alite (tricalcium silicate) (Beck et al., 2003; Lioy et al., 2002). Al were thought of coming from breaking and demolition of aluminium windows, steel beams and concrete since alumina (Al_2O_3) is integral

component of cement (Azarmi et al., 2015b). There are sources such as sea salt and fuel oil fly ash for S (see Table D3) but this is expected to be predominantly arising from diesel exhaust emissions from the construction machinery (Dorado et al., 2003). Furthermore, Na and Cl were mostly likely due to the effect of sea salt brought by the south-westerly winds to the site (Figure 7.3). Zn and Mg were expected to be contributed by on-site exhaust emissions from construction machinery and soil dust, respectively. The above results reflect the dominance of Si and Al in particles and the ability of building demolition works to effectively aerosolise both friable and non-friable building materials to the surrounding environment.

Table 7.4: The elemental composition of the all the filters (quantitative EDS analyses).

Sample 1 (Reference)		Sample 2 (Background)		Sample 3 (Fixed site)		Sample 4 (Mobile measurements)		Sample 5 (Different distances)	
Name	Fraction (%)	Name	Fraction (%)	Name	Fraction (%)	Name	Fraction (%)	Name	Fraction (%)
C	30.6	C	46.2	C	16.7	C	19.3	C	21.0
-	-	O	24.3	O	48.5	O	48.9	O	22.9
F	69.3	-	-	F	3.5	F	1.4	F	40.8
-	-	-	-	Si	17.8	Si	14.0	Si	10.5
-	-	S	1.2	S	2.3	S	4.2	-	-
-	-	-	-	Al	5.1	Al	4.5	Al	4.2
-	-	-	-	Mg	1.4	Mg	2.6	Mg	0.3
-	-	Cl	4.4	Cl	1.9	Cl	1.5	-	-
-	-	Na	2.6	Na	2.5	-	-	-	-
-	-	N	21.0	-	-	-	-	-	-
-	-	-	-	-	-	Zn	3.1	-	-

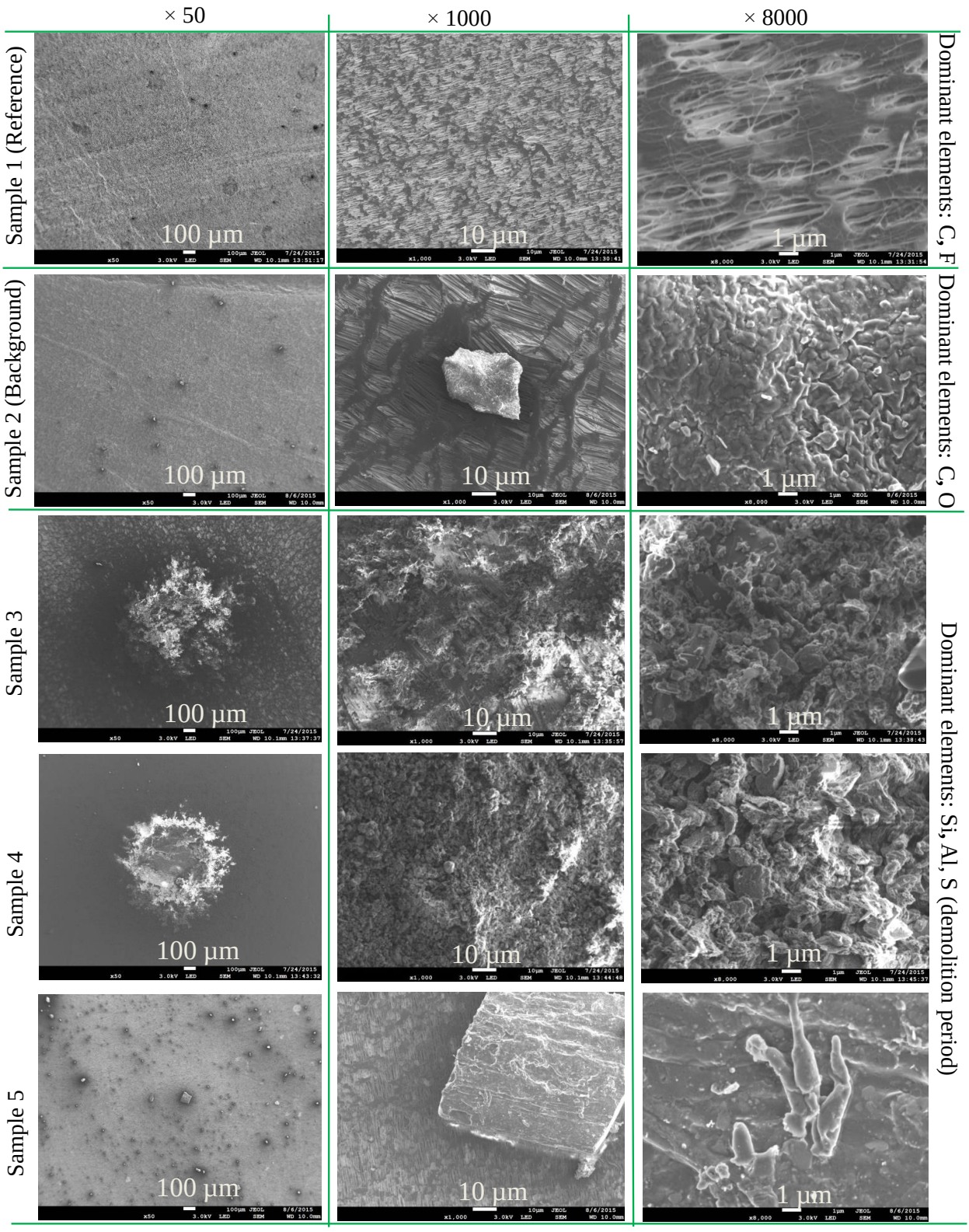

Figure 7.9: SEM images of the surface morphology of the particles collected on blank filter, background measurements, sample 3, sample 4 and sample 5 at ×50, ×1000 and ×8000 resolution.

7.3.7 Exposure to demolition workers and engineers

The average respiratory deposited doses (RDD) of coarse and fine particles were estimated using the methodology described in Section 3.5.2 for people on and around the demolition sites (i.e. workers, individuals around the demolition site, engineers inside a temporary on-site offices and drivers inside the excavator vehicle cabin) during heavy and light exercise levels (Table 7.5). Compared to the local background (pre-demolition) exposure levels, the RDD of coarse and fine particles were found to be 58- and 5-times in the excavator vehicle cabin, respectively, which happens to be the highest exposure among all the assessed categories. This was followed by the fixed-site "downwind" measurements where RDD rate for coarse (and fine) particles were 20- (and 3-) times over the background, followed by 32- (and 4-) times at the downwind of mobile measurements on the routes A compared to only 9- (and 3-) times at the route B and 13- (and 2-) times in the on-site temporary office (Figure 7.10). Given a logarithmic decay of emissions away from the site (Section 7.3.4), the distance from the demolition site was an important variable to describe the differences in RDD. For example, highest RDD were calculated at the closed locations to the source, such as at the excavator vehicle cabin (see Figure D8). As expected, downwind RDD of coarse (and fine) particles during mobile measurements were 10- (and 3-) times higher for route A, and 3- (and 4-) times higher for route B, respectively, compared to those in upwind of demolition site. These downwind exposures are much higher than those reported during walking on typical urban routes. For instance, the PM_{10} and $PM_{2.5}$ concentrations measured by Gulliver and Briggs (2004) during walking on suburban routes in Northampton, UK were used to calculate RDD for comparison. Their RDD for coarse (and fine) particles were found to be up to 8- (and 2-) and 2- (and 0.8-)

times less than downwind RDD of this study during the mobile measurements at route A and route B, respectively.

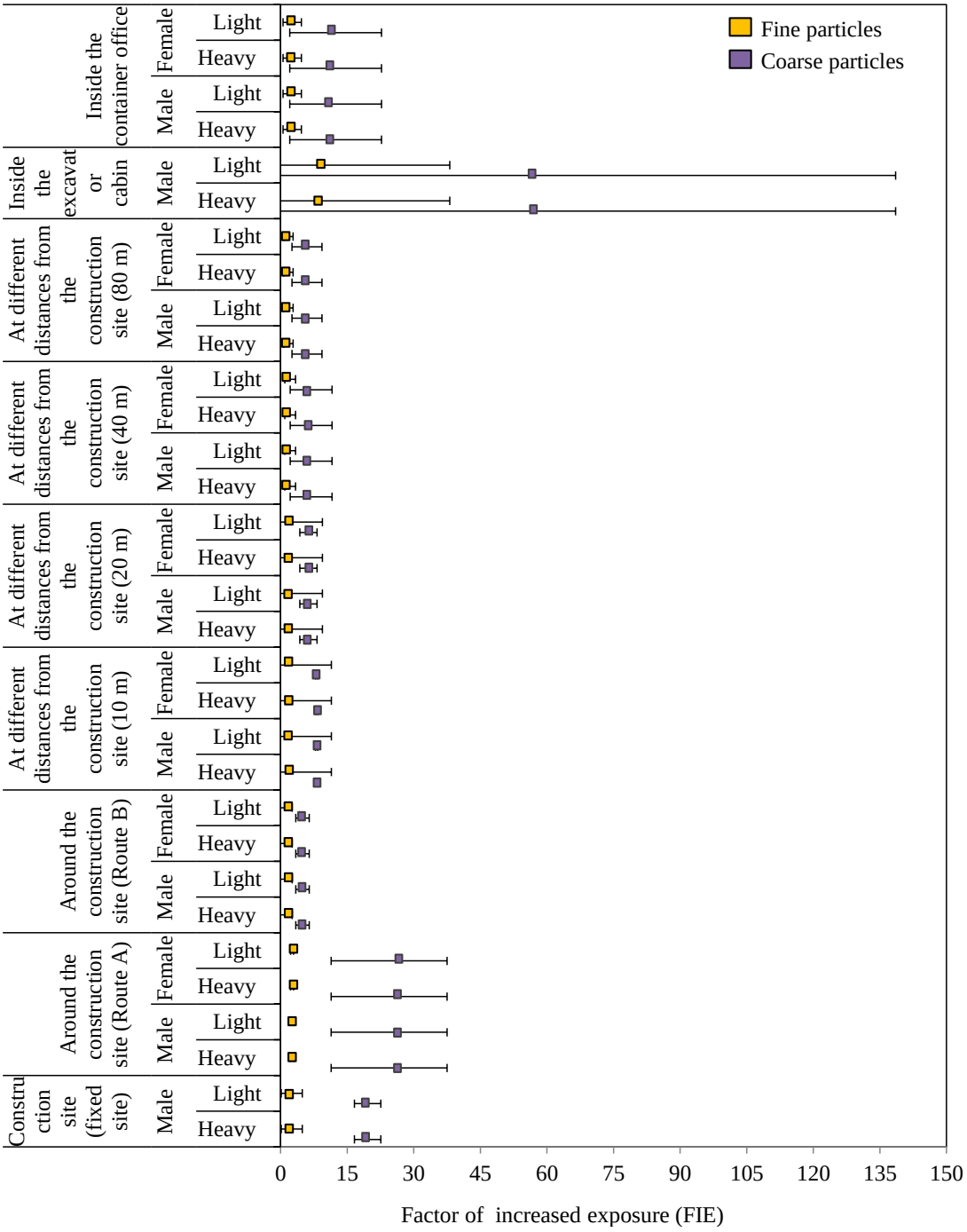

Figure 7.10: Factor of increased exposure (FIE) representing a ratio of respiratory deposition doses during the activities over the background level in coarse and fine particles range during each activity.

Table 7.5: The RDD rates of coarse and fine particles.

Location	Gender	Exercise level	Total RDD (μg $min^{-1} \times 10^{-2}$) ±STD	
			Coarse particles	Fine particles
Construction site (fixed site)	Male	Heavy	572.8±52.7	34.7±14.6
		Light	290.0±26.6	17.5±7.4
Around the construction site (route A)	Male	Heavy	956.0±231.8	64.8±2.5
		Light	484.1±117.3	32.8±1.2
	Female	Heavy	827.6±200.6	56.1±2.2
		Light	383.4±92.9	26.0±1.0
Around the construction site (route B)	Male	Heavy	249.7±26.8	38.0±11.2
		Light	126.4±13.5	19.2±5.6
	Female	Heavy	216.1±23.2	32.9±9.7
		Light	100.1±10.7	15.2±4.5
At different distances from the construction site (10 m)	Male	Heavy	238.7±4.7	39.5±26.9
		Light	120.8±2.4	20.2±13.6
	Female	Heavy	206.6±4.1	34.2±23.3
		Light	95.7±1.9	15.8±10.8
At different distances from the construction site (20 m)	Male	Heavy	185.1±34.4	32.0±22.4
		Light	93.7±17.4	16.2±11.3
	Female	Heavy	160.3±29.8	27.7±19.4
		Light	74.2±13.8	12.8±8.9
At different distances from the construction site (40 m)	Male	Heavy	202.9±84.0	18.7±4.7
		Light	102.7±42.5	9.5±2.3
	Female	Heavy	175.3±72.7	16.2±4.0
		Light	81.3±33.6	7.5±1.8
At different distances from the construction site (80 m)	Male	Heavy	175.5±60.3	15.4±4.1
		Light	88.8±30.5	7.8±2.0
	Female	Heavy	151.9±52.2	13.3±3.5
		Light	70.4±24.1	6.1±1.6
Inside the excavator cabin	Male	Heavy	1662.8±1422.3	78.3±38.2
		Light	842.0±720.2	39.6±19.3
Inside the temporary office	Male	Heavy	365.4±184.3	30.7±10.9
		Light	185.0±93.3	15.5±5.5
	Female	Heavy	316.3±159.5	26.5±9.4
		Light	146.5±73.9	12.3±4.3
Background	Male	Heavy	29.3±17.7	15.2±6.8
		Light	14.8±8.9	7.7±3.4
	Female	Heavy	25.3±15.3	13.1±5.9
		Light	11.7±7.1	6.1±2.7

Result of this study also showed that exposure to coarse particle is greater compared with fine particles due to the disproportionate increments in concentrations of coarse particles from demolition works (Sections 7.3.1-7.3.3). Since male subjects breathe and inhale higher doses of coarse and fine particles, compared with female subjects, due to differences in body tidal volume and higher frequency of breathing (Section 3.7.2), male workers are expected to inhale more particles than female workers (Figure 7.10). Furthermore, given that breathing rate and frequency are higher during heavy exercises such as removing and segregating demolished materials for re-use or recycling, exposure rates could vary substantially depending on the nature of work workers are involved even if all the workers are exposed to same emission source (see Section D6).

7.4 Chapter summary and conclusions

Size-resolved mass distributions of particles were measured in the 0.22–10 µm size range through a combination of measurement strategies (e.g. fixed-site and mobile). The objectives of this study were to assess emission characteristics of PM emissions in various size ranges during the mechanical demolition of a building, in addition to understand their physicochemical characteristics and the occupational exposure of workers to PM_{10}, $PM_{2.5}$ and PM_1 on and around the demolition site.

The following conclusions are drawn:

- The mass concentrations of average PM_{10}, $PM_{2.5}$ and PM_1 were found to be about 11-, 3- and 4-times above the local background levels during fixed-site measurements at the downwind of the demolition site. The coarse particles ($PM_{2.5-10}$) contributed majority (89%) of the total PMCs. The largest PM_{10}, $PM_{2.5}$ and PM_1 were detected in the

excavator cabin during the demolition of building's ceiling and walls.

- The overall average PM_{10}, $PM_{2.5}$ and PM_1 during mobile measurements at route A were found to be 4-, 2- and 1.5-times higher than those at the route B (larger periphery of the site), mainly due to route A being the closed periphery of the demolition site. Segregation of the data in the downwind of the demolition site showed up to 8- and 2.5-times higher PM_{10} and $PM_{2.5}$ concentrations than those in the upwind of the mobile routes, respectively. These observations substantiate my previous findings that the demolition activities produce much larger PM_{10} emissions compared with $PM_{2.5}$. The exposure to high PMCs can be minimised by staying indoors or being positioned upwind of demolition sites.
- ΔPM_{10}, $\Delta PM_{2.5}$ and ΔPM_1 values during the demolition period in the downwind direction showed a logarithmic decay with distance ($R^2 \approx 0.90$). Such decay profiles are important for extrapolating emissions in downwind of building demolition and incorporate them in dispersion models such as were used in PMEF modelling. PM_{10} and $PM_{2.5}$ concentrations meet the daily mean EU and WHO limit values at about 50 and 15 m, respectively, suggesting this as a public exclusion zone in this particular case.
- Average emission factors during fixed-site monitoring of demolition activity were calculated as 35.3±12.7, 12.2±3.6 and 3.9±0.5 μg m^{-2} s^{-1} for PM_{10}, $PM_{2.5}$ and PM_1, respectively. Such emission factors are currently lacking, but are key input to dispersion models for accurately estimating the affected area around demolition sites and design appropriate measures to limit the exposure of nearby public.

- SEM images indicated irregular, aggregated and crystal shaped particles during the demolition works while the EDS analysis suggested the dominance of Si and Al in the particles. The escape of these elements along with others such as S, Zn and Mg suggest towards appropriate protection measures of population, particularly sensitive subgroups (e.g. elderly and children) and those in nearby sensitive areas (e.g. hospitals, retirement home or nurseries).
- The downwind distance from the demolition site was an important factor to dictate the exposure doses. For example, highest exposure doses to coarse (and fine) particles were found to be inside the excavator vehicle cabin, which were up to 6- (and 5-), 5- (and 3-) and 17- (and 6-) times higher than those in downwind at the fixed-site, downwind of the mobile route A and temporary on-site office, respectively. Other factors affecting the exposure doses of individual workers depend on their nature of work and type of physical exercise and therefore the RDD rates could be different to workers involved in heavy and light exercise, site engineers or drivers even if they are exposed to same level of particle concentrations.

This study focuses on PM_{10}, $PM_{2.5}$ and PM_1 generated from the demolition of a 3-storey brick-walled concrete building. The results showed effect of PM emissions on the exposure to people on and around such sites. The elevated PMCs during the demolition represent a potential health risk due to exposure to a wide variety of toxic elemental species. The results are also important for the development of mitigation strategies prior to the demolition operations and accordingly choose special protective equipment to limit exposures during the demolition activities. The male subjects inhale more doses of particles

than female subjects, because of their higher body tidal volume and breathing frequency and that the rate of deposited particles could considerably increase during heavy exercises by workers for the same emission source. This suggests varying RDD rates to individual workers depending on their nature of work. Further personal monitoring studies, focusing on individual workers with different level of physical activities at large-scale demolition sites, are recommended to advance the understanding of occupational exposure of on-site workers.

Chapter 8. Summary, conclusions and future work

This chapter presents a summary and conclusion of this thesis drawn from the preceding chapters. It also presents recommendations for future research.

8.1 Summary

Building works including refurbishment, construction and demolition, are now common in both the developing and developed world. However, PM emitted from such activities in the coarse, fine and ultrafine particle size ranges contain a wide variety of toxic organic substances, and may adversely affect the respiratory health of on-site workers and nearby residents (Kumar et al., 2012; Azarmi et al., 2014). This research thus set out to conduct a series of laboratory, indoor and outdoor field measurements to determine the impact of PM types arising from a range of building activities. The other objectives of this thesis were to determine the emission characteristics and occupational exposure to PM_{10}, $PM_{2.5}$, PM_1 and ultrafine particles, and gain an understanding of the physicochemical properties, of those particles such as shape, size and composition, which are currently poorly understood. Chapter 1 outlined the background, motivation, objectives and approach of this thesis. A comprehensive literature review of the existing knowledge and relevant published studies of airborne PM and ultrafine particles are presented in Chapter 2. At the beginning of Chapter 2, the definitions of ultrafine particles and PM and their

emissions features from various building activities were also discussed. This was followed by an assessment of the likely indoor and outdoor sources of particles, with a detailed focus on particles derived from specific building activities. In addition, the physical and chemical characterisations of particles were examined using physiochemical analysis such as SEM, EDS, XPS and IBA. The review of current literature suggests that the existing knowledge requires more extensive research to monitor the impact of building activities on the air quality of areas surrounding building works, and to assess their potential impact and levels of occupational exposure.

A set of experiments were set up in order to fill the research gap, as reviewed in Chapter 3, so as to achieve the research objectives described in Chapter 1. Chapter 3 focused on the methodologies, materials and methods which were used in the experiments, and provides information on site descriptions and sampling set ups. The following chapters (Chapters 4-7) presented the results obtained from the laboratory and field experiments, with a related discussion about the measurements of particle mass, number concentrations and size distributions. The summary of experiments, findings and conclusions were described in the following Section 8.2 and Section 8.3 of this Chapter 8.

8.1.1 Simulated laboratory investigations

Building activities generate coarse, fine and ultrafine particles making it necessary to understand both the exposure levels of operatives on site and the dispersion of ultrafine particles into the surrounding environment. This study investigates the release of PM and ultrafine particles, during the mixing of concrete (combining Portland cement with ground granulated blastfurnace slag, GGBS or pulverised fuel ash, PFA) and the subsequent

drilling and cutting of hardened concrete. Particles were measured in the 5-10,000 nm size range using a GRIMM particle spectrometer and a fast response differential mobility spectrometer (DMS50). The mass concentrations of coarse particles contributed ~52-64% of total mass released. The ultrafine particles dominated the total particle number concentrations; being 74, 82, 95 and 97% for mixing with GGBS, mixing with PFA, drilling and cutting, respectively. Peak values measured during the drilling and cutting activities were 4 and 14 times the background. Equivalent emission factors were calculated and the total respiratory deposition dose rates for PNCs for drilling and cutting were $32.97\pm9.41 \times10^{8}$ min^{-1} and $88.25\pm58.82 \times10^{8}$ min^{-1}. These are a step towards establishing number and mass emission inventories for particle exposure during construction activities.

8.1.2 Release of particles from indoor activities of building refurbishment

Understanding of the emissions of coarse, fine and ultrafine particles from refurbishment activities and their dispersion into the nearby environment is of primary importance for developing efficient risk assessment and management strategies in the construction and demolition industry. This study investigates the release, occupational exposure and physicochemical properties of PM and ultrafine particles, from over 20 different indoor refurbishment activities occurring at an operational building site. Particles were measured in the 5–10,000 nm size range using a fast response differential mobility spectrometer and a GRIMM particle spectrometer for 55 hours over 8 days. The ultrafine particles were found to account for >90% of the total particle number concentrations and <10% of the total mass concentrations released during the recorded activities. The highest ultrafine particle concentrations were 4860, 740, 650 and 500 times above the background value during wall chasing, drilling, cementing and general demolition activities,

respectively. Scanning electron microscopy, X-ray photoelectron spectroscopy and ion beam analysis were used to identify physicochemical characteristics of particles and attribute them to probable sources considering the size and the nature of the particles. The results confirm that refurbishment activities produce significant levels (both number and mass) of airborne particles, indicating a need to develop appropriate regulations for the control of occupational exposure of operatives undertaking building refurbishment.

8.1.3 Assessment of PM_{10} and $PM_{2.5}$ particles from outdoor construction activities

Construction activities are common across cities, yet the studies assessing their contribution to airborne PM_{10} and $PM_{2.5}$ particles on the surrounding air quality are limited. Here, we assessed the impact of PM_{10} and $PM_{2.5}$ arising from outdoor construction works in and around London. Measurements were made at 17 different monitoring stations around three construction sites between January 2002 and December 2013. Tapered element oscillating micro balance (TEOM 1400) and OSIRIS (2315) particle monitors were used to measure PM_{10} and $PM_{2.5}$ fractions in the 0.1–10 µm size range along with the ambient meteorological data. The data were analysed using bivariate concentration polar plots and k-means clustering techniques. Daily mean concentrations of PM_{10} were found to exceed European Union target limit value of 50 µg m^{-3} at 11 monitoring stations but remained within the allowable 35 exceedances per year, except at two monitoring stations. In general, construction works found to influence downwind concentrations of PM_{10} relatively more than $PM_{2.5.}$ Splitting of the data between working (0800-1800 h; local time) and non-working (1800-0800 h) periods showed about 2.2-fold higher concentrations of PM_{10}

during working hours compared with non-working hours. However, these observations did not allow concluding that this increment was from the construction emissions. Together, the polar concentration roses and the k-means cluster analysis applied to a pair of monitoring stations across the construction sites (i.e. one in upwind and the other in downwind) confirmed the contribution of construction sources on the measured concentrations. Furthermore, pairing the monitoring stations in downwind of construction sites showed a logarithmic decrease (with R^2 about 0.9) in PM_{10} and $PM_{2.5}$ concentration with the distance. Findings of this study clearly indicate an impact of construction activities on the nearby downwind areas and a need for developing mitigation measures to limit their escape from the construction sites.

8.1.4 Exposure to particles from outdoor building demolition activities

Demolition of buildings produce large quantities of PM that could be inhaled by on-site workers and people living in the neighbourhood, but studies assessing occupational exposure at the real-world demolition sites are rare. Concentrations of PM_{10}, $PM_{2.5}$ and PM_1 were measured along with local meteorology for 54 working hours over the demolition period. The measurements were carried out at (i) a fixed-site in the downwind of demolished building, (ii) around the site during demolition operation through mobile monitoring, (iii) different distances away from the demolition site through sequential monitoring, and (iv) inside an excavator vehicle cabin and on-site temporary office for engineers. Position of the PM instrument was continuously recorded using a Global Positioning System on a second basis during mobile measurements. Fraction of coarse particles contributed 89 (with mean particle mass concentration, PMC ≈ 133±17 μg m^{-3}),

83 (100±29 μg m^{-3}), and 70% (59±12 μg m^{-3}) of total PMC during the fixed-site, mobile monitoring and sequential measurements, respectively, compared with only 50% (mean 12±6 μg m^{-3}) during the background measurements. The corresponding values for fine particles ($PM_{2.5}$) were 11, 17 and 30% compared with 50% during background, showing a much greater release of coarse particles during demolition. The openair package in R and map source software (ArcGIS) were used to assess spatial variation of PMCs in downwind and upwind of the demolition site. A modified box model was developed to determine the emission factors, which were 210, 73 and 24 μg m^{-2} s^{-1} for PM_{10}, $PM_{2.5}$ and PM_{1}, respectively. The average respiratory deposited doses to coarse (and fine) particles inside the excavator cabin and on-site temporary office increased by 57 (and 5) and 13 (and 2) times compared with the local background level, respectively. The monitoring stations in downwind direction illustrated a logarithmic decrease of PM with distance. Energy-dispersive X-ray spectroscopy and scanning electron microscopy were used to assess physicochemical features of particles. The minerals such as silica were found as a marker of demolition dust and elements such as sulphur coming from construction machinery emissions. Findings of this study highlight a need to limit occupational exposure of individuals to coarse and fine particles by enforcing effective engineering controls.

8.2 Conclusions

This thesis presents a comprehensive data set on particle mass and number distributions and concentrations in the coarse, fine and ultrafine size ranges in the context of building-related activities. The key conclusions obtained from the overall analysis covered in the chapters of this thesis are summarised as follows:

- Ultrafine particles were found to dominate the total PNCs with a proportion of 74-97% during the laboratory simulated experiments and the indoor building refurbishment activities, with the highest proportion of ultrafine particles arising from the cutting of concrete, drilling and wall chasing activities. In addition, the average PNCs values were found to be up to 38- and 84-times higher than background levels during the laboratory simulated and indoor refurbishment activities, respectively.
- The results also confirm that the simulated laboratory building activities studied here have the potential to release PM_{10}, $PM_{2.5}$ and PM_1 at levels above those encountered in the normal background. The mechanical attrition between the surfaces of instruments and materials during the activities and the re-suspension of existing particles appear to be the main reasons for the production of larger-sized particles.
- The highest concentrations of PM_{10} and $PM_{2.5}$ were observed at the paired monitoring stations during the construction works when the winds were blowing from the construction sites toward the monitoring stations. PM_{10} were found about ~24, 18 and 120%, and $PM_{2.5}$ were about 11% larger during the working periods compared with those during non-working periods at the three construction sites, which can thus be attributed to the construction works, as indicated by the bivariate concentration polar plots and k-means clustering analysis. Moreover, the highest PM_{10}, $PM_{2.5}$ and PM_1 concentrations were detected in the excavator cabin during the demolition of the building's ceiling and walls. This was followed by PM_{10}, $PM_{2.5}$ and PM_1 concentrations measured during downwind mobile measurements at route A (close periphery of the demolition site), which were up to 7.7-, 2.3- and 2.1-times higher than those upwind of the route, respectively.

- Downwind concentrations of PM_{10} were found to be relatively more influenced by construction (Chapter 6) and demolition works (Chapter 7) at the downwind of the sites than $PM_{2.5}$ concentrations. Also, the coarse particles contributed most of the total PMCs during field construction and demolition works. Exposure to high levels of PMCs can be minimised by staying indoors or being positioned upwind of construction and demolition sites.
- PM_{10}, $PM_{2.5}$ and PM_1 values during both construction and demolition works in the downwind direction showed a logarithmic decay relative to distance ($R^2 \approx 0.90$). Such decay profiles are important for extrapolating emissions downwind of building works to incorporate them into dispersion models such as those used in PMEF modelling. The daily mean EU limit of value for PM_{10} was breached on two occasions due to construction operations on downwind monitoring stations while measurements were being taken between 2002 and 2013. Moreover, PM_{10} and $PM_{2.5}$ concentrations met the daily mean EU and WHO limit values during demolition works at about 50 and 15 m, respectively suggesting this as a public exclusion zone in this particular case.
- Average particle number and mass-based emission rates were estimated for building simulated activities (i.e. mixing with GGBS, PFA, drilling and cutting of concrete) and average emission factors were calculated for building demolition activity. Such emission factors are currently lacking, but are key inputs into dispersion models for accurately estimating the affected area around the sites and for designing appropriate measures to limit the exposure of the nearby public.
- Occupational exposures for workers on the both construction and demolition sites were found to contribute much higher exposure over background exposure levels compared

with the occupational exposure for workers on indoor building works. The downwind distance from the source was another important factor influencing exposure doses. Other factors affecting the exposure doses of individual workers included the nature of work and the type of physical exercise; therefore, the RDD rates could be different for workers involved in heavy and light exercise, site engineers or drivers, even if they were exposed to the same level of particle concentrations.

- SEM images indicated irregular, aggregated and crystal shaped particles during building refurbishment (indoor) and demolition works (outdoor). However, combining the results of EDS, XPS and IBA analysis suggested the dominance of elements such Si, Al, and S on the collected samples. These elements were presumably released from the building equipment and materials (e.g. concrete, bricks and metals) involved in refurbishment and demolition activities. The escape of these elements, along with others such as Zn and Mg, suggests the appropriateness of protection measures for the populace, particularly sensitive subgroups (e.g. elderly and children) and those in nearby sensitive areas (e.g. hospitals, retirement homes or nurseries).

8.3 Recommendations for future research

This subject and area of research offers a good scope for further work to understand the formation mechanism of particles, their dispersion behaviour and mitigation methods. These are some recommendations that should be considered for future work:

- The findings of laboratory investigations have implications both for the owners of buildings and regulatory bodies, which appear to be unaware of the potential for indoor building works to produce to ultrafine particles at levels significantly above a typical

background. Further studies covering different types of simulated building activities with a longer time duration, are needed to better understand variations of PNCs, PMCs and associated exposure doses.

- These high levels of ultrafine particles during indoor refurbishment activities suggest that there is a need to design more detailed and appropriate risk mitigation strategies to limit exposure of on-site workers in indoor operation sites. It is also recommended to perform decay profiles of PM_{10}, $PM_{2.5}$, PM_1 and ultrafine particles to evaluate the variations in PMCs and PNCs at different indoor distances, which can be used in future dispersion modelling studies of indoor field activities. More investigations are also needed by repeating the same experiments under varying meteorological conditions and on different operational sites, in order to develop emission inventories for PM_{10}, $PM_{2.5}$, PM_1 and ultrafine particles.
- The findings of outdoor construction measurements will enable authorities to develop risk assessment and mitigation strategies for the construction industry. Further research is required to monitor and understand the physicochemical properties of PM, and also the emission levels of ultrafine particles arising from the construction works in different meteorological conditions, to establish suitable exposure limits for on-site workers.
- In order to provide adequate protection for workers and for the populations living in the neighborhood of outdoor demolition works, further studies, involving monitoring of size-resolved particles from a wide variety of building demolition works within different urban morphological and meteorological settings are recommended. Dedicated studies are also needed in the future that can allow the PND signatures of

outdoor building activities to be quantified, as well as the formation pathways and emission levels of particles in the ultrafine particles size range during different seasons and atmospheric stability conditions.

References

Abbey, D.E., Ostro, B.E., Fraser, G., Vancuren, T., Burchette, R.J., 1994. Estimating fine particulates less than 2.5 microns in aerodynamic diameter ($PM_{2.5}$) from airport visibility data in California. Journal of Exposure Analysis and Environmental Epidemiology 5, 161-180.

Abu-Allaban, M., Gillies, J., Gertler, A., Clayton, R., Proffitt, D., 2007. Motor vehicle contributions to ambient PM_{10} and $PM_{2.5}$ at selected urban areas in the USA. Environmental Monitoring and Assessment 132, 155-163.

Abu-Allaban, M., Hamasha, S., Gertler, A., 2006. Road dust resuspension in the vicinity of limestone quarries in Jordan. Journal of the Air & Waste Management Association 56, 1440-1444.

Adachi, K., Tainosho, Y., 2004. Characterization of heavy metal particles embedded in tire dust. Environment International 30, 1009-1017.

Adhami, S., Abel, M.L., Lowe, C., Watts, J.F., 2012. Failure of a waterborne primer applied to zinc coated steel. Surface and Interface Analysis 44, 1054-1058.

Adhami, S., Abel, M.L., Lowe, C., Watts, J.F., 2014. The role of the adhesion promoter in a model water-borne primer. Surface and Interface Analysis 46, 1005-1008.

Akbar-Khanzadeh, F., Brillhart, R.L., 2002. Respirable crystalline silica dust exposure during concrete finishing (grinding) using hand-held grinders in the construction industry. Annals of Occupational Hygiene 46, 341-346.

Akbar-Khanzadeh, F., Milz, S., Ames, A., Susi, P.P., Bisesi, M., Khuder, S.A., Akbar-Khanzadeh, M., 2007. Crystalline Silica Dust and Respirable Particulate Matter During Indoor Concrete Grinding-Wet Grinding and Ventilated Grinding Compared with Uncontrolled Conventional Grinding. Journal of Occupational and Environmental Hygiene 4, 770-779.

Al-Dabbous, A.N., Kumar, P., 2014. The influence of roadside vegetation barriers on airborne nanoparticles and pedestrians exposure under varying wind conditions. Atmospheric Environment 90, 113-124.

Amato, F., Pandolfi, M., Escrig, A., Querol, X., Alastuey, A., Pey, J., Perez, N., Hopke, P.K., 2009. Quantifying road dust resuspension in urban environment by multilinear engine: a comparison with PMF2. Atmospheric Environment 43, 2770-2780.

Anderson, H.R., 2009. Air pollution and mortality: a history. Atmospheric Environment 43, 142-152.

Andrews, G.E., Andrews, I.D., Dixon-Hardy, D.W., Gibbs, B.M., Li, H., Wright, S., 2010. Airport PM_{10} emissions: development of a first order approximation (FOA) methodology for aircraft and airport particulate mass emissions, ASME turbo expo 2010: power for land, sea, and air. American Society of Mechanical Engineers, 363-375.

Authority, G.L., Councils, L., 2006. The control of dust and emissions from construction and demolition. Best Practice Guidance.

Ayers, G.P., Keywood, M.D., Gras, J.L., 1999. TEOM vs. manual gravimetric methods for determination of $PM_{2.5}$ aerosol mass concentrations. Atmospheric Environment 33, 3717-3721.

Azarmi, F., Kumar, P., Marsh, D., Fuller, G.W., 2015a. Assessment of long-term impacts of PM_{10} and $PM_{2.5}$ particles from construction works on surrounding areas. Environmental Science: Processes & Impacts 18, 208-221.

Azarmi, F., Kumar, P., Mulheron, M., 2014. The exposure to coarse, fine and ultrafine particle emissions from concrete mixing, drilling and cutting activities. Journal of Hazardous Materials 279, 268-279.

Azarmi, F., Kumar, P., Mulheron, M., Colaux, J., Jeynes, C., Adhami, S., Watts, J., 2015b. Physicochemical characteristics and occupational exposure to coarse, fine and ultrafine particles during building refurbishment activities. Journal of Nanoparticle Research 17, 343, doi: 10.1007/s11051-015-3141-z.

Balaras, C.A., Gaglia, A.G., Georgopoulou, E., Mirasgedis, S., Sarafidis, Y., Lalas, D.P., 2007. European residential buildings and empirical assessment of the Hellenic

building stock, energy consumption, emissions and potential energy savings. Building and Environment 42, 1298-1314.

Barradas, N., Jeynes, C., 2008. Advanced physics and algorithms in the IBA DataFurnace. Nuclear Instruments and Methods in Physics Research Section B: Beam Interactions with Materials and Atoms 266, 1875-1879.

Barratt, B.M., Fuller, G.W., 2014. Intervention assessments in the control of PM_{10} emissions from an urban waste transfer station. Environmental Science: Processes & Impacts 16, 1328-1337.

Bates, T.S., Quinn, P.K., Coffman, D., Schulz, K., Covert, D.S., Johnson, J.E., Williams, E.J., Lerner, B.M., Angevine, W.M., Tucker, S.C., Brewer, W.A., Stohl, A., 2008. Boundary layer aerosol chemistry during TexAQS/GoMACCS 2006: Insights into aerosol sources and transformation processes. Journal of Geophysical Research: Atmospheres 113, D00F01.

Batonneau, Y., Bremard, C., Gengembre, L., Laureyns, J., Le Maguer, A., Le Maguer, D., Perdrix, E., Sobanska, S., 2004. Speciation of PM_{10} Sources of airborne nonferrous metals within the 3-km Zone of Lead/Zinc smelters. Environmental Science & Technology 38, 5281-5289.

Beck, C.M., Geyh, A., Srinivasan, A., Breysse, P.N., Eggleston, P.A., Buckley, T.J., 2003. The impact of a building implosion on airborne particulate matter in an urban community. Journal of the Air & Waste Management Association 53, 1256-1264.

Bello, D., Wardle, B.L., Zhang, J., Yamamoto, N., Santeufemio, C., Hallock, M., Virji, M.A., 2010. Characterization of exposures to nanoscale particles and fibers during solid core drilling of hybrid carbon nanotube advanced composites. International Journal of Occupational and Environmental Health 16, 434-450.

Bergdahl, I., Toren, K., Eriksson, K., Hedlund, U., Nilsson, T., Flodin, R., Järvholm, B., 2004. Increased mortality in COPD among construction workers exposed to inorganic dust. European Respiratory Journal 23, 402-406.

Britter, R., Hanna, S., 2003. Flow and dispersion in urban areas. Annual Review of Fluid Mechanics 35, 469-496.

Broekhuizen, P., Broekhuizen, F., Cornelissen, R., Reijnders, L., 2011. Use of nanomaterials in the European construction industry and some occupational health aspects thereof. Journal of Nanoparticle Research 13, 447-462.

Brook, R.D., Rajagopalan, S., Pope, C.A., Brook, J.R., Bhatnagar, A., Diez-Roux, A.V., Holguin, F., Hong, Y., Luepker, R.V., Mittleman, M.A., 2010. Particulate matter air pollution and cardiovascular disease an update to the scientific statement from the American Heart Association. Circulation 121, 2331-2378.

Brouwer, D., 2010. Exposure to manufactured nanoparticles in different workplaces. Toxicology 269, 120-127.

Brunekreef, B., Holgate, S.T., 2002. Air pollution and health. The Lancet 360, 1233-1242.

Brunekreef, B., Forsberg, B., 2005. Epidemiological evidence of effects of coarse airborne particles on health. European Respiratory Journal 26, 309-318.

Burt, S., Eden, P., 2004. The August 2003 heatwave in the United Kingdom. Part 2 - the hottest sites. Weather 59, 239-246.

Buseck, P. R., Posfai, M., 1999. Airborne minerals and related aerosol particles: Effects on climate and the environment. Proceedings of the National Academy of Sciences 96, 3372-3379.

Buonanno, G., Lall, A., Stabile, L., 2009. Temporal size distribution and concentration of particles near a major highway. Atmospheric Environment 43, 1100-1105.

Buonanno, G., Morawska, L., Stabile, L., 2011. Exposure to welding particles in automotive plants. Journal of Aerosol Science 42, 295-304.

Cadle, S.H., Mulawa, P.A., Hunsanger, E.C., Nelson, K., Ragazzi, R.A., Barrett, R., Gallagher, G.L., Lawson, D.R., Knapp, K.T., Snow, R., 1999. Composition of light-duty motor vehicle exhaust particulate matter in the Denver, Colorado Area. Environmental Science & Technology 33, 2328-2339.

Caggiano, R., Macchiato, M., Trippetta, S., 2010. Levels, chemical composition and sources of fine aerosol particles (PM_1) in an area of the Mediterranean basin. Science of the Total Environment 408, 884-895.

Cao, C., Jiang, W., Wang, B., Fang, J., Lang, J., Tian, G., Jiang, J., Zhu, T.F., 2014. Inhalable microorganisms in Beijing's $PM_{2.5}$ and PM_{10} pollutants during a severe smog event. Environmental Science & Technology 48, 1499-1507.

Carpentieri, M., Kumar, P., 2011. Ground-fixed and on-board measurements of nanoparticles in the wake of a moving vehicle. Atmospheric Environment 45, 5837-5852.

Carslaw, D.C., Beevers, S.D., 2013. Characterising and understanding emission sources using bivariate polar plots and k-means clustering. Environmental Modelling & Software 40, 325-329.

Carslaw, D.C., Ropkins, K., 2012. Openair, an R package for air quality data analysis. Environmental Modelling & Software 27–28, 52-61.

Cavallari, J.M., Eisen, E.A., Chen, J.-C., Fang, S.C., Dobson, C.B., Schwartz, J., Christiani, D.C., 2007. Night heart rate variability and particulate exposures among boilermaker construction workers. Environmental Health Perspectives, 1046-1051.

Chaloulakou, A., Kassomenos, P., Spyrellis, N., Demokritou, P., Koutrakis, P., 2003. Measurements of PM_{10} and $PM_{2.5}$ particle concentrations in Athens, Greece. Atmospheric Environment 37, 649-660.

Chalupa, D.C., Morrow, P.E., Oberdörster, G., Utell, M.J., Frampton, M.W., 2004. Ultrafine particle deposition in subjects with asthma. Environmental Health Perspectives 112, 879.

Charron, A., Harrison, R.M., 2003. Primary particle formation from vehicle emissions during exhaust dilution in the roadside atmosphere. Atmospheric Environment 37, 4109-4119.

Chen, M., Wang, X., Yu, Y., Pei, Z., Bai, X., Sun, C., Huang, R., Wen, L., 2000. X-ray photoelectron spectroscopy and auger electron spectroscopy studies of Al-doped ZnO films. Applied Surface Science 158, 134-140.

Chen, J., Yao, H., Zhang, P.A., Xiao, L., Luo, G., Xu, M., 2011. Control of PM_1 by kaolin or limestone during O_2/CO_2 pulverized coal combustion. Proceedings of the Combustion Institute 33, 2837-2843.

Cheng, M.T., Tsai, Y.I., 2000. Characterization of visibility and atmospheric aerosols in urban, suburban, and remote areas. Science of the Total Environment 263, 101-114.

Cheng, Y. H., Li, Y. S., 2010. Influences of traffic emissions and meteorological conditions on ambient PM_{10} and $PM_{2.5}$ levels at a highway toll station. Aerosol and Air Quality Research 10, 456-462.

Cheng, Y., Zou, S.C., Lee, S.C., Chow, J.C., Ho, K.F., Watson, J.G., Han, Y.M., Zhang, R.J., Zhang, F., Yau, P.S., Huang, Y., 2011. Characteristics and source apportionment of PM_1 emissions at a roadside station. Journal of Hazardous Materials 195, 82-91.

Cheung, H.-C., Wang, T., Baumann, K., Guo, H., 2005. Influence of regional pollution outflow on the concentrations of fine particulate matter and visibility in the coastal area of southern China. Atmospheric Environment 39, 6463-6474.

Claeys, M., Graham, B., Vas, G., Wang, W., Vermeylen, R., Pashynska, V., Cafmeyer, J., Guyon, P., Andreae, M.O., Artaxo, P., Maenhaut, W., 2004. Formation of secondary organic aerosols through photooxidation of isoprene. Science 303, 1173-1176.

Chow, J.C., Chen, L.W.A., Watson, J.G., Lowenthal, D.H., Magliano, K.A., Turkiewicz, K., Lehrman, D.E., 2006. $PM_{2.5}$ chemical composition and spatiotemporal variability during the California Regional PM_{10}/$PM_{2.5}$ Air Quality Study (CRPAQS). Journal of Geophysical Research: Atmospheres 111, 1-17.

CPCB, 2010. National ambient air quality status and trend in India. Ambient air quality monitoring series NAAQMS/35/2011-2012.

Chow, J.C., Watson, J.G., Mauderly, J.L., Costa, D.L., Wyzga, R.E., Vedal, S., Hidy, G.M., Altshuler, S.L., Marrack, D., Heuss, J.M., 2006. Health effects of fine particulate air pollution: lines that connect. Journal of the Air & Waste Management Association 56, 1368-1380.

Coakley, J.A., Cess, R.D., Yurevich, F.B., 1983. The effect of tropospheric aerosols on the earth's radiation budget: a parameterization for climate models. Journal of the Atmospheric Sciences 40, 116-138.

Cohen, D.D., Bailey, G.M., Kondepudi, R., 1996. Elemental analysis by PIXE and other IBA techniques and their application to source fingerprinting of atmospheric fine particle pollution. Nuclear Instruments and Methods in Physics Research Section B: Beam Interactions with Materials and Atoms 109, 218-226.

Conny, J.M., 2013. Internal composition of atmospheric dust particles from focused ion-beam dcanning electron microscopy. Environmental Science & Technology 47, 8575-8581.

Cook Jr, C., Harris, K.L., 1992. Well bore drilling direction changing method. Patent number US 5086850 A. http://www.google.com.lb/patents/US5086850 [accessed 15 April 2014].

Corbett, J.J., Winebrake, J.J., Green, E.H., Kasibhatla, P., Eyring, V., Lauer, A., 2007. Mortality from ship emissions: a global assessment. Environmental Science & Technology 41, 8512-8518.

Croteau, G.A., Guffey, S.E., Flanagan, M.E., Seixas, N.S., 2002. The effect of local exhaust ventilation controls on dust exposures during concrete cutting and grinding activities. American Industrial Hygiene Association Journal 63, 458-467.

Cyrys, J., Dietrich, G., Kreyling, W., Tuch, T., Heinrich, J., 2001. $PM_{2.5}$ measurements in ambient aerosol: comparison between Harvard impactor (HI) and the tapered element oscillating microbalance (TEOM) system. Science of the Total Environment 278, 191-197.

D'amato, G., Cecchi, L., D'amato, M., Liccardi, G., 2010. Urban air pollution and climate change as environmental risk factors of respiratory allergy: an update. Journal of Investigational Allergology and Clinical Immunology 20, 95-102.

Dall'Osto, M., Thorpe, A., Beddows, D.C.S., Harrison, R.M., Barlow, J.F., Dunbar, T., Williams, P.I., Coe, H., 2011. Remarkable dynamics of nanoparticles in the urban atmosphere. Atmospheric Chemistry and Physics 11, 6623-6637.

Davila, A.F., Rey, D., Mohamed, K., Rubio, B., Guerra, A.P., 2006. Mapping the sources of urban dust in a coastal environment by measuring magnetic parameters of Platanus hispanica leaves. Environmental Science & Technology 40, 3922-3928.

DeCarlo, P.F., Slowik, J.G., Worsnop, D.R., Davidovits, P., Jimenez, J.L., 2004. Particle morphology and density characterization by combined mobility and aerodynamic diameter measurements. Part 1: Theory. Aerosol Science and Technology 38, 1185-1205.

Defra, F., 2009. Local Air Quality Management Technical Guidance LAQM. TG (09).

Dhir, R.K., Hewelett, P., Csetenyi, L.J., 2002. Innovations and development in concrete materials and construction". UK: Thomas Telford, 533-544.

Diapouli, E., Papamentzelopoulou, A., Chaloulakou, A., 2013. Survey of airborne particulate matter concentration at a marvle processing facility workers exposure assessment. Global NEST Journal 15, 204-208.

Directive, C., 1999. Council Directive 1999/30/EC of 22 April 1999 relating to limit values for sulphur dioxide, nitrogen dioxide and oxides of nitrogen, particulate matter and lead in ambient air. Journal of the European Communities 50, 41-60.

Directive, E., 2008. Council Directive 2008/50/EC, on ambient air quality and cleaner air for Europe. Official Journal of the European Communities L 151, 1-44.

Dorado, M.P., Ballesteros, E., Arnal, J.M., Gomez, J., Lopez, F.J., 2003. Exhaust emissions from a Diesel engine fueled with transesterified waste olive oil. Fuel 82, 1311-1315.

Dorevitch, S., Demirtas, H., Perksy, V.W., Erdal, S., Conroy, L., Schoonover, T., Scheff, P.A., 2006. Demolition of high-rise public housing increases particulate matter air pollution in communities of high-risk asthmatics. Journal of the Air & Waste Management Association 56, 1022-1032.

Dosho, Y., 2007. Development of a sustainable concrete waste recycling system-Application of recycled aggregate concrete produced by aggregate replacing method. Journal of Advanced Concrete Technology 5, 27-42.

ECI, 2005. 40% House Report. Environmental Change Institute. Availabe at :http://www.eci.ox.ac.uk/research/energy/40house.php. [last access 12th October 2015].

EEA Technical report, 2008: Annual European Community LRTAP Convention emission inventory report 1990–2006 submission to EMEP through the executive secretary of the UNECE. EEA Technical report. No 7/2008. ISBN 978-92-9167-366-7.

Egbu, C.O., 1999. Skills, knowledge and competencies for managing construction refurbishment works. Construction Management and Economics 17, 29-43.

Eggleston, P.A., Buckley, T.J., Breysse, P.N., Wills-Karp, M., Kleeberger, S.R., Jaakkola, J., 1999. The environment and asthma in US inner cities. Environmental Health Perspectives 107, 439-450.

Elangasinghe, M.A., Singhal, N., Dirks, K.N., Salmond, J.A., Samarasinghe, S., 2014. Complex time series analysis of PM_{10} and $PM_{2.5}$ for a coastal site using artificial neural network modelling and k-means clustering. Atmospheric Environment 94, 106-116.

EMEP-EEA., 2013. EMEP/EEA air pollutant emission inventory guidebook. Technical guidance to prepare national emission inventories. Publications Office of the European Union, Luxembourg (2013), available at: http://dx.doi.org/10.2800/92722, [last access 12th October 2015].

Engel, A., Colliex, C., 1993. Application of scanning transmission electron microscopy to the study of biological structure. Current Opinion in Biotechnology 4, 403-411.

EPA., 2011. Environmental Protection Agency, AP-42, compilation of air pollutant emission factors, volume 1: stationary point and area sources. (Fifth Edition), available at: http://www.epa.gov/ttn/chief/ap42/, [last access 12th October 2015].

Everitt, B., Landau, S., Leese, M., Stahl, D., 2011. Cluster Analysis (Wiley Series in Probability and Statistics). Wiley, UK, Fifth Edition, pp. 330.

Falkovich, A.H., Ganor, E., Levin, Z., Formenti, P., Rudich, Y., 2001. Chemical and mineralogical analysis of individual mineral dust particles. Journal of Geophysical Research: Atmospheres (1984–2012) 106, 18029-18036.

Flower, D.J., Sanjayan, J.G., 2007. Green house gas emissions due to concrete manufacture. The International Journal of Life Cycle Assessment 12, 282-288.

Fischer, A., Richter, K., Emmenegger, L., Künniger, T., 2005. PM_{10} emissions caused by the woodworking industry in Switzerland. Holz als Roh-und Werkstoff 63, 245-250.

Flanagan, M.E., Seixas, N., Becker, P., Takacs, B., Camp, J., 2006. Silica exposure on construction sites: results of an exposure monitoring data compilation project. Journal of Occupational and Environmental Hygiene 3, 144-152.

Font, A., Baker, T., Mudway, I.S., Purdie, E., Dunster, C., Fuller, G.W., 2014. Degradation in urban air quality from construction activity and increased traffic arising from a road widening scheme. Science of the Total Environment 497–498, 123-132.

Fujitani, Y., Kobayashi, T., Arashidani, K., Kunugita, N., Suemura, K., 2008. Measurement of physical properties of aerosols in a fullerene factory for inhalation exposure assessment. Journal of Occupational and Environmental Hygiene 5, 380-389.

Fujitani, Y., Kumar, P., Tamura, K., Fushimi, A., Hasegawa, S., Takahashi, K., Tanabe, K., Kobayashi, S., Hirano, S., 2012. Seasonal differences of the atmospheric particle size distribution in a metropolitan area in Japan. Science of the Total Environment 437, 339-347.

Fuller, G.W., Carslaw, D.C., Lodge, H.W., 2002. An empirical approach for the prediction of daily mean PM_{10} concentrations. Atmospheric Environment 36, 1431-1441.

Fuller, G.W., Green, D., 2004. The impact of local fugitive from building works and road works on the assessment of the European union limit value. Atmospheric Environment 38, 4993-5002.

Goel, A., Kumar, P., 2014. A review of fundamental drivers governing the emissions, dispersion and exposure to vehicle-emitted nanoparticles at signalised traffic intersections. Atmospheric Environment 97, 316-331.

Goel, A., Kumar, P., 2015. Characterisation of nanoparticle emissions and exposure at traffic intersections through fast–response mobile and sequential measurements. Atmospheric Environment 107, 374-390.

Goyal, R., Kumar, P., 2013. Indoor–outdoor concentrations of particulate matter in nine microenvironments of a mix-use commercial building in megacity Delhi. Air Quality, Atmosphere and Health 6, 747-757.

Green, D., Fuller, G., Barratt, B., 2001. Evaluation of TEOM TM 'correction factors' for assessing the EU Stage 1 limit values for PM_{10}. Atmospheric Environment 35, 2589-2593.

Green, D.C., Fuller, G.W., Baker, T., 2009. Development and validation of the volatile correction model for PM_{10}–An empirical method for adjusting TEOM measurements for their loss of volatile particulate matter. Atmospheric Environment 43, 2132-2141.

Grimm, H., Eatough, D.J., 2009. Aerosol Measurement: The use of optical light scattering for the determination of particulate size distribution, and particulate mass, including the semi-volatile fraction. Journal of the Air and Waste Management Association 59, 101-107.

GroBmann, A., Hohmann, F., Wiebe, K., 2013. PortableDyme-A simplified software package for econometric model building. Macroeconomic Modelling For Policy Evaluation 120, pp. 33.

Gulliver, J., Briggs, D., 2004. Personal exposure to particulate air pollution in transport microenvironments. Atmospheric Environment 38, 1-8.

Gustafsson, M., Blomqvist, G., Gudmundsson, A., Dahl, A., Swietlicki, E., Bohgard, M., Lindbom, J., Ljungman, A., 2008. Properties and toxicological effects of particles from the interaction between tyres, road pavement and winter traction material. Science of the Total Environment 393, 226-240.

Hagler, G.S.W., Baldauf, R.W., Thoma, E.D., Long, T.R., Snow, R.F., Kinsey, J.S., Oudejans, L., Gullett, B.K., 2009. Ultrafine particles near a major roadway in

Raleigh, North Carolina: Downwind attenuation and correlation with traffic-related pollutants. Atmospheric Environment 43, 1229-1234.

Hansen, D., Blahout, B., Benner, D., Popp, W., 2008. Environmental sampling of particulate matter and fungal spores during demolition of a building on a hospital area. Journal of Hospital Infection 70, 259-264.

Hartog, J.J.d., Hoek, G., Mirme, A., Tuch, T., Kos, G.P.A., Brink, H.M.t., Brunekreef, B., Cyrys, J., Heinrich, J., Pitz, M., Lanki, T., Vallius, M., Pekkanen, J., Kreyling, W.G., 2005. Relationship between different size classes of particulate matter and meteorology in three European cities. Journal of Enviromental Monitoring 7, 302-312.

Haynes, R., Savage, A., 2007. Assessment of the health impacts of particulates from the redevelopment of Kings Cross. Environmental Monitoring and Assessment 130, 47-56.

He, C., Morawska, L., Hitchins, J., Gilbert, D., 2004. Contribution from indoor sources to particle number and mass concentrations in residential houses. Atmospheric Environment 38, 3405-3415.

He, H., Zhou, Q., Frost, R.L., Wood, B.J., Duong, L.V., Kloprogge, J.T., 2007. A X-ray photoelectron spectroscopy study of HDTMAB distribution within organoclays. Spectrochimica Acta Part A: Molecular and Biomolecular Spectroscopy 66, 1180-1188.

Heal, M.R., Kumar, P., Harrison, R.M., 2012. Particles, air quality, policy and health. Chemical Society Reviews 41, 6606-6630.

Hicks, J.B., McCarthy, S.A., Mezei, G., Sayes, C.M., 2011. PM_1 particles at coal-and gas-fired power plant work areas. Annals of Occupational Hygiene 56, 182-193.

Hinds, W.C., 1999. Aerosol Technology: properties, behaviour and measurement of airborne particles. John Wiley & Sons, USA, Second Edition, pp. 483.

Hitchins, J., Morawska, L., Wolff, R., Gilbert, D., 2000. Concentrations of submicrometre particles from vehicle emissions near a major road. Atmospheric Environment 34, 51-59.

Ho, K., Lee, S., Chow, J.C., Watson, J.G., 2003. Characterization of PM_{10} and $PM_{2.5}$ source profiles for fugitive dust in Hong Kong. Atmospheric Environment 37, 1023-1032.

Hoet, P.H., Brüske-Hohlfeld, I., Salata, O.V., 2004. Nanoparticles–known and unknown health risks. Journal of Nanobiotechnology 2, 1-15.

Hofmann, W., 2011. Modelling inhaled particle deposition in the human lung – a review. Journal of Aerosol Science 42, 693-724.

Hopke, P.K., Lamb, R.E., Natusch, D.F.S., 1980. Multielemental characterization of urban roadway dust. Environmental Science & Technology 14, 164-172.

Horvath, H., 1995. Estimation of the average visibility in central Europe. Atmospheric Environment 29, 241-246.

Hosseini, S., Li, Q., Cocker, D., Weise, D., Miller, A., Shrivastava, M., Miller, J.W., Mahalingam, S., Princevac, M., Jung, H., 2010. Particle size distributions from laboratory-scale biomass fires using fast response instruments. Atmospheric Chemistry and Physics 10, 8065-8076.

HSE, 2006. Construction (design and management) regulations, Health and Safety Excutive. http://www.hse.gov.uk/construction/cdm/2015/legal.htm [last access on 10th September 2015].

HSE, 2011. Health and Safety Executive, Control of Substances Hazardous to Health (COSHH). Essentials Guidance Publications http://www.hse.gov.uk/pubns/guidance/index.htm [last access on 10th October 2015].

Hu, S., Fruin, S., Kozawa, K., Mara, S., Winer, A.M., Paulson, S.E., 2009. Aircraft emission impacts in a neighborhood adjacent to a general aviation airport in Southern California. Environmental Science & Technology 43, 8039-8045.

Hunt, A., Johnson, D.L., Watt, J.M., Thornton, I., 1992. Characterizing the sources of particulate lead in house dust by automated scanning electron microscopy. Environmental Science & Technology 26, 1513-1523.

Iavicoli, I., Leso, V., Fontana, L., Cottica, D., Bergamaschi, A., 2013. Characterization of inhalable, thoracic, and respirable fractions and ultrafine particle exposure during grinding, brazing, and welding activities in a mechanical engineering factory. Journal of Occupational and Environmental Medicine 55, 430-445.

Isaxon, C., Pagels, J., Gudmundsson, A., Asbach, C., John, A.C., Kuhlbusch, T.A.J., Karlsson, J.E., Kammer, R., Tinnerberg, H., Nielsen, J., Bohgard, M., 2009. Characteristics of welding fume aerosol investigated in three Swedish workshops. IOP Conference Publishing Series: Physics 151, 1-5.

ICRP, 1994. Human respiratory tract model for radiological protection, a report of a task group of the international commission on radiological protection. ICRP Publication 66, 1-482.

Int Panis, L., de Geus, B., Vandenbulcke, G., Willems, H., Degraeuwe, B., Bleux, N., Mishra, V., Thomas, I., Meeusen, R., 2010. Exposure to particulate matter in traffic: A comparison of cyclists and car passengers. Atmospheric Environment 44, 2263-2270.

Jaecker-Voirol, A., Pelt, P., 2000. PM_{10} emission inventory in Ile de France for transport and industrial sources: PM_{10} re-suspension, a key factor for air quality. Environmental Modelling & Software 15, 575-581.

Jamriska, M., Morawska, L., 2001. A model for determination of motor vehicle emission factors from on-road measurements with a focus on submicrometer particles. Science of the Total Environment 264, 241-255.

Janssen, N.A., Fischer, P., Marra, M., Ameling, C., Cassee, F.R., 2013. Short-term effects of $PM_{2.5}$, PM_{10} and $PM_{2.5–10}$ on daily mortality in the Netherlands. Science of the Total Environment 463–464, 20-26.

Jenkins, N.T., Eagar, T.W., 2005. Chemical analysis of welding fume particles. Welding Journal 84, 87-93.

Jenkins, G., Perry, M., Prior, J., 2009. The climate of the United Kingdom and recent trends. Met Office Hadley Centre (UKCIP09), UK, Revised Edition, pp. 120.

JEOL, 2015. JSM-7100F Schottky Field Emission Scanning Electron Microscope. JEOL Ltd Japan. http://www.jeol.co.jp/en/products/detail/JSM-7100F.html, [last access 14th October 2015].

Jeynes, C., Bailey, M., Bright, N., Christopher, M., Grime, G., Jones, B., Palitsin, V., Webb, R., 2012. "Total IBA"–Where are we? nuclear instruments and methods in physics research section B. Beam Interactions with Materials and Atoms 271, 107-118.

Jones, A.M., Harrison, R.M., Baker, J., 2010. The wind speed dependence of the concentrations of airborne particulate matter and NO_x. Atmospheric Environment 44, 1682-1690.

Joodatnia, P., Kumar, P., Robins, A., 2013a. The behaviour of traffic produced nanoparticles in a car cabin and resulting exposure rates. Atmospheric Environment 65, 40-51.

Joodatnia, P., Kumar, P., Robins, A., 2013b. Fast response sequential measurements and modelling of nanoparticles inside and outside a car cabin. Atmospheric Environment 71, 364-375.

Joseph, J., Patil, R.S., Gupta, S.K., 2009. Estimation of air pollutant emission loads from construction and operational activities of a port and harbour in Mumbai, India. Environmental Monitoring and Assessment 159, 85-98.

Junninen, H., Mønster, J., Rey, M., Cancelinha, J., Douglas, K., Duane, M., Forcina, V., Müller, A., Lagler, F., Marelli, L., Borowiak, A., 2009. Quantifying the impact of residential heating on the urban air quality in a typical European coal combustion region. Environmental Science & Technology 43, 7964-7970.

Kampa, M., Castanas, E., 2008. Human health effects of air pollution. Environmental Pollution 151, 362-367.

Kan, H., London, S.J., Chen, G., Zhang, Y., Song, G., Zhao, N., Jiang, L., Chen, B., 2007. Differentiating the effects of fine and coarse particles on daily mortality in Shanghai, China. Environment International 33, 376-384.

Kan, H., Chen, R., Tong, S., 2012. Ambient air pollution, climate change, and population health in China. Environment International 42, 10-19.

Kaur, S., Nieuwenhuijsen, M., Colvile, R., 2005. Personal exposure of street canyon intersection users to $PM_{2.5}$, ultrafine particle counts and carbon monoxide in Central London, UK. Atmospheric Environment 39, 3629-3641.

Kean, A.J., Sawyer, R.F., Harley, R.A., 2000. A Fuel-Based Assessment of off-Road diesel engine emissions. Journal of the Air & Waste Management Association 50, 1929-1939.

Kim, K.Y., Kim, Y.S., Roh, Y.M., Lee, C.M., Kim, C.N., 2008. Spatial distribution of particulate matter (PM_{10} and $PM_{2.5}$) in Seoul metropolitan subway stations. Journal of Hazardous Materials 154, 440-443.

Kim, Y.J., Kim, K.W., Oh, S.J., 2001. Seasonal characteristics of haze observed by continuous visibility monitoring in the urban atmosphere of Kwangju, Korea. Environmental Monitoring and Assessment 70, 35-46.

Kittelson, D.B., 1998. Engines and nanoparticles – a review. Journal of Aerosol Science 29, 575-588.

Kittelson, D. B., Watts, W. F., Johnson, J. P., 2004. Nanoparticle emissions on Minnesota highways. Atmospheric Environment, 38, 9-19.

Knibbs, L.D., Cole-Hunter, T., Morawska, L., 2011. A review of commuter exposure to ultrafine particles and its health effects. Atmospheric Environment 45, 2611-2622.

Kohler, N., Hassler, U., 2002. The building stock as a research object. Building Research & Information 30, 226-236.

Kothai, P., Prathibha, P., Saradhi, I.V., Pandit, G.G., Puranik, V.D., 2009. Characterization of atmospheric particulate matter using pixe technique. International Journal of Environmental Science and Technology 1, 27-30.

Kousa, A., Kukkonen, J., Karppinen, A., Aarnio, P., Koskentalo, T., 2002a. A model for evaluating the population exposure to ambient air pollution in an urban area. Atmospheric Environment 36, 2109-2119.

Kousa, A., Oglesby, L., Koistinen, K., Künzli, N., Jantunen, M., 2002b. Exposure chain of urban air $PM_{2.5}$-associations between ambient fixed site, residential outdoor, indoor, workplace and personal exposures in four European cities in the EXPOLIS-study. Atmospheric Environment 36, 3031-3039.

Kuhlbusch, T.A.J., Neumann, S., Fissan, H., 2004. Number size distribution, mass concentration, and particle composition of PM_1, $PM_{2.5}$, and PM_{10} in bag filling areas of carbon black production. Journal of Occupational and Environmental Hygiene 1, 660-671.

Kumar, P., 2009. Measurements and modelling of the dispersion of nanoparticles in the urban environment (Doctoral dissertation, University of Cambridge), pp. 226.

Kumar, P., Azarmi, F., Mulheron, M., 2012a. Enlightening and noxious shades of nanotechnology application in concrete. Nanotechnology: Volume 7 Civil / Construction Engineering. (Studium Press LLC, USA; Govil, J.N. Eds.). ISBN: 1-62699-009-3. pp. 255-287.

Kumar, P., Fennell, P., Britter, R., 2008. Effect of wind direction and speed on the dispersion of nucleation and accumulation mode particles in an urban street canyon. Science of the Total Environment 402, 82-94.

Kumar, P., Gurjar, B.R., Nagpure, A.S., Harrison, R.M., 2011a. Preliminary estimates of nanoparticle number emissions from road vehicles in megacity Delhi and associated health impacts. Environmental Science & Technology 45, 5514-5521.

Kumar, P., Jain, S., Gurjar, B., Sharma, P., Khare, M., Morawska, L., Britter, R., 2013a. New Directions: Can a "blue sky" return to Indian megacities?. Atmospheric Environment 71, 198-201.

Kumar, P., Ketzel, M., Vardoulakis, S., Pirjola, L., Britter, R., 2011b. Dynamics and dispersion modelling of nanoparticles from road traffic in the urban atmospheric environment – a review. Journal of Aerosol Science 42, 580-603.

Kumar, P., Martani, C., Morawska, L., Norford L.K., Choudhary R., Leach, M., 2016. Indoor air quality and energy management through real-time sensing in commercial buildings. Energy and Buildings 111, 145-153.

Kumar, P., Morawska, L., 2013. Energy-Pollution Nexus for Urban Buildings. Environmental Science & Technology 47, 7591-7592.

Kumar, P., Morawska, L., 2014. Recycling Concrete: an undiscovered source of ultrafine particles. Atmospheric Environment 90, 51-58.

Kumar, P., Morawska, L., Birmili, W., Paasonen, P., Hu, M., Kulmala, M., Harrison, R.M., Norford, L., Britter, R., 2014. Ultrafine particles in cities. Environment International 66, 1-10.

Kumar, P., Mulheron, M., Fisher, B., Harrison, R.M., 2012b. New Directions: Airborne ultrafine particle dust from building activities – A source in need of quantification. Atmospheric Environment 56, 262-264.

Kumar, P., Mulheron, M., Som, C., 2012c. Release of ultrafine particles from three simulated building processes. Journal of Nanoparticle Research 14, doi: 10.1007/s11051-012-0771-2.

Kumar, P., Pirjola, L., Ketzel, M., Harrison, R.M., 2013b. Nanoparticle emissions from 11 non-vehicle exhaust sources – a review. Atmospheric Environment 67, 252-277.

Kumar, P., Robins, A., Vardoulakis, S., Britter, R., 2010. A review of the characteristics of nanoparticles in the urban atmosphere and the prospects for developing regulatory controls. Atmospheric Environment 44, 5035-5052.

Kumar, P., Robins, A., Vardoulakis, S., Quincey, P., 2011c. Technical challenges in tackling regulatory concerns for urban atmospheric nanoparticles. Particulogy 9, 566-571.

Kupiainen, K., Tervahattu, H., Raisanen, M., 2003. Experimental studies about the impact of traction sand on urban road dust composition. Science of the Total Environment 308, 175-184.

Labban, R., Veranth, J.M., Chow, J.C., Engelbrecht, J.L., Watson, J.G., 2004. Size and geographical variation in PM_1, $PM_{2.5}$ and PM_{10}: Source profiles from soils in the western United States. Water, Air, and Soil Pollution 157, 13-31.

Lawson, N., Douglas, I., Garvin, S., McGrath, C., Manning, D., Vetterlein, J., 2001. Recycling construction and demolition wastes-a UK perspective. Environmental Management and Health 12, 146-157.

Li, G., 2004. Properties of high-volume fly ash concrete incorporating nano-SiO_2. Cement and Concrete Research 34, 1043-1049.

Li, G., Zhao, X., 2003. Properties of concrete incorporating fly ash and ground granulated blast-furnace slag. Cement and Concrete Composites 25, 293-299.

Lim, J.M., Lee, J.H., Moon, J.H., Chung, Y.S., Kim, K.H., 2010. Source apportionment of PM_{10} at a small industrial area using positive matrix factorization. Atmospheric Research 95, 88-100.

Lim, S.S., Vos, T., Flaxman, A.D., Danaei, G., Shibuya, K., Adair-Rohani, H., AlMazroa, M.A., Amann, M., Anderson, H.R., Andrews, K.G., 2013. A comparative risk assessment of burden of disease and injury attributable to 67 risk factors and risk factor clusters in 21 regions, 1990–2010: a systematic analysis for the global burden of disease study 2010. The Lancet 380, 2224-2260.

Lioy, P.J., Weisel, C.P., Millette, J.R., Eisenreich, S., Vallero, D., Offenberg, J., Buckley, B., Turpin, B., Zhong, M., Cohen, M.D., Prophete, C., Yang, I., Stiles, R., Chee, G., Johnson, W., Porcja, R., Alimokhtari, S., Hale, R.C., Weschler, C., Chen, L.C., 2002. Characterization of the dust/smoke aerosol that settled east of the World Trade Center (WTC) in lower Manhattan after the collapse of the WTC 11 September 2001. Environmental Health Perspectives 110, 703-714.

Liu, Y.J., Harrison, R.M., 2011. Properties of coarse particles in the atmosphere of the United Kingdom. Atmospheric Environment 45, 3267-3276.

Lo, I.M.C., Tang, C.I., Li, X.D., Poon, C.S., 2000. Leaching and microstructural analysis of cement-based solidified wastes. Environmental Science & Technology 34, 5038-5042.

Lonati, G., Ozgen, S., Giugliano, M., 2007. Primary and secondary carbonaceous species in $PM_{2.5}$ samples in Milan (Italy). Atmospheric Environment 41, 4599-4610.

Loomis, D., 2000. Sizing up air pollution research. Epidemiology 11, 2-4.

Mangelson, N.F., Lewis, L., Joseph, J.M., Cui, W., Machir, J., Eatough, D.J., Rees, L.B., Wilkerson, T., Jensen, D.T., 1997. The contribution of sulfate and nitrate to atmospheric fine particles during winter inversion fogs in Cache Valley, Utah. Journal Of The Air & Waste Management Association 47, 167-175.

Majewski, G., Czechowski, P.O., Badyda, A., Brandyk, A., 2014. Effect of air pollution on visibility in urban conditions, Warsaw case study. Environment Protection Engineering 40, 47-64.

Mazzuckelli, L., Methner, M., Birch, M., Evans, D., Ku, B., Crouch, K., Hoover, M., 2007. Identification and characterization of potential sources of worker exposure to carbon nanofibres during polymer composite laboratory operations. Journal of Occupational and Environmental Hygiene 4, 125-130.

McGee, J.K., Chen, L.C., Cohen, M.D., Chee, G.R., Prophete, C.M., Haykal-Coates, N., Wasson, S.J., Conner, T.L., Costa, D.L., Gavett, S.H., 2003. Chemical analysis of World Trade Center fine particulate matter for use in toxicologic assessment. Environmental Health Perspectives 111, 972-980.

Meinshausen, M., Meinshausen, N., Hare, W., Raper, S.C., Frieler, K., Knutti, R., Frame, D.J., Allen, M.R., 2009. Greenhouse-gas emission targets for limiting global warming to 2C. Nature 458, 1158-1162.

Methner, M., Hodson, L., Dames, A., Geraci, C., 2009. Nanoparticle emission assessment technique (NEAT) for the identification and measurement of potential inhalation exposure to engineered nanomaterials-Part B: Results from 12 field studies. Journal of Occupational and Environmental Hygiene 7, 163-176.

Meyer, M.B., Patashnick, H., Ambs, J.L., Rupprecht, E., 2000. Development of a sample equilibration system for the TEOM continuous PM monitor. Journal of the Air & Waste Management Association 50, 1345-1349.

Mickaityte, A., Zavadskas, E.K., Kaklauskas, A., Tupenaite, L., 2008. The concept model of sustainable buildings refurbishment. International Journal of Strategic Property Management 12, 53-68.

Mouzourides, P., Kumar, P., Marina Neophytou, K.A., 2015. Assessment of long-term measurements of particulate matter and gaseous pollutants in South-East Mediterranean. Atmospheric Environment 107, 148-165.

Muleski, G.E., Cowherd, C., Kinsey, J.S., 2005a. Particulate Emissions from Construction Activities. Journal of the Air & Waste Management Association 55, 772-783.

NAEI, 2013. National Atmospheric Emissions Inventory, http://naei.defra.gov.uk/data/ef-all [last access on 10th October 2015].

Namdeo, A., Bell, M.C., 2005. Characteristics and health implications of fine and coarse particulates at roadside, urban background and rural sites in UK. Environment International 31, 565-573.

Nakamura, S., Kondo, Y., 2002. Recycling, landfill consumption, and CO_2 emission: analysis by waste input–output model. Journal of Material Cycles and Waste Management, 4, 2-11.

Nowack, B., Bucheli, T.D., 2007. Occurrence, behavior and effects of nanoparticles in the environment. Environmental Pollution 150, 5-22.

Oberdörster, G., 2000. Pulmonary effects of inhaled ultrafine particles. International Archives of Occupational and Environmental Health 74, 1-8.

Oberg, E., Jones, F., McCauley, C., Heald, R., 2004. Machinery's Handbook: a reference book for the mechanical engineer, designer, manufacturing engineer, draftsman, toolmaker, and machinist. Industrial Press, USA, Twenty Sixth Edition, pp. 260.

Omer, A.M., 2008. Renewable building energy systems and passive human comfort solutions. Renewable and Sustainable Energy Reviews 12, 1562-1587.

Ostro, B., Lipsett, M., Reynolds, P., Goldberg, D., Hertz, A., Garcia, C., Henderson, K.D., Bernstein, L., 2010. Long-term exposure to constituents of fine particulate air pollution and mortality: results from the California Teachers Study. Environmental Health Perspectives 118, 363-369.

Pacca, S., Horvath, A., 2002. Greenhouse gas emissions from building and operating electric power plants in the upper Colorado river Basin. Environmental Science & Technology 36, 3194-3200.

Paoletti, L., De Berardis, B., Diociaiuti, M., 2002. Physico-chemical characterisation of the inhalable particulate matter (PM_{10}) in an urban area: an analysis of the seasonal trend. Science of the Total Environment 292, 265-275.

Pattanaik, S., Huggins, F.E., Huffman, G.P., 2012. Chemical speciation of Fe and Ni in residual Oil Fly Ash fine particulate matter using X-ray absorption spectroscopy. Environmental Science & Technology 46, 12927-12935.

Pearce, D.W., Cline, W.R., Achanta, A.N., Fankhauser, S., Pachauri, R.K., Tol, R.S., Vellinga, P., 1996. The social costs of climate change: greenhouse damage and the benefits of control. Climate Change 1995: Economic and Social Dimensions of Climate Change, 179-224.

Pekkanen, J., Timonen, K.L., Ruuskanen, J., Reponen, A., Mirme, A., 1997. Effects of ultrafine and fine particles in urban air on peak expiratory flow among children with asthmatic symptoms. Environmental Research 74, 24-33.

Peng, R.D., Chang, H.H., Bell, M.L., McDermott, A., Zeger, S.L., Samet, J.M., Dominici, F., 2008. Coarse particulate matter air pollution and hospital admissions for cardiovascular and respiratory diseases among medicare patients. Journal of the American Medical Association 299, 2172-2179.

Perez, N., Pey, J., Cusack, M., Reche, C., Querol, X., Alastuey, A., Viana, M., 2010. Variability of particle number, black carbon, and PM_{10}, $PM_{2.5}$, and PM_1 levels and speciation: influence of road traffic emissions on urban air quality. Aerosol Science and Technology 44, 487-499.

Pey, J., Querol, X., Alastuey, A., Rodriguez, S., Putaud, J.P., Van Dingenen, R., 2009. Source apportionment of urban fine and ultra-fine particle number concentration in a Western Mediterranean city. Atmospheric Environment 43, 4407-4415.

Plog, B.A., Quinlan, P., 2002. Fundamentals of industrial hygiene. National Safety Council Press, USA, Fifth Edition, pp. 1080.

Pope, C.A., 2000. What do epidemiologic findings tell us about health effects of environmental aerosols?. Journal of Aerosol Medicine 13, 335-354.

Pope III, C.A., Dockery, D.W., 2006. Health effects of fine particulate air pollution: lines that connect. Journal of the Air & Waste Management Association 56, 709-742.

Potgieter-Vermaak, S.S., Godoi, R.H.M., Grieken, R.V., Potgieter, J.H., Oujja, M., Castillejo, M., 2005. Micro-structural characterization of black crust and laser cleaning of building stones by micro-Raman and SEM techniques. Spectrochimica Acta Part A: Molecular and Biomolecular Spectroscopy 61, 2460-2467.

Ragheb, A.F., 2011. Towards environmental profiling for office building using life cycle assessment (Doctoral dissertation, University of Michigan), pp.163.

Raki, L., Beaudoin, J., Alizadeh, R., Makar, J., Sato, T., 2010. Cement and concrete nanoscience and nanotechnology. Materials 3, 918-942.

Rana, A.K., Rana, S.B., Kumari, A., Kiran, V., 2009. Significance of nanotechnology in construction engineering international. Journal of Recent Trends in Engineering 1, 46-48.

Rao, A., Jha, K.N., Misra, S., 2007. Use of aggregates from recycled construction and demolition waste in concrete. Resources, Conservation and Recycling 50, 71-81.

Reid, J.S., Eck, T.F., Christopher, S.A., Koppmann, R., Dubovik, O., Eleuterio, D.P., Holben, B.N., Reid, E.A., Zhang, J., 2005. A review of biomass burning emissions part III: intensive optical properties of biomass burning particles. Atmospheric Chemistry and Physics 5, 827-849.

Roberts, S., 2008. Altering existing buildings in the UK. Energy Policy 36, 4482-4486.

Rodriguez, S., Querol, X., Alastuey, A., Viana, M.a.-M., Alarcon, M., Mantilla, E., Ruiz, C.R., 2004. Comparative PM_{10}–$PM_{2.5}$ source contribution study at rural, urban and industrial sites during PM episodes in Eastern Spain. Science of the Total Environment 328, 95-113.

Rogula-Kozłowska, W., Pastuszka, J.S., Talik, E., 2008. Influence of vehicular traffic on concentration and particle surface composition of PM_{10} and $PM_{2.5}$ in Zabrze, Poland. Polish Journal of Environmental Studies 17, 539-548.

Rosenfeld, D., Rudich, Y., Lahav, R., 2001. Desert dust suppressing precipitation: A possible desertification feedback loop. Proceedings of the National Academy of Sciences 98, 5975-5980.

Sabbagh-Kupelwieser, N., Horvath, H., Szymanski, W.W., 2010. Urban Aerosol studies of PM_1 size fraction with reference to ambient conditions and visibility. Aerosol and Air Quality Resarch 10, 425-432.

Sachse, S., Silva, F., Irfan, A., Zhu, H., Pielichowski, K., Leszczynska, A., Blazquez, M., Kazmina, O., Kuzmenko, O., Njuguna, J., 2012. Physical characteristics of nanoparticles emitted during drilling of silica based polyamide 6 nanocomposites. IOP Conference Publishing Series: Materials Science and Engineering 40, 1-8.

Saitoh, K., Sera, K., Shiral, T., Sato, T., Odaka, M., 2003. Determination of elemental and ionic compositions for diesel exhaust particles by particle induced X-ray emission and ion chromatography analysis. Analytical Sciences 19, 525-528.

Saliba, N., El Jam, F., El Tayar, G., Obeid, W., Roumie, M., 2010. Origin and variability of particulate matter (PM_{10} and $PM_{2.5}$) mass concentrations over an Eastern Mediterranean city. Atmospheric Research 97, 106-114.

Sartori, I., Bergsdal, H., Müller, D.B., Brattebø, H., 2008. Towards modelling of construction, renovation and demolition activities: Norway's dwelling stock, 1900-2100. Building Research & Information 36, 412-425.

Saxe, H., Larsen, T., 2004. Air pollution from ships in three Danish ports. Atmospheric Environment 38, 4057-4067.

Schaap, M., van Loon, M., ten Brink, H.M., Dentener, F.J., Builtjes, P.J.H., 2004. Secondary inorganic aerosol simulations for Europe with special attention to nitrate. Atmospheric Chemistry and Physics 4, 857-874.

Schopp, W., Amann, M., Cofala, J., Heyes, C., Klimont, Z., 1998. Integrated assessment of European air pollution emission control strategies. Environmental Modelling & Software 14, 1-9.

Seinfeld, J.H., Pandis, S.N., 2006. Atmospheric chemistry and physics: from air pollution to climate change. John Wiley & Sons, USA, Second Edition, pp. 1232.

Senlin, L., Zhenkun, Y., Xiaohui, C., Minghong, W., Guoying, S., Jiamo, F., Paul, D., 2008. The relationship between physicochemical characterization and the potential toxicity of fine particulates ($PM_{2.5}$) in Shanghai atmosphere. Atmospheric Environment 42, 7205-7214.

Shekari, A.H., Razzaghi, M.S., 2011. Influence of nanoparticles on durability and mechanical properties of high performance concrete. Procedia Engineering 14, 3036-3041.

Shi, Y., Chen, J., Hu, D., Wang, L., Yang, X., Wang, X., 2014. Airborne submicron particulate (PM_1) pollution in Shanghai, China: Chemical variability, formation/dissociation of associated semi-volatile components and the impacts on visibility. Science of the Total Environment 473, 199-206.

Sjogren, B., Fossum, T., Lindh, T., Weiner, J., 2002. Welding and ischemic heart disease. International Journal of Occupational and Environmental Health 8, 309-311.

Smethurst, H.E., Witham, C., Robins, A.G., Murray, V.S.G., 2012. An exceptional case of long range odorant transport. Journal of Wind Engineering and Industrial Aerodynamics 103, 60-72.

Smith, S.D., Wood, G.S., Gould, M., 2000. A new earthworks estimating methodology. Construction Management & Economics 18, 219-228.

Spencer-Hwang, R., Knutsen, S.F., Soret, S., Ghamsary, M., Beeson, W.L., Oda, K., Shavlik, D., Jaipaul, N., 2011. Ambient air pollutants and risk of fatal coronary heart disease among kidney transplant recipients. American Journal of Kidney Diseases 58, 608-616.

Srivastava, A., Jain, V., Srivastava, A., 2009. SEM-EDX analysis of various sizes aerosols in Delhi India. Environmental Monitoring and Assessment 150, 405-416.

Stern, F., Lehman, E., Ruder, A., 2001. Mortality among unionized construction plasterers and cement masons. American Journal of Industrial Medicine 39, 373-388.

Sunikka, M., Boon, C., 2003. Environmental policies and efforts in social housing: the Netherlands. Building Research & Information 31, 1-12.

Tam, V. W., 2008. Economic comparison of concrete recycling: a case study approach. Resources, Conservation and Recycling, 52, 821-828.

Tai, A.P., Mickley, L.J., Jacob, D.J., 2010. Correlations between fine particulate matter ($PM_{2.5}$) and meteorological variables in the United States: Implications for the sensitivity of $PM_{2.5}$ to climate change. Atmospheric Environment 44, 3976-3984.

Tang, I., Munkelwitz, H., 1994. Water activities, densities, and refractive indices of aqueous sulfates and sodium nitrate droplets of atmospheric importance. Journal of Geophysical Research: Atmospheres (1984–2012) 99, 18801-18808.

Tao, J., Ho, K.F., Chen, L., Zhu, L., Han, J., Xu, Z., 2009. Effect of chemical composition of $PM_{2.5}$ on visibility in Guangzhou, China, 2007 spring. Particuology 7, 68-75.

Tasic, V., Jovasevic-Stojanovic, M., Vardoulakis, S., Milosevic, N., Kovacevic, R., Petrovic, J., 2012. Comparative assessment of a real-time particle monitor against the reference gravimetric method for PM_{10} and $PM_{2.5}$ in indoor air. Atmospheric Environment 54, 358-364.

Tian, G., Fan, S., Li, G., Qin, J., 2007. Characteristics of fugitive dust emission from paved road near construction activities. Journal of Huanjing Kexue 28, 2626-2629.

Tiwari, S., Srivastava, A.K., Bisht, D.S., Bano, T., Singh, S., Behura, S., Srivastava, M.K., Chate, D.M., Padmanabhamurty, B., 2009. Black carbon and chemical characteristics of PM_{10} and $PM_{2.5}$ at an urban site of North India. Journal of Atmospheric Chemistry 62, 193-209.

Toledo, V.E., de Almeida Júnior, P.B., Quiterio, S.L., Arbilla, G., Moreira, A., Escaleira, V., Moreira, J.C., 2008. Evaluation of levels, sources and distribution of toxic elements in PM_{10} in a suburban industrial region, Rio de Janeiro, Brazil. Environmental Monitoring and Assessment 139, 49-59.

Tsai, C.J., Huang, C.Y., Chen, S.C., Ho, C.E., Huang, C.H., Chen, C.W., Chang, C.P., Tsai, S.J., Ellenbecker, M., 2011. Exposure assessment of nano-sized and respirable particles at different workplaces. Journal of Nanoparticle Research 13, 4161-4172.

Tsai, C.J., Lin, G.Y., Liu, C.N., He, C.E., Chen, C.W., 2012. Characteristic of nanoparticles generated from different nano-powders by using different dispersion methods. Journal of Nanoparticle Research 14, 1-12.

Tsai, C.J., Wu, C.H., Leu, M.L., Chen, S.C., Huang, C.Y., Tsai, P.-J., Ko, F.H., 2009. Dustiness test of nanopowders using a standard rotating drum with a modified sampling train. Journal of Nanoparticle Research 11, 121-131.

Turner, M.C., Krewski, D., Pope, C.A., Chen, Y., Gapstur, S.M., Thun, M.J., 2011. Long-term ambient fine particulate matter air pollution and lung cancer in a large cohort of never-smokers. American Journal of Respiratory and Critical Care Medicine 184, 1374-1381.

Unal, Y. S., Toros, H., Deniz, A., Incecik, S., 2011. Influence of meteorological factors and emission sources on spatial and temporal variations of PM_{10} concentrations in Istanbul metropolitan area. Atmospheric Environment, 45, 5504-5513.

Vajanapoom, N., Shy, C.M., Neas, L.M., Loomis, D., 2001. Estimation of particulate matter from visibility in Bangkok, Thailand. Journal of Exposure Analysis & Environmental Epidemiology 11, 97-102.

Vecchi, R., Marcazzan, G., Valli, G., Ceriani, M., Antoniazzi, C., 2004. The role of atmospheric dispersion in the seasonal variation of PM_1 and $PM_{2.5}$ concentration and composition in the urban area of Milan (Italy). Atmospheric Environment 38, 4437-4446.

Verma, D.K., Kurtz, L.A., Sahai, D., Finkelstein, M.M., 2003. Current chemical exposures among Ontario construction workers. Applied Occupational and Environmental Hygiene 18, 1031-1047.

Viana, M., Kuhlbusch, T., Querol, X., Alastuey, A., Harrison, R., Hopke, P., Winiwarter, W., Vallius, M., Szidat, S., Prevot, A., 2008. Source apportionment of particulate

matter in Europe: a review of methods and results. Journal of Aerosol Science 39, 827-849.

Vineis, P., Forastiere, F., Hoek, G., Lipsett, M., 2004. Outdoor air pollution and lung cancer: Recent epidemiologic evidence. International Journal of Cancer 111, 647-652.

Voliotis, A., Benzantakos, S., Gaimarelou, M., Valenti, M., Kumar, P., Biskos, G., 2014. Nanoparticle emissions from traditional pottery manufacturing. Environmental Science: Process & Impacts 16, 1489-1494.

Walker, S., Jamieson, H., Rasmussen, P., 2011. Application of synchrotron microprobe methods to solid-phase speciation of metals and metalloids in house dust. Environmental Science & Technology 45, 8233-8240.

Wan, J.M., Lin, M., Chan, C.Y., Zhang, Z.S., Engling, G., Wang, X.M., Chan, I.N., Li, S.Y., 2011. Change of air quality and its impact on atmospheric visibility in central-western Pearl River Delta. Environmental Monitoring and Assessment, 172, 339-351.

Ward, T.J., Smith, G.C., 2005. The 2000/2001 Missoula Valley $PM_{2.5}$ chemical mass balance study, including the 2000 wildfire season-seasonal source apportionment. Atmospheric Environment 39, 709-717.

Watt, I.M., 1997. The principles and practice of electron microscopy. Cambridge University Press, UK, Second Edition. pp. 484.

Watts, J.F., 1990. An introduction to surface analysis by electron spectroscopy. Oxford university Press, UK, First Edition, pp. 65.

Watts, J.F., Wolstenholme, J., 2003. An introduction to surface analysis by XPS and AES. An introduction to surface analysis by XPS and AES. Wiley, UK, First Edition, pp.224.

Weichenthal, S., Van Ryswyk, K., Kulka, R., Sun, L., Wallace, L., Joseph, L., 2014. In-vehicle exposures to particulate air pollution in Canadian metropolitan areas: the urban transportation exposure study. Environmental Science & Technology 49, 597-605.

Weng, C.H., Hu, C.C., Yen, T.H., Huang, W.H., 2015. Association between environmental particulate matter and arterial stiffness in patients undergoing hemodialysis. BMC Cardiovascular Disorders 15, 1-7.

Westmoreland, E.J., Carslaw, N., Carslaw, D.C., Gillah, A., Bates, E., 2007. Analysis of air quality within a street canyon using statistical and dispersion modelling techniques. Atmospheric Environment 41, 9195-9205.

WHO, 2006. Air quality guidelines: global update 2005: particulate matter, ozone, nitrogen dioxide, and sulfur dioxide. World Health Organization. Available at: http://www.euro.who.int/document/e90038.pdf.

Wood, S., 2006. Generalized additive models: an introduction with R. CRC press, USA, First Edition, pp. 410.

Woskie, S.R., Kalil, A., Bello, D., Virji, M.A., 2002. Exposures to quartz, diesel, dust, and welding fumes during heavy and highway construction. American Industrial Hygiene Association Journal 63, 447-457.

Zereini, F., Wiseman, C.L., Puttmann, W., 2012. In vitro investigations of platinum, palladium, and rhodium mobility in urban airborne particulate matter (PM_{10}, $PM_{2.5}$, and PM_1) using simulated lung fluids. Environmental Science & Technology 46, 10326-10333.

Zhang, Y.H., Shao, M., Cheng, C.L., 2006. Quantitative relationship between visibility and mass concentration of $PM_{2.5}$ in Beijing. Journal of Environmental Sciences 18, 475-481.

Appendix A

A1. Average and cumulative concentration against size during the activities

The average number and mass concentrations of particles measured during mixing with GGBS, PFA, drilling and cutting activities are presented in Figure A1 and Figure A2, respectively. Similarly, cumulative number concentration of particles for each activity are presented in Figure A3 and Figure A4. The cutting of concrete cubes took place in the laboratory displayed considerable increase in cumulative number of particles in contradiction of intermediate background readings.

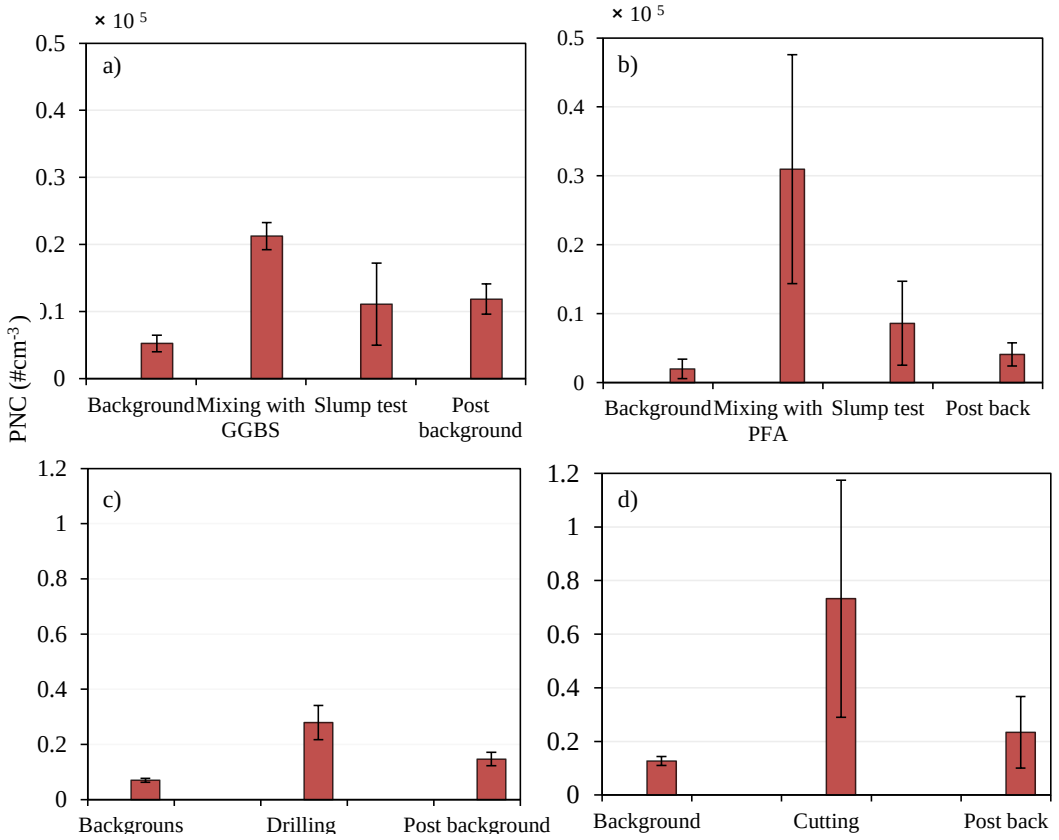

Figure A1: Average of PNCs during (a) mixing with GGBS, (b) mixing with PFA (c) drilling, and (d) cutting activities.

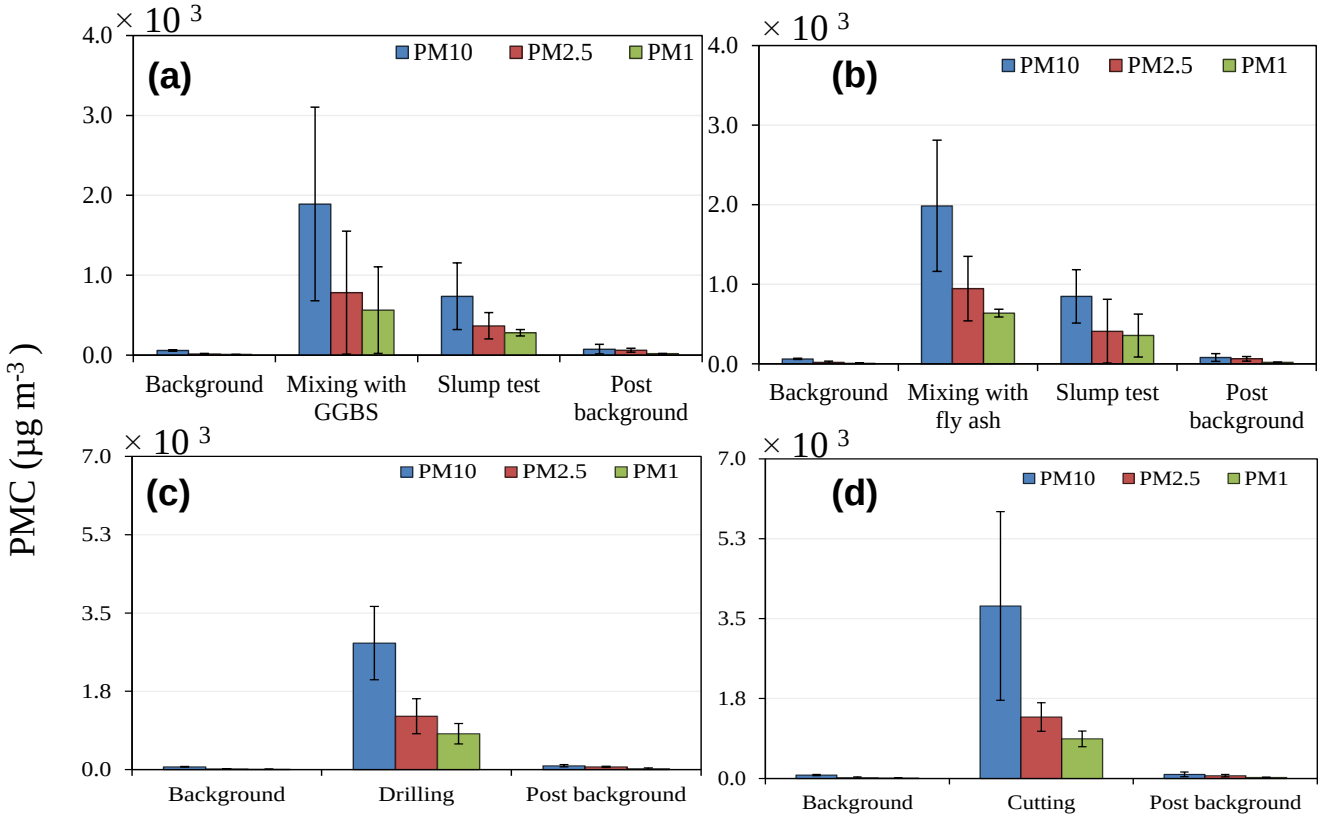

Figure A2: Average of PMCs during (a) mixing with GGBS, (b) mixing with PFA (c) drilling, and (d) cutting activities. The error bars indicate the standard deviation values.

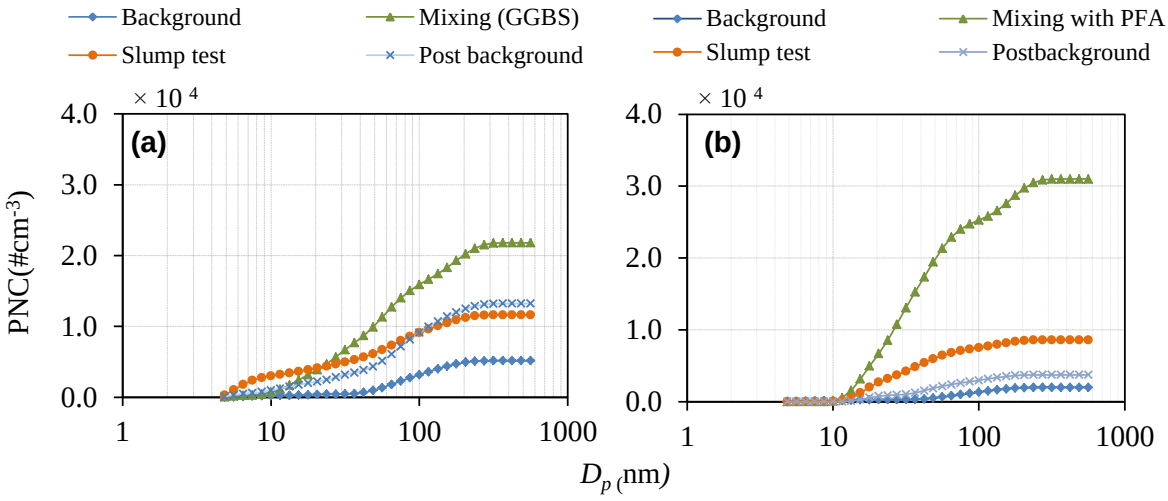

Figure A3: Cumulative concentration for (a) mixing with GGBS (b) for mixing with PFA.

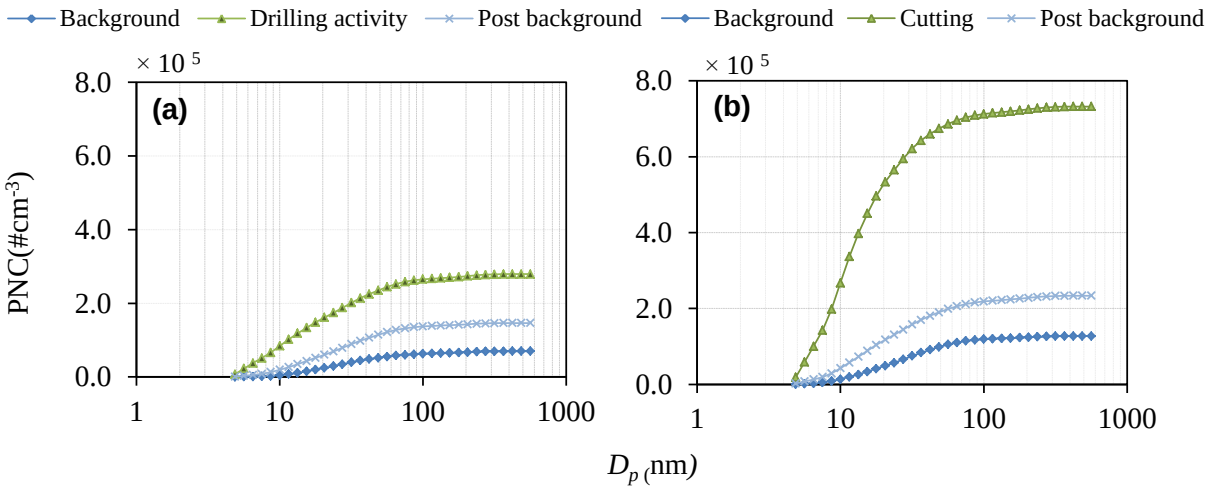

Figure A4: Cumulative concentration of particles during or (a) drilling and (b) cutting.

Table A1: Details of materials were used in mixing with GGBS.

Material	Quantity (kg)
Water	3.48
Cement	3.00
GGBS	3.00
10 mm aggregates	3.76
20 mm aggregates	3.76
Sand	4.00

Table A2: Details of materials were used in mixing with PFA.

Materials	Quantity (kg)
Water	3.48
Cement	3.00
PFA	3.00
10 mm aggregate	3.76
20 mm aggregate	3.76
Sand	4.00

Table A3: Emission factors of PMs for mixing with GGBS, PFA, drilling and cutting activities.

	PM_{10} ($\times 10^{-4}$)			$PM_{2.5}$($\times 10^{-4}$)			PM_{1}($\times 10^{-4}$)		
Activities	$\mu g\ s^{-1}$	$\mu g\ s^{-1}\ kg^{-1}$	$\mu g\ kg^{-1}$	$\mu g\ s^{-1}$	$\mu g\ s^{-1}\ kg^{-1}$	$\mu g\ kg^{-1}$	$\mu g\ s^{-1}$	$\mu g\ s^{-1}\ kg^{-1}$	$\mu g\ kg^{-1}$
Mixing with GGBS	366.56 ±240.60	17.45 ±11.45	7331.31 ±4812.04	153.45 ±152.90	7.30 ±7.28	3069.13 ±3058.12	111.14 ±106.94	5.29 ±5.09	2222.82 ±2138.92
Mixing with PFA	393.48 ±163.20	18.73 ±7.77	7869.65 ±3264.12	185.31 ±78.16	8.82 ±3.72	3706.35 ±1563.28	125.89 ±9.24	5.99 ±0.44	2517.89 ±184.88
Drilling	552.77 ±162.70	4606.45 ±1355.86	276387.14 ±81352.22	235.68 ±77.60	1964.05 ±646.68	117843.51 ±38801.10	158.90 ±45.27	1324.39 ±377.31	79454.39 ±22639.03
Cutting	740.53 ±410.38	9142.43 ±5066.45	548545.96 ±303987.11	265.81 ±58.34	3281.70 ±720.25	196902.26 ±43215.40	172.12 ±33.96	2125.01 ±419.30	127500.67 ±25158.51

Table A4: Net emission factors of particles numbers for mixing with GGBS, PFA, drilling and cutting activities.

	Particle number based EFs			
Activities	# s^{-1} ($\times 10^4$)	# $s^{-1}\ kg^{-1}$ ($\times 10^4$)	# kg^{-1} ($\times 10^4$)	Typical activity duration (sec)
Mixing with GGBS	173.41±8.43	8.25± 4.09	3468.33± 168.79	420
Mixing with PFA	314.01±164.55	14.95±7.83	6280.30±3291.06	420
Drilling	2266.81±593.32	18890.12±4944.36	1133407± 296661.70	60
Cutting	6553.34±4613.34	80905.44±56954.83	4854326±341728.91	60

Table A5: The deposited doses of particle numbers with fitted and variable DFs.

Activity	Duration (s)	Dose with constant DF(dose min^{-1}) ±STD	Dose with variable DF (dose min^{-1}) ±STD
Mixing GGBS	2,777	[a] 1.99×±1.80 $\times 10^8$	[a]2.35±0.31 $\times 10^8$
		[b]1.50±0.72 $\times 10^8$	[b]1.81±0.32 $\times 10^8$
Mixing PFA	4,255	[a] 2.90±1.55 $\times 10^8$	[a] 3.40±2.17 $\times 10^8$
		[b]2.72±1.42 $\times 10^8$	[b]3.19±2.18 $\times 10^8$
Drilling	1,953	[a] 26.12±5.80 $\times 10^8$	[a] 32.97±9.41 $\times 10^8$
		[b]19.58±5.13 $\times 10^8$	[b]25.09±9.38 $\times 10^8$
Cutting	3,888	[a] 68.54±41.41 $\times 10^8$	[a] 88.25± 58.82 $\times 10^8$
		[b]56.62±39.86 $\times 10^8$	[b]73.75± 58.82 $\times 10^8$

[a]Total deposited doses (including background). [b]Net deposited doses (after subtracting background from total).

Appendix B

B1. Activities frequency and site description during the experiment days

The list of refurbishment activities are presented in Tables B1 and B2 during the sampling period. About 20 number of different refurbishment activities were counted such as demolition and cutting of concrete, welding, wall chasing, painting, cutting abrasive blasting, cementing, hammering, impact driving and sawing were carried out at an indoor refurbishment site (Chemistry Laboratory) at the University of Surrey (Figure 5.1).

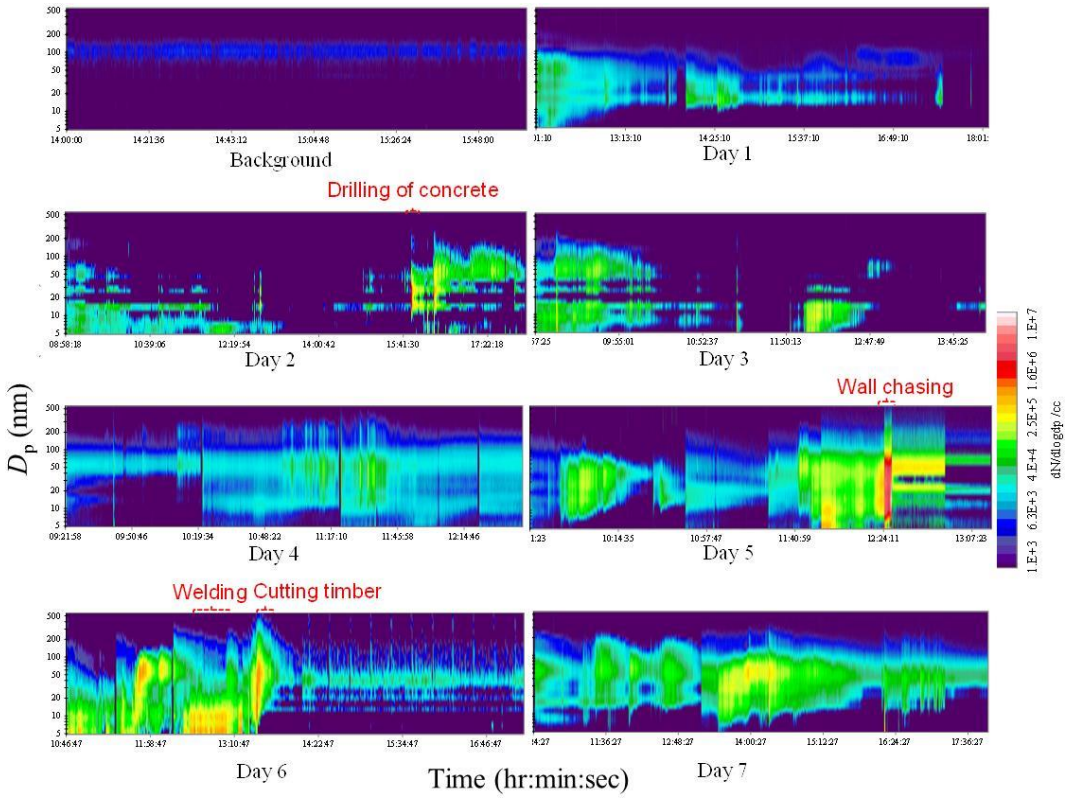

Figure B1: The contour plots of PNCs during the background, activity and non-activity periods (see Table B1 for details of activities time).

Table B1: PNCs and PMCs for each activity during the seven days of refurbishment; stdev refers to standard deviation.

Date	Time	Activity type	PNCs ±stdev ($\times 10^4$ # cm^{-3})	PM_{10} ±stdev ($\times 10^4$ µg m^{-3})	$PM_{2.5}$ ±stdev ($\times 10^4$ µg m^{-3})	PM_1 ±stdev ($\times 10^4$ µg m^{-3})
02/07/2013	12:04:00-12:07:00	Hot Air torching	3.76±0.43	4.14±1.42	0.39±0.08	0.12±0.009
02/07/2013	12:07:00-12:09:00	Metal cutting	3.12±0.38	2.65±0.86	0.36±0.08	0.12±0.006
02/07/2013	12:44:58-13:08:34	Ceiling drilling	1.54±0.69	1.23±0.41	0.27±0.04	0.11±0.005
02/07/2013	13:48:00-13:50:00	Galvanising spray	1.11±0.71	3.32±0.55	0.38±0.08	0.14±0.01
02/07/2013	14:02:00-14:21:02	Drilling of concrete beam	1.92±0.81	19.21±10.66	1.11±0.49	0.22±0.05
02/07/2013	14:23:52-14:32:00	Emptying of concrete waste bin	2.55±1.84	5.09±1.40	0.45±0.09	0.13±0.009
02/07/2013	17:23:12-17:28:41	Floor sweeping	1.24±0.83	11.00±4.70	0.70±0.26	0.15±0.02
02/07/2013	17:51:28-17:52:01	Wrenching	1.86±1.80	2.20±0.40	0.30±0.07	0.11±0.005
03/07/2013	08:58:20-09:14:58	Cutting timber	2.53±0.92	10.02±5.28	0.59±0.3	0.09±0.03
03/07/2013	09:15:00-09:37:24	Punching of timber boards	2.14±1.09	6.05±3.15	0.41±0.23	0.07±0.02
03/07/2013	09:37:24-09:55:34	Drilling of ceiling	1.98±0.75	3.56±1.72	0.29±0.15	0.05±0.01
03/07/2013	09:56:00-10:08:43	Hammering	1.66±0.55	3.59±2.25	0.26±0.16	0.05±0.01
03/07/2013	10:38:00-10:59:00	Punching of timber boards	1.10±0.62	4.27±3.79	0.34±0.30	0.08±0.04
03/07/2013	11:03:03-11:17:01	Taking out construction waste materials	0.95±0.19	15.41±5.64	0.95±0.33	0.13±0.03
03/07/2013	11:20:01-11:26:59	Sawing air ducts	0.63±0.08	19.20±3.48	1.33±0.23	0.18±0.02
03/07/2013	11:34:00-11:40:00	Drilling of celling	1.40±0.3	11.17±2.27	0.7±0.21	0.11±0.02
03/07/2013	12:05:00-12:15:59	PVC drilling	1.10±0.27	30.28±30.01	1.92±2.20	0.22±0.18
03/07/2013	12:35:00-12:38:59	Metal drilling	0.14±0.09	7.73±3.15	0.64±0.25	0.10±0.02
03/07/2013	12:49:53-12:52:42	Timber sanding	8.17±7.7	5.10±4.35	0.33±0.28	0.07±0.02
03/07/2013	12:52:42-12:59:58	Timber cutting	0.36±0.18	4.32±2.53	0.37±0.21	0.07±0.02

03/07/2013	14:54:40-15:03:59	Drilling of concrete slabs on ceiling	0.76±0.56	9.11±7.72	0.54±0.54	0.09±0.06
03/07/2013	15:04:00-15:14:14	V seprate saw for cutting	0.31±0.25	6.80±4.67	0.47±0.43	0.08±0.05
03/07/2013	15:44:00-15:46:50	Sawing old pipes	1.15±1.13	19.16±9.65	1.11±0.73	0.16±0.09
03/07/2013	15:55:00-15:59:59	Welding with auto welding Jig	7.91±1.66	23.59±10.45	1.64±0.77	0.26±0.09
03/07/2013	16:10:09-16:35:00	Concrete drilling	10.01±8.03	21.75±23.76	1.44±1.70	0.23±0.23
03/07/2013	16:35:01-17:00:00	Concrete slab drilling	2.88±0.87	6.23±4.50	0.53±0.43	0.09±0.05
03/07/2013	17:13:00-17:15:06	Hammering	2.94±0.55	3.93±2.93	0.28±0.21	0.06±0.02
03/07/2013	17:15:08-17:19:58	Welding	3.22±0.41	9.19±6.88	0.50±0.39	0.09±0.03
03/07/2013	17:20:01-17:27:01	GF machining	3.20±0.85	3.93±2.54	0.29±0.18	0.06±0.02
03/07/2013	17:27:01-17:34:40	Preparation to finish	4.73±0.88	4.87±3.77	0.34±0.20	0.07±0.02
04/07/2013	08:58:00-09:16:00	Demolition of bricks	5.17±4.74	41.60±18.51	3.20±1.24	0.36±0.12
04/07/2013	09:17:44-09:30:00	Concrete drilling	5.17±2.11	6.42±5.01	0.57±0.39	0.09±0.04
04/07/2013	09:30:00-09:47:00	Moving demolished debris	6.87±3.01	2.23±2.53	0.23±0.23	0.05±
04/07/2013	09:53:00-10:04:00	GF machining	2.78 ±1.87	27.46±25.45	1.69±1.48	0.20±
04/07/2013	10:04:24-10:09:11	Ground cleaning	2.35±1.27	20.28±3.98	1.60±0.37	0.18±0.03
04/07/2013	10:10:00-10:17:00	Painting	2.19±1.40	9.27±3.17	0.76±0.23	0.10±0.02
04/07/2013	11:17:03-11:18:17	Devices movement	1.32±1.27	8.42±9.69	0.47±0.80	0.08±0.09
04/07/2013	12:01:47-12:21:49	Sanding	6.03±3.47	6.33±5.12	0.48±0.38	0.09±0.04
04/07/2013	12:27:25-12:39:49	Timber sanding	1.71±0.91	4.25±2.63	0.31±0.19	0.07±0.02
04/07/2013	13:57:00-14:05:00	Spraying	4.84±3.98	2.49±1.80	0.30±0.16	0.09±0.01
05/07/2013	09:36:37-10:07:27	Oiling of instrument	0.60±0.47	15.04±2.34	1.10±1.66	0.12±0.17
05/07/2013	10:07:27-10:19:59	Carrying metal bars to the site	0.96±0.56	36.08±28.17	2.81±2.21	0.29±0.21
05/07/2013	10:20:00-10:48:03	Ground sweeping	1.52±1.04	4.99±6.17	0.58±0.61	0.06±0.05

05/07/2013	10:54:04-11:19:59	Ground sweeping	2.77±1.82	16.38±18.74	1.46±1.48	0.16±0.15
05/07/2013	11:20:01-11:40:00	Demolition of blocks	4.30±3.56	7.17±3.55	12.22±0.56	0.19±0.07
06/07/2013	09:42:13-17:20:30	Background measurement	0.11±0.08	0.19±0.04	0.16±0.009	0.14±0.004
09/07/2013	09:32:43-09:44:00	Pipe sawing	0.89± 0.46	12.15±12.26	1.01±1.00	0.16±0.13
09/07/2013	09:48:43-09:53:40	Cementing	6.26± 3.00	6.82±1.85	0.71±0.20	0.13±0.02
09/07/2013	09:54:00-10:05:40	Wall chasing	8.25± 2.94	12.71±7.20	1.18±0.57	0.23±0.10
09/07/2013	10:30:51-10:40:08	Hammering	1.63±1.17	7.52±4.82	0.63±0.37	0.10±0.03
09/07/2013	10:42:38-10:47:47	Embedding electrical facilities in the wall	0.63± 0.33	1.48±0.46	0.21±0.005	0.05±0.007
09/07/2013	11:26:55-11:40:10	Welding with blow torch	1.94± 0.49	1.36±0.85	0.46±0.006	0.08±0.005
09/07/2013	11:40:53-11:54:06	Hammering	8.30± 3.76	3.02±2.25	0.30±0.17	0.10±0.03
09/07/2013	11:54:07-12:07:45	Demolition of ceramics	18.53± 7.07	3.39±1.53	0.27±0.09	0.06±0.01
09/07/2013	12:10:49-12:14:55	Using Monkey Wrench on the duct	1.17± 2.33	11.25±4.30	0.67±0.33	0.10±0.02
09/07/2013	12:18:58-12:53:50	Wall chasing	44.36±9.32	17.71±14.83	1.54±1.07	0.21±0.16
09/07/2013	12:54:40-13:16:52	Grinding of dropped pieces	1.57±0.50	5.14±232.59	0.67±0.24	0.09±0.02
10/07/2013	10:49:00-11:16:00	Drilling of concrete beam	7.08± 3.36	4.50±2.29	0.64±0.25	0.16±0.03
10/07/2013	11:44:47-11:52:47	Ladder movement	4.21± 3.08	6.01±1.48	0.94±0.26	0.30±0.08
10/07/2013	12:04:00-12:17:00	Drilling of duct	6.82±5.16	6.63±2.99	0.71±0.19	0.18±0.02
10/07/2013	12:21:00-12:29:47	Placing air duct	4.99± 2.64	4.20±0.74	0.43±0.06	0.12±0.01
10/07/2013	12:29:50-12:35:47	Drilling of concrete beam	10.69± 6.07	3.89±0.62	0.41±0.06	0.11±0.01
10/07/2013	12:41:49-12:56:47	Welding with auto welding JIG	17.98± 6.74	3.83±1.66	0.39±0.09	0.12±0.01
10/07/2013	13:38:00-13:53:00	Cutting timber	4.81± 4.59	1.11±0.60	0.19±0.06	0.08±0.01
10/07/2013	13:54:00-14:11:00	Sawing of timber	9.70± 6.56	2.76±1.50	0.52±0.33	0.15±0.07
10/07/2013	14:12:00-15:12:00	Drilling of concrete beam with VEKA	12.44±4.21	5.54±2.47	0.78±0.35	0.18±0.06
10/07/2013	15:12:02-15:33:59	Impact driving	9.96± 6.41	14.15±9.65	1.10±0.45	0.23±0.06

10/07/2013	15:36:00-16:00:47	Cementing	18.27± 18.53	8.51±3.18	1.38±0.60	0.37±0.19
10/07/2013	16:19:01-16:54:00	Spraying of air duct	0.98±0.73	3.20±1.55	0.43±0.16	0.14±0.01
11/07/2013	10:26:07-10:30:54	Cutting wood to small cubes	4.71±2.18	12.32±1.86	1.62±0.15	0.35±0.02
11/07/2013	10:30:55-10:34:59	Wall grinding	3.85 ±0.54	9.84±1.38	1.30±0.21	0.30±0.03
11/07/2013	10:35:00-10:46:59	Carrying wasted materials from grinding	2.62±0.45	5.75±1.16	0.96±0.32	0.23±0.03
11/07/2013	10:47:00-10:49:50	Sawing	2.33±0.41	3.93±0.80	0.65±0.37	0.18±0.04
11/07/2013	11:06:00-11:09:00	Carrying stone materials to the site	2.54±1.20	12.81±3.28	0.85±0.35	0.19±0.03
11/07/2013	11:13:00-11:14:59	Steel cutting	1.78 ±0.31	12.47±3.10	1.05±0.33	0.24±0.02
11/07/2013	11:15:00-11:24:59	Drilling of ceiling	5.41±1.83	16.36±4.79	1.53±0.43	0.36±0.04
11/07/2013	11:25:00-12:02:59	VEKA drilling	3.69±1.78	15.68±5.19	1.26±0.59	0.27±0.08
11/07/2013	12:05:07-12:07:00	Sawing	1.90±0.42	16.81±1.50	1.26±0.52	0.23±0.06
11/07/2013	12:07:01-12:11:00	Dragging electricity cables on the ground	2.47 ±0.67	25.82±8.00	1.86±0.24	0.30±0.03
11/07/2013	12:11:01-12:13:59	Spraying (galvanising spray)	3.60±1.11	19.02±2.76	1.46±0.26	0.26±0.03
11/07/2013	12:15:00-12:16:00	Drilling of ceiling concrete	5.51±0.96	21.79±7.10	1.94±0.16	0.38±0.01
11/07/2013	12:16:01-12:19:59	Hammering	6.82±0.46	19.45±4.81	1.69±0.18	0.33±0.02
11/07/2013	12:20:00-12:45:56	Displacement of air tubes and wiring	3.32±1.75	17.87±6.52	1.61±0.12	0.33±0.01
11/07/2013	13:40:00-13:44:58	Grinding of timber parts	4.00±0.27	3.28±2.03	0.31±0.03	0.09±0.01
11/07/2013	13:45:00-14:07:58	Timber sawing with chain saw	3.80 ±0.38	6.68±5.16	0.49±0.04	0.11±0.01
11/07/2013	14:08:00-14:14:23	Grinding	9.04±3.99	10.58±2.85	0.67±0.17	0.13±0.02
11/07/2013	14:15:00-14:19:58	Engineering work on electricity box	13.17±2.17	14.84±3.08	0.91±0.16	0.16±0.01
11/07/2013	14:20:00-14:20:59	impact driver on woody boards	14.71 ±0.95	14.14±1.28	0.96±0.13	0.16±0.01
11/07/2013	14:21:00-14:33:00	Welding	12.74 ±1.64	9.44±3.74	0.70±0.20	0.14±0.01
11/07/2013	14:54:00-15:49:00	Metal cutting	6.67±2.39	9.11±3.66	0.82±0.16	0.16±0.01

11/07/2013	15:50:00-16:09:30	Fiberglass cutting	2.95±0.69	9.52±3.34	0.92±0.26	0.17±0.03
11/07/2013	16:25:00-16:29:00	Ladder movement	1.95±1.22	23.43±16.04	1.67±0.21	0.26±0.03
11/07/2013	16:29:21-16:30:20	drilling	15.49 ±15.45	38.27±16.92	4.28±0.22	0.75±0.03
11/07/2013	16:39:00-16:58:30	Wall drilling	3.41±1.22	14.25±4.92	1.05±0.21	0.20±0.03
11/07/2013	16:59:01-17:01:20	grinding	4.93±3.58	6.64±0.90	0.65±0.05	0.15±0.009
11/07/2013	17:05:29-16:06-29	Hot air torching	3.21±0.82	8.02±1.82	0.61±0.09	0.15±0.009
11/07/2013	17:07:30-17:40:40	Preparation to finish	3.32±1.82	9.59±2.12	0.79±0.10	0.17±0.09

Table B2: Peak diameters of PND observed during different activities. It is worth noting that these peak diameters represent the size distributions when the activities below were occurring dominantly at the sample site and do not represent the direct emissions from an activity.

Activity name	Peak diameter 1 (nm)	Peak diameter 2 (nm)	Peak diameter 3 (nm)
Wall chasing	15.4	27.4	48.7
Cementing	15.4	27.4	48.7
Welding and hot air torching	15.4	27.4	48.7
Drilling	6.0	15.0	27.0
Cutting	15.4	27.4	56.2
Sawing	5.6	10.0	15.4
General Demolition[a]	5.6	10.0	48.7
Hammering	15.4	27.4	56.2
Sanding	5.6	15.4	27.4
GF machining[b]	5.6	15.4	27.4
Ground cleaning and sweeping	15.4	27.4	56.2
Spraying	15.4	20.5	48.7
Empting of waste materials	7.5	15.4	27.4
Wrenching	5.6	15.4	27.4
Ladder and staff movement	5.6	8.6	15.4
Grinding	15.4	27.4	48.7
Impact driving	5.6	10.0	27.4
Punching of timber	5.6	15.4	27.4
Preparation works to finish	15.4	27.4	56.2
Other activities (e.g. painting, oiling, carrying metal bars to the site and moving demolished debris)	15.4	27.4	48.7

[a]Breaking of materials such as concrete, brick and ceramic; [b]Straightening of metal tubing.

Table B3: Averages PNCs and PMCs for each activity, during the seven days of refurbishment activities.

Activity name	Average PNCs ±stdev ($\times 10^4$ # cm^{-3})	PM_{10} ±stdev ($\times 10^2$ µg m^{-3})	$PM_{2.5}$ ±stdev ($\times 10^2$ µg m^{-3})	PM_1 ±stdev ($\times 10^2$ µg m^{-3})
Wall chasing	26.30±25.53	15.21±3.53	1.36±0.25	0.22±0.01
Cementing	12.23±8.44	7.66±1.20	1.05±0.47	0.25±0.17
Welding and hot air torching	7.25±6.03	8.51±7.31	0.67±0.44	0.14±0.05
Drilling	5.22±4.44	12.74±10.17	1.09±0.94	0.21.±0.16
Cutting	2.96±1.46	8.34±4.96	0.77±0.47	0.16±0.09
Sawing	2.59±3.08	10.94±6.79	0.86±0.35	0.16±0.04
General demolition[a]	9.33±7.97	20.01.±19.58	1.52±1.51	0.18±0.15
Hammering	4.27±3.09	7.50±6.90	0.63±0.61	0.13±0.11
Sanding	5.30±3.29	5.23±1.04	0.37±0.09	0.07±0.009
GF machining[b]	2.99±0.30	15.69±16.63	0.99±0.98	0.13±0.09
Ground cleaning and sweeping	1.92±0.62	11.02±7.49	0.93±0.56	0.13±0.04
Spraying	1.54±1.39	6.46±8.42	0.58±0.58	0.15±0.07
Empting of waste materials	1.75±1.12	10.25±7.29	0.70±0.35	0.13±0.0005
Wrenching	8.55±9.46	6.73±6.40	0.48±0.25	0.11±0.005
Ladder and staff movement	2.67±1.35	11.75±8.77	1.00±0.59	0.21±0.10
Grinding	4.67±2.73	7.09±3.09	0.72±0.35	0.15±0.08
Impact driving	12.33±3.36	14.33±0.26	1.03±0.09	0.20±0.04
Punching of timber	2.14±1.10	5.16±1.25	0.37±0.05	0.07±0.004
Preparation works to finish	4.02±0.99	7.23±3.33	0.57±0.32	0.12±0.07
Other activities (e.g. painting, oiling, carrying metal bars to the site and moving demolished debris)	4.32±4.87	13.92±11.94	1.04±0.92	0.13±0.08

[a]Breaking of materials such as concrete, brick and ceramic; [b] Straightening of metal tubing.

B2. XPS results

Figure B2 shows the binding energy of the peak and the elemental composition of all the five samples described in Table 5.1. XPS spectra were picked up by applying a Thermo digital twin anode source, which was operated using the Al Kα at 300W. Also quantitative surface chemical analyses were calculated from the high resolution, core level spectra following the removal of a non-linear background.

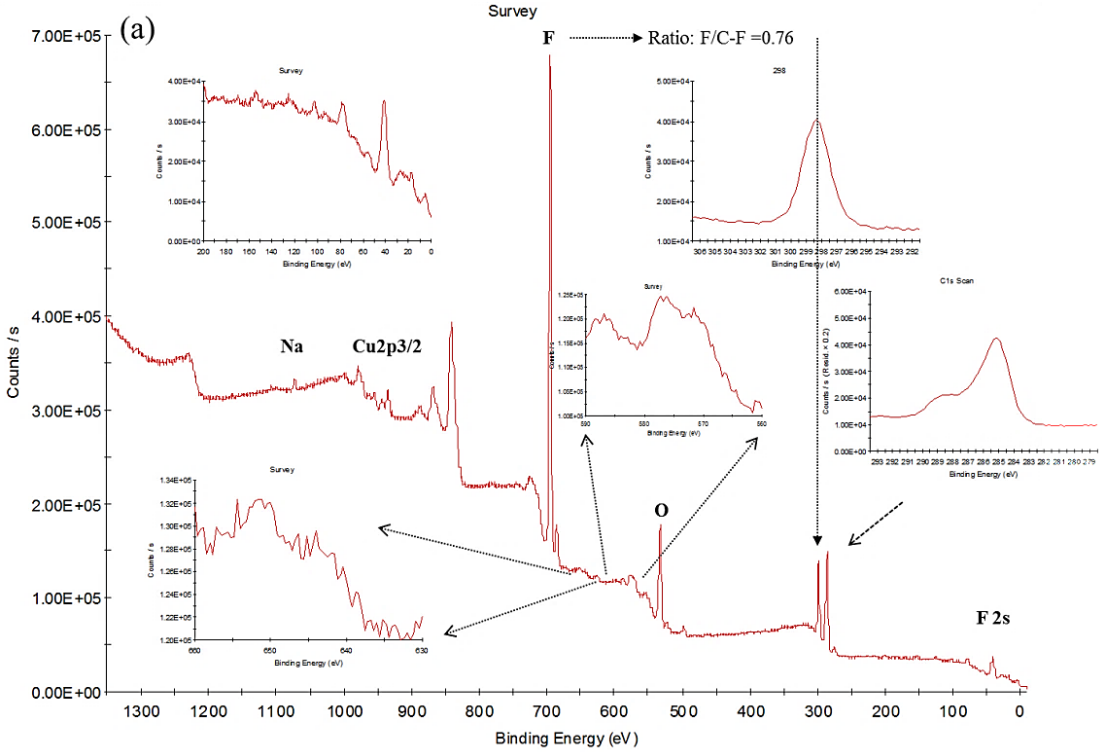

Figure B2: Survey spectra for all samples (a) blank sample (b) background (c) sample 1 (d) sample 2 and (e) sample 5.

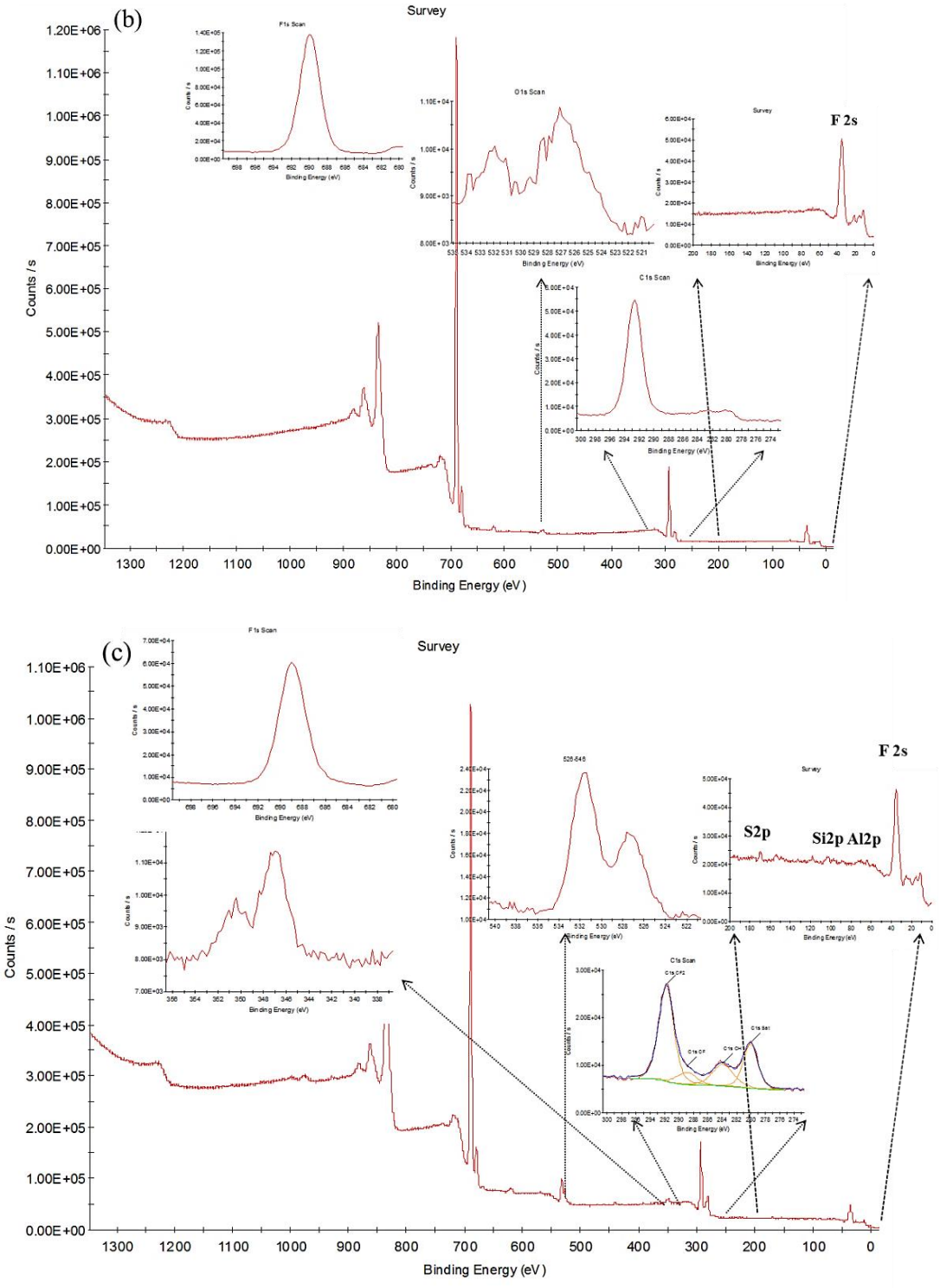

Figure B2: Survey spectra for all samples (a) blank sample (b) background (c) sample 1 (d) sample 2 and (e) sample 5.

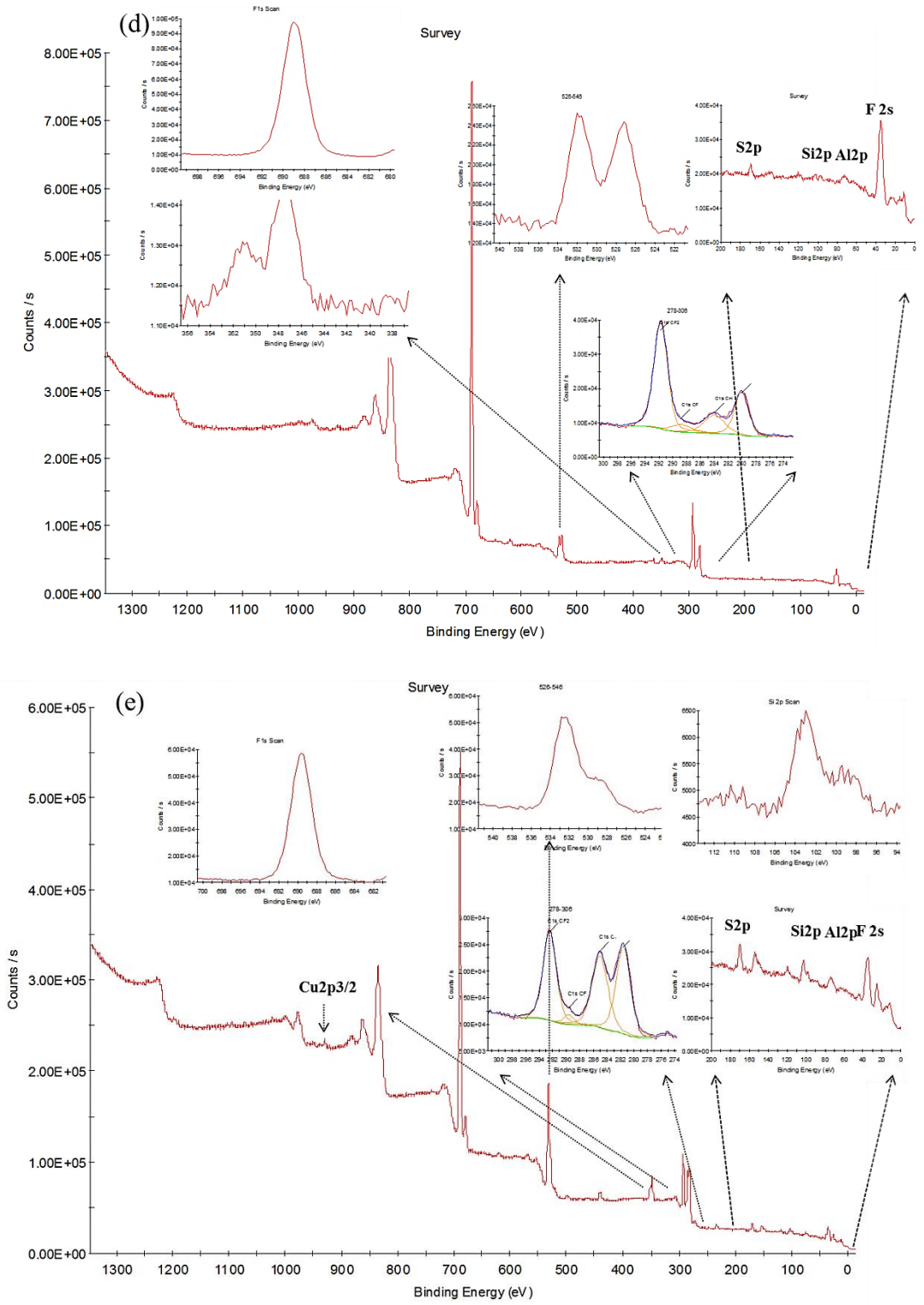

Figure B2: Survey spectra for all samples (a) blank sample (b) background (c) sample 1 (d) sample 2 and (e) sample 5.

Table B4: Summary of the results obtained by the IBA. The contents and uncertainties are given in ppm (atomic part per million). MLD refers to minimum level of detection.

	Sample 1		Sample 2		Sample 3		Sample 4		Sample 5		MLD
	Content	Uncertainty	Content	Uncertainty	Content	Uncertainty	Content	Uncertainty	Content	Uncertainty	
Si	67.3	17.7	<MLD	<MLD	<MLD	<MLD	<MLD	<MLD	36.7	13.2	5.2
S	52.0	5.3	<MLD	<MLD	<MLD	<MLD	<MLD	<MLD	11.7	3.5	1.4
K	1.3	1.3	<MLD	<MLD	<MLD	<MLD	<MLD	<MLD	<MLD	<MLD	0.6
Ca	64.7	2.1	1.6	1.0	<MLD	<MLD	<MLD	<MLD	19.0	1.3	0.6
Fe	6.7	1.2	0.5	0.7	6.7	2.7	1.3	1.1	6.0	1.0	0.5
Zn	<MLD	<MLD	<MLD	<MLD	<MLD	<MLD	<MLD	<MLD	1.3	1.4	0.6

B3. The respiratory deposited doses

Following the methodology and results described in Section 3.5, the calculated values of the respiratory deposited doses at the sampling location during the refurbishment activities are presented in Table B5.

Table B5: The deposited doses of particle numbers with fixed and variable DFs.

Activity	Dose with constant DF(dose min^{-1}) ±stdev	Dose with variable DF (dose min^{-1}) ±stdev
Drilling	[a]4.892±4.165 $\times 10^8$	[a] 6.883×±5.860 $\times 10^8$
	[b]4.782±4.089 $\times 10^8$	[b]6.680±5.712 $\times 10^8$
Cutting	[a] 2.770±1.371 $\times 10^8$	[a] 3.448±1.707 $\times 10^8$
	[b]2.660±1.296 $\times 10^8$	[b]3.330±1.622 $\times 10^8$
Sawing	[a] 2.427±2.885 $\times 10^8$	[a] 3.184±3.785 $\times 10^8$
	[b]2.317±2.809×10^8	[b]3.066±3.718×10^8
General Demolition[c]	[a] 8.740±7.468 $\times 10^8$	[a] 11.440±9.775 $\times 10^8$
	[b]8.630±7.392 $\times 10^8$	[b]11.320±9.697 $\times 10^8$
Hammering	[a] 3.997±2.896 $\times 10^8$	[a] 4.755±3.445 $\times 10^8$
	[b]3.887±2.821 $\times 10^8$	[b]4.636±3.364 $\times 10^8$
Welding and hot air torching	[a] 6.791±5.653 $\times 10^8$	[a] 8.110±6.751 $\times 10^8$
	[b]6.681±5.577 $\times 10^8$	[b]7.991±6.671 $\times 10^8$
GF machining[d]	[a] 2.804±0.280 $\times 10^8$	[a] 3.286±0.329 $\times 10^8$
	[b]2.694±0.205 $\times 10^8$	[b]3.167±0.241 $\times 10^8$

Ground cleaning and sweeping	[a] 1.801±0.586 ×10^8 [b]1.691±0.511 ×10^8	[a] 2.250±0.733 ×10^8 [b]2.132±0.644 ×10^8
Wall chasing	[a] 24.621±23.902 ×10^8 [b]24.511±23.827 ×10^8	[a] 30.023±29.147 ×10^8 [b]29.904±29.068 ×10^8
Spraying	[a] 1.446±1.308 ×10^8 [b]1.366±1.233 ×10^8	[a] 1.763±1.595 ×10^8 [b]1.644±1.517 ×10^8
Empting of waste materials	[a] 1.640± 1.052 ×10^8 [b]1.530±0.976 ×10^8	[a] 2.101±1.348 ×10^8 [b]1.983±1.266 ×10^8
Wrenching	[a] 8.003±8.858 ×10^8 [b]7.893±8.782 ×10^8	[a] 10.035±11.107 ×10^8 [b]9.916±11.03 ×10^8
Ladder and staff movement	[a] 2.501±1.269 ×10^8 [b]2.391±1.194 ×10^8	[a] 3.389±1.719 ×10^8 [b]3.270±1.632 ×10^8
Cementing	[a] 11.450±7.903 ×10^8 [b]11.340±7.828 ×10^8	[a] 13.792±9.520 ×10^8 [b]13.674±9.439 ×10^8
Grinding	[a] 4.379±2.558 ×10^8 [b]4.269±2.483 ×10^8	[a] 5.252±3.069 ×10^8 [b]5.134±2.986 ×10^8
Sanding	[a] 4.966±3.082 ×10^8 [b]4.586±3.007 ×10^8	[a] 4.890±3.035 ×10^8 [b]4.772±2.955 ×10^8
Punching of timber	[a] 1.522±0.692 ×10^8 [b]1.412±0.616 ×10^8	[a] 2.103±0.956 ×10^8 [b]1.985±0.866 ×10^8
Preparation to finish	[a] 3.769±0.932 ×10^8 [b]3.659±0.857 ×10^8	[a] 4.333±1.072 ×10^8 [b]4.215 ±0.987 ×10^8
Impact driving	[a] 11.546±3.146 ×10^8 [b]11.436±3.070 ×10^8	[a] 14.770±4.024 ×10^8 [b]14.652±3.935 ×10^8
[e]Other activities	[a] 4.050±4.567 ×10^8 [b]3.940±4.492 ×10^8	[a] 4.962±5.596 ×10^8 [b]4.843±5.521 ×10^8
Non-activity	[a] 2.861±2.179 ×10^8 [b]2.759±2.104 ×10^8	[a] 3.573±2.721 ×10^8 [b]3.455±2.641 ×10^8
Background	[a] 0.118±0.002 ×10^8 [b]0±0.000 ×10^8	[a] 0.109± 0.081 ×10^8 [b]0± 0.000× 10^8

[a]Total deposited doses (including background);
[b]Net deposited doses (after subtracting background from total);
[c]Breaking of materials such as concrete, brick and ceramic;
[d]Straightening of metal tubing;
[e]Painting, oiling, carrying metal bars to the site and moving demolished debris.

Appendix C

C1. Particle mass concentrations

Figures C1 and C2 show the average PM_{10} and $PM_{2.5}$ during the activity and non-activity periods at the CS_1, CS_2 and CS_3, respectively (Tables C1- C4).

C2. Variation of PM_{10} and $PM_{2.5}$ during different years

In order to understand the variability in concentrations during individual years, we plotted Figures C3 and C4 that present the annual mean PM_{10} concentrations obtained from monitoring stations (MS_1 to MS_9) around the CS_1. These annual mean concentrations of PM_{10} and $PM_{2.5}$ ranged from 10 to 80 μg m^{-3} (Figure C3) and 5 to 55 μg m^{-3} (Figure C4), respectively. Figure C3 also shows PM_{10} values at 6 monitoring stations during 5 years (2009-2013) of measurements around the CS_2. The annual mean PM_{10} concentrations obtained from monitoring stations (MS_{10} to MS_{15}) around the CS_2 ranged from 5 to 62 μg m^{-3}. Moreover Figure C3 shows PM_{10} values during 2011 and 2012 at MS_{16} and MS_{17} around the CS_3. The annual mean PM_{10} concentrations were found to be in the 6 to 90 μg m^{-3} range with the mean of 28.90 and 32.99 μg m^{-3} at MS_{16} and MS_{17}, respectively. Moreover, Figure C5 presents a total number of exceedences over the EU limit value at the individual monitoring stations.

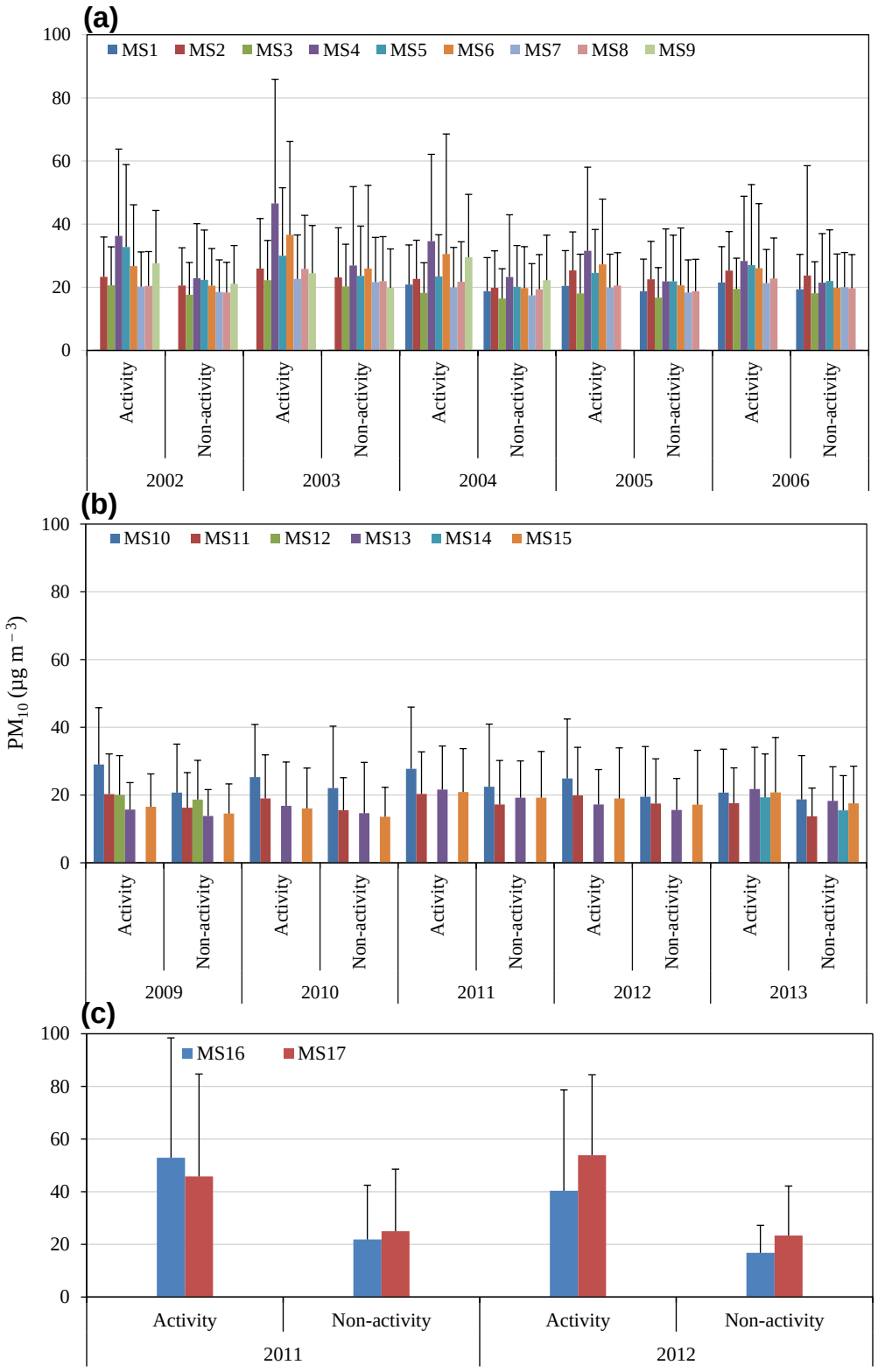

Figure C1: The average concentrations of PM_{10} (17 monitoring stations) during the working and non-working periods at the (a) CS_1, (b) CS_2, and (c) CS_3.

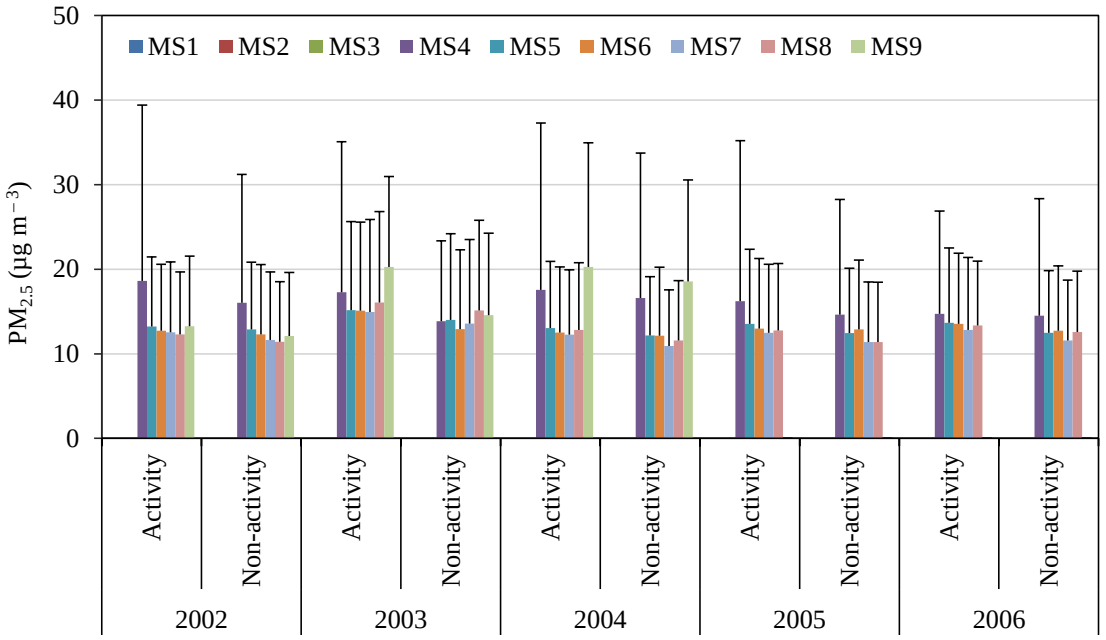

Figure C2: The average concentrations of $PM_{2.5}$ (monitoring stations) during the working and non-working periods at CS_1.

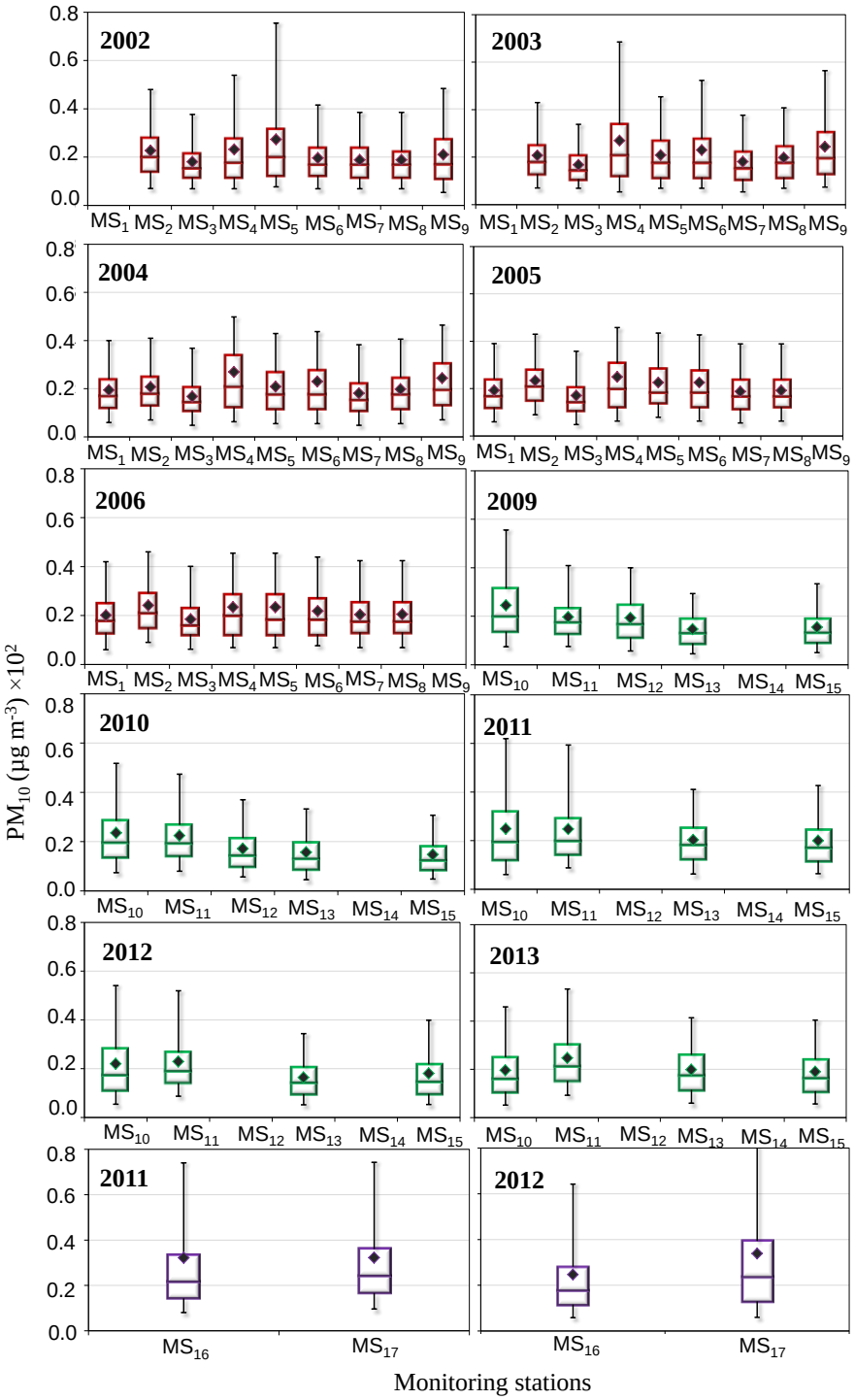

Figure C3: The Box and whiskers plots showing mean, upper, middle, and lower lines of "boxes" indicated seventy-fifth, fiftieth, and twenty-fifth percentiles of PM_{10} values during the activity and non-activity periods at the monitoring stations at CS_1 (red colour), CS_2 (green colour), and CS_3 (violet colour).

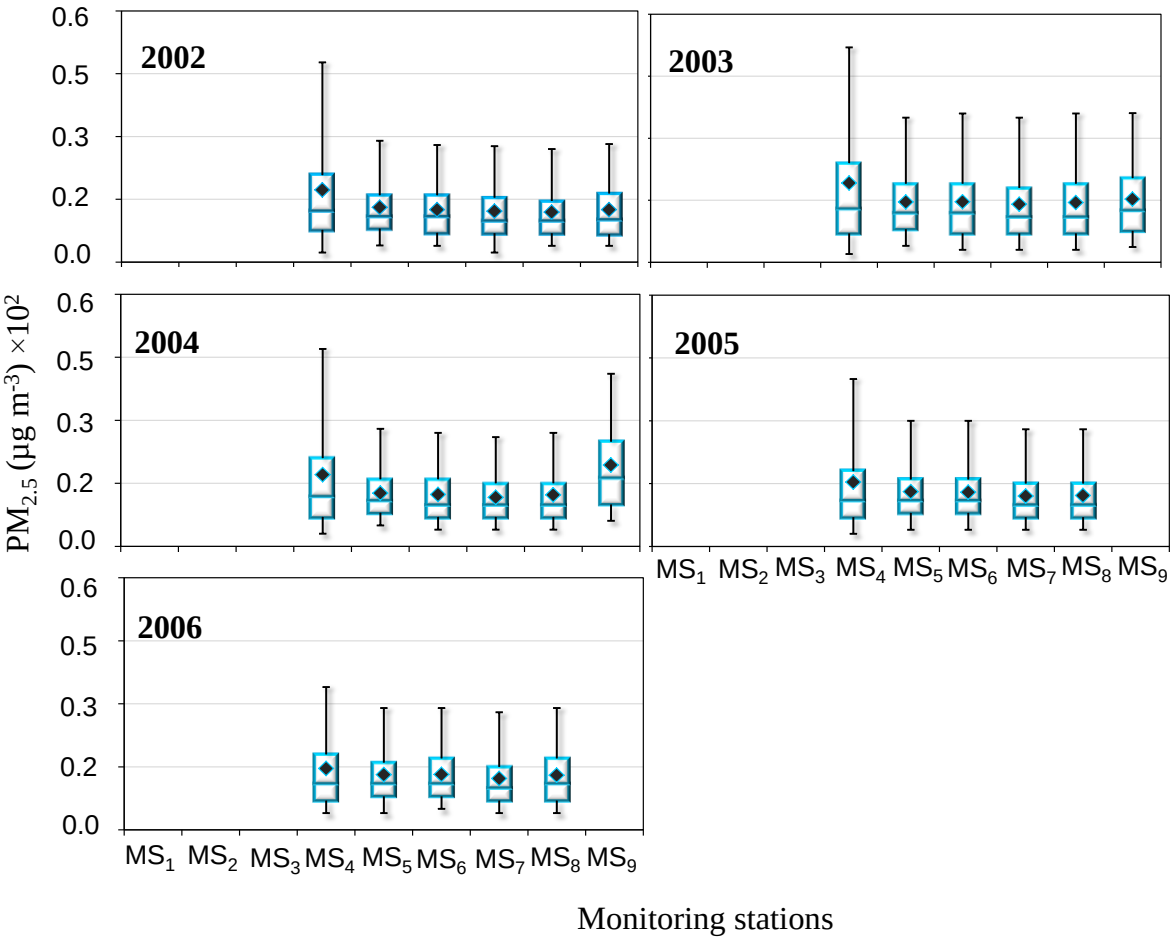

Figure C4: The Box and whiskers plots showing mean, upper, middle, and lower lines of "boxes" indicated seventy-fifth, fiftieth, and twenty-fifth percentiles of $PM_{2.5}$ values during the activity and non-activity periods at the monitoring stations at CS_1.

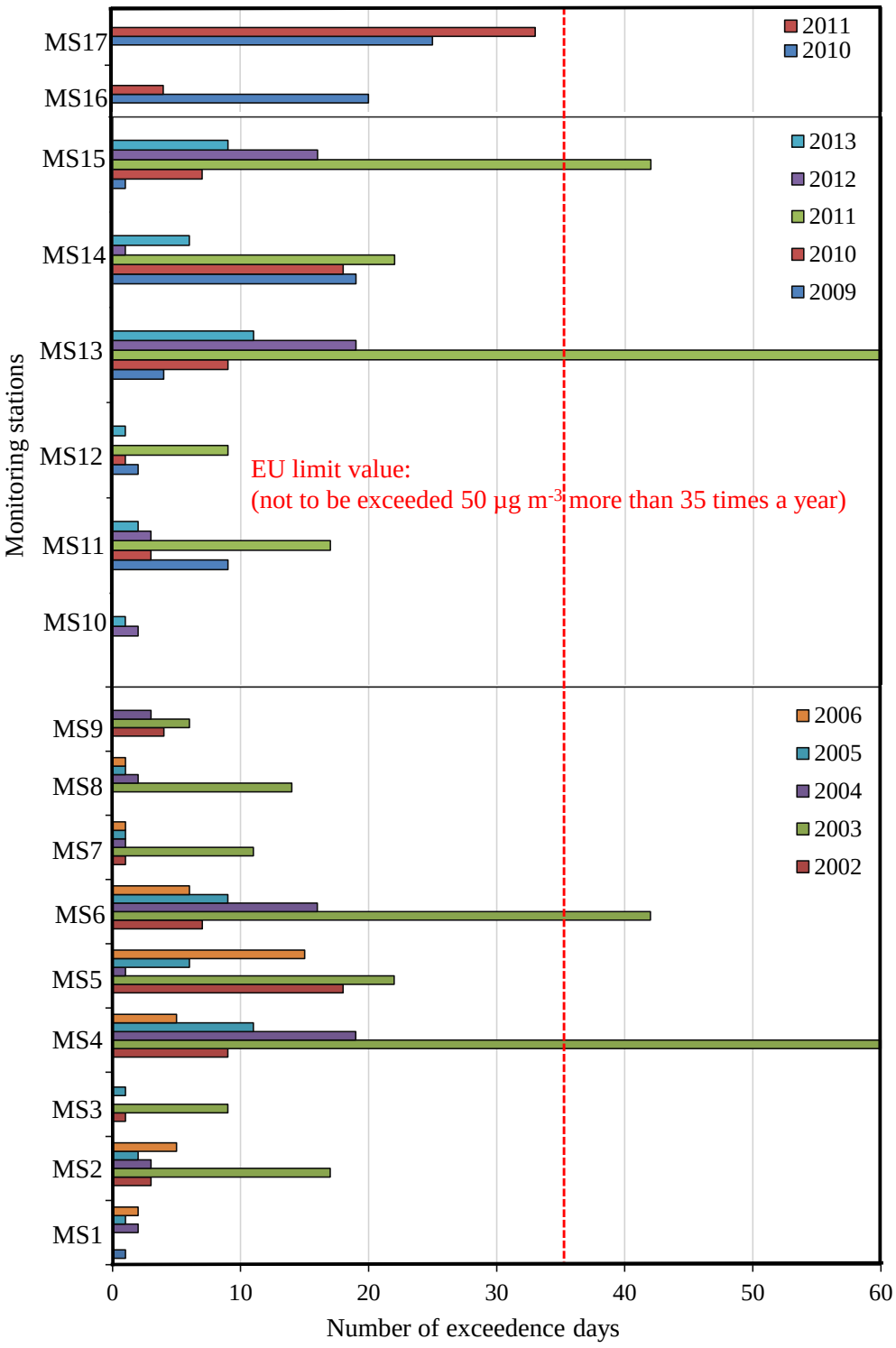

Figure C5: Total number of exceedences over the EU limit value at the individual monitoring stations.

Table C1: The concentrations of PM_{10} during the working and non-working periods at the CS_2; STD refers to standard deviation and "–" to the unavailability of data.

		Monitoring stations					
Year	PM_{10}	MS_{10}	MS_{11}	MS_{12}	MS_{13}	MS_{14}	MS_{15}
2009	Working	29.006±16.77	20.30±11.82	20.05±11.60	15.69±8.01	_	16.57±9.67
	Non-working	20.72±14.30	16.26±10.35	18.64±11.58	13.81±7.79	_	14.52±8.77
2010	Working	25.31±15.51	18.97±12.89	_	16.84±12.89	_	16.05±11.90
	Non-working	22.06±18.27	15.57±9.57	_	14.64±14.97	_	13.57±8.71
2011	Working	27.74±18.23	20.35±12.43	_	21.59±12.89	_	20.91±12.81
	Non-working	22.46±18.46	17.22±12.95	_	19.22±10.88	_	19.20±13.68
2012	Working	24.92±17.53	19.88±14.22	_	17.22±10.27	_	18.98±14.93
	Non-working	19.48±14.82	17.48±13.19	_	15.62±9.28	_	17.16±16.05
2013	Working	20.71±12.82	17.60±10.39	_	21.75±12.36	19.36±12.76	20.77±16.22
	Non-working	18.72±12.90	13.68±8.40	_	18.30±10.04	15.50±10.21	17.54±10.97
Overall	Working	25.54±3.18	19.42±1.15	20.056±0.00	18.36±2.84	19.36±0.00	18.66±2.27
Overall	Non-working	20.69±1.60	16.04±0.33	18.64±0.00	16.32±2.33	15.50±0.00	16.40±2.30

Table C2: The concentrations of PM_{10} during the working and non-working periods at the CS_3; STD refers to standard deviation.

		Monitoring stations	
Year	PM_{10}	MS_{16}	MS_{17}
2011	Working	29.006±16.77	20.30±11.82
	Non-working	20.72±14.30	16.26±10.35
2012	Working	25.31±15.51	18.97±12.89
	Non-working	22.06±18.27	15.57±9.57
Overall	Working	46.62±8.82	49.84±5.66
Overall	Non-working	19.30±3.62	24.16±1.11

Table C3: The concentrations of PM_{10} during the working and non-working periods at the CS_1; STD refers to standard deviation, W to working, N-w to non-working and "–" to the unavailability of data.

		Monitoring stations								
Year	PM_{10}	MS_1	MS_2	MS_3	MS_4	MS_5	MS_6	M S_7	M S8	M S9
2002	W	_	23.34±12.60	20.64±12.19	36.29±27.47	32.74±26.12	26.71±19.46	20.19±11.04	20.45±10.89	27.64±16.69
	N-w	_	20.54±11.95	17.65±10.20	22.89±17.30	22.37±15.79	20.51±11.78	18.56±10.11	18.38±9.53	21.08±12.14
2003	W	_	25.98±15.82	22.23±12.60	46.56±39.31	30.04±21.49	36.67±29.53	22.67±13.91	25.81±16.99	24.46±15.09
	N-w	_	23.16±15.68	20.28±13.37	26.90±24.96	23.61±15.80	25.95±26.33	21.65±14.15	21.94±14.09	19.83±12.33
2004	W	20.84±12.57	22.66±12.25	18.22±9.59	34.62±27.47	23.46±13.20	30.56±37.97	19.96±12.64	21.74±12.69	29.56±19.90
	N-w	18.78±10.60	19.85±11.72	16.42±9.45	23.27±19.70	20.15±13.08	19.73±13.13	17.48±10.02	19.38±10.96	22.25±14.26
2005	W	20.42±11.17	25.34±12.22	18.07±12.42	31.54±26.51	24.58±13.74	27.28±20.65	19.94±10.55	20.54±10.41	_
	N-w	18.78±10.15	22.51±12.05	16.76±9.47	21.88±16.62	21.89±14.61	20.62±18.16	18.37±10.32	18.78±10.06	_
2006	W	21.54±11.35	25.27±12.37	19.49±9.76	28.32±20.52	27.03±25.51	26.07±20.45	21.33±10.65	22.78±12.87	_
	N-w	19.37±11.06	23.76±34.76	18.15±9.95	21.44±15.53	21.99±16.22	19.85±10.67	20.01±11.02	19.65±10.68	_
Overall	W	20.93±0.56	24.52±1.43	19.73±1.74	35.47±6.90	27.56±3.83	29.46±4.38	20.82±1.18	22.26±2.43	27.22±2.57
Overall	N-w	18.98±0.34	21.92±1.69	17.85±1.52	23.27±2.15	22.00±1.23	21.33±2.61	19.21±1.63	19.63±1.38	21.06±1.21

Table C4: The concentrations of $PM_{2.5}$ during the working and non-working periods at the CS_1; STD refers to standard deviation, W to working, N-w to non-working and "–" to the unavailability of data.

		Monitoring stations								
Year	$PM_{2.5}$	MS_1	MS_2	MS_3	MS_4	MS_5	MS_6	MS_7	MS8	MS9
2002	W	_	_	_	18.60±20.81	13.22±8.23	12.72±7.87	12.55±8.29	12.30±7.39	13.27±8.26
	N-w	_	_	_	16.04±15.15	12.89±7.95	12.30±8.24	11.62±8.06	11.42±7.08	12.09±7.53
2003	W	_	_	_	17.28±17.77	15.16±10.48	15.09±10.47	14.95±10.91	16.06±10.76	20.27±10.66
	N-w	_	_	_	13.84±9.50	14.00±10.19	12.90±9.38	13.57±9.94	15.12±10.66	14.56±9.71
2004	W	_	_	_	17.57±19.70	13.05±7.87	12.51±7.76	12.26±7.64	12.81±7.95	20.27±14.65
	N-w	_	_	_	16.59±17.13	12.16±6.95	12.14±8.09	10.93±6.63	11.58±7.07	18.55±11.92
2005	W	_	_	_	16.21±18.96	13.55±8.80	12.98±8.27	12.49±8.08	12.75±7.92	_
	N-w	_	_	_	14.62±13.63	12.44±7.66	12.88±8.19	11.38±7.09	11.40±7.05	_
2006	W	_	_	_	14.71±12.16	13.67±8.84	13.53±8.35	12.80±8.59	13.33±7.60	_
	N-w	_	_	_	14.50±13.82	12.47±7.34	12.73±7.65	11.57±7.13	12.55±7.21	_
Overall	W	_	_	_	16.88±1.47	13.73±0.83	13.37±1.03	13.01±1.10	13.45±1.50	17.94±2.90
Overall	N-w	_	_	_	15.12±1.14	12.79±0.72	12.59±0.347	11.81±1.01	12.41±1.58	15.06±3.26

Appendix D

D1. Calibration of PM mass

Tables D1 show the description of GRIM 1.107 E calibration by the manufacturer and also the values measured during the building demolition activity.

Table D1: Description of GRIMM 1.107 E calibration by the manufacturer.

Measurement values at calibration tower (sample volume: 0.018 m^3/sample time : 15 min)			
Mean value	Reference unit ($\mu g\ m^{-3}$)	Calibrated unit ($\mu g\ m^{-3}$)	Deviation (%)
PM_{10}	305.5	308.3	0.9
$PM_{2.5}$	119.3	118.0	1.1
PM_1	42.3	41.9	0.9
Measurement values at ambient air (sample volume: 0.9 m^3 and sample time : 823 min)			
Mean value	Reference unit ($\mu g\ m^{-3}$)	Calibrated unit ($\mu g\ m^{-3}$)	Deviation (%)
PM_{10}	4.7	4.5	4.3
$PM_{2.5}$	4.1	3.9	4.9
PM_1	3.5	3.3	5.7

D2. Particles mass concentrations during the fixed–site measurements at the downwind of demolition site

The average concentrations of PM_{10}, $PM_{2.5}$ and PM_1, relative wind speed and relative humidity during two days of fixed site measurements are shown in Figure D1. Moreover, Figure D2 shows histograms of PM_{10}, $PM_{2.5}$ and PM_1 concentrations which were made using the SPSS statistical software. In addition, variation in PM concentrations and fractions for all runs during mobile measurements at route A and route B are presented in Figure D3.

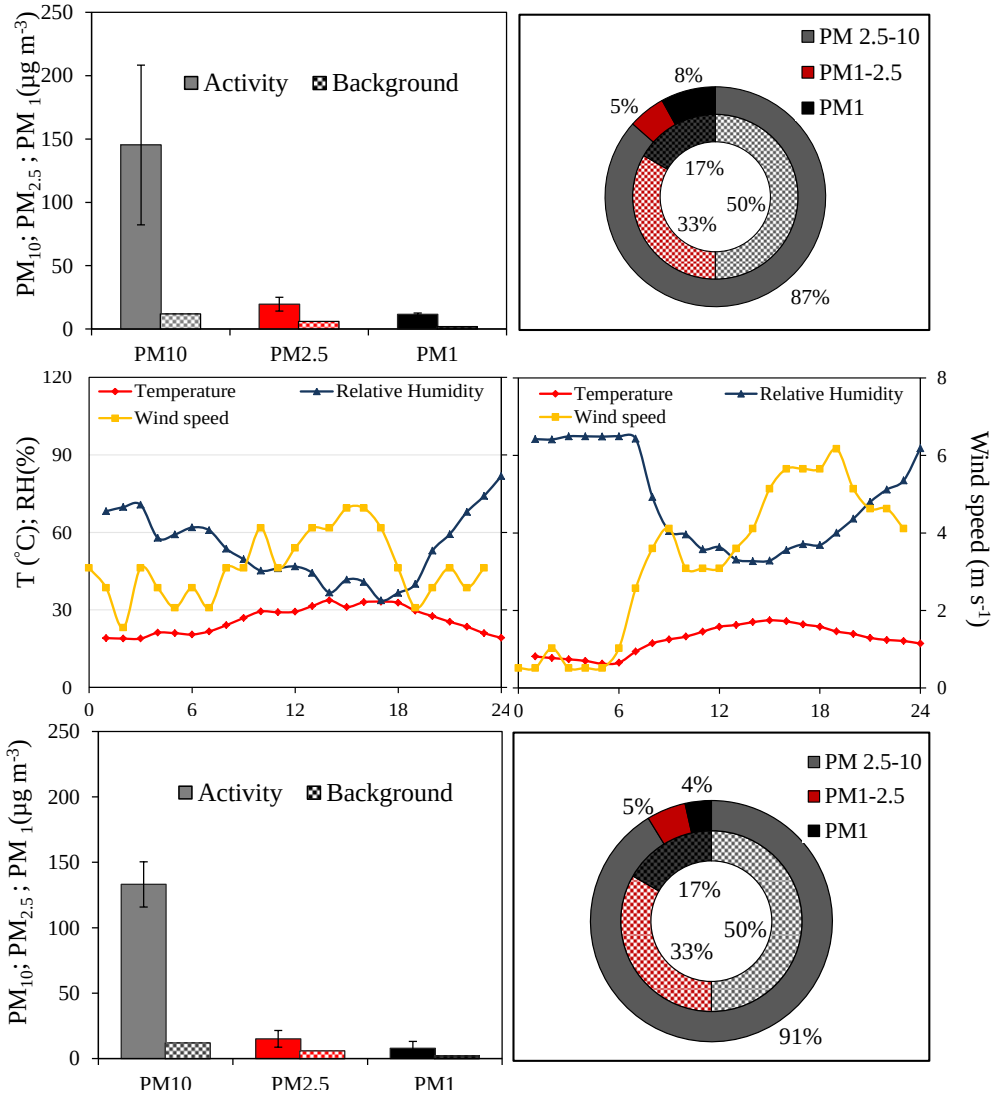

Figure D1: The concentrations of PM_{10}, $PM_{2.5}$ and PM_1, temperature and relative humidity during two days of fixed site measurements. The inner and outer circles represent fractions of PMCs in various size ranges during the background and activity periods, respectively.

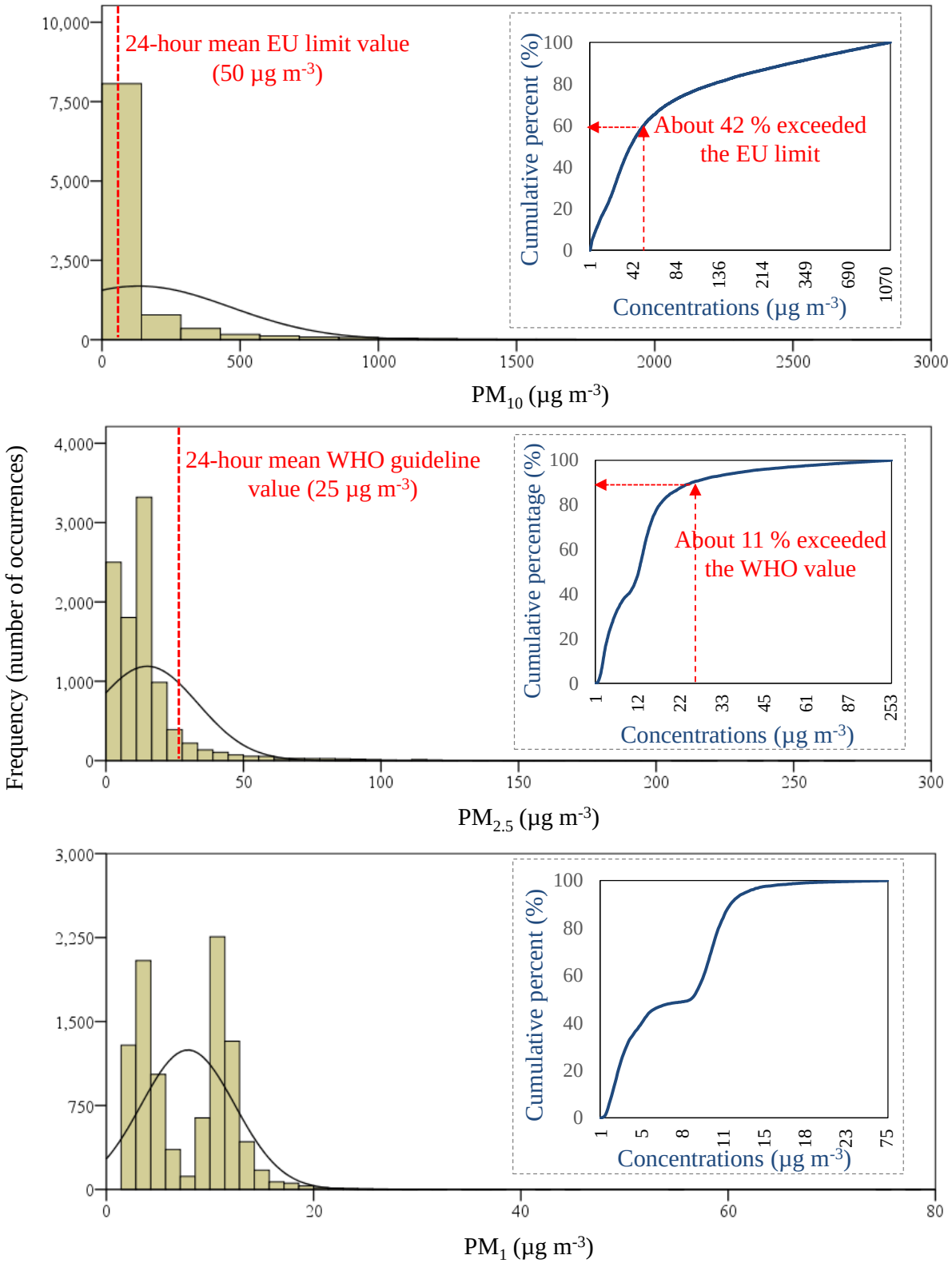

Figure D2. The concentrations of PM_{10}, $PM_{2.5}$ and PM_1 related cumulative frequency during the all days of fixed site measurements.

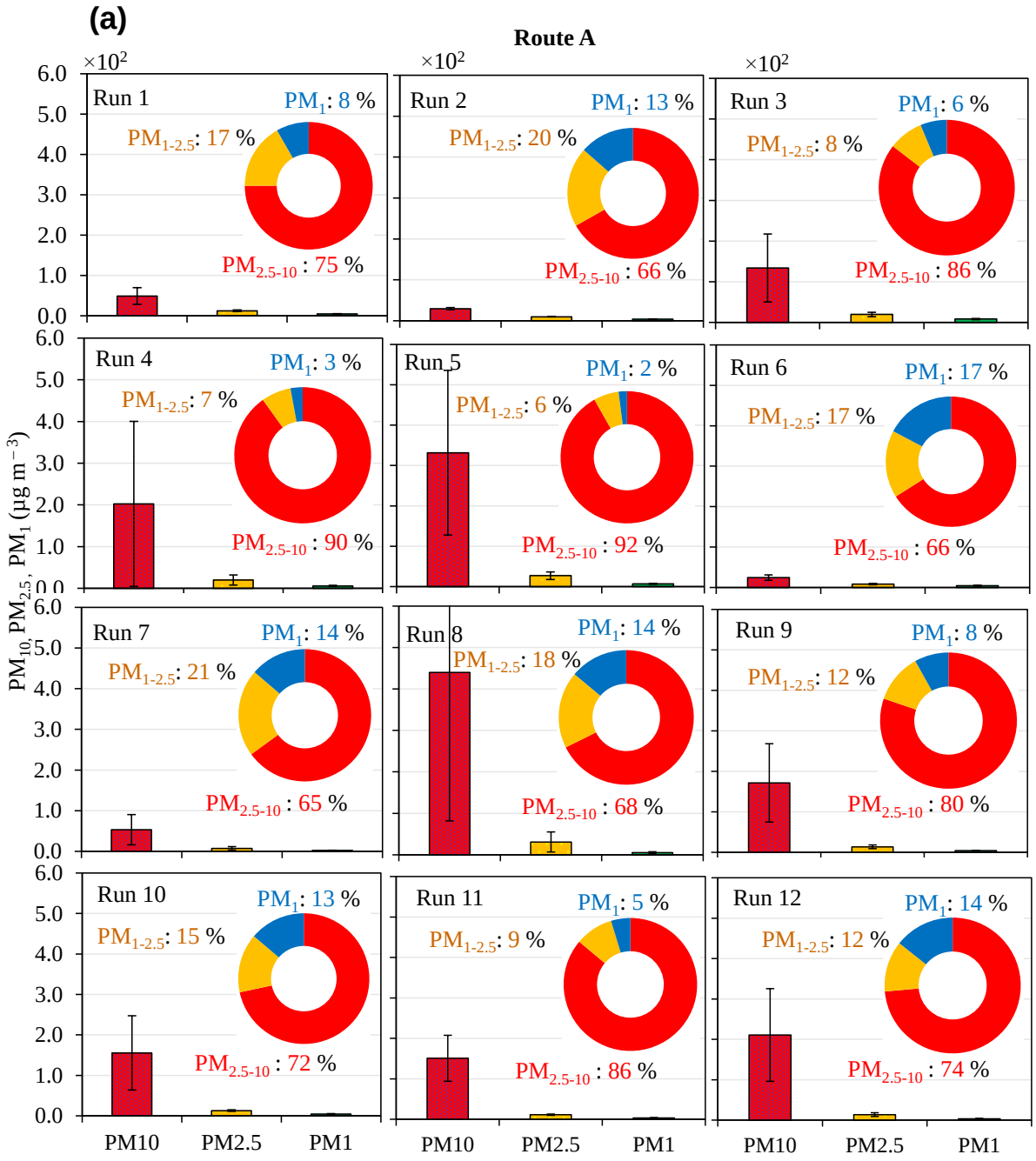

Figure D3: The variations of PM_{10}, $PM_{2.5}$ and PM_1 concentrations during mobile measurements at route A and route B.

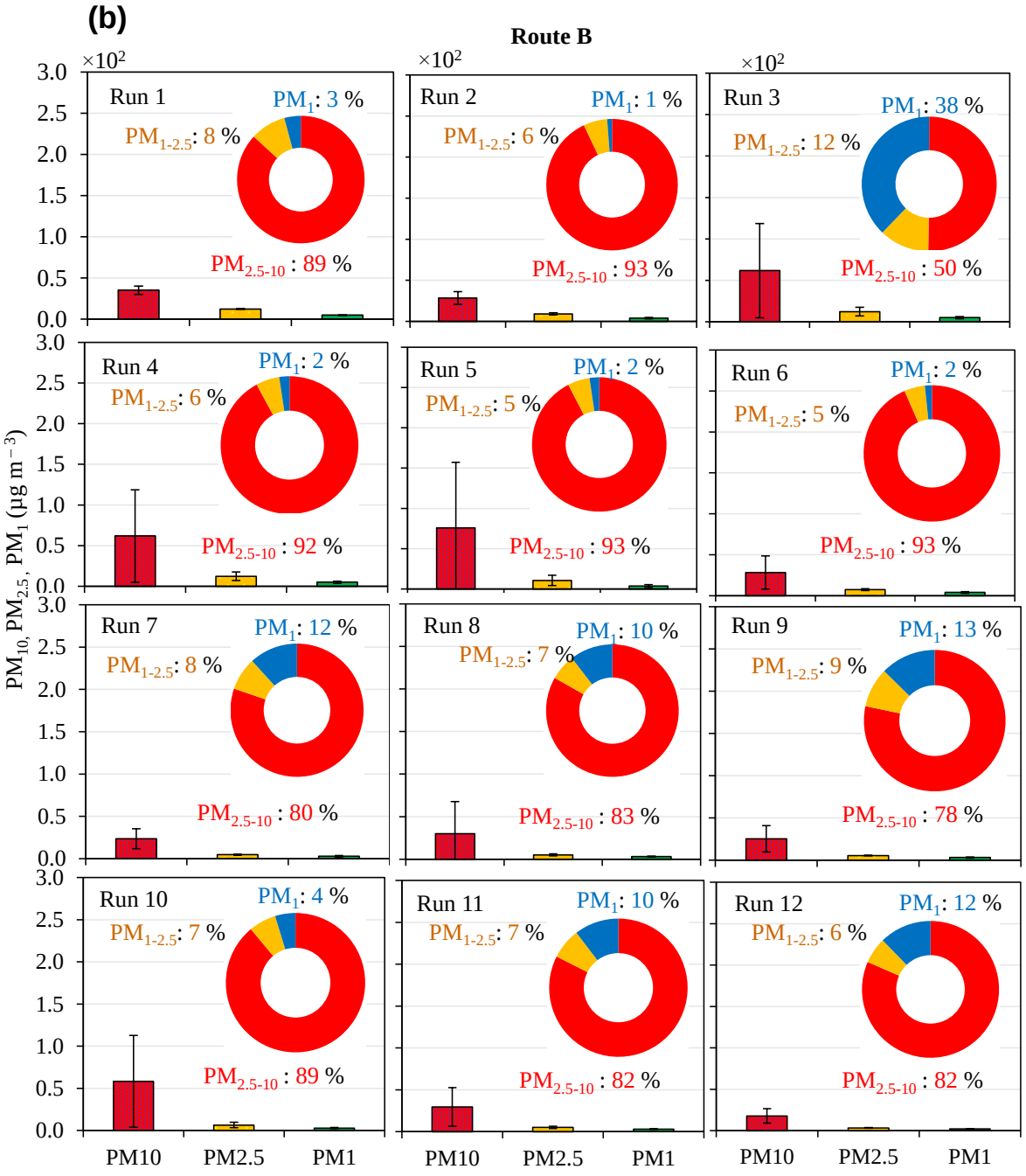

Figure D3: The variations of PM_{10}, $PM_{2.5}$ and PM_1 concentrations during mobile measurements at route A and route B.

D3. Decay profiles of PM

Figure D4 shows the variation in net concentrations of PM_{10}, $PM_{2.5}$ and PM_1 at different distances (i.e. at 10, 20, 40 and 80 m) in the downwind of the demolition site. The ΔPM concentrations at downwind distances presented in a correlated exponential decay

profiles form with R^2 values as 0.85 (ΔPM_{10}), 0.89 ($\Delta PM_{2.5}$) and 0.68 (ΔPM_1). Moreover, concentrations of PM_{10} and $PM_{2.5}$ against distances and their comparison with EU and WHO limit values are shown in Figure D5.

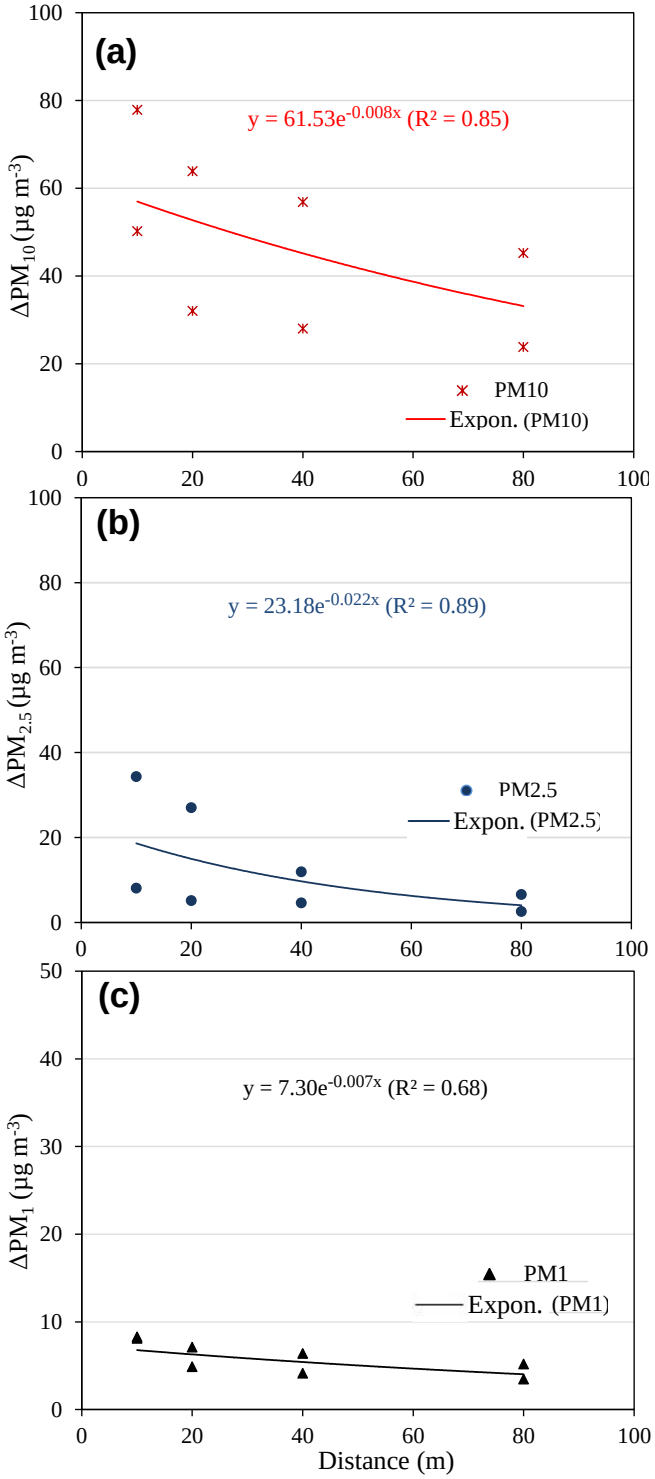

Figure D4. (a) ΔPM_{10}, (b) $\Delta PM_{2.5}$ and (c) ΔPM_1 concentration decay at demolition site during days of measurements (average of day 6 and day 7) versus distance in the downwind direction of

demolition site. In equations, *x* and *y* expresses distance from principal demolition site and ΔPM values, respectively.

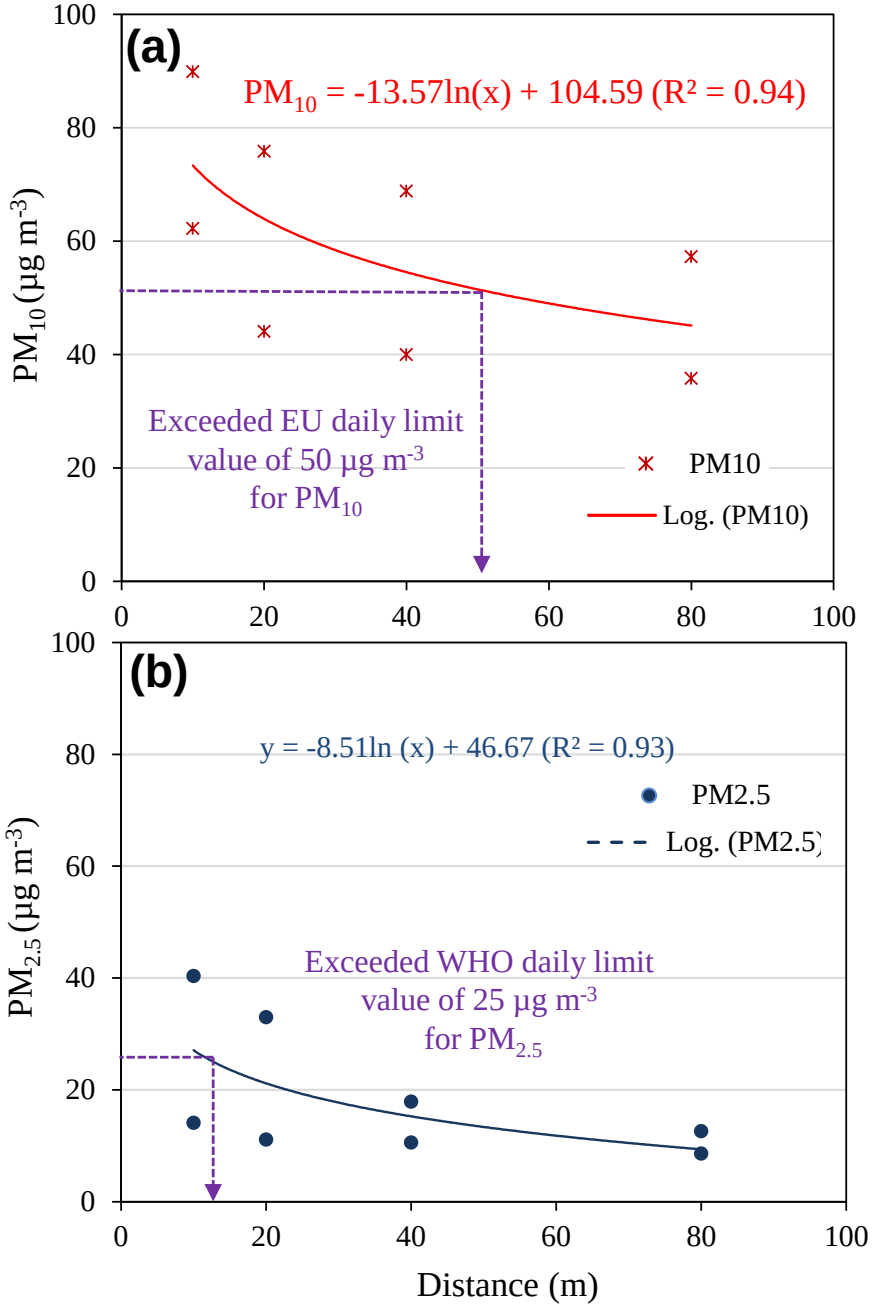

Figure D5: (a) PM_{10}, and (b) $PM_{2.5}$ decay at demolition site during measurements (average of day 6 and day7) with distance in the downwind direction of demolition site. In equations, *x* and *y* expresses distance from principal demolition site and total PM values (including background), respectively.

D4. Estimation of particle mass emission factors (PMEF)

Emission factors of PM_{10}, $PM_{2.5}$ and PM_1 from demolition works (applying the modified box model) is shown in Table D2 and their summary is presented in Figure D6.

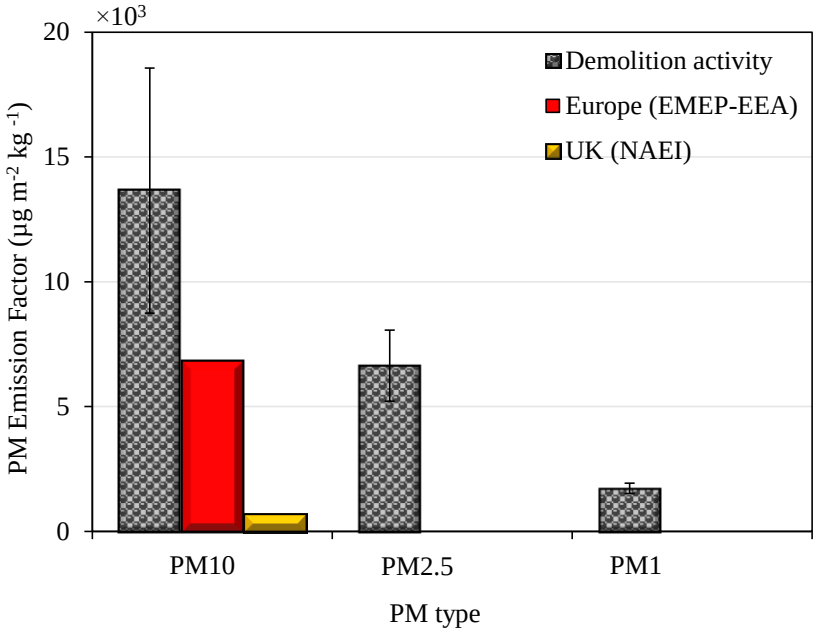

Figure D6. Particle mass concentration based PMEFs demolition activity.

Table D2. Net PM_{10}, $PM_{2.5}$ and PM_1 emission factors from demolition work activity after applying the modified box model.

PM_{10}, $PM_{2.5}$ and PM_1 net emission factors (excluding background values)									
	ΔPM_{10} ($\mu g\ m^{-3}$)	$\Delta PM_{2.5}$ ($\mu g\ m^{-3}$)	ΔPM_1 ($\mu g\ m^{-3}$)	U_X ($m\ s^{-1}$)	H_m (m)	W (m)	EF_{PM10} ($\mu g\ m^{-2}\ s^{-1}$)	$EF_{PM2.5}$ ($\mu g\ m^{-2}\ s^{-1}$)	EF_{PM1} ($\mu g\ m^{-2}\ s^{-1}$)
Day 1	123.81	60.19	15.66	0.50	8.40	15.00	34.67±17.09	16.85±3.07	4.38±0.03
Day 2	123.81	60.19	15.66	0.52	8.40	15.00	36.05±8.15	17.52±4.32	4.56±1.07
Average	123.81	60.19	15.66	0.51	8.40	15.00	35.36±12.72	17.19±3.69	4.47±0.54

D5. Energy dispersive X-ray spectroscopy technique (EDS) analysis

Figure D7 shows the EDS survey spectra and binding energy of the peak for understanding the elemental composition of all the five samples described in Table 3.5. In

addition, Table D3 shows potential sources of captured elements on the filters in the typical urban environment.

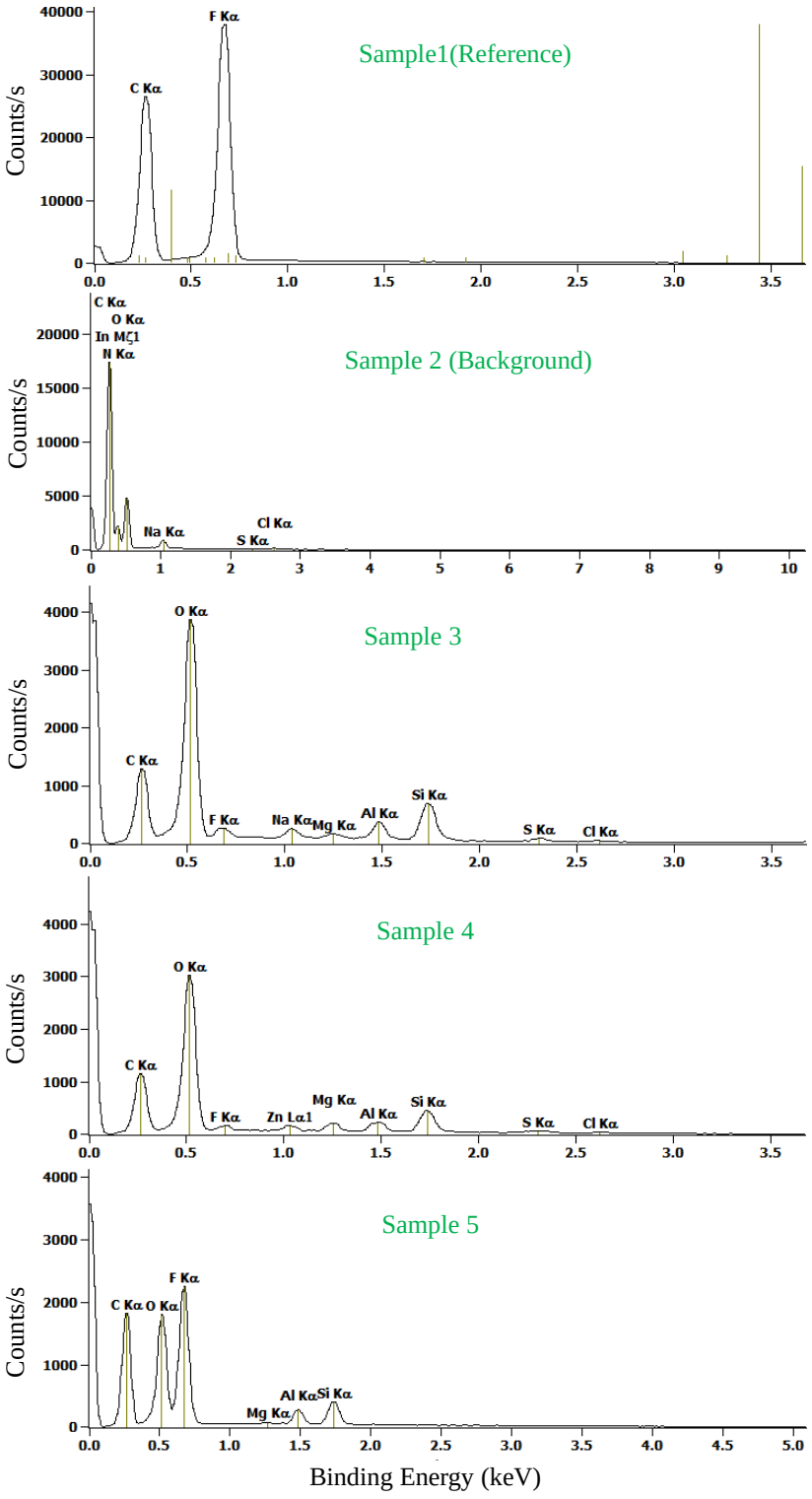

Figure D7. EDS survey spectra for sample 1 (reference), sample 2 (background) and samples 3-5 (demolition period).

Table D3. Main potential sources of captured elements on the filters (Friedlander, 1973; Fuge and Andrews, 1988; Kowalczyk et al., 1982; Miguel et al., 1997; Viana et al., 2008).

Elements	Possible sources in urban environments	Possible links with building demolition
C	Tire dust; Auto exhaust; Fuel oil fly ash	Could be released from exhaust of the construction heavy vehicular in the form calcium carbonate as filler in many construction materials
O	Sea spray; Tire dust; Auto exhaust; Fuel oil fly ash	Contributing to the elements in oxide form
F	Fuel oil fly ash	Could be found in building materials (steel)
Na	Sea spray; Soil dust	Could be found in building materials (Portland cement)
N	Sea spray; Soil dust; Auto exhaust	Could be found in building materials such incandescent and fluorescent light bulbs
S	Sea spray; Auto exhaust; Fuel oil fly ash	Could be found in building materials (Portland cement)
Cl	Sea spray; Auto exhaust	Could be found in building materials (Gypsum)
Al	Soil dust; Auto exhaust	Could be found in building materials (Metal and Ceramic)
Mg	Sea spray; Tire dust; Fuel oil fly ash	Could be found in building materials (Portland cement)
Si	Soil dust; Fuel oil fly ash	Could be found in building materials (Portland cement, bricks, asbestos)
Zn	Auto exhaust; Fuel oil fly ash	Could be found in building materials (metals)

D6. Estimation of the respiratory deposited doses (RDD)

The average RDD of coarse and fine particles during demolition works were calculated using the approach described in Section 3.5 and were shown in Figure D8.

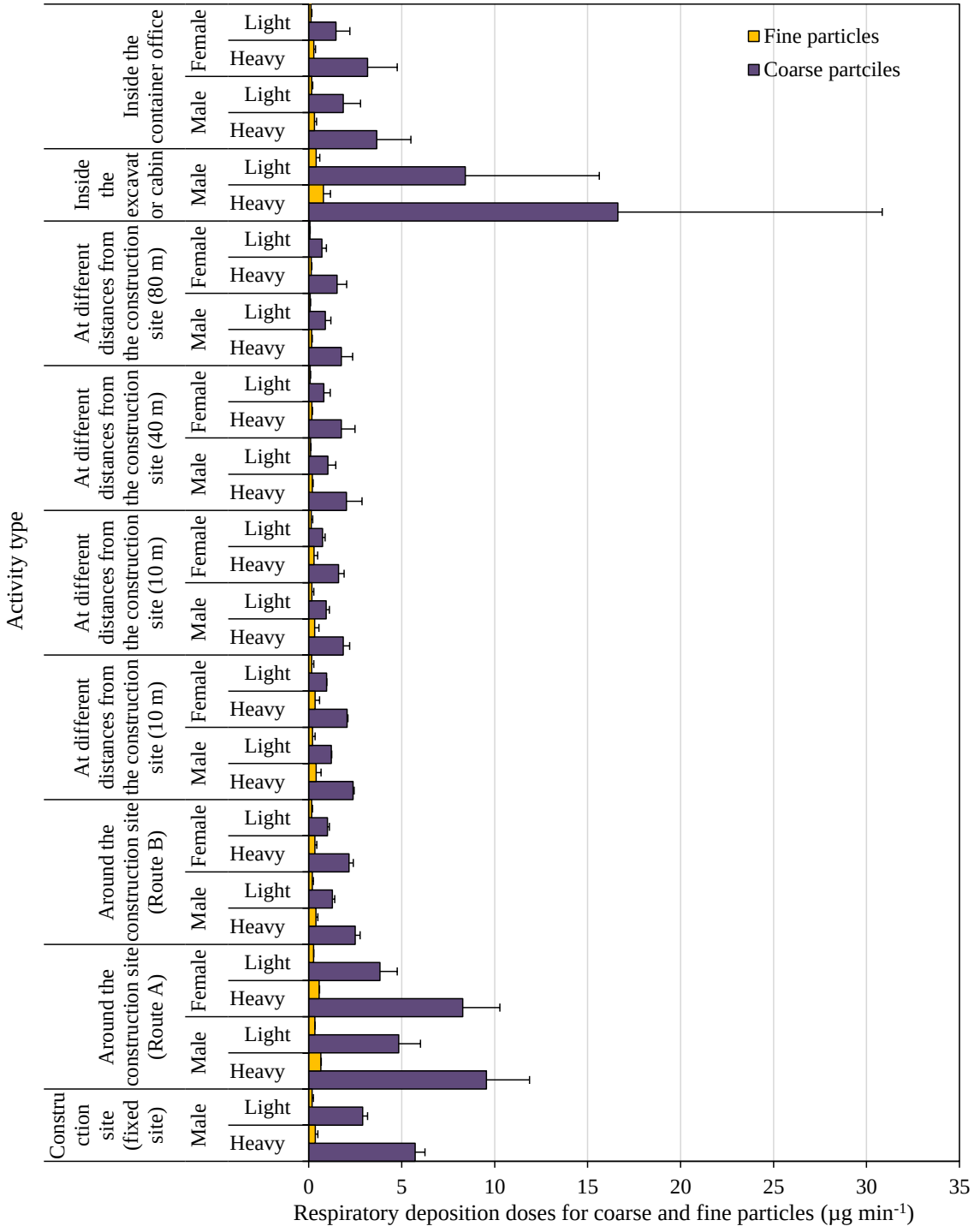

Figure D8. Respiratory deposition dose (RDD) rate (μg min^{-1}) calculated using a constant DF and the average PMCs for coarse and fine particles during each activity.

References

Friedlander, S.K., 1973. Chemical element balances and identification of air pollution sources. Environmental Science & Technology 7, 235-240.

Fuge, R., Andrews, M., 1988. Fluorine in the UK environment. Environmental Geochemistry and Health 10, 96-104.

Kowalczyk, G.S., Gordon, G.E., Rheingrover, S.W., 1982. Identification of atmospheric particulate sources in Washington, D.C. using chemical element balances. Environmental Science & Technology 16, 79-90.

Miguel, E.D., Llamas, J.F., Chacon, E., Berg, T., Larssen, S., Royset, O., Vadset, M., 1997. Origin and patterns of distribution of trace elements in street dust: Unleaded petrol and urban lead. Atmospheric Environment 31, 2733-2740.

Viana, M., Kuhlbusch, T., Querol, X., Alastuey, A., Harrison, R., Hopke, P., Winiwarter, W., Vallius, M., Szidat, S., Prevot, A., 2008. Source apportionment of particulate matter in Europe: a review of methods and results. Journal of Aerosol Science 39, 827-849.